

SYNTHESIS, CHARACTERISATION AND POTENTIAL APPLICATION OF VANADIUM COMPLEXES

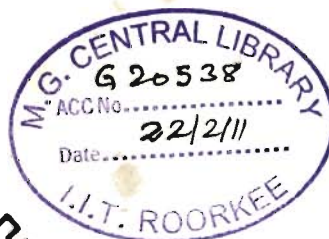
A THESIS

***Submitted in partial fulfilment of the
requirements for the award of the degree***

of
DOCTOR OF PHILOSOPHY
in
CHEMISTRY

by

AFTAB ALAM KHAN



**DEPARTMENT OF CHEMISTRY
INDIAN INSTITUTE OF TECHNOLOGY ROORKEE
ROORKEE-247 667 (INDIA)**

AUGUST, 2010

**©INDIAN INSTITUTE OF TECHNOLOGY ROORKEE, ROORKEE, 2010
ALL RIGHTS RESERVED**



INDIAN INSTITUTE OF TECHNOLOGY ROORKEE

CANDIDATE'S DECLARATION

I hereby certify that the work which is being presented in the thesis entitled **SYNTHESIS, CHARACTERISATION AND POTENTIAL APPLICATION OF VANADIUM COMPLEXES** in partial fulfilment of the requirements for the award of the Degree of Doctor of Philosophy and submitted in the Department of Chemistry of the Indian Institute of Technology Roorkee is an authentic record of my own work carried out during a period from July, 2006 to August, 2010 under the supervision of Dr. Mannar R. Maurya, Professor, Department of Chemistry, Indian Institute of Technology Roorkee, Roorkee.

The matter presented in the thesis has not been submitted by me for the award of any other degree of this or any other Institute.

(Aftab Alam Khan)

This is to certify that the above statement made by the candidate is correct to the best of my knowledge.

Date: 20.08.2010

(Mannar R. Maurya)
Supervisor

The Ph. D. Viva-Voce Examination of **Mr. Aftab Alam Khan**, Research Scholar, has been held on

Signature of Supervisor

Signature of External Examiner

ABSTRACT

Vanadium with atomic number 23 and electronic configuration $[\text{Ar}]3d^34s^2$, is a soft and silvery gray ductile transition metal. Concentration of vanadium is about 136 ppm in the earth's crust and is nineteenth element in the order of abundance. It is also present at very low concentrations ($<10^{-8}$ M) in the cells of plants and animals. Metallic vanadium is not found in nature, but is known to exist in about 65 different minerals.

Vanadium has been reported to be an essential bio-element for certain organisms, including tunicates, bacteria and some fungi. The physiological role of vanadium is not known but its importance has been indicated for the normal growth and development. Vanadium exhibits formal oxidation states from +V down to -III. The most stable oxidation states +IV and +V under normal conditions are generally stabilized through V-O bond and oxocations $[\text{VO}]^{2+}$, $[\text{VO}]^{3+}$ and $[\text{VO}_2]^+$ are most common for biological systems. Vanadium in these oxidation states comfortably binds with O, N and S donor ligands. Much attention was focused on oxovanadium(IV) complexes in mid 70s. The discovery of vanadium(V) in vanadium based enzymes in 90s, e.g., vanadate-dependent haloperoxidases and vanadium nitrogenase attracted attention of researcher to develop coordination chemistry of vanadium(V) in search of good models for vanadium-containing biomolecules. Studies on the metabolism and detoxification of vanadium compounds under physiological conditions, their stability and speciation in biofluids have further influenced the coordination chemistry of vanadium with multidentate ligands. Medicinal aspects of vanadium compounds were increased with the discovery of insulin-mimetic, antituberculosis and antiamoebic properties of vanadium complexes. Vanadium(IV) and vanadium(V) salts have been extensively tested both in vivo and in vitro in a considerable variety of experimental models of diabetes. A significant effect on the antitumor

activity of the vanadium complexes by structural modifications on the semicarbazone moiety has been indicated. Recently, several papers have also appeared in the literature on the potential application of vanadium complexes as catalysts for different oxidation reactions [whole issue of *Coord. Chem. Rev.*, 237 (2003) and an issue of *Pure Appl. Chem.*, 81(2009)].

In view of the above it may clearly be conceived that the coordination chemistry of vanadium is of increasing potential interest and therefore was considered desirable to study the coordination chemistry of vanadium that would provide: (i) structural and functional models of haloperoxidases, and (ii) medicinal as well as catalytic potentials. The present thesis is therefore, aimed to describe the coordination chemistry of vanadium considering biologically important ligands in biologically relevant oxidation states. Stability, structural and reactivity studies have been carried out to model the role of vanadium in vanadium based enzymes. The isolated complexes have been screened for their potential catalytic and medicinal applications.

For convenient the work embodied in the thesis has been divided into following chapters:

First chapter is introductory one and deals with the general remarks on vanadium, their occurrence in nature and biological systems. Applications of vanadium complexes in different areas (biological, medicinal and catalytic) and literature on model studies as well as general coordination chemistry have also been included.

The synthesis of dinuclear oxidovanadium(IV) and dioxidovanadium(V) complexes of two hydrazones $\{\text{CH}_2(\text{H}_2\text{sal-nah})_2$, **2.I** $\}$ and $\{\text{CH}_2(\text{H}_2\text{sal-inh})_2$, **2.II** $\}$ derived from 5,5'-methylenebis(salicylaldehyde) $\{\text{CH}_2(\text{Hsal})_2\}$ and nicotinic acid hydrazide (nah) or isonicotinic acid hydrazide (inh) is described in **second chapter**. The compounds are characterized in the solid state and in solution, namely by spectroscopic techniques (IR, UV-Vis, EPR, ^1H , ^{13}C and ^{51}V NMR). It has been demonstrated that the oxidovanadium(IV) complexes $[\text{CH}_2\{\text{V}^{\text{IV}}\text{O}(\text{sal-}$

nah)(H₂O)}₂] (**2.1**) and [CH₂{V^{IV}O(sal-inh)(H₂O)}₂] (**2.2**) are catalyst precursors for the catalytic oxidation, by peroxide, of methyl phenyl sulfide and diphenyl sulfide, yielding the corresponding sulfoxide and sulfone. It has also been shown that the dioxidovanadium(V) complexes K₂[CH₂{V^VO₂(sal-nah)}₂]·2H₂O (**2.3**), Cs₂[CH₂{V^VO₂(sal-nah)}₂]·2H₂O (**2.4**) and Cs₂[CH₂{V^VO₂(sal-inh)}₂]·2H₂O (**2.5**) of **2.I** and **2.II** are active in the oxidative bromination of salicylaldehyde, by H₂O₂, therefore acting as functional models of vanadium dependent haloperoxidases. Plausible intermediates involved in these catalytic processes are established by UV-Vis, EPR and ⁵¹V NMR studies. The dioxidovanadium(V) complexes along with ligands **2.I** and **2.II** were also screened against HM1:1MSS strains of *Entamoeba histolytica*, the results showed that the IC₅₀ value of compound **2.3** and **2.5** are less than the IC₅₀ value of metronidazole. The toxicity studies against human cervical (HeLa) cells line showed that the compounds **2.3** and **2.5** are toxic as compared to metronidazole.

Third chapter describes the interaction of binucleating hydrazones CH₂(H₂sal-bhz)₂ (**3.I**) and CH₂(H₂sal-fah)₂ (**3.II**), derived from 5,5'-methylbis(salicylaldehyde) and benzoylhydrazide or 2-furoylhydrazide with [V^{IV}O(acac)₂] to give dinuclear V^{IV}O-complexes [CH₂{V^{IV}O(sal-bhz)(H₂O)}₂] **3.1** and [CH₂{V^{IV}O(sal-fah)(H₂O)}₂] (**3.4**), respectively. In the presence of KOH or CsOH·H₂O, oxidation of (**3.1**) and (**3.4**) results in the formation of dioxidovanadium(V) complexes, K₂[CH₂{V^VO₂(sal-bhz)}₂]·2H₂O (**3.2**), K₂[CH₂{V^VO₂(sal-fah)}₂]·2H₂O (**3.5**), Cs₂[CH₂{V^VO₂(sal-bhz)}₂]·2H₂O (**3.3**) and Cs₂[CH₂{V^VO₂(sal-fah)}₂]·2H₂O (**3.6**). These complexes have also been prepared by aerial oxidation of in situ prepared oxidovanadium(IV) complexes **3.1** and **3.4**. The compounds were characterized by IR, electronic, EPR, ¹H, ¹³C and ⁵¹V NMR spectroscopy, elemental analyses and thermogravimetric patterns. Single crystal X-ray analysis of Cs₂[CH₂{V^VO₂(sal-bhz)}₂]·2H₂O (**3.3**) confirms the coordination of the ligand in the dianionic (ONO²⁻) enolate tautomeric form. The

V^VO_2 -complexes were used to catalyze the oxidative bromination of salicylaldehyde, therefore acting as functional models of vanadium dependent haloperoxidases, in aqueous H_2O_2/KBr in presence of $HClO_4$ at room temperature. It has been shown that the $V^{IV}O$ -complexes $[CH_2\{V^{IV}O(sal-bhz)(H_2O)\}_2]$ (**3.1**) and $[CH_2\{V^{IV}O(sal-fah)(H_2O)\}_2]$ (**3.4**) are catalyst precursors for the catalytic oxidation of organic sulphides using aqueous H_2O_2 . Plausible intermediates involved in these catalytic processes have been established by UV-Vis, EPR and ^{51}V NMR studies. The vanadium complexes along with ligands $CH_2(H_2sal-bhz)_2$ (**3.I**) and $CH_2(H_2sal-fah)_2$ (**3.II**) have also been screened against HM1:1MSS strains of *Entamoeba histolytica*, the results showing that the IC_{50} values of compounds $Cs_2[CH_2\{V^VO_2(sal-bhz)\}_2] \cdot 2H_2O$ (**3.3**) and $Cs_2[CH_2\{V^VO_2(sal-fah)\}_2] \cdot 2H_2O$ (**3.6**) are lower than that of metronidazole. The toxicity studies against human cervical (HeLa) cancer cell line also showed that although compounds **3.3** and **3.6** are more toxic than metronidazole towards this cell line, the corresponding IC_{50} values are relatively high, the cell viability therefore not being much affected.

Syntheses of dinuclear oxidovanadium(IV) and dioxidovanadium(V) complexes of two thiohydrazones $\{CH_2(H_2sal-sbdt)_2$, **4.I** and $\{CH_2(H_2sal-smdt)_2$, **4.II** derived from 5,5'-methylenebis(salicylaldehyde) $\{CH_2(Hsal)_2\}$ and S-benzyldithiocarbazate (sbdt) or S-methyldithiocarbazate (smdt) have been described in **Chapter 4**. Reactions of $[VO(acac)_2]$ with $CH_2(H_2sal-sbdt)_2$ or $CH_2(H_2sal-smdt)_2$ in 2:1 molar ratio in refluxing methanol gave the dinuclear oxidovanadium(IV) complexes $[CH_2\{VO(sal-sbdt)(H_2O)\}_2]$ (**4.1**) and $[CH_2\{VO(sal-smdt)(H_2O)\}_2]$ (**4.2**), respectively. Oxidation of $[CH_2\{VO(sal-sbdt)(H_2O)\}_2]$ and $[CH_2\{VO(sal-smdt)(H_2O)\}_2]$ in the presence KOH or CsOH gave the corresponding dioxidovanadium(V) species $K_2[CH_2\{VO_2(sal-sbdt)_2\}] \cdot 2H_2O$ (**4.3**), $Cs_2[CH_2\{VO_2(sal-sbdt)_2\}] \cdot 2H_2O$ (**4.4**), $K_2[CH_2\{VO_2(sal-smdt)_2\}] \cdot 2H_2O$ (**4.5**) and $Cs_2[CH_2\{VO_2(sal-smdt)_2\}] \cdot 2H_2O$ (**4.6**), respectively.

These complexes can also be isolated directly by the reaction of $[\text{VO}(\text{acac})_2]$ with $\text{CH}_2(\text{H}_2\text{sal-sbdt})_2$ or $\text{CH}_2(\text{H}_2\text{sal-smdt})_2$ in 2:1 ratio in refluxing methanol followed by aerial oxidation in the presence of corresponding hydroxides. These compounds have been characterized in the solid state and in solution by spectroscopic techniques (IR, UV-Vis, ^1H , and ^{51}V NMR). Complexes $\text{Cs}_2[\text{CH}_2\{\text{VO}_2(\text{sal-sbdt})_2\}]\cdot 2\text{H}_2\text{O}$ (**4.4**), $\text{Cs}_2[\text{CH}_2\{\text{VO}_2(\text{sal-smdt})_2\}]\cdot 2\text{H}_2\text{O}$ (**4.6**) have been used as catalysts for the oxidation and oxidative bromination of organic substrates in the presence of H_2O_2 . Reactivity of these complexes with H_2O_2 and HCl has been studied to obtain possible intermediate involved in catalytic reactions. Oxidovanadium(IV) and dioxidovanadium(V) complexes along with ligands **4.I** and **4.II** have also been screened against HM1:1MSS strains of *Entamoeba histolytica* and results showed that metallation of ligands reduced the IC_{50} value considerably and all dioxidovanadium(V) complexes have IC_{50} value much less than the IC_{50} value of metronidazole.

Acknowledgements

I am on the verge of giving a final shape to my dream with the grace of Allah. It is pleasant and exhilarating moment of my life to acknowledge the persons who are directly or indirectly associated with this gigantic task.

I owe this opportunity as my distinct privilege to acknowledge with great pleasure my deep sense of gratitude and reverence to my mentor and guide Prof. M.R. Maurya, who exemplified to me the meaning of research with their distinct vision and meticulous guidance. At this stage of my career, when I pause to look back to my research period I find that at every stage their perpetual encouragement, constructive criticism and above all morale boosting inspiration served as a vital source to bring the present research work to conclusion. Further their bold initiative and uncompromising gesture made by highly challenging path feasible. My heartfelt thank to him for guiding me to achieve my goal successfully. I have no words to express my gratitude to him.

I am highly thankful to Prof. A. Head Kamaluddin and Prof. Ravi Bhushan former Head, Department of Chemistry, Indian Institute of Technology Roorkee, Roorkee for providing me essential infrastructural facilities to carry out this research work.

I am also thankful to the Head, Institute Instrumentation Centre of our institute for providing me necessary instrumentation facilities for my research work. My sincere thank to Mr. Abdul Haque, Mr. V.P. Saxena, Mr. Hem Singh Panwar, Mr. Madan Pal, and Mr. Tilak Ram for helping me for timely help for my research work. I am also grateful to all the members of Chemistry Department for their cooperation in many ways.

I am also thankful to Prof. Joao Costa-Pessoa and Dr. Amit Kumar, Instituto Superior Tecnico, Portugal for carrying out the EPR studies and ^{51}V NMR spectra of some of my samples. I am also thankful to Prof. Fernando Avecilla, Departamento de Química Fundamental, Facultad de Ciencias, Universidade da Coruña, Spain for carrying out Single crystal data of some of my samples.

My special thanks to Prof. Amir Azam, Department of Chemistry, Jamia Malia Islamia, New Delhi to carry out antiamebic activities.

The words are not enough to express all my regards, love and thankfulness to my (late) Papa, Mummy and Mama Mohd Zakī Khan for their blessings, love encouragement, consistent support and motivation at every moment and throughout my study. Their presence always kept me energetic and full of spirits. I humbly acclaim my indebtedness to them for prudently shaping my life. I am in dearth of words in expressing my warm feelings to my sister Aafrin, Noorsabana and Aamina. I am in dearth of proper words to express my abounding feeling to my Nani, Khala, Khalu, Mami, Sana Khan, Humaira Khan, Arsh Khan, Mamoon Khan, Masoom Khan and Maroof Khan.

My heartfelt thanks to my seniors and laboratory colleagues Dr. Shalu Agarwal, Dr. Sweta, Dr. Umesh, Dr. Maneesh, Dr. Aarti, Manisha Bisht, Priyanka Saini and Ruchi for their lively company and motivation for the completion of my work. I own my special thanks to lab mate Chanchal Halder his selfless support.

My sincere thanks to Dr. Shahraj Ali for his selfless support, guidance, suggestions and vibrant company during the period of my thesis.

My convivial and humungous thank to my seniors and friends Mohd Ashfaue, Sheikh Altaf, Mohd Arif Khan, Dr. Moinuddin Ahmad, Dr. Sudhansu, Dr. Vipin Bansal, Ashis Sahu, Ehtesham, Saba Khan, Khan, Madan, Lal Jitendra, Sushil Kumar and Firoz Khan for their affectionate company, cooperation and moral support. I will always remain very grateful to them to be with me in all the circumstances.

I would like to thank Indian Institute of Technology Roorkee, Roorkee for awarding me the Institute fellowship.

The financial assistance provided by Council of Scientific and Industrial Research (CSIR), New Delhi is gratefully acknowledged.

Last but not least I wish to acknowledge all those, whose names have not figured above, but helped me in any form during the entire period of my research work.

(Aftab Alam Khan)

LIST OF PUBLICATIONS

1. M. R. Maurya, A. A. Khan, A. Azam, S. Ranjan, N. Mondal, A. Kumar, and J. Costa Pessoa, Dinuclear oxidovanadium(IV) and dioxidovanadium(V) complexes of 5,5'-methylenebis(dibasic tridentate) ligands: Synthesis, spectral characterisation, reactivity, and catalytic and antiamoebic activities *Eur. J. Inorg. Chem.*, 5377–5390 (2009).
2. M. R. Maurya, A. A. Khan, A. Azam, S. Ranjan, N. Mondal, A. Kumar, F. Avecilla and J. Costa Pessoa, Vanadium complexes having $[V^{IV}O]^{2+}$ and $[V^VO_2]^+$ cores with binucleating dibasic tetradentate ligands: Synthesis, characterization, catalytic and antiamoebic activities, *Dalton Trans.*, 1345–1360 (2010).
3. M. R. Maurya, A. A. Khan, A. Azam, A. Kumar and J. Costa Pessoa, Synthesis, characterization, catalytic and antiamoebic activities of vanadium complexes with 5,5'-methylenebis(dibasic tridentate ONS donor) system, *In preparation*.

Papers presented in Symposia / Conferences

1. M.R. Maurya and **A.A. Khan**, Binuclear and polymer vanadium (V) complexes of binucleating ligands derived from methylenebis(salicylaldehyde), National symposium on modern trends in chemical sciences, PP-26 (2006), October 6 – 7, 2006. Kurukshetra University, Kurukshetra.
2. M.R. Maurya and **A.A. Khan**, Synthesis, structural and antiamoebic activity studies of oxovanadium(IV) and dioxidovanadium(V) complexes of binucleating tetradentate ligands derived from 5, 5'-methylenebis(salicylaldehyde) and nicotinic acid hydrazide or isonicotinic acid hydrazide, 27th Annual Conference of Indian Council of Chemists, Gurukul Kangri University, Haridwar, December 26 – 28 2008, IP-CYSA-06.

INDIAN COUNCIL OF CHEMISTS




YOUNG SCIENTIST AWARD

*This is to certify that Dr/Sri/Ms. Aftab Alam Khan
of Deptt. of Chemistry, Indian Instt. of Tech. Roorkee, Roorkee
has been awarded the **Young Scientist Award** for the best **POSTER** presentation
of his/her paper in **Inorganic Chemistry Section** in the 27th Annual Conference
of the Indian Council of Chemists held at Gurukul Kangri Vishwavidyalaya, Haridwar on
26th, 27th & 28th December, 2008.*


Prof. Rajesh Dhakarey
Secretary

Haridwar
28th December, 2008


Dr. G. C. Saxena
President

CONTENTS

	Page No.
CANDIDATE'S DECLARATION	(i)
ABSTRACT	(ii)
ACKNOWLEDGEMENTS	(vii)
LIST OF PUBLICATIONS	(ix)
CONTENTS	(x)
LIST OF FIGURES	(xiii)
LIST OF TABLES	(xx)

CHAPTER 1

Introduction and literature survey

1.1 General	1
1.2 Vanadium in naturally occurring system	3
1.3 Structural models of haloperoxidases, nitrogenases and amvadin	8
1.4 Vanadium in biology	21
1.5 Vanadium complexes of biomolecules and their speciation in biofluids	22
1.6 Vanadium compounds in medicine	24
1.7 Functional model of haloperoxidases	30
1.8 Catalytic activity of supported or encapsulated vanadium complexes	40
1.9 Objective of the present investigation	46

CHAPTER 2

Binuclear oxidovanadium(IV) and dioxidovanadium(V) Complexes of 5, 5'-methylenebis(dibasic tridentate) ligands: Synthesis, spectral characterisation, reactivity, catalytic and antiamoebic activities

2.1 Introduction	48
2.2 Experimental	49
2.2.1 Materials	49

2.2.2	Characterization Procedures	50
2.2.3	Preparations	50
2.2.4	Catalytic activity studies	53
2.2.5	In vitro testing against E. Histolytica	54
2.3	Results and Discussion	57
2.3.1	Thermogravimetric studies	59
2.3.2	IR Spectral studies	59
2.3.3	Electronic spectral studies	60
2.3.4	^1H and ^{13}C NMR studies	61
2.3.5	Solution behaviour of $\text{K}_2[\text{CH}_2\{\text{V}^{\text{V}}\text{O}_2(\text{sal-nah})\}_2]\cdot 2\text{H}_2\text{O}$ (2.3)	64
2.3.6	Solution behaviour of $\text{Cs}_2[\text{CH}_2\{\text{V}^{\text{V}}\text{O}_2(\text{sal-nah})\}_2]\cdot 2\text{H}_2\text{O}$ (2.4)	70
2.3.7	Solution behavior of $\text{Cs}_2[\text{CH}_2\{\text{V}^{\text{V}}\text{O}_2(\text{sal-inh})\}_2]\cdot 2\text{H}_2\text{O}$ (2.5)	74
2.3.8	Catalytic activity studies	88
2.3.9	Antiamoebic activity study	95
2.4	Conclusions	98

CHAPTER 3

Vanadium complexes having $[\text{V}^{\text{V}}\text{O}]^{2+}$ and $[\text{V}^{\text{V}}\text{O}_2]^+$ cores with binucleating dibasic tetradentate ligands: Synthesis, characterization, catalytic and antiamoebic activities

3.1	Introduction	101
3.2	Experimental	103
3.2.1.	Materials	103
3.2.2.	Characterization procedures	103
3.2.3.	Preparations	103
3.2.4.	Catalytic activity studies	106
3.2.5.	In vitro testing against E. Histolytica	107
3.2.6.	X-Ray crystal structure determination of $\text{Cs}_2[\text{CH}_2\{\text{V}^{\text{V}}\text{O}_2(\text{sal-bhz})\}_2]\cdot 2\text{H}_2\text{O}$ (3.3)	108
3.3.	Results and Discussion	110
3.3.1.	Crystal and molecular structure of $\text{Cs}_2[\text{CH}_2\{\text{V}^{\text{V}}\text{O}_2(\text{sal-bhz})\}_2]\cdot 2\text{H}_2\text{O}$	112
3.3.2.	IR Spectral studies	119
3.3.3.	Electronic spectral studies	120
3.3.4.	^1H NMR studies	120

3.3.5. ^{13}C NMR studies	122
3.3.6. ^{51}V NMR studies	123
3.3.7. EPR and UV/Vis studies	129
3.3.8. Catalytic activity studies	138
3.3.9. Antiamoebic activity study	144
3.4. Conclusions	149

CHAPTER 4

Synthesis, characterisation, catalytic and antiamoebic activities of vanadium complexes with 5,5'-methylenebis(dibasic tridentate ONS donor) system

4.1. Introduction	151
4.2. Experimental	151
4.2.1. Materials	151
4.2.2. Characterization procedures	152
4.2.3. Preparations	152
4.2.4. Catalytic activity studies	155
4.2.5. In vitro testing against E. Histolytica	156
4.3. Results and Discussion	158
4.3.1. IR spectral studies	160
4.3.2. Electronic spectral studies	162
4.3.3. ^1H NMR studies	162
4.3.4. ^{51}V NMR studies	164
4.3.5. Reaction with H_2O_2	164
4.3.6. Reaction with HCl	171
4.3.7. Catalytic activity studies	173
4.3.8. Antiamoebic activity study	179
4.4. Conclusions	182

REFERENCES	183
------------	-----

SUMMARY AND CONCLUSION	215
------------------------	-----

LIST OF FIGURES

- Figure 1.1 Crystals of “Vanadite”.
- Figure 1.2 1910 “Ford Model T” where chassis of the car has vanadium containing steel. Source Wikipedia.
- Figure 1.3 *Amanita muscaria*. Source: Wikipedia.
- Figure 1.4 Active site structure of vanadate-dependent bromoperoxidases from *Ascophyllum nodosum*.
- Figure 1.5 Active site structures of vanadium chloroperoxidases (VCIPO) in the native (**2**) and peroxo forms (**3**) from *Curvularia inequalis*.
- Figure 1.6 Proposed vanadium environmental vanadium-nitrogenase, based on XAS finding and analogy to molybdenum-nitrogenase.
- Figure 1.7 ORTEP plot (at 50 % probability level) of [VO(OMe)(MeOH)(sal-nah)] (above) and [VO(OMe)(MeOH)(sal-fah)] (below). Taken from.
- Figure 1.8 Titration of [K(H₂O)₂][VO₂(pydx-bhz)] with a saturated solution of HCl in MeOH; the spectra were recorded after addition of 2 drops portions MeOH-HCl to 10 ml of ca. 10⁻⁴ M solution of complex in MeOH.
- Figure 1.9 Titration of [VO₂(sal-aebmz)] with 30% H₂O₂ in MeOH. The spectra were recorded after successive addition of 1-drop portions of H₂O₂ dissolved in MeOH to 10 mL of a ca. 1 × 10⁻⁴ M solution of [VO₂(sal-aebmz)].
- Figure 1.10 Examples of model peroxo complexes.
- Figure 1.11 Structural models of vanadium-nitrogenase.
- Figure 1.12 Structure of complexes studied for insulin-mimetic activity.
- Figure 1.13 Structure of complexes studied for insulin-mimetic activity by Rehder *et al.*
- Figure 1.14 Complexes tested for antiamoebic activity.

- Figure 1.15 Proposed catalytic reaction mechanism of V-ClPO.
- Figure 1.16 Structures of ligands that are used to design functional models of haloperoxidases.
- Figure 1.17 Complex used for functional model study.
- Figure 1.18 Polymeric complexes having catalytic potential.
- Figure 1.19 Homogeneous oxovanadium(IV) catalysts.
- Figure 1.20 (S,S)- and (R,R)-dDioxovanadium(V) complexes.
- Figure 1.21 Perspective view of complex with atomic numbering scheme (ellipsoids at the 40% level).
- Figure 1.22 View of an ORTEP plot of complex with ellipsoids at the 50% level.
- Figure 1.23 Complexes prepared by Ando *et al.* for catalytic activity.
- Figure 1.24 Ligands used to prepared oxovanadium(IV) complexes having catalytic potential.
- Figure 1.25 PS-[VO(hmbmz)₂], a polystyrene supported complex used for catalytic activity.
- Figure 1.26 Complexes having catalytic potential for the oxidation of methyl phenyl sulfide.
- Figure 1.27 Polymer supported complexes.
- Figure 2.1 ⁵¹V NMR spectra for solutions (ca. 4 mM) of K₂[CH₂{V^VO₂(sal-nah)}₂].2H₂O (**2.3**): (a) in MeOH, and (b-h) after stepwise additions of an aqueous solution of 30% H₂O₂; (b) 0.5 equiv H₂O₂ added; (c) 2 equiv H₂O₂ (total) added; (d) 4.0 equiv H₂O₂ (total) added; (e) 6.0 equiv H₂O₂ (total) added; (f) 8.0 equiv H₂O₂ (total) added; (g) 10 equiv H₂O₂ (total) added; (h) solution of (g) after 2 h leaving tube open; (i) solution of (h) after 36 h leaving tube open.
- Figure 2.2A ⁵¹V NMR spectra for K₂[CH₂{V^VO₂(sal-nah)}₂].2H₂O (**2.3**): (a) in DMSO (ca. 4 mM), (b) solution of (a) after addition of 3.0 equiv of an aqueous solution of HClO₄ (15.8 M), the pH being ~3.1; (c) solution of (b) after addition of MeOH, the solution now containing equal volumes of DMSO and MeOH; (d) solution of (a) after

addition of 3.0 equiv of an aqueous solution of HCl (11.6 M), the pH being ~ 3.3 ; (e) solution of (d) after addition of MeOH, the solution now containing equal volumes of DMSO and of MeOH.

Figure 2.2B ^{51}V NMR spectra for $\text{K}_2[\text{CH}_2\{\text{V}^{\text{V}}\text{O}_2(\text{sal-nah})\}_2]\cdot 2\text{H}_2\text{O}$ (**2.3**): (a) in MeOH, ca. 4 mM; (b) after addition of 2.0 equiv of an aqueous solution of HCl (11.6 M); (c) solution of spectrum (b) after standing for ca. 15h.

Figure 2.3 ^{51}V NMR spectra for $\text{Cs}_2[\text{CH}_2\{\text{V}^{\text{V}}\text{O}_2(\text{sal-nah})\}_2]\cdot 2\text{H}_2\text{O}$ (**2.4**): (a) in MeOH (ca. 4mM of **2.4**), and upon stepwise addition of aqueous 30% solution H_2O_2 : (b) 1.0 equiv H_2O_2 ; (c) 4.0 equiv H_2O_2 ; (d) 6.0 equiv H_2O_2 ; (e) 8.0 equiv H_2O_2 ; (f) solution of (e) after 24 h leaving the tube open (g) solution of (e) after 36 h of leaving the tube open.

Figure 2.4 ^{51}V NMR spectra for $\text{Cs}_2[\text{CH}_2\{\text{V}^{\text{V}}\text{O}_2(\text{sal-nah})\}_2]\cdot 2\text{H}_2\text{O}$ (**2.4**): (a) in MeOH (ca. 4 mM of **2.4**), and after addition of an aqueous solution of HCl (11.6 M) (b) 1.0 equiv HCl and (c) 2.0 equiv HCl added.

Figure 2.5 ^{51}V NMR spectra for $\text{Cs}_2[\text{CH}_2\{\text{V}^{\text{V}}\text{O}_2(\text{sal-nah})\}_2]\cdot 2\text{H}_2\text{O}$ (**2.4**): (a) in DMSO and after additions of aqueous acids: (b) 2.0 equiv HCl and (d) 2.0 equiv HClO_4 . Upon addition of MeOH to the solutions of spectra (b) and (d) so that the mixtures contain equal volumes of MeOH and DMSO, spectra (c) and (e), respectively, were recorded.

Figure 2.6 ^{51}V NMR spectra for $\text{Cs}_2[\text{CH}_2\{\text{V}^{\text{V}}\text{O}_2(\text{sal-inh})\}_2]$ (**2.5**): (a) in MeOH, and after addition of aqueous 30% solution of H_2O_2 : (b) 3.0 equiv H_2O_2 and (c) 5.0 equiv H_2O_2 .

Figure 2.7 ^{51}V NMR spectra for $\text{Cs}_2[\text{CH}_2\{\text{V}^{\text{V}}\text{O}_2(\text{sal-inh})\}_2]$ (**2.5**): (a) in MeOH and after addition of an aqueous solution (11.6 M) of HCl: (b) 1.0 equiv HCl; (c) 2.0 equiv HCl.

Figure 2.8 ^{51}V NMR spectra for $[\text{Cs}(\text{H}_2\text{O})]_2[\text{CH}_2\{\text{V}^{\text{V}}\text{O}_2(\text{sal-inh})\}_2]$ (**2.5**): (a) in DMSO and after additions of aqueous of either HCl or HClO_4 : (b) 2.0 equiv HCl and (d) 2.0 equiv HClO_4 . Upon addition of MeOH to the solutions of spectra (b) and of (d) so that the mixtures contain equal volumes of MeOH and DMSO, spectra (c) and (e), respectively, were recorded.

Figure 2.9 EPR spectra of frozen solution (4 mM) samples of $[\text{CH}_2\{\text{V}^{\text{IV}}\text{O}(\text{sal-nah})(\text{H}_2\text{O})\}_2]$ (**2.1**) (a) and $[\text{CH}_2\{\text{V}^{\text{IV}}\text{O}(\text{sal-inh})(\text{H}_2\text{O})\}_2]$ (**2.2**) (b) in DMSO.

- Figure 2.10 1st derivative EPR spectra (at 77 K) of a solution of $[\text{CH}_2\{\text{VO}(\text{sal-nah})(\text{H}_2\text{O})\}_2]$ (**2.1**): (a) in DMSO (ca. 4 mM); (b) after addition of an equal volume of MeOH; (c) after addition of 0.5 equiv of an aqueous 30% H_2O_2 solution.
- Figure 2.11 1st derivative EPR spectra (at 77 K) of a solution of $[\text{CH}_2\{\text{V}^{\text{IV}}\text{O}(\text{sal-inh})(\text{H}_2\text{O})\}_2]$ (**2.2**): (a) in DMSO (ca. 4 mM); (b) after addition of an equal volume of MeOH; (c) after addition of 0.5 equiv of an aqueous 30% H_2O_2 solution (see text).
- Figure 2.12 ^{51}V NMR spectra for $[\text{CH}_2\{\text{V}^{\text{IV}}\text{O}(\text{sal-inh})(\text{H}_2\text{O})\}_2]$ (**2.2**): (a) in DMSO after standing in air for 3 days, (b) upon adding 2.0 equiv H_2O_2 ; (c) upon adding 3.0 equiv H_2O_2 (total); (e) upon adding 5.0 equiv H_2O_2 ; (d) after 12 h of adding 10 equiv methyl phenyl sulfide addition to solution of (e).
- Figure 2.13 UV-Vis spectrum of 20 mL of ca. 4.135×10^{-5} M methanolic solution of $\text{Cs}_2[\text{CH}_2\{\text{V}^{\text{V}}\text{O}_2(\text{sal-inh})\}_2] \cdot 2\text{H}_2\text{O}$ (**2.5**) and spectral changes observed with time after addition of 30 % aqueous H_2O_2 (30 drops, 18.04 mmol). Each spectrum was recorded with 25 min interval.
- Figure 2.14 UV-Vis spectrum of 20 mL of ca. 5×10^{-5} M methanolic solution of ca. 5×10^{-5} M of $\text{K}_2[\text{CH}_2\{\text{V}^{\text{V}}\text{O}_2(\text{sal-nah})\}_2] \cdot 2\text{H}_2\text{O}$ (**2.3**) and spectral changes observed with time after addition of 30 % aqueous H_2O_2 (30 drops, 18.04 mmol). Each spectrum was recorded with 25 min interval.
- Figure 2.15 UV-Vis spectrum of 20 mL of ca. 5×10^{-5} M methanolic solution of $\text{Cs}_2[\text{CH}_2\{\text{V}^{\text{V}}\text{O}_2(\text{sal-nah})\}_2] \cdot 2\text{H}_2\text{O}$ (**2.4**) and spectral changes observed with time after addition of 30 % aqueous H_2O_2 (30 drops, 18.04 mmol). Each spectrum was recorded after every 25 min interval.
- Figure 2.16 Spectral changes obtained during titration of 20 mL of 6.535×10^{-5} M methanolic solution of $\text{Cs}_2[\text{CH}_2\{\text{V}^{\text{V}}\text{O}_2(\text{sal-inh})\}_2] \cdot 2\text{H}_2\text{O}$ (**2.5**) with HCl gas saturated in methanol; the spectra were recorded after the successive additions of 1-drop portions.
- Figure 2.17 Spectral changes obtained during titration of 20 mL of 5×10^{-5} M methanolic solution of $\text{K}_2[\text{CH}_2\{\text{V}^{\text{V}}\text{O}_2(\text{sal-nah})\}_2] \cdot 2\text{H}_2\text{O}$ (**2.3**) with

HCl gas saturated in methanol; the spectra were recorded after the successive addition of 1-drop portions.

- Figure 2.18 Spectral changes obtained during titration of 20 mL of 5×10^{-5} M methanolic solution of $\text{Cs}_2[\text{CH}_2\{\text{V}^{\text{V}}\text{O}_2(\text{sal-nah})\}_2] \cdot 2\text{H}_2\text{O}$ (**2.4**) with HCl gas saturated in methanol; the spectra were recorded after the successive addition of 1-drop portions.
- Figure 2.19 Effect of oxidant on the oxidation of methyl phenyl sulfide. Reaction conditions: methylphenyl sulfide (1.24 g, 10 mmol), catalyst $[\text{CH}_2\{\text{V}^{\text{IV}}\text{O}(\text{sal-nah})(\text{H}_2\text{O})\}_2]$ (**2.1**) (0.015 g) and petroleum ether (10 ml).
- Figure 2.20 Effect of catalyst $[\text{CH}_2\{\text{V}^{\text{IV}}\text{O}(\text{sal-nah})(\text{H}_2\text{O})\}_2]$ (**2.1**) on the oxidation of methyl phenyl sulfide. Reaction conditions: methyl phenyl sulfide (1.24 g, 10 mmol), H_2O_2 (2.27 g, 20 mmol) and petroleum ether (10 ml).
- Figure 2.21 Conversion of methyl phenyl sulfide and variation in the selectivity of different reaction products as a function of time using $[\text{CH}_2\{\text{V}^{\text{IV}}\text{O}(\text{sal-nah})(\text{H}_2\text{O})\}_2]$ (**2.1**) as catalyst: (a) conversion of methyl phenyl sulfide, (b) selectivity of methyl phenyl sulfoxide, (c) selectivity of methyl phenyl sulfone and (d) other unidentified product.
- Figure 2.22 Percentage of viable cells after 24 h, 48 h and 72 h on human cervical (HeLa) cells on incubation with various concentrations of compound $\text{K}_2[\text{CH}_2\{\text{V}^{\text{V}}\text{O}_2(\text{sal-nah})\}_2] \cdot 2\text{H}_2\text{O}$ (**2.3**) or vehicle (DMSO). Cell survival was determined by the MTT assay.
- Figure 2.23 Percentage of viable cells after 24 h, 48 h and 72 h on human cervical (HeLa) cells on incubation with various concentrations of compound $\text{Cs}_2[\text{CH}_2\{\text{V}^{\text{V}}\text{O}_2(\text{sal-inh})\}_2] \cdot 2\text{H}_2\text{O}$ (**2.5**) or vehicle (DMSO). Cell survival was determined by the MTT assay.
- Figure 3.1 ORTEP diagram with the thermal ellipsoids of the non-hydrogen atoms drawn at the 30% probability level representing one of the four moieties of the asymmetric unit of $\text{Cs}_2[\text{CH}_2\{\text{V}^{\text{V}}\text{O}_2(\text{sal-bhz})\}_2] \cdot 2\text{H}_2\text{O}$ (**3.3**).
- Figure 3.2 The four dinuclear molecules present in the unit cell of compound $\text{Cs}_2[\text{CH}_2\{\text{V}^{\text{V}}\text{O}_2(\text{sal-bhz})\}_2] \cdot 2\text{H}_2\text{O}$ (**3.3**).

- Figure 3.3 Space filling representation of the crystal packing of compound $\text{Cs}_2[\text{CH}_2\{\text{V}^{\text{V}}\text{O}_2(\text{sal-bhz})\}_2]\cdot 2\text{H}_2\text{O}$ (**3.3**), showing cation π -interactions. In red: oxygen, pink: caesium, gray: carbon, green: vanadium, dark blue: nitrogen and white: hydrogen atoms.
- Figure 3.4 ^{51}V NMR spectrum of a 4 mM solution of $\text{K}_2[\text{CH}_2\{\text{V}^{\text{V}}\text{O}_2(\text{sal-fah})\}_2]$ (**3.5**) in DMSO; (b) addition of 0.5 M methanol to the solution of (a).
- Figure 3.5 ^{51}V NMR spectra for $\text{K}_2[\text{CH}_2\{\text{V}^{\text{V}}\text{O}_2(\text{sal-fah})\}_2]$ (**3.5**): (a) in MeOH, (b) after addition of 3.0 equiv H_2O_2 (30%) to the solution of (a); (c) after addition of a total of 5 equiv H_2O_2 (30%) to the solution of (a); (d) after addition of a total of 8.0 equiv H_2O_2 (30%) to the solution of (a).
- Figure 3.6 ^{51}V NMR spectra for $\text{K}_2[\text{CH}_2\{\text{V}^{\text{V}}\text{O}_2(\text{sal-fah})\}_2]$ (**3.5**): (a) in DMSO, (b) 3.0 equiv HCl to the solution (a); (c) addition of methanol to solution of (b) [final MeOH ca. 50% v/v]; (d) 3.0 equiv HClO_4 to the solution (a); (e) addition of methanol to solution of (d) [final MeOH ca. 50% v/v].
- Figure 3.7 EPR spectra for 4 mM $[\text{CH}_2\{\text{V}^{\text{IV}}\text{O}(\text{sal-bhz})\}_2]$ (**3.1**) (a) in DMSO; (b) after addition of 1.0 equiv. of HCl [aqueous solution (11.6 M)] (c) after addition of a total of 2.0 equiv. of HCl [aqueous solution (11.6 M)].
- Figure 3.8 EPR spectra for 4 mM $[\text{CH}_2\{\text{V}^{\text{IV}}\text{O}(\text{sal-fah})\}_2]$ (**3.5**) (a) in DMSO; (b) after addition of 1.0 equiv. of HCl [aqueous solution (11.6 M)] (c) after addition of a total of 2.0 equiv. of HCl [aqueous solution (11.6 M)], (d) after addition of a total of 3.0 equiv. of HCl [aqueous solution (11.6 M)].
- Figure 3.9 Spectral changes obtained during titration of 20 mL of 2.86×10^{-5} M methanolic solution of $\text{Cs}_2[\text{CH}_2\{\text{V}^{\text{V}}\text{O}_2(\text{sal-bhz})\}_2]\cdot 2\text{H}_2\text{O}$ with dilute solution of 30% aqueous H_2O_2 (0.401 g, 3.01 mmol in 20 mL MeOH). Spectra were recorded after 25 min of each stepwise addition of dilute H_2O_2 solution up to a total of ca. 18 mmol (see text).
- Figure 3.10 Spectral changes obtained during titration of 20 mL of 4.2×10^{-5} M methanolic solution of $\text{Cs}_2[\text{CH}_2\{\text{V}^{\text{V}}\text{O}_2(\text{sal-bhz})\}_2]\cdot 2\text{H}_2\text{O}$ with a methanolic solution saturated with HCl gas. The spectra were recorded after the successive addition of 1-drop portions.
- Figure 4.1 Spectral changes obtained after adding two drop dilute solution of

30% aqueous H_2O_2 (3.214 g, 28.35 mmol dissolved in 30 mL MeOH) to 20 mL of ca. 20 mL of $6.429 \times 10^{-5} \text{ M}$ methanolic solution of $[\text{CH}_2\{\text{V}^{\text{IV}}\text{O}(\text{sal-sbdt})(\text{H}_2\text{O})\}_2](\mathbf{4.1})$. Spectra were recorded at every 15 min. interval. Bottom plots are expanded region of 300 to 500 nm of top.

Figure 4.2 Spectral changes obtained during titration of 20 mL of $5.76 \times 10^{-3} \text{ M}$ DMSO solution of $[\text{CH}_2\{\text{V}^{\text{IV}}\text{O}(\text{sal-sbdt})(\text{H}_2\text{O})\}_2](\mathbf{4.1})$ with a dilute solution of 30% aqueous H_2O_2 (1.256 g, 11.1 mmol in 5 mL DMSO). Spectra were recorded after the successive addition of 1-drop portions.

Figure 4.3 Spectral changes obtained during titration of 20 mL of $8.76 \times 10^{-3} \text{ M}$ DMSO solution of $[\text{CH}_2\{\text{V}^{\text{IV}}\text{O}(\text{sal-smdt})(\text{H}_2\text{O})\}_2]$ with a dilute solution of 30% aqueous H_2O_2 (1.256 g, 11.085 mmol in 5 mL DMSO). Spectra were recorded after the successive addition of 1-drop portions.

Figure 4.4 Spectral changes obtained after adding two drop dilute solution of 30% aqueous H_2O_2 (3.214 g, 28.36 mmol dissolved in 30 mL MeOH) to 20 mL of ca. 20 mL of $6.327 \times 10^{-5} \text{ M}$ methanolic solution of $[\text{CH}_2\{\text{V}^{\text{IV}}\text{O}(\text{sal-smdt})(\text{H}_2\text{O})\}_2](\mathbf{4.2})$. Spectra were recorded at every 10 min. Bottom plots are expanded region of 300 to 500 nm of top.

Figure 4.5 Spectral changes obtained after adding one drop dilute solution of 30% aqueous H_2O_2 (3.214 g, 28.358 mmol dissolved in 30 mL MeOH) to 20 mL of ca. $3.124 \times 10^{-5} \text{ M}$ methanolic solution of $\text{Cs}_2[\text{CH}_2\{\text{V}^{\text{V}}\text{O}_2(\text{sal-sbdt})\}_2] \cdot 2\text{H}_2\text{O} (\mathbf{4.4})$. Spectra were recorded at every 10 min.

Figure 4.6 Expanded spectra (300 – 500 nm) of Figure 4.5.

Figure 4.7 Spectral changes obtained after adding one drop dilute solution of 30% aqueous H_2O_2 (3.214 g, 28.358 mmol dissolved in 30 mL MeOH) to 20 mL of ca. $3.326 \times 10^{-5} \text{ M}$ methanolic solution of $\text{Cs}_2[\text{CH}_2\{\text{V}^{\text{V}}\text{O}_2(\text{sal-smdt})\}_2] \cdot 2\text{H}_2\text{O}$. Spectra were recorded at every 13 min.

Figure 4.8 Expanded spectrum (300 – 500 nm) of Figure 4.7.

Figure 4.9 Spectral changes obtained during titration of 20 mL of ca. $2.851 \times 10^{-5} \text{ M}$ methanolic solution of $\text{Cs}_2[\text{CH}_2\{\text{V}^{\text{V}}\text{O}_2(\text{sal-sbdt})\}_2] \cdot 2\text{H}_2\text{O}$

with drop wise addition of HCl (3.877×10^{-3} M) dissolved in MeOH. The spectra were recorded after the successive addition of 1-drop portions.

- Figure 4.10 Spectral changes obtained during titration of 20 mL of ca. 2.643×10^{-5} M methanolic solution of $\text{Cs}_2[\text{CH}_2\{\text{V}^{\text{V}}\text{O}_2(\text{sal-smdt})\}_2] \cdot 2\text{H}_2\text{O}$ with drop wise addition of HCl (3.877×10^{-3} M) dissolved in MeOH. The spectra were recorded after the successive addition of 1-drop portions.
- Figure 4.11 Effect of amount of catalyst per unit weight of styrene. (a) 0.001 g, (b) 0.0035 g and (c) 0.005 g. For other reaction conditions see text.
- Figure 4.12 Effect of H_2O_2 concentration (H_2O_2 : styrene molar ratio) on oxidation of styrene. For reaction conditions see text.
- Figure 4.13 Effect of solvent (methanol) on oxidation of styrene. (a) 5 mL, (b) 7 mL and (c) 10 mL. For reaction conditions see text.
- Figure 4.14 Effect of amount of catalyst, $\text{Cs}_2[\text{CH}_2\{\text{V}^{\text{V}}\text{O}_2(\text{sal-sbdt})\}_2] \cdot 2\text{H}_2\text{O}$ per unit weight of styrene. For reaction conditions see text.

LIST OF TABLES

- Table 1.1 Total concentrations of components in computer model of serum.
- Table 2.1 IR spectra of compounds (ν in cm^{-1}).
- Table 2.2 Electronic spectral data of compounds.
- Table 2.3 ^1H NMR spectral data.
- Table 2.4 ^{13}C NMR chemical shifts observed; for the atom labelling see scheme.
- Table 2.5 Spin Hamiltonian parameters obtained by simulation of the experimental EPR spectra recorded for DMSO solutions of complexes $[\text{CH}_2\{\text{V}^{\text{IV}}\text{O}(\text{sal-nah})(\text{H}_2\text{O})\}_2]$ (2.1) and $[\text{CH}_2\{\text{V}^{\text{IV}}\text{O}(\text{sal-}$

inh)(H₂O)₂] (2.2) at 77K.

Table 2.6	Percent conversion ^a of methyl phenyl sulfide and diphenyl sulfide along with the turn over frequency and selectivity of the reaction products after 7 h of reaction time.
Table 2.7	Conversion of salicylaldehyde and selectivity of oxidative brominated products data after 7 h of contact time.
Table 2.8	Vanadium Complexes, antiamoebic activity against HM1 : IMSS strain of <i>E. histolytica</i> and toxicity profile of compound K ₂ [CH ₂ {V ^V O ₂ (sal-nah)} ₂].2H ₂ O (2.3) and Cs ₂ [CH ₂ {V ^V O ₂ (sal-inh)} ₂].2H ₂ O (2.5).
Table 3.1	Crystal data and structure refinement parameters for Cs ₂ [CH ₂ {VO ₂ (sal-bhz)} ₂].2H ₂ O 3.3.
Table 3.2	Selected bond lengths (Å) and angles (°) for [Cs] ₂ [CH ₂ {V ^V O ₂ (sal-bhz)} ₂] (3.3).
Table 3.3	Summary of IR spectra of compounds (ν in cm ⁻¹).
Table 3.4	Electronic spectral data of compounds recorded in methanol.
Table 3.5	¹ H NMR spectral data (δ in ppm) for ligands 3.I and 3.II and the V ^V O ₂ -complexes recorded in DMSO-d ₆ .
Table 3.6	¹³ C NMR chemical shifts observed; for the atom labelling see scheme below.
Table 3.7	¹³ C NMR chemical shifts observed; for the atom labelling see scheme below.
Table 3.8	Summary of the ⁵¹ V NMR data (ppm) and assignment of the vanadium complexes studied in this work (see text and Scheme 3.3).
Table 3.9	Spin Hamiltonian parameters obtained by simulation of the experimental EPR spectra recorded for solutions of complexes CH ₂ {V ^{IV} O(sal-bhz)(H ₂ O) ₂] (3.1) and [CH ₂ {V ^{IV} O(sal-fah)(H ₂ O) ₂] (3.4) at 77K.
Table 3.10	Results of oxidative bromination of salicylaldehyde catalyzed by V ^V O ₂ -complexes (K ₂ [CH ₂ {V ^V O ₂ (sal-bhz)} ₂].2H ₂ O (3.2), Cs ₂ [CH ₂ {V ^V O ₂ (sal-bhz)} ₂].2H ₂ O (3.3), K ₂ [CH ₂ {V ^V O ₂ (sal-

fah)}₂].2H₂O (3.5) and Cs₂[CH₂{V^VO₂(sal-fah)}₂].2H₂O (3.6). Conversion and products obtained after 7 h of contact time.

Table 3.11 Percent conversion^a of methyl phenyl sulfide and diphenyl sulfide along with the turn over frequency and selectivity of the reaction products after 7 h of reaction time. [CH₂{V^{IV}O(sal-bhz)(H₂O)}₂] (3.1) and [CH₂{V^{IV}O(sal-fah)(H₂O)}₂] (3.4).

Table 3.12 Antiamoebic activity against HM1:IMSS strain of *E. histolytica* and toxicity profile of vanadium Complexes.

Table 4.1 IR spectra of compounds (ν in cm⁻¹).

Table 4.2 Electronic spectral data of compounds.

Table 4.3 ¹H NMR spectral data (δ in ppm) of ligands and complexes.

Table 4.4 Products selectivity and percent conversion of styrene after 6 h of reaction time.

Table 4.5 Results of oxidative bromination of salicylaldehyde catalysed by K₂[CH₂{VO^V(sal-sbdt)}₂].2H₂O (4.3), Cs₂[CH₂{VO^V(sal-sbdt)}₂].2H₂O (4.4), K₂[CH₂{VO^V(sal-smdt)}₂].2H₂O (4.5) and Cs₂[CH₂{VO^V(sal-smdt)}₂].2H₂O (4.6). Conversion and products obtained in after 7 h.

Table 4.6 Results of oxidative bromination of styrene catalysed by Cs₂[CH₂{VO^V(sal-sbdt)}₂].2H₂O (4.4) and Cs₂[CH₂{VO^V(sal-smdt)}₂].2H₂O (4.6). Conversion and products obtained after 4 h.

Table 4.7 Vanadium complexes, Antiamoebic activity against HM1:IMSS strain of *E. histolytica*.

Chapter-1

Introduction and literature survey

1.1. General

Vanadium with atomic number 23 and electronic configuration $[\text{Ar}]3d^34s^2$, is a soft, silvery gray, ductile transition metal. Vanadium was originally discovered by Andrés Manuel del Río, a Spanish-born Mexican mineralogist, in 1801. Del Río extracted the element from a sample of Mexican "brown lead" ore, and named it vanadinite. In 1831, the Swedish chemist, Nils Gabriel Sefström, rediscovered the element in a new oxide form while working with iron ores. Sefström chose a name beginning with V. He called the element *vanadium* after Vanadis (another name for Freya, the Norse goddess of beauty and fertility), because of the many beautifully colored chemical compounds it produces [1]. Later that same year, Friedrich Wöhler confirmed del Río's earlier work. [1].

Concentration of vanadium is about 136 ppm in the earth's crust and is nineteenth element in the order of abundance. It is also present at very low concentrations ($<10^{-8}$ M) in the cells of plants and animals. Metallic vanadium is not found in nature, but is known to exist in about 65 different minerals. Economically significant examples include patronite (VS_4), vanadinite ($\text{Pb}_5(\text{VO}_4)_3\text{Cl}$, Figure 1.1), and carnotite ($\text{K}_2(\text{UO}_2)_2(\text{VO}_4)_2 \cdot 3\text{H}_2\text{O}$). Much of the world's vanadium production is sourced from vanadium-bearing magnetite found in ultramafic gabbro bodies.



Figure 1.1. Crystals of “Vanadite”.

The first large scale industrial use of vanadium in steels was found in the chassis of the Ford Model T (Figure 1.2), inspired by French race cars. Vanadium containing steel allowed to control the weight while simultaneously increasing tensile strength [2].



Figure 1.2. 1910 “Ford Model T” where chassis of the car has vanadium containing steel. Source Wikipedia.

Vanadium has been reported to be an essential bio-element [3] for certain organisms, including tunicates, bacteria and some fungi. The physiological role of vanadium is not known but its importance has been indicated for the normal growth and development [4]. Vanadium exhibits formal oxidation states from +V down to -III. Oxidation states -III, -I and 0 are generally stabilized by carbonyl ligand (e.g. $[\text{V}(\text{CO})_5]^{3-}$, $[\text{V}(\text{CO})_6]^-$ and $[\text{V}(\text{CO})_6]$). Complex $[\text{V}(\text{dipy})_3]^+$ having vanadium in the +I oxidation state is well known [5]. Oxidation states II and III are, though, reducing in nature, a variety of vanadium(III) complexes are known [6 -10]. The most stable oxidation states +IV and +V under normal conditions are generally stabilized through V-O bond and oxocations $[\text{VO}]^{2+}$, $[\text{VO}]^{3+}$ and $[\text{VO}_2]^+$ are most common for biological systems. Vanadium in these oxidation states comfortably binds with O, N and S donor ligands.

The discovery of vanadium(V) in vanadium based enzymes e.g. vanadate-dependent haloperoxidases and vanadium nitrogenase attracted attention of researcher to develop coordination chemistry of vanadium(V) in search of good

models for vanadium-containing biomolecules. Studies on the metabolism and detoxification of vanadium compounds under physiological conditions, their stability and speciation in biofluids, and potential therapeutic, catalytic and other applications have further influenced the coordination chemistry of vanadium with multidentate ligands. Some aspects of vanadium complexes are given below.

1.2 Vanadium in naturally occurring system

Vanadium has been found in several plants and animals, coal and crude oils. Anthropogenic sources include the combustion of fossil fuels, particularly residual fuel oils, which make up the single largest overall release of vanadium to the atmosphere. Blood cells of several ascidians accumulate very high concentrations of vanadium in lower oxidation states. Amavadine, a naturally occurring vanadium(IV) complex has been isolated from *Amanita muscaria* (Figure 1.3) and other members of the genus Amanitae.



Figure 1.3. *Amanita muscaria*. Source: Wikipedia.

Biological systems have developed haloperoxidases enzymes to catalyze the oxidation of chloride, bromide and iodide by hydrogen peroxide. On the basis of their cofactor requirement haloperoxidases are classified into the following three groups: heme-containing, vanadium-containing [11] and metal-free

haloperoxidases [12]. Among them, vanadium haloperoxidase (VHPO) appears to be the most ubiquitous [13]. The vanadium haloperoxidases represent a group of peroxidases that possess a single bound vanadate ion in a prosthetic group.

The historical nomenclature convention of HPO is based on the most electronegative halide that the enzyme can oxidize (i.e., the chloroperoxidases (ClPO) can oxidize both Cl^- and Br^- and bromoperoxidases (BrPO) can oxidize Br^-). HPO does not have the driving force to oxidize the fluoride; however a fluorinating enzyme, fluorinase, has recently been isolated and is proposed to act by SN_2 mechanism [14, 15].

In 1983, a naturally occurring vanadium-containing enzyme, vanadium bromoperoxidase (VBrPO), was discovered in the marine brown alga *Ascophyllum nodosum* [16]. The bromoperoxidases involve in the polymerization of polyphenols holding the zygote to the membrane during the reproductive cycle of the cell [17]. It has trigonal bipyramidal coordination sphere including apical histidine and a meridionally bound oxo group; Figure 1.4 [18].

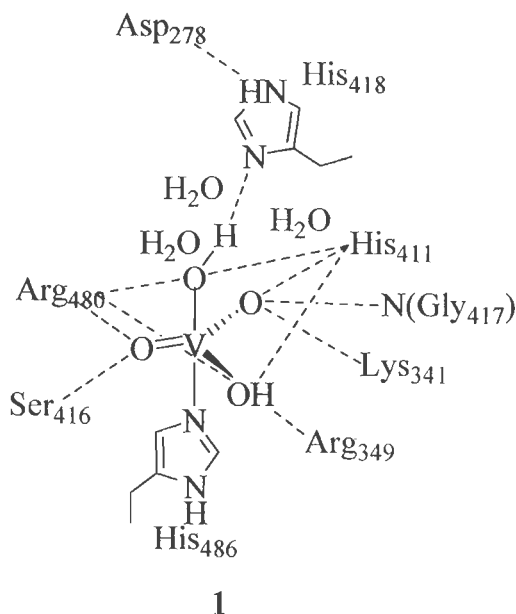


Figure 1.4. Active site structure of vanadate-dependent bromoperoxidases from *Ascophyllum nodosum*.

The oxidation state of the vanadium is +V and it does not change when hydrogen peroxide bind to give activated peroxo-intermediate species. Vanadium chloroperoxidases (VCIPO), in the native and peroxo forms (Figure 1.5), have been isolated from the fungus *Curvularia inaequalis* [19, 20]. The active site is located at the top of the bundles [21]. A five-coordinated trigonal bipyramidal $V^{(V)}$ moiety (**2** of Figure 1.5) is present in the native form which is coordinated by three nonprotein oxo groups in the equatorial plane and one His₄₉₆ and a hydroxy group at the axial positions. The oxygens are hydrogen bonded to several amino acid residues of the protein chain. The nitrogen of His₄₉₆ coordinates to vanadium and hence is the only direct bond from the protein to the metal center. The apical V-O bond length is 1.93 Å and the V-N bond is 1.96 Å, three equatorial V-O bonds are about 1.65 Å long.

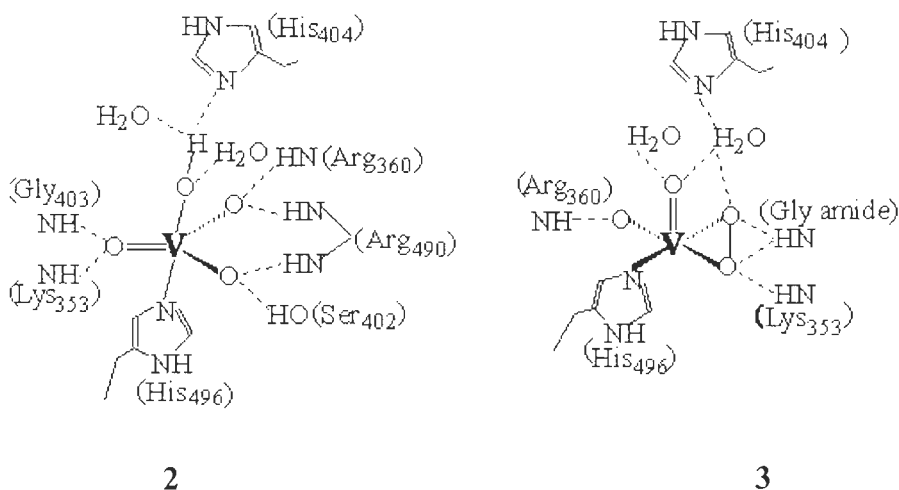


Figure 1.5. Active site structures of vanadium chloroperoxidases (VCIPO) in the native (**2**) and peroxo forms (**3**) from *Curvularia inaequalis*.

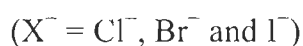
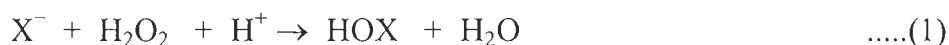
In the peroxo form (**3** of Figure 1.5), the peroxide ligand is bound in a η^2 -manner in the equatorial plane. The apical oxygen ligand detaches and gives a distorted tetragonal pyramidal coordination geometry around the vanadium centre with the two peroxo oxygens having V-O bond length ~ 1.87 Å and O-O is 1.47 Å.

One oxygen (V-O bond length 1.93 Å) and the nitrogen (V-N bond length 2.19 Å) are in the basal plane while one oxygen (V-O bond length 1.60 Å) is in the apical position.

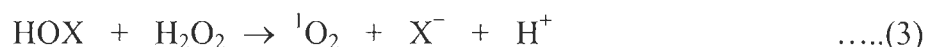
Carallina officinalis has been isolated from red algae and shows a high degree of amino acid homology in their active centre and has almost identical structural feature as have been reported for other enzymes [22].

These enzymes catalyze the oxidation of suitable electrophilic halides (X^-) to the corresponding hypohalous acid (HOX) according to equation (1) using H_2O_2 as an oxidant followed by non-enzymatically halogenation of organic compounds, equation (2).

The presence of such enzyme in nature could do some way to explaining the formation of at least some of the wide diversity of halogenated compounds in environment [23].



Without suitable organic substrate, the two-electron oxidation of halide may turn to produce singlet oxygen, equation (3).



In the last decade peroxidases, particularly chloroperoxidase have been shown to catalyse a variety of synthetically useful oxygen transfer reactions with H_2O_2 , including enantioselective oxidation of sulfides [24, 25]. Vanadium haloperoxidases, such as vanadium chloroperoxidase from *Curvularia inaequalis* are much more stable. The vanadium-dependent bromoperoxidase from *Corallina officinalis* mediates the enantioselective oxidation of aromatic sulfides [26, 27]. The brown seaweed *Ascophyllum nodosum* mediate the formation of the (R)-enantiomer of the methyl phenyl sulfoxide with 91 % enantiomeric excess, whereas the red seaweed *Corallina pilulifera* mediates formation of the (S)-

enantiomer (55 % enantiomeric excess) under optimal reaction conditions [28]. Recently Butler *et al.* have reported vanadium bromoperoxidase catalyzed biosynthesis of halogenated marine natural products [29].

In 1986, a vanadium nitrogenase enzyme was isolated from each of the two soil bacteria, *Azotobacter chroococcum* [30] and *A. vinelandii* [31, 32]. In vanadium-nitrogenases, vanadium is in II / III oxidation state as an integral part of an iron-sulphur cluster [33] which activates and reductively protonates various unsaturated substrates [34]. The coordination sphere around vanadium is probably octahedral (4, Figure 1.6) and is similar to that of molybdenum in the structurally characterized molybdenum-nitrogenase [33, 35]. Thus, in vanadium-nitrogenase, vanadium is coordinated to histidine and the vicinal hydroxide and carboxylate groups of homocitrate in addition to three sulphide ions from iron-cluster.

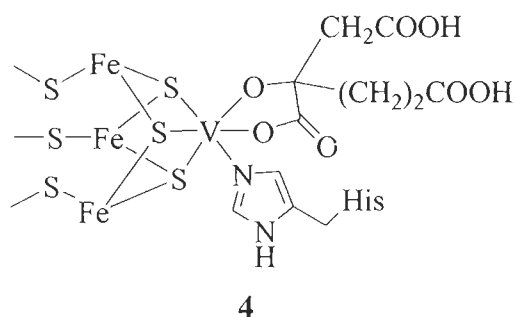
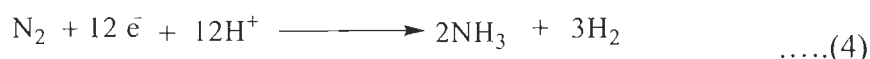


Figure 1.6. Proposed vanadium environment vanadium-nitrogenase, based on XAS finding and analogy to molybdenum-nitrogenase [33, 35].

The vanadium-iron protein of vanadium nitrogenases extracted from *Azotobacter chroococcum* contains an iron-vanadium cofactor. It is suggested that the nitrogen fixation requires specific interactions between Fe-V cofactor (Fe-Vaco) or Fe-Mo cofactor (Fe-Moco) and their respective polypeptides [36]. The vanadium nitrogenases [37] are multicomponent metalloenzyme complexes that are capable of reducing dinitrogen to ammonia, and hence to a form accessible by plants [38].



Many nitrogenases consist of a Fe-S cluster and a molybdenum-dependent component [39]. The first vanadium containing nitrogenase, *i.e.* a V-Fe-protein, was isolated and purified in 1986 from certain nitrogen-fixing bacteria [30].

1.3. Structural models of haloperoxidases, nitrogenases and amvadin

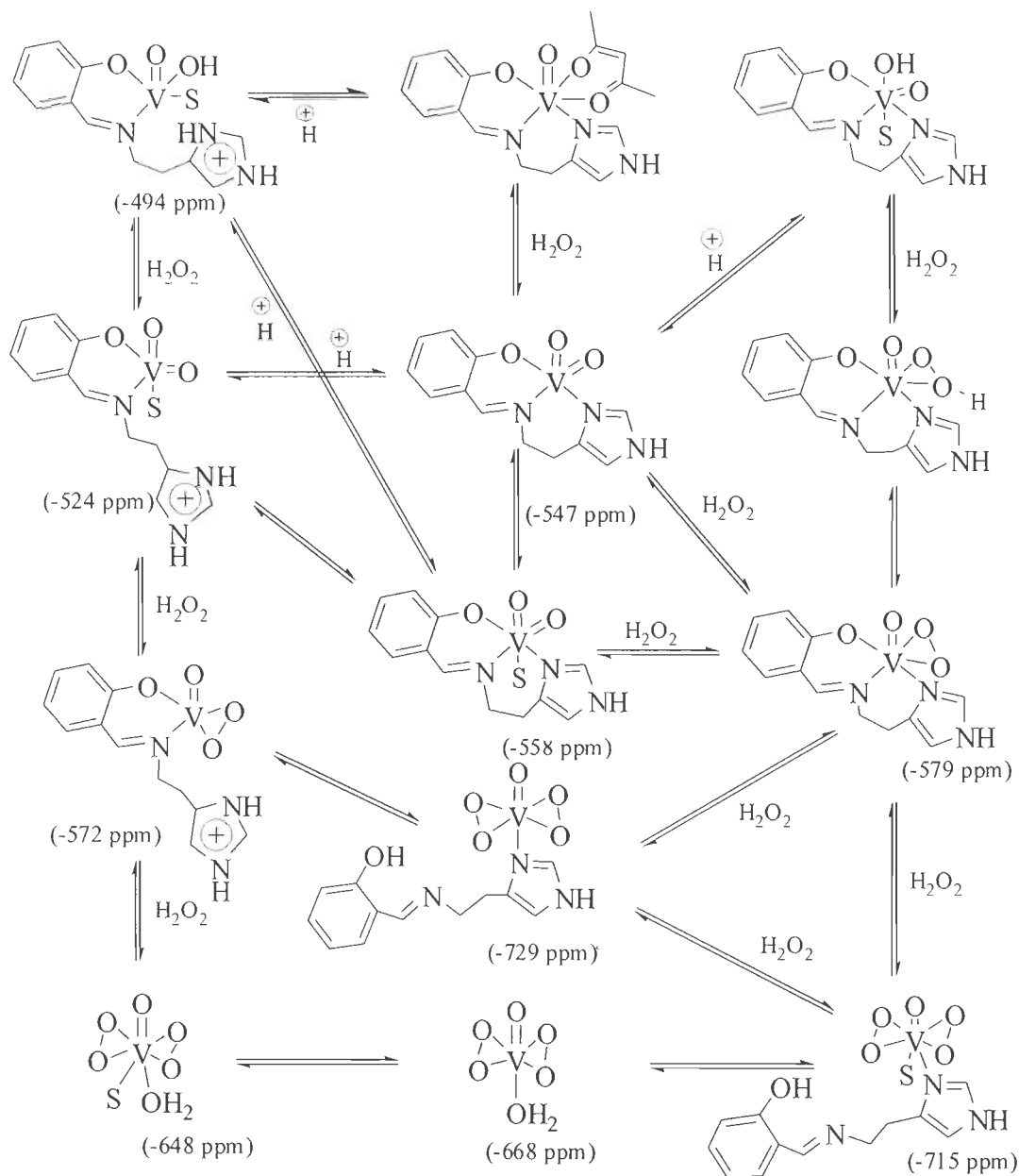
The active site structure of vanadate-dependent haloperoxidases has O_4N coordination environment where vanadate(V) is coordinated to the histidine of the protein matrix. The stability of vanadium(V) complexes under aerobic conditions has allowed the design of structural and/or functional models for the haloperoxidases and to isolate or generate species having above group in solution. [40]. A large number of imidazole coordinated vanadium complexes have been synthesized in order to model the active site of haloperoxidases. Complexes, $[VO(acac)(sal-his)]$, $[VO(sal)(sal-his)]$ and $[VO(sal-his)_2]$ ($H_2sal-his = 4-(2-(salicylideneamino)ethylimidazole)$) represent model characters observed for the reduced form of vanadate-bromo peroxidase. Upon acidification, protonation of coordinated imidazole (in $[VO(acac)(sal-im)]$, $[VO(sal)(sal-his)]$) or non-coordinated imidazole (in $[VO(sal-his)_2]$) have been suggested in these complexes [41 - 43]. Electron Spin-Echo Envelop Modulation (ESEEM) study, however, suggested that the azomethine nitrogen of the Schiff base of $[VO(acac)(sal-his)]$ is protonated and detached from vanadium upon addition of one equivalent of acid. [44]. $[VO(acac)(sal-his)]$ reacts with catechol, pyrogallol and acetohydroxamic acid in solvent to give corresponding mixed chelate complexes. Aerial oxidation of $[VO(acac)(sal-his)]$ in the presence of a few drops of aqueous 30% H_2O_2 results in the formation of dioxidovanadium(V) complex $[V^VO_2(sal-his)]$. Solution of $[V^{IV}O(sal-his)(acac)]$ in methanol is sensitive towards addition of H_2O_2 , as monitored by electronic absorption spectroscopy, yielding oxoperoxo species [45].

Solutions of $[V^VO_2(sal-his)]$ in methanol are also sensitive to pH changes, and were also monitored by ^{51}V NMR spectroscopy. Addition of 1 equiv HCl to a

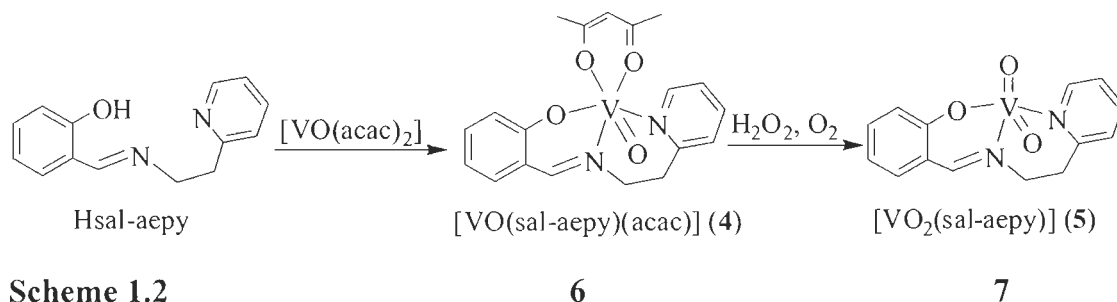
methanolic solution of $[V^V O_2(\text{sal-his})]$ resulted in a reduction in intensity of the $\delta = -547$ ppm and $\delta = -558$ ppm peaks, while a new signal at $\delta = -524$ ppm was detected. Further addition of 1 equiv of HCl gave a spectrum with only one intense signal at $\delta = -524$ ppm. This has been assigned to the protonation of the imidazole N atom, the sal-his ligand becoming bidentate and the solvent also coordinating $[V^V O_2(\text{sal-Hhis})(\text{MeOH})]$ ($\delta = -524$ ppm).

As compound $[V^{IV} O(\text{sal-his})(\text{acac})]$ is paramagnetic as no signal was observed by ^{51}V NMR spectroscopy when dissolved in methanol. However, after addition of 0.5 equiv H_2O_2 , three signals ($\delta = -494$, -547 and -558 ppm) appear, and we tentatively assign them to $[V^V O(\text{OH})(\text{sal-Hhis})(\text{MeOH})]$ ($\delta = -494$ ppm), $[V^V O_2(\text{sal-his})]$ ($\delta = -547$ ppm) and $\{[V^V O_2(\text{sal-his})(\text{MeOH})]\}$ ($\delta = -558$ ppm). Upon further addition of 0.5 equiv of H_2O_2 another three signals at: $\delta = -579$, -524 and -572 ppm were detected, which we tentatively assign as $[V^V O(\text{O}_2)(\text{sal-his})]$ ($\delta = -579$ ppm), $\{[V^V O_2(\text{sal-Hhis})(\text{MeOH})]\}$ ($\delta = -524$ ppm) and $[V^V O(\text{O}_2)(\text{sal-Hhis})]^+$ ($\delta = -572$ ppm). Further addition of 0.5 equiv H_2O_2 originated the formation of the peak at -729 ppm (see above), and $[\text{VO}(\text{O}_2)_2(\text{H}_2\text{O})(\text{MeOH})]^-$ ($\delta = -648$ ppm). Tentative assignments of various species, on addition of aqueous H_2O_2 and HCl, formed in methanolic solutions of $[V^{IV} O(\text{sal-his})(\text{acac})]$ and $[V^V O_2(\text{sal-his})]$ based on ^{51}V NMR spectroscopy are presented in Scheme 1.1.

Similarly, the reaction of $[\text{VO}(\text{acac})_2]$ with an equimolar amount of Hsal-aepy (Hsal-aepy = Schiff base derived from salicylaldehyde and 2-aminoethylpyridine in acetonitrile at room temperature yielded the oxidovanadium(IV) complex $[V^{IV} O(\text{sal-aepy})(\text{acac})]$ while $[V^V O_2(\text{sal-aepy})]$ was obtained by aerobic oxidation of $[V^{IV} O(\text{sal-aepy})(\text{acac})]$ in solvent in the presence of a small amount of H_2O_2 ; Scheme 1.2.[46].



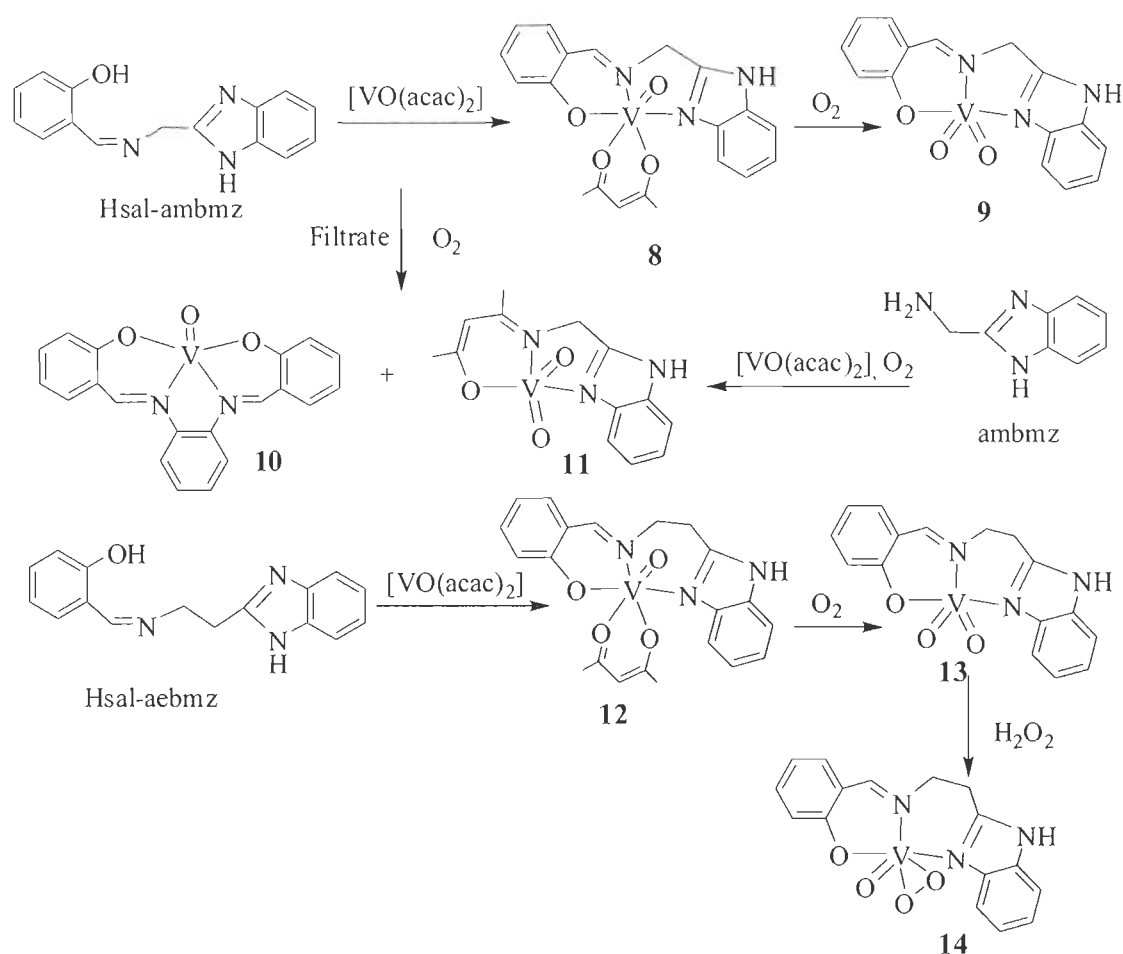
Scheme 1.1. Proposed reaction scheme (see text) and tentative assignments of the ^{51}V NMR chemical shifts involving oxidovanadium(V)-, dioxidovanadium(V)-, monoperoxovanadium(V)- and bisperoxovanadium(V)-species formed in methanolic solutions of $[\text{V}^{\text{IV}}\text{O}(\text{sal-his})(\text{acac})]$ and $[\text{V}^{\text{V}}\text{O}_2(\text{sal-his})]$ based on ^{51}V NMR spectroscopy, on addition of aqueous H_2O_2 and HCl . S indicates solvent.



In histidine derived dioxovanadium(V) complex $[\text{VO}_2(\text{hydrox-his})]$ ($\text{H}_2\text{hydrox-his}$ = Schiff base derived from 2-hydroxy-1-naphthaldehyde and histidine), nitrogen of the histidine moiety is not involved in coordination [47]. Oxovanadium(IV) and dioxovanadium(V) complexes having benzimidazole unit in the ligand system provide model for the coordination of histidine in the enzyme. [48] Other imidazole (or its derivatives) as well as benzimidazole containing complexes have also been reported where these are acting as a coligand [49 -56].

Reaction of $[\text{VO}(\text{acac})_2]$ and benzimidazole derived ligands Hsal-ambmz or Hsal-aebmz (Scheme 1.3) in dry, refluxing methanol gave the brown oxovanadium(IV) complexes $[\text{VO}(\text{acac})(\text{sal-ambmz})]$ or $[\text{VO}(\text{acac})(\text{sal-aebmz})]$, respectively. Aerial oxidation of 1 and 2 in methanol, yielded the dioxovanadium(V) complexes $[\text{VO}_2(\text{sal-ambmz})]$ and $[\text{VO}_2(\text{sal-aebmz})]$, respectively. Further, $[\text{VO}_2(\text{sal-ambmz})]$ and $[\text{VO}_2(\text{sal-aebmz})]$ were obtained from the reaction of the respective ligand with aeri ally oxidized solution of $[\text{VO}(\text{acac})_2]$ in methanol.

Exposing the filtrate obtained after separating $[\text{VO}(\text{acac})(\text{sal-ambmz})]$ to air, resulted in the formation of $[\text{VO}_2(\text{acac-ambmz})]$ and the known complex $[\text{VO}(\text{sal-phen})]$. Apparently, the formations of these complexes proceed through a complex reaction pattern as depicted in Scheme 1.3.[57]. The complex $[\text{VO}_2(\text{acac-aebmz})]$ can also be prepared directly by reacting $[\text{VO}(\text{acac})_2]$ with Haebmz followed by aerial oxidation.

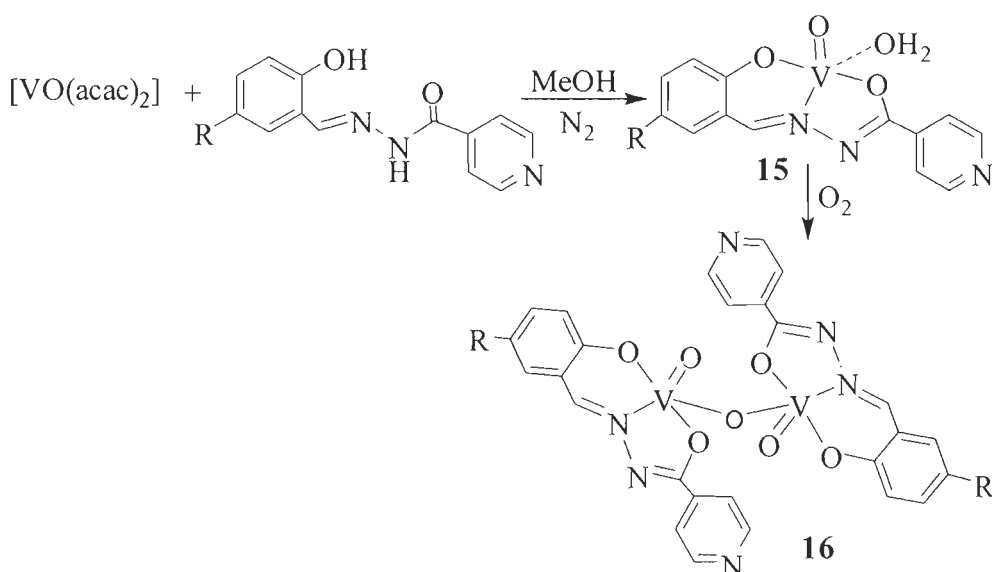


Scheme 1.3

Other type of ligands e.g. Schiff bases, amino acid derivatives, ligands having peptide moiety etc. have been frequently used to model active site of haloperoxidases, the details of such ligands and their complexes are presented in preceding sections.

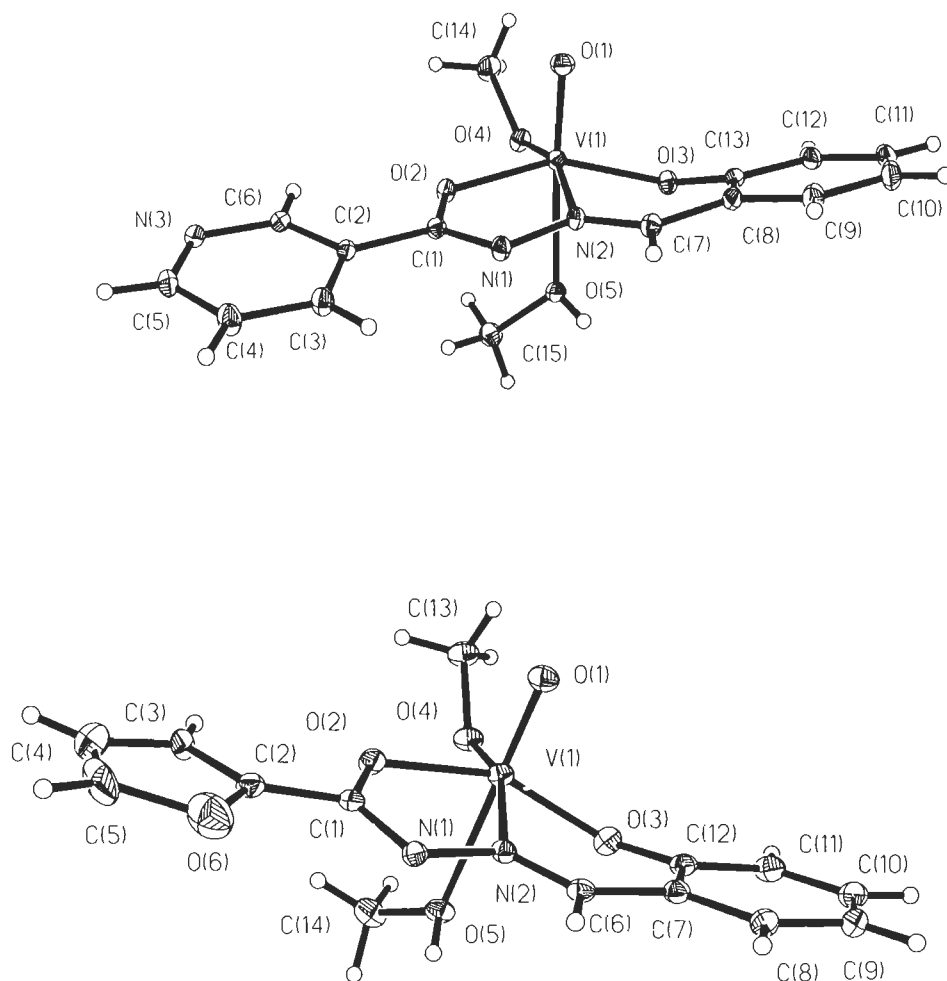
The dioxovanadium(V) complexes $[\text{K}(\text{H}_2\text{O})][\text{VO}_2(\text{sal-inh})]$ and $[\text{K}(\text{H}_2\text{O})][\text{VO}_2(\text{Cl-sal-inh})]$ (H_2L = Schiff base derived from salicylaldehyde or 5-chlorosalicylaldehyde and isonicotonylhydrazide) have been isolated by the reaction of potassium vanadate(V), prepared in situ by dissolving V_2O_5 in aqueous KOH, and potassium salt of ligands at pH ca. 7.5. The final pH of the reaction mixture plays an important role in that a decrease in pH (to ca. 6.5) causes the formation of oxo-bridged binuclear complexes $[\{\text{VO}(\text{sal-inh})\}_2\mu\text{-O}]$ and

$[\{\text{VO}(\text{Cl-sal-inh})\}_2\mu\text{-O}]$ along with the respective anionic species. Similarly, reaction of $\text{NH}_4[\text{VO}_3]$ and the sodium salt of $\text{H}_2\text{sal-inh}$ results in the formation of the corresponding ammonium salt $\text{NH}_4[\text{VO}_2(\text{sal-inh})(\text{H}_2\text{O})]$ and $[\{\text{VO}(\text{sal-inh})\}_2\mu\text{-O}]$. The binuclear complexes have also been synthesized by allowing equimolar amounts of $[\text{VO}(\text{acac})_2]$ and ligand to react in acetone, followed by aerial oxidation as shown in Scheme 1.4. Intermediate oxovanadium(IV) complexes $[\text{VO}(\text{sal-inh})(\text{H}_2\text{O})]$ and $[\text{VO}(\text{Cl-sal-inh})(\text{H}_2\text{O})]$ can also be isolated as a stable solid [58].



Scheme 1.4

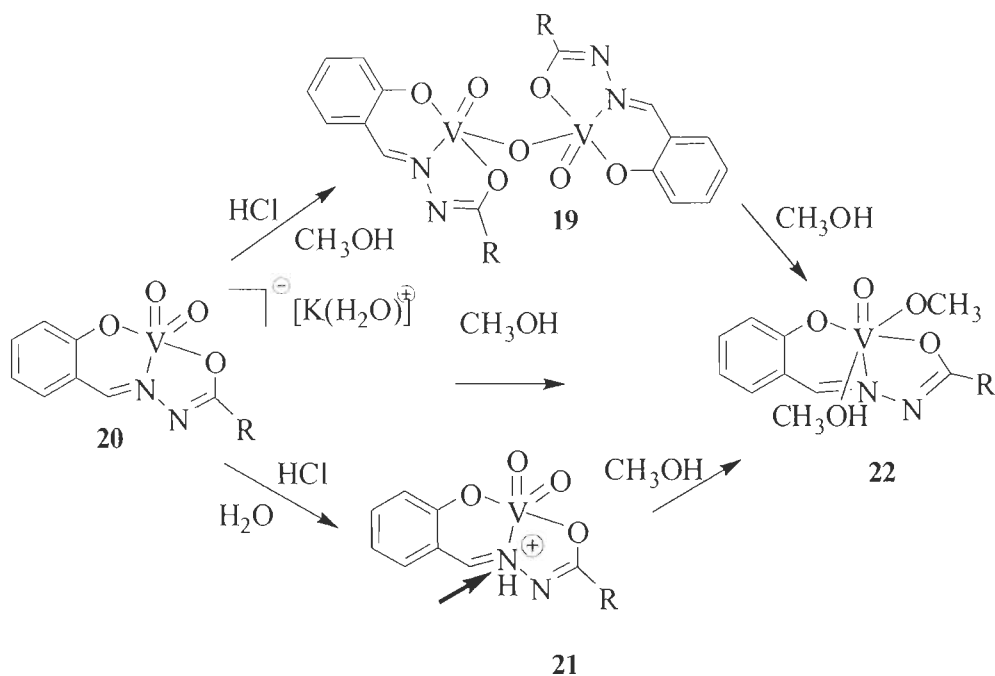
Neutral complexes $[\{\text{VO}(\text{sal-nah})\}_2\mu\text{-O}]$ and $[\{\text{VO}(\text{sal-fah})\}_2\mu\text{-O}]$ ($\text{H}_2\text{sal-nah}$ = Schiff base derived from salicylaldehyde and nicotonylhydrazide and $\text{H}_2\text{sal-fah}$ = Schiff base derived from salicylaldehyde and furoylhydrazide) isolated as described above are, though, stable in the solid state, they undergo deoxygenation process slowly in methanol to give $[\text{VO}(\text{OMe})(\text{MeOH})(\text{sal-nah})]$ and $[\text{VO}(\text{OMe})(\text{MeOH})(\text{sal-fah})]$, respectively. The molecular structure of these oxomethoxo complexes are presented in Figure 1.7 [59]. Reactivities of these complexes are presented in Scheme 1.5.



18

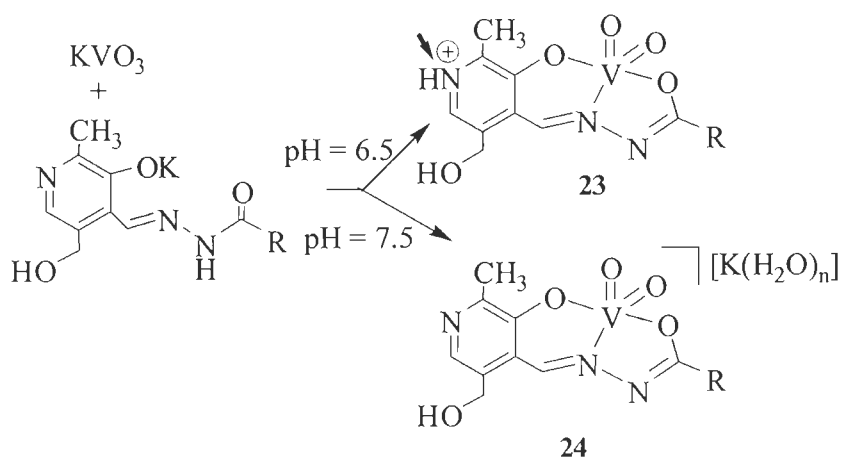
Figure 1.7. ORTEP plot (at 50 % probability level) of [VO(OMe)(MeOH)(sal-nah)] (above) and [VO(OMe)(MeOH)(sal-fah)] (bellow). Taken from [59].

Ghosh et al. [60 - 63] and Plass et al. [64] have also reported chemistry of mixed-ligand methoxy bonded oxidovanadium(V) and dioxovanadium(V) complexes with a family of hydrazone ligands.



Scheme 1.5. Reactivity patterns of complexes; R = various groups.

Anionic dioxovanadium(V) complexes $[K(H_2O)_3][VO_2(pydx-inh)]$, $[VO_2(Hpydx-inh)]$ $[K(H_2O)_2][VO_2(pydx-nah)]$ and $[K(H_2O)_2][VO_2(pydx-bhz)]$ presented in Scheme 1.6 presents good model of haloperoxidases. Here, final pH of the reaction mixture plays an important role [65].



R = 3-pyridyl, 4-pyridyl, ph; n = 2 or 3

Scheme 1.6

For the catalytic activity of vanadate-dependent haloperoxidases, the presence of a coordinated hydroxo ligand has been proposed on the basis of kinetic investigations. The generation of oxo-hydroxo species has been accomplished for $[\text{K}(\text{H}_2\text{O})_2][\text{VO}_2(\text{pydx-bhz})]$ on reaction with HCl ; Figure 1.8. Corresponding results have also been obtained with HClO_4 (dissolved in a minimum amount of methanol and added drop-wise to a methanolic solution of $[\text{K}(\text{H}_2\text{O})_2][\text{VO}_2(\text{pydx-bhz})]$).

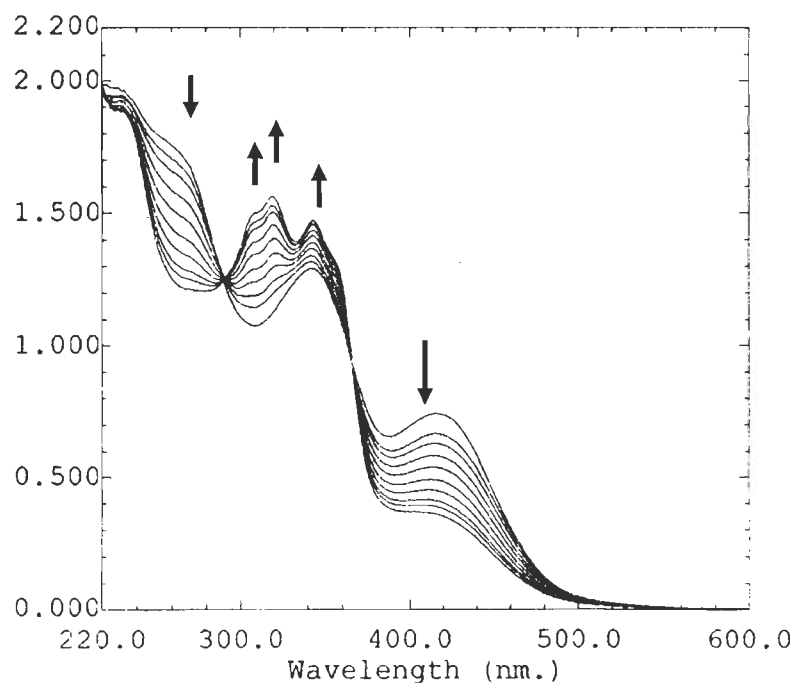


Figure 1.8. Titration of $[\text{K}(\text{H}_2\text{O})_2][\text{VO}_2(\text{pydx-bhz})]$ (**25**) with a saturated solution of HCl in MeOH ; the spectra were recorded after addition of 2 drops portions MeOH-HCl to 10 ml of $\text{ca. } 10^{-4} \text{ M}$ solution of complex in MeOH .

During turnover of haloperoxidases, a peroxovanadium(V) intermediate has been reported to form. The peroxo form of the enzyme from the fungus *Curvularia inaequalis* has been isolated and structurally characterized. In the peroxo form, the active site has η^2 -peroxo group. The peroxovanadium(V) complexes with biologically relevant ligands, therefore, represent a useful model for the haloperoxidases.

The dioxido complex $[\text{VO}_2(\text{sal-aebmz})]$ can be converted into the peroxido complex $[\text{VO}(\text{O}_2)(\text{sal-aebmz})]$ by treatment with H_2O_2 , and thus to an intermediate in the catalytic cycle representing the activity of VHPO. The formation of the peroxo complex has also been established in solution by the treatment of $[\text{VO}_2(\text{sal-aebmz})]$ with H_2O_2 and following the changes by electronic absorption spectroscopy, Figure 1.9 [57].

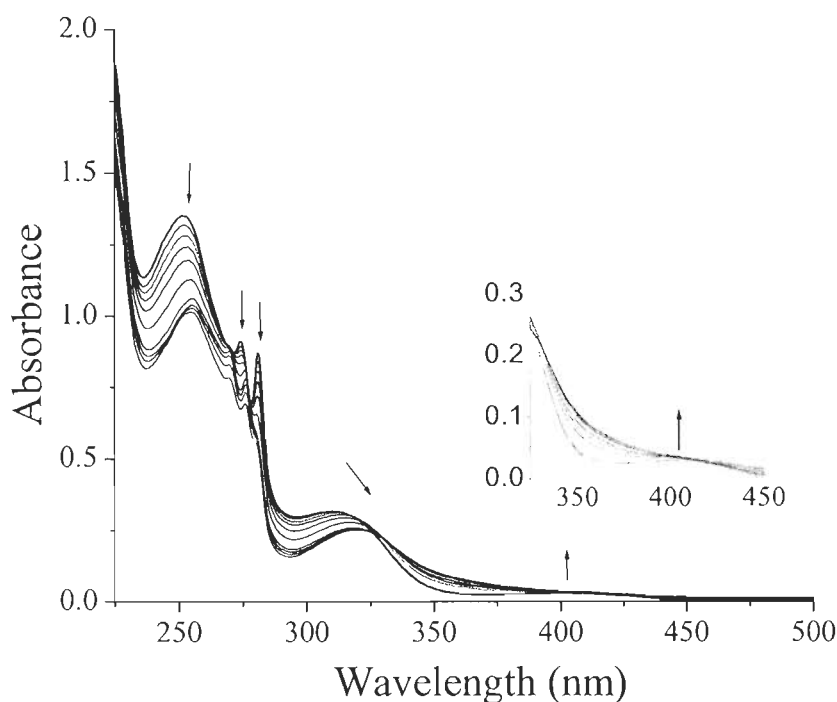


Figure 1.9. Titration of $[\text{VO}_2(\text{sal-aebmz})]$ (**26**) with 30% H_2O_2 in MeOH. The spectra were recorded after successive addition of 1-drop portions of H_2O_2 dissolved in MeOH to 10 mL of a ca. 1×10^{-4} M solution of $[\text{VO}_2(\text{sal-aebmz})]$.

Djordjevic et al. and others have isolated a whole range of oxoperoxovanadium(V) complexes with heteroligands e.g. nicotinic acid, nicotinic acid N-oxide, cystine, adenine, , adenosine, citric acid, malonic acid, tartaric acid, nitrilotriacetic acid, iminodiacetic acid, ethylenediaminetetraacetic acid, 2,2'-

dipyridyl, *o*-phenanthroline etc. The stability of these complexes towards decomposition in the solid state, mother liquid and pure water depends upon the heteroligand [66 - 74].

Tetradentate glycine-derived ligands, nitrilotriacetic acid (nta), aminodiacetic acid (ada), N-(carbamoylmethyl)iminodiacetic acid (H_2cmida) and N-(carbamoylethyl) iminodiacetic acid (H_2ceida) give oxoperoxovanadium(V) complexes in presence of H_2O_2 . The X-ray structure analyses of $Ba[VO(O_2)(nta)] \cdot 3H_2O$ and $K[VO(O_2)(ceida)] \cdot 2H_2O$ (**27**) reveal a mononuclear structure of the complex anions with a typical pentagonal bipyramidal arrangement around vanadium [75, 76]. A glycyglycine complex of monoperoxovanadate, $[NEt_4][VO(O_2)_2(glygly)] \cdot 1.58 H_2O$ (where Hglygly = glycyglycine) has been isolated by reacting glycyglycine with vanadate in presence of H_2O_2 . Complex $[NEt_4][VO(O_2)_2(glygly)] \cdot 1.58 H_2O$ has pentagonal bipyramidal structure where axial positions are occupied by the oxo ligand and by one oxygen of the peroxo group of the adjacent anion (**28** of Fig. 1.10). The equatorial positions are occupied by the peroxo group and the tridentate ligand [77]. Monoperoxo complexes, $M_2[VO(O_2)(acmaa)(H_2O)]$ (where $M = K^+$ and NH_4^+) and $M_2[VO(O_2)(Hacmaa)(H_2O)]$ (where $M = K^+$, Cs^+ and NBu_4^+ , $H_3acmaa = R,S$ -N-(carboxymethyl)aspartic acid) exist in two isomeric forms *exo* and *endo* with their ^{51}V NMR chemical shift at ca. -590 and -600 ppm, respectively. While *endo*-form partially decomposes with pH variations, it has no influence on the chemical shifts of the diastereomers [78].

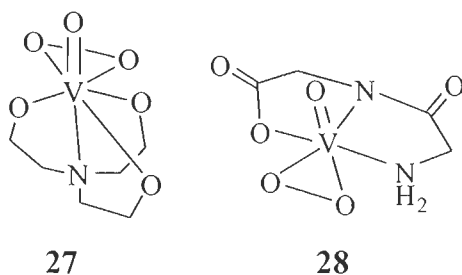


Figure 1.10. Examples of model peroxo complexes.

Formation of peroxovanadate(V) adducts with hetero ligands in presence of H_2O_2 has also been studied in solution using various techniques [79]. Reactivity of dioxovanadium(V) complexes e.g. $[\text{VO}_2(\text{bpg})]$, $[\text{VO}_2(\text{pmida})]^-$, $[\text{VO}_2(\text{ada})]^-$ with H_2O_2 in solution to give oxoperoxovanadium(V) species has been monitored spectroscopically and various kinetic parameters obtained [80]. Reaction between KVO_3 and N-(2-pyridylmethyl)-6-amino)iminodiacetic acid (H_2pmida) in presence of H_2O_2 gave $\text{K}[\text{VO}(\text{O}_2)(\text{pmida})]$. In presence of H_2O_2 and Br, bromination of pyridine ring occurred in complex $\text{K}[\text{VO}(\text{O}_2)(\text{pmida})]$. Both the complexes are structurally characterized bromoperoxidase model that show significant intra-molecular hydrogen bonding between a pendant amine functionality and peroxo oxygen [81]. H_2VO_4^- , in presence of H_2O_2 forms several mononuclear species with L- α -alanyl-L-histidine (ah) in aqueous solution. The peroxo species $[\text{VO}(\text{O}_2)_2(\text{ah})]^-$ is quite stable and exhibits coordination through the imidazole residue and thus exhibits a good model for the peroxo form of chloroperoxidase [82]. Guevara-Garcia *et al.* have reviewed bis-peroxovanadium(V) complexes of peptides having histidine group [83].

Complexes have also been designed that model parts of the structure of the V-Fe cofactor. The coordination atom is S in place of N and/or O coordination. Dioxovanadium(V) complexes (**29**, **30**, **31**, **32**, **34** of Figure 1.11) having O, N, and S atoms have been prepared and structurally characterized in order to model in order to model nitrogenases [84 - 89].

Complexes having the general formula $[\text{VO}(\text{OMe})(\text{tbhsR})]$ (H_2tbhsR = Schiff bases derived from thiobenzhydrazide and 5-substituted salicylaldehydes; R = H, OMe, Cl, Br and NO_2) have been prepared by the reaction of $[\text{VO}(\text{acac})_2]$ with H_2tbhsR in methanol. The complex where R= NO_2 , crystallizes as a hexacoordinated species due to coordination of a methanol O-atom at the vacant sixth site. The bond parameters associated with the metal ions and the physical properties of the complexes are consistent with the +5 oxidation state of the metal ion in all the complexes [90].

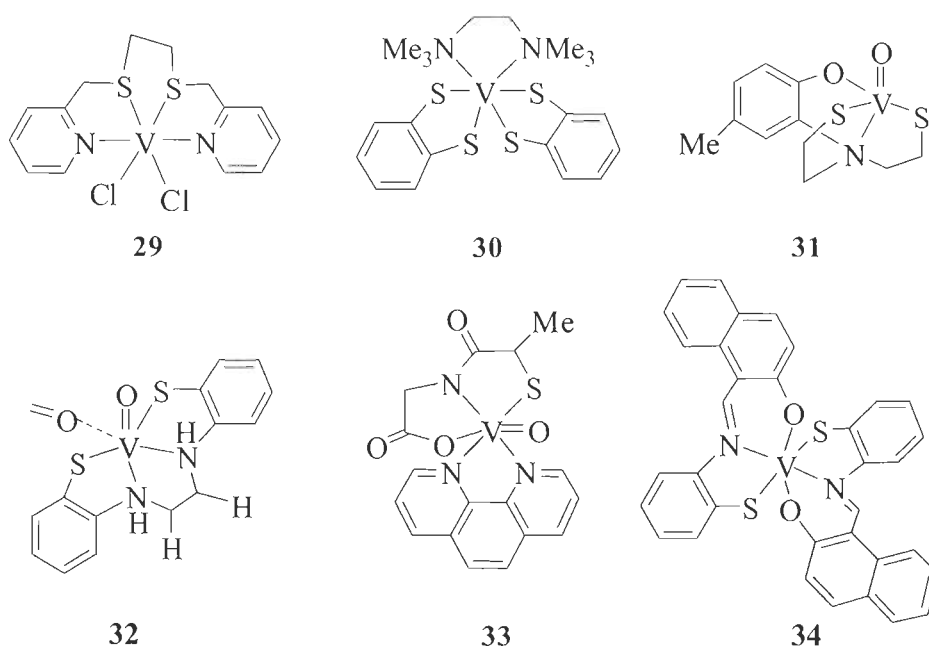


Figure 1.11. Structural models of vanadium-nitrogenase.

The tetragonal-pyramidal oxovanadium(IV) complexes $[\text{VO}\{(\text{RSC}=\text{S})=\text{N}-\text{N}=\text{X}\}_2]$ were synthesized by the reactions of $\text{VO}(\text{OCHMe}_2)_3$ with the dithiocarbazate ligands $\text{RSC}(=\text{S})-\text{NH}-\text{N}=\text{X}$, where X = cyclopentyl, cyclohexyl or $4\text{-Me}_2\text{N}-\text{C}_6\text{H}_4-\text{CH}_3$, and $\text{R} = \text{CH}_3$ or $\text{CH}_2\text{C}_6\text{H}_5$. These complexes present good models for the interaction of VO^{2+} with thiofunctional ligands [91].

Complex $[\text{V}^{\text{IV}}(\text{HIDPA})_2]^{2-}$ ($\text{HIDPA} = 2,2'$ -(hydroxyimino)dipropionate) is known as amavadin, a vanadium-containing natural product present in the *Amanita muscaria* mushroom and is responsible for vanadium accumulation in nature. Two non-oxo eight coordinate distorted dodecahedral model vanadium complexes, $[\text{PPh}_4][\text{V}^{\text{V}}(\text{HIDPA})_2]$ and $[\text{PPh}_4][\text{V}^{\text{V}}(\text{HIDA})_2]$ ($\text{HIDA} = 2,2'$ -(hydroxyimino)diacetate) have been prepared and investigated by solid-state ^{51}V NMR spectroscopy and DFT calculations. Both complexes were isolated by oxidizing their reduced forms: $[\text{V}^{\text{IV}}(\text{HIDPA})_2]^{2-}$ and $[\text{V}^{\text{IV}}(\text{HIDA})_2]^{2-}$. The quadrupolar coupling constants, C_Q , are found to be moderate, 5.0–6.4 MHz while the chemical shift anisotropies are relatively small for vanadium complexes, -420

and -360 ppm. The isotropic chemical shifts in the solid state are -220 and -228 ppm for the two compounds [92].

The tetradentate ONNO Schiff base ligands benzildihydrazone of 2-aminobenzoylhydrazine, benzildihydrazone of 2-hydroxybenzoylhydrazine, benzildihydrazone of benzoylhydrazine, pentane-2,3-dihydrazone of 2-aminobenzoylhydrazine, pentane-2,3-dihydrazone of 2-hydroxybenzoylhydrazine, and pentane-2,3-dihydrazone of benzoylhydrazine have been used to prepare non-amavadine model octacoordinated vanadium(IV) complexes from various oxovanadium(IV/V) compounds. These ligands have special affinity for the non-oxo V^{IV} center manifested in the facile synthesis of VL_2 -type complexes [93].

1.4. Vanadium in biology

Many essential/ trace elements play an important role in a number of biological processes by activating or inhibiting enzymatic reactions, by competing the permeability of cell membranes, maintaining genomic stability and/or by other mechanisms [94].

The role of vanadium in biochemistry has attracted attention for the last three decades. It could be used as inhibitor for nucleases and phosphatases [95]. Cantley and coworkers revealed a potent inhibitor of $Na^+/K^+ - ATPase$, widely used to study the mechanism of the sodium-potassium pump [96, 97]. This pump is necessary for proper transport of materials across cell membranes to maintain ionic equilibrium.

Vanadium(V) ($H_2VO_4^-$) enters into cells probably through the phosphate transport mechanism and reduced to vanadium(IV) through one-electron reduction in the gastrointestinal tract. VO^{2+} undergoes auto oxidation to vanadate in the presence of oxygen, whereas glutathione, ascorbate, cysteine and similar reducing agents can reduce vanadate. Thus, endogenous reducing agents and dissolved oxygen ensure that both vanadium(V) and vanadium(IV) species are present in serum. Vanadium has been found in its +IV oxidation state in mammalian lung

and heart tissues [98] whereas +V oxidation state is common in kidney, liver and erythrocytes. It has also been suggested that extra cellular vanadium exists primarily as vanadium(V) and exclusively vanadium(IV) inside the cells [99]. The processes of interactions between vanadium species and serum albumin are still a challenge for scientists. However, the deposition of the vanadium in different tissue, obtained from *in vitro* experiments performed in different laboratories on several animals, follows the order: bone > kidney > liver > spleen > intestine \approx stomach, blood, muscle, testes, lungs and brain. The excretion of the small fraction of ingested and not retained vanadium occurs mainly through urine, as low molecular weight VO_2^+ complexes. Biliar excretion seems to be a secondary route [100 - 103].

1.5. Vanadium complexes of biomolecules and their speciation in biofluids

Blood serum consists of various components which are classified as high molecular mass (hmm) and low molecular mass (lmm) components. The chemical compositions of these components are presented in Table 1.1.

Mainly oxovanadium(IV) (VO^{2+}) and vanadate(V) (H_2VO_4^-) are the most common species present under physiological conditions. Thus, the binding ability of vanadium(IV) with lmm components of the blood serum such as oxalate, lactate, citrate, and phosphate have been studied in detail. Oxalate, citrate and lactate form stable oxovanadium(IV) complexes at lower pH while at higher pH, where hydroxide ion dominates, formation of different species with various compositions occurs. Inorganic monophosphate binds oxovanadium(IV) weakly in the acidic pH range followed by precipitation in the 4.0 to 8.5 pH range. Dioxovanadium(V) complex, $\text{Cs}_2[\{\text{VO}_2(\text{lact})\}_2] \cdot 2\text{H}_2\text{O}$ [lact = lactate(2-)] has also been isolated and structurally characterized [104]. Binding capacity of other higher phosphonic acids with oxovanadium(IV) has also been studied [105]. The transferrin and albumin both binds with oxovanadium(IV) strongly. In fact, transferrin binds with

oxovanadium(IV) about six times more than albumin in vitro [106].

Table 1.1. Total concentrations of components in computer model of serum^a

Components	Concentration
High molecular mass (hmm)	
Albumin	630 μM
Transferrin	37.0 μM
Low molecular mass (lmm)	
Histidine	77.0 μM
Lactate	1.51 mM
Oxalate	9.20 μM
Phosphate	1.10 mM
Citrate	99.0 μM
Carbonate	24.9 mM
Cistine	10.9 μM
Cysteine	33.0 μM
Glycine	2.30 μM
Glutamate	60.0 μM
Sulfate	330 μM
H ⁺ (free ion)	39.8 nM
OH ⁻ (free ion)	417 nM
Al ³⁺	3.0 mM
Ca ²⁺ (free)	1.37 mM
Mg ²⁺ (free)	580 μM
Zn ²⁺	10.0 μM

a) W.R. Harris, *J. Clin. Chem.*, 1992, **39**, 1809.

Interaction of oxovanadium(IV) with other biomolecules and knowledge of various species form in the solid as well as in solution is important to understand the vanadium biochemistry. Interaction of biomolecules such as l-ascorbic acid (Vitamin C), carboxylic acids, amino acids and peptides (di- and tripeptides), nucleotides (ribonucleases and ATPases), carbohydrates, cysteine and derivatives etc. with vanadium(IV) have been studied in detail [107]. Interaction of

oxovanadium(IV) ion with oxidized glutathione in aqueous solution has been studied in the pH range 2 to 11 by a combination of pH potentiometry and spectroscopy and plausible structures for each species have been provided [108].

The formation of insulin mimetic complexes such as $[\text{VO}(\text{maltolate})_2]$, $[\text{VO}(\text{picolinate})_2]$, $[\text{VO}(6\text{-methylpicolinate})_2]$ has been studied in various pH ranges. The neutral bis complex $[\text{VO}(\text{maltolate})_2]$ dominates in the 5 – 7.5 pH range while $[\text{VO}(\text{picolinate})_2]$ in the 2 – 7 pH range. Complex $[\text{VO}(6\text{-methylpicolinate})_2]$ exists in the pH range 4–6. The formation of parent complexes, $[\text{VO}(\text{maltolate})]^{+}$ and $[\text{VO}(\text{maltolate})_2]$ are only slightly affected by the presence of low molecular mass component phosphate and dominate above pH 4. In the pH range 2 – 4, the formation of ternary complexes occurs but never become dominant. However, such ternary complexes are favored with picolinic acid and 6-methyl picolinic acid [109]. Similarly, formation and stability of $[\text{VO}(\text{picolinate})_2]$, $[\text{VO}(6\text{-methylpicolinate})_2]$ complexes are affected in the presence of low molecular mass components like oxalic acid, citric acid and lactic acid at physiological pH [110]. Speciation of these complexes in presence of human transferrin has also been studied [111].

1.6. Vanadium compounds in medicine

In early 1900s vanadium compounds were used for treating tuberculosis, anaemia and diabetes and were present in antiseptics or tonics. Medicinal aspects of vanadium compounds were increased with the discovery of insulin-mimetic property of vanadium ions in 1979 [112] / 1980 [113, 114], though orally administered sodium vanadate was reported to improve diabetes mellitus (DM) in human diabetes in 1899 [115]. Diabetes mellitus (DM) is a chronic metabolic disease that occurs when the body is not able to use sugar for growth and energy for daily activities. There are two main types of diabetes mellitus: insulin-dependent (Type I) and insulin independent (Type II). Insulin-dependent diabetes

mellitus (IDDM) results in hyperglycemia owing to the deficiency of insulin, causing many serious secondary complications. Insulin, secreted by pancreas, influences the glucose and the fatty acid metabolism by stimulating the uptake of glucose by the liver and splanchnic as well as peripheral tissues (adipose and muscle) from the blood stream for further storage and utilization. Insulin also influences the action of other hormones which are responsible for the breakdown of glycogen into glucose, lipids into fatty acids and proteins into amino acids. In Type II, though pancreas continues to produce insulin, the diabetic patients remain hyperglycemic as liver and peripheral tissues fail to respond efficiently to insulin. About 90 % of the diabetic patients belong to Type II category [116]. Vanadium(IV) and vanadium(V) salts have been extensively tested both in vivo and in vitro in a considerable variety of experimental models of diabetes [117]. In vitro studies demonstrated that streptozotocin (STZ)-induced diabetic animals partially or completely restored liver and muscle enzyme activities involved in glycolysis, lipolysis and glycogenesis by giving vanadium(V) orally [118 -121]. Oral treatment with vanadate ion also improves insulin sensitivity in skeletal muscle of type –II diabetic patients, reduces fasting plasma glucose concentration and suppresses hepatic glucose production [122 - 124]

Bis(maltolato)oxovanadium(IV) (BMOV) is the first most widely tested complex among many proposed insulin mimetic vanadium complexes [125 -129]. Its interaction with human serum albumin (HSA) is possibly responsible for the efficacy of the drug [130]. Peters *et al.* have suggested the generation of VO_4 from BMOV in ‘physiologic’ solutions and uncomplexed vanadium is the active component [131]. The closely related analogue bis(ethylmaltolato)oxovanadium(IV) (BEOV) has completed phase I clinical trials for the treatment of type II diabetes mellitus and study suggests that there were no adverse health effects in any of the (nondiabetic) volunteers [132].

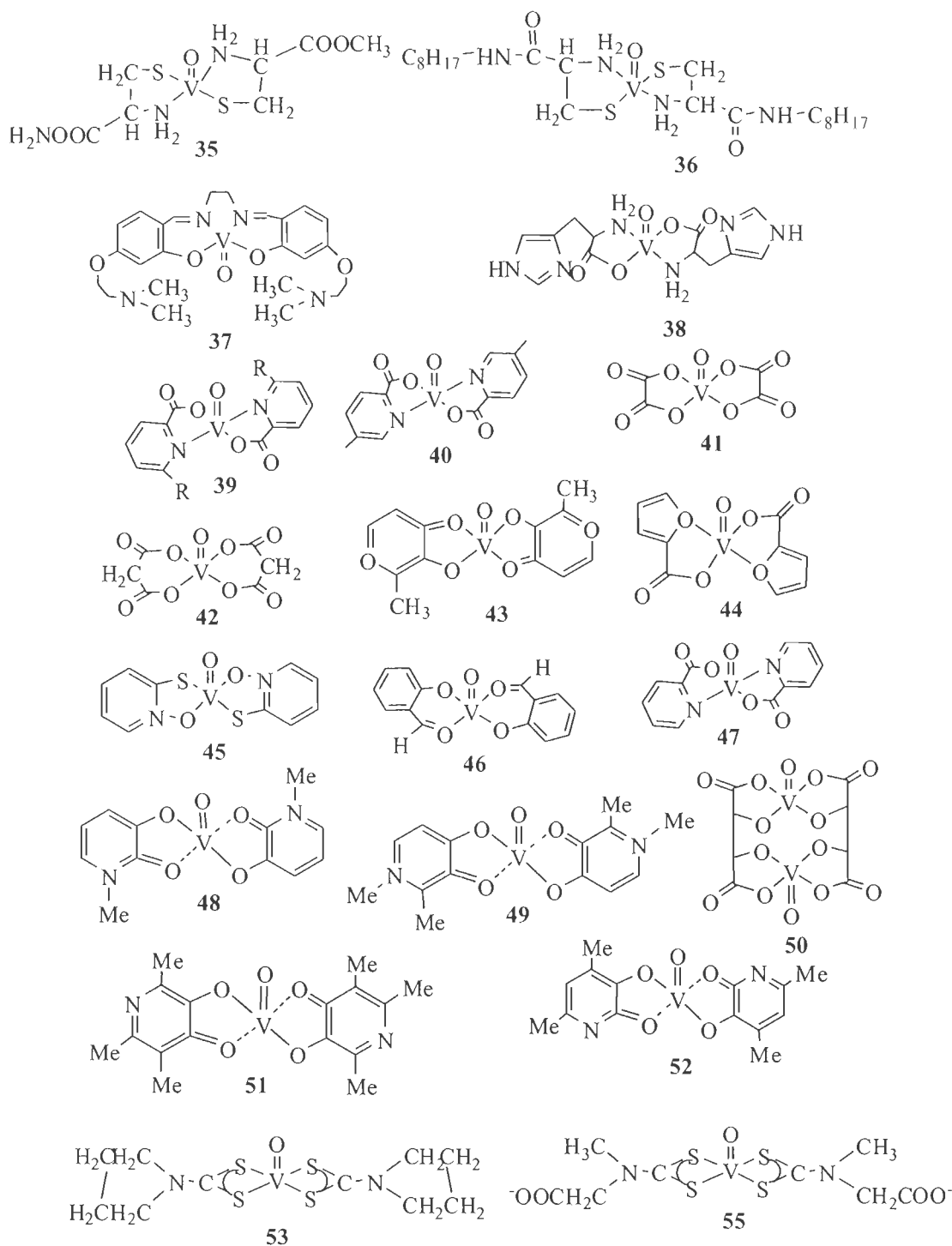


Figure 1.12. Structure of complexes studied for insulin-mimetic activity.

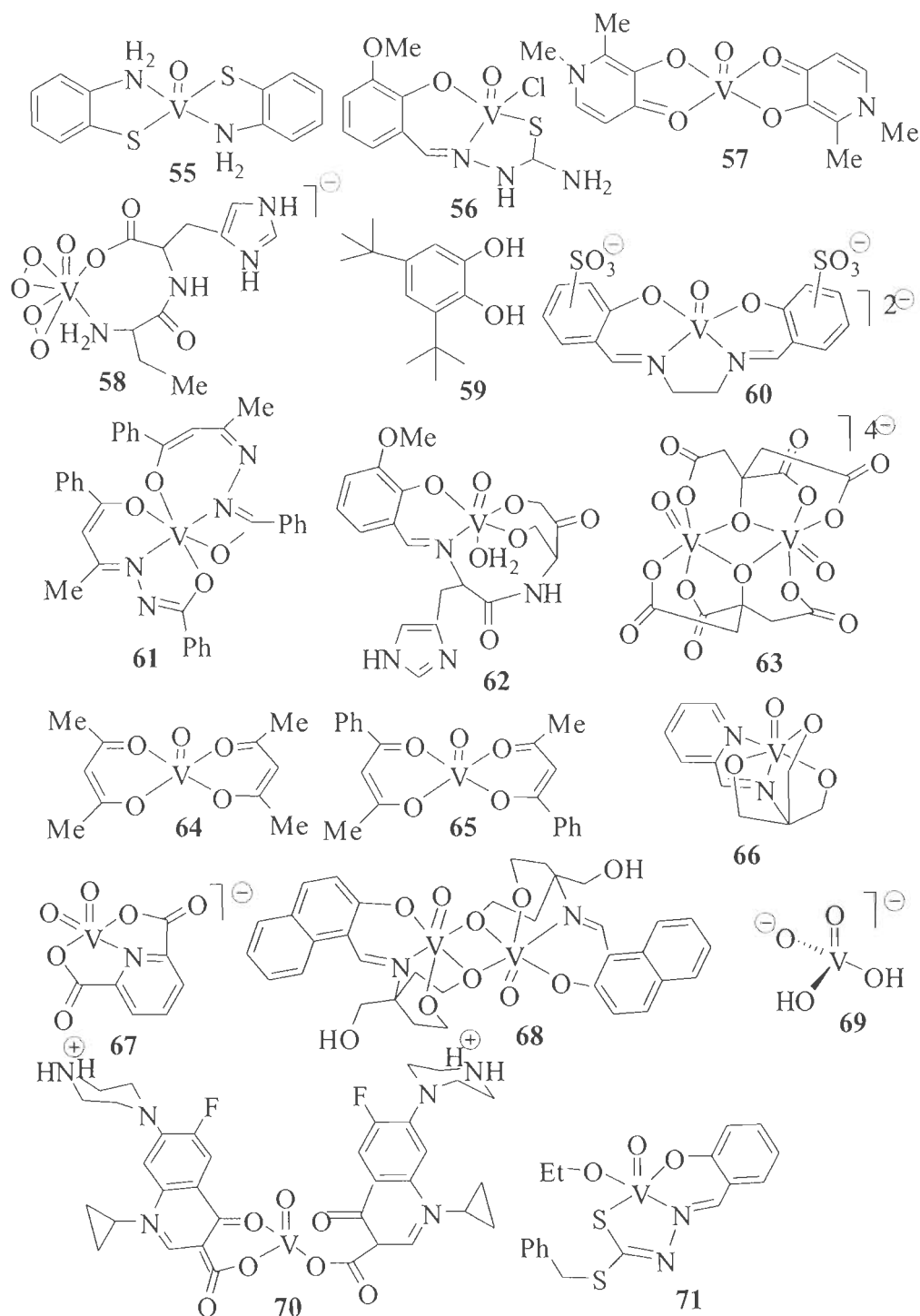


Figure 1.13. Structure of complexes studied for insulin-mimetic activity by

Rehder *et al.* [139].

Oxidation state of metal ion, interaction of complexes with human serum albumin (HSA) [133] and design of ligands have been indicated to play important role in modifying the biological effects of metal based drugs [134]. While studying the activity, it has also been found that (i) vanadium complexes must cross the biological membranes, (ii) most vanadium in normal rats treated with vanadate exist in vanadyl form and (iii) vanadyl ion is less toxic to rats than the vanadate [135]. Thus, several types of neutral and low molecular weight vanadium(IV) complexes with organic ligands have been designed and investigated in animal model systems for the treatment of diabetes. Figure 1.12 lists some of these complexes while review articles provide details of these complexes used in the study [136 -138] Rehder *et al.* have screened toxicity and insulin mimetic activity of a whole range of oxovanadium(IV), oxovanadium(V) and oxoperoxovanadium(V) complexes presented in Figure 1.13 along with some of the complexes presented in Figure 1.12 [139]. Vanadium-picolinate complexes also exhibit the insulin-enhancing properties. [140] The activity is further enhanced on taking halogen substituted picoline. [141]

Simple peroxo compounds have also been screened for their insulin-mimetic action [142, 143]. It was observed that the mixture of H_2O_2 and vanadate or vanadium(V) oxide were more potent in controlling the blood glucose level in rats than either vanadate or H_2O_2 alone. [144] Insulin-mimetic properties of peroxovanadium(V) compounds with nucleic bases such as uracil and cytosine have also been reported in the literature [145].

McLauchlan *et al.* have prepared a series of V(III), V(IV) and V(V) complexes with bidentate ligands, anthranilic acid and imidazole-4-carboxylic acid. A phosphatase inhibition assay using *p*-nitrophenylphosphate (pNPP) as a substrate has been used to study the inhibition kinetics of these vanadium complexes and they have shown to directly decrease the activity of three different

phosphatases (acid, alkaline, and tyrosine (PTP1B) phosphatase). However, the degree of inhibition of each enzyme varied and was a function of the complex added [146].

Vanadium complexes have also shown positive results towards antitumor activity. Peroxovanadates(V) with or without organic ligands exhibit antitumor activity. A special nature of electron transfer within the peroxovanadium(V) moiety was proposed to be responsible for this phenomenon. The active role of hetero ligand in modifying the antitumor and toxicity of peroxovanadium(V) has also been indicated. A set of 14 oxoperovanadium(V) complexes of the types $(\text{NH}_4)_4[\text{O}\{\text{VO}(\text{O}_2)_2\}_2]$, $\text{M}_3[\text{VO}(\text{O}_2)_2(\text{C}_2\text{O}_4)]$ and $\text{M}[\text{VO}(\text{O}_2)\text{L}]$ (L = malate, citrate, iminodiacetate, nitrilotriacetate and ethylenedianinetetraacetate) were tested for toxicity and antitumor activity against L1210 murine leukemia to examine the biological properties and about 25 % increase in life span was observed with some of these complexes [147]. Dioxovanadium(V) complexes, $[\text{VO}_2(\text{X-sal-tsc})]$ (where $\text{H}_2\text{X-sal-tsc}$ = Schiff base derived from salicylaldehyde, 5-bromosalicylaldehyde, 2-hydroxy-1-naphthaldehyde and semicarbazide, N^4 -n-butylsemicarbazide and N^4 -(2-naphthyl)semicarbazide) exhibit selective cytotoxicity on TK-10 human tumor cell lines. A significant effect on the antitumor activity of the vanadium complexes by structural modifications on the semicarbazone moiety has been indicated [148]. $[\text{VO}(\text{acac})(\text{aptsc})]$, $[\text{VO}(\text{acac})(\text{apmtsc})]$ and $[\text{VO}(\text{acac})(\text{apptsc})]$ (acac = acetylacetonate; Haptsc = 2-acetylpyridinethiosemicarbazone; Hapmtsc = 2-acetylpyridine-N(4)-methyl-thiosemicarbazone and Happtsc = 2-acetylpyridine-N(4)-phenyl-thiosemicarbazone) and their corresponding cis-dioxovanadium(V) complexes $[\text{VO}_2(\text{aptsc})]$, $[\text{VO}_2(\text{apmtsc})]$ and $[\text{VO}_2(\text{apptsc})]$ show comparable or larger anti-mycobacterium tuberculosis activities than the free thiosemicarbazone ligands, with MIC values within 62.5–1.56 (lg/mL) [149].

Vanadium complexes have also shown encouraging results on the in vitro antiamebic activity. Amoebiasis, a world-wide disease due to protozoan parasite *Entamoeba histolytica*, affects millions of individuals in developing countries.

Metronidazole [MNZ, 1-(2-hydroxyethyl)-2-methyl-5-nitroimidazole] is the most effective antiamoebic medication [150]. This, however, induces certain tumors in rodents and is mutagenic towards bacteria [151]. In vitro tests of the antiamoebic activity of dioxovanadium(V) complexes $[K(H_2O)_n[VO_2(X\text{-sal-sbdt})]]$ ($n = 2$ or 3 , $H_2X\text{-sal-sbdt} =$ Schiff base derived from salicylaldehyde and S-benzylthiocarbazate, $X = H, 5\text{-Cl}, 5\text{-Br}$) against *Entamoeba histolytica*, show comparable (when $X = H$ and 5-Cl) or substantially better (when $X = 5\text{-Br}$) amoebocidal action than metronidazole [152]. Similarly anionic and neutral complexes **41**, **42**, **43** and **44** (Fig. 1.14) have been found to be more effective than metronidazole [153, 154].

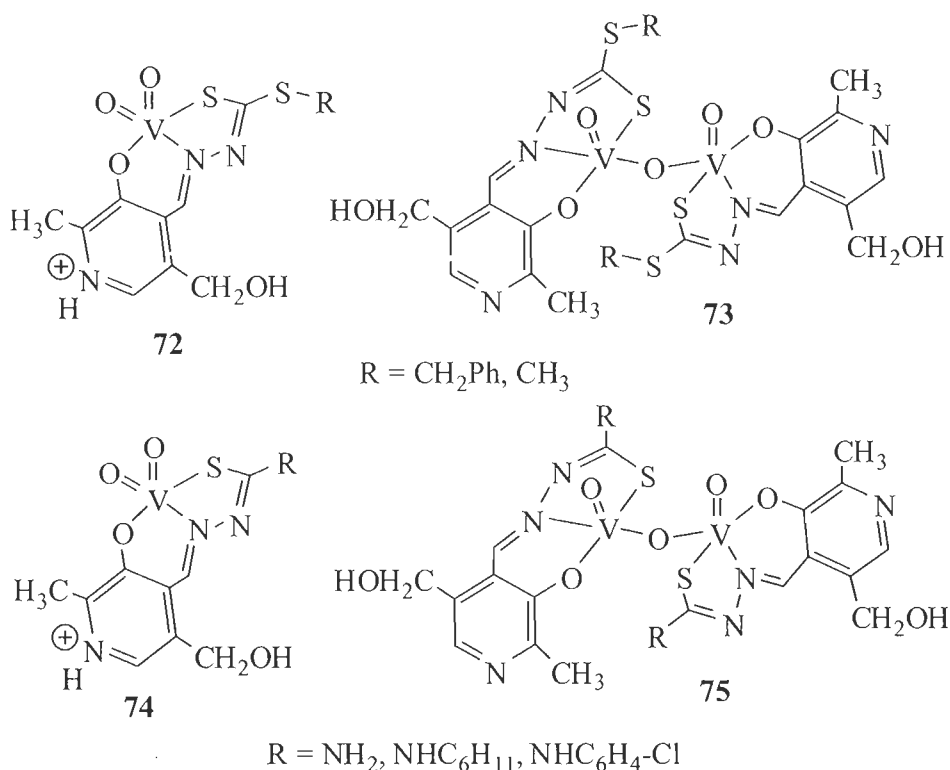


Figure 1.14. Complexes tested for antiamoebic activity.

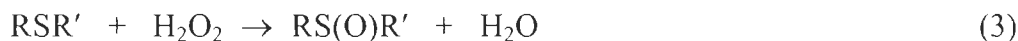
1.7. Functional model of haloperoxidases

Haloperoxidases catalyse the oxidation, by peroxide, of halides to

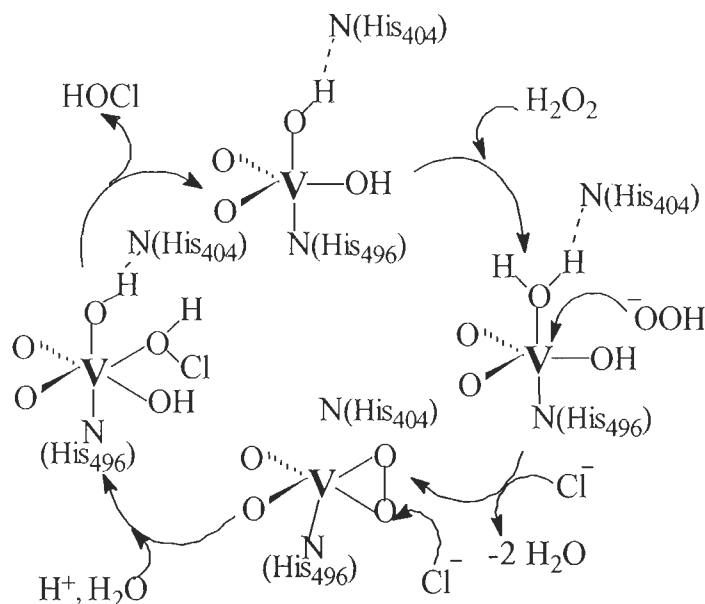
hypohalous acid followed by non-enzymatically halogenation of hydrocarbon.



also oxidise (prochiral)sulfide to (chiral) sulfoxide



An organic substance 2-chloro-5,5-dimethyl-1,3-cyclohexane dione (mcd) has been used as the standard substrate for the determination of haloperoxidases activity using H_2O_2 as the oxidant [155]. Figure 1.15 presents the widely accepted mechanism after carrying out many spectroscopic studies.



76

Figure 1.15. Proposed catalytic reaction mechanism of V-ClPO.

Oxo- and dioxovanadium(V) complexes of multidentate ligands (47-58) that presented the active functional models for bromoperoxidases are presented in Figure 1.16. Efforts were made to get a better understanding of the working mechanism of the vanadium haloperoxidase enzymes and to determine the role of

vanadium [156 -158].

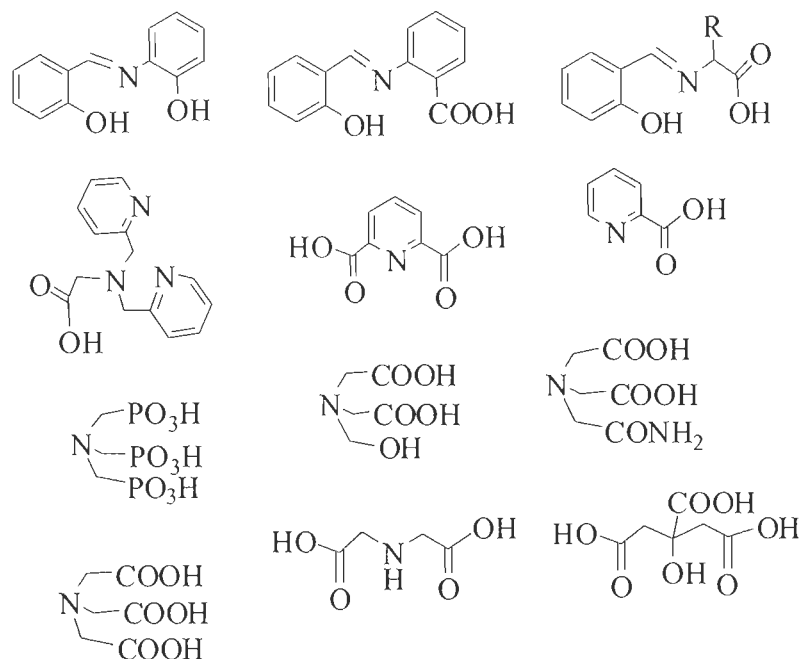


Figure 1.16. Structures of ligands that are used to design functional models of haloperoxidases.

The first functional mimic of bromoperoxidase to catalyse the bromination of 1,3,5-trimethoxybenzene (TMB) was reported by Butler *et al.* [156] using cis-dioxovanadium(V) complex in acidic aqueous solution. The brominated product 2-bromo-1,3,5-trimethoxybenzene was obtained when the reaction was catalysed by [VO(OMe)(MeOH)(sal-oap)] using H₂O₂ as oxidant. Complexes [VO(hybeb)]²⁻ and [VO(hybeb)]⁻ (H₂hybeb = 1,2-bis(2-hydroxybenzylamido)benzene) have also shown catalytic activity for the bromination of 1,3,5-trimethoxybenzene to some extent [157].

Oxidative bromination of salicylaldehyde to 5-bromosalicylaldehyde and 3,5-dibromosalicylaldehyde catalysed by polymeric oxovanadium(IV) complexes (**59** of Figure 1.17) [159].

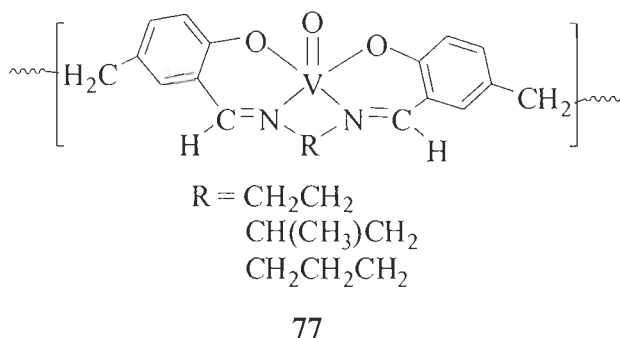


Figure 1.17. Complex used for functional model study.

These polymeric coordination complexes (Fig. 1.9) have also been used to catalyze the oxidation of phenol using H_2O_2 as an oxidant. Under the optimized reaction conditions, the selectivity of catechol was found to be 90 – 98 %. Similar complexes (Figure 1.18) were able to catalyze oxidation of styrene, cyclohexene and *trans*-stilbene using TBHP as an oxidant [160].

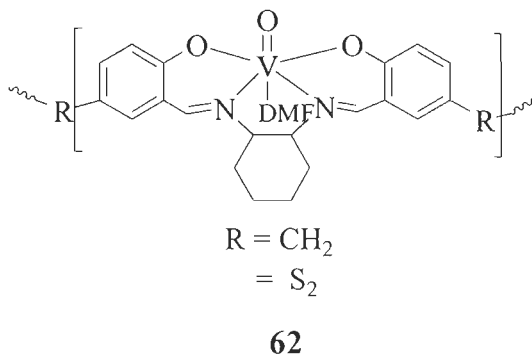


Figure 1.18. Polymeric complexes having catalytic potential.

Homogeneous oxovanadium(IV) catalysts **79** (Figure 1.19) have been reported by Rayati et. al.[161]. Catalytic potential of these complexes was tested for the oxidation of cyclooctene and styrene using tertbutylhydroperoxide (TBHP) as oxidant. The effects of molar ratio of oxidant to substrate, temperature and solvent have been studied. Excellent selectivity of epoxidation for cyclooctene and good selectivity for styrene were obtained. The mechanism of oxidation has also been discussed. Oxovanadium complex, $[\text{VO}(3,5\text{-}^t\text{Bu}_2\text{-salophen})]$ ($\text{H}_2[3,5\text{-}^t\text{Bu}_2\text{-}$

salophen] = Schiff base derived from 3,5-di-tert-butylsalicylaldehyde and *o*-phenylenediamine) has also been reported. This complex should exhibit a good catalytic activity but only characterization of the complex has been reported [162]. The chiral V^{IV}-salen and V^{IV}-salan (H₂salan = reduced form of chiral H₂salen type ligands) have been tested as catalysts in the oxidation of styrene, cyclohexene, cumene, and methyl phenyl sulfide with H₂O₂ and *t*-BuOOH as oxidants. Overall, the V-salan complexes show higher activity and normally better selectivity in alkene oxidation and higher activity and enantioselectivity for sulfoxidation than their parent V-salen complexes, therefore being an advantageous alternative ligand system for oxidation catalysis. The better performance of V-salan complexes probably results from their significantly higher hydrolytic stability [163].

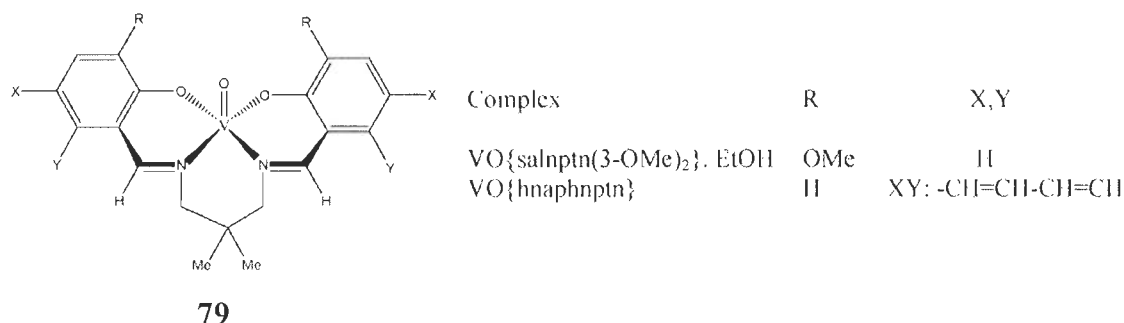


Figure 1.19. Homogeneous oxovanadium(IV) catalysts.

The (S,S)- and (R,R)-dioxovanadium(V) complexes bearing the methoxy substituent in positions 3 or 5 of the salicylidene moiety (Figure 1.20) also catalyze the oxidation of phenyl methyl sulfide by cumene hydroperoxide to the corresponding sulfoxide almost quantitatively [164, 165].

This oxidation reaction was also catalysed by oxovanadium(V) complexes of Schiff bases derived from 6-phenylsalicylaldehyde or 6-(2-hydroxyphenyl)salicylaldehyde and different amines using H₂O₂ as an oxidant. Conversion was quantitative and formation of sulfones was only small. [166].

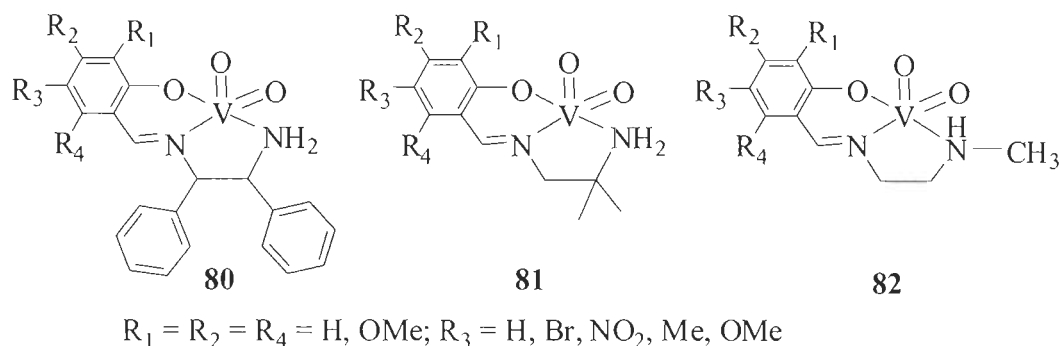


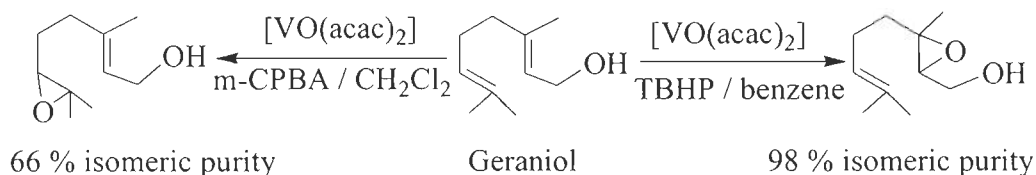
Figure 1.20. (S,S)- and (R,R)-dDioxovanadium(V) complexes

The α -cyclodextrin (α -CD) inclusion complex $\text{K}[\text{VO}_2(\text{salhybiph})(\alpha\text{-CD})_2]$ ($\text{H}_2\text{salhybiph}$ = Schiff-base obtained from the condensation of salicylaldehyde and biphenyl-4-carboxylic acid hydrazide) and the analogous 1:1 inclusion compound with β -CD have also been tested as catalyst in the oxidation of methyl phenyl sulfide (thioanisole) using hydrogen peroxide as oxidant in a water/ethanol mixture, under neutral as well as acidic conditions [167].

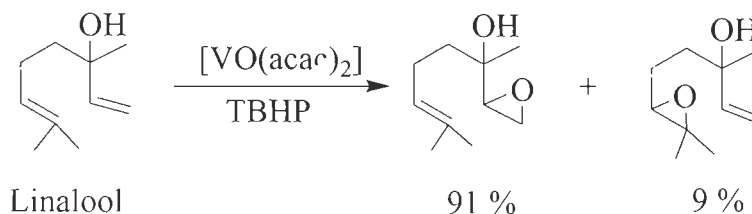
Various chiral complexes e.g. $[(\text{S,S-VO}(\text{OMe})\text{L}^1)]$ ($\text{H}_2\text{L}^1 = (\text{S,S-bis}(2\text{-hydroxypropyl})\text{-(S)-1-(phenylethylamine)})$), $[\text{S,S-VO}(\text{OMe})\text{L}^2]$ ($\text{H}_2\text{L}^2 = (\text{S,S-bis}(2\text{-hydroxypropyl})\text{-(benzylamine)})$) catalyse the asymmetric oxidation of prochiral sulfide such as methyl-*p*-tolylsulfide using cumylhydroperoxide as an oxidant to give *S*-methyl-*p*-tolylsulfoxide in 31% enantiometric excess. Nearly 100% conversion has been obtained after 150 min. at 0 °C [168]. Oxovanadium(V) complex, $(\text{RRR})\text{-}[\text{VO}(\text{OMe})\text{L}]$ ($\text{H}_2\text{L} = (\text{R,R-bis}(2\text{-phenylethanol})\text{-(R)-1-phenylethylamine})$), or complex generated in situ by the reaction of $[\text{VO}(\text{O}^i\text{Pr})_3]$ and ligand in methanol, has also been able to catalyse the oxidation of methyl-*p*-tolylsulfide with cumylhydroperoxide to an enantiomeric excess (ee) of 25 % [169].

Review articles by Conte *et al.* [170, 171] and Ligtenbarg *et al.* [158] present a detail account of vanadium complexes used as catalysts. Epoxidation of geraniol was achieved in presence of *tert*-butylhydroperoxide using $[\text{VO}(\text{acac})_2]$ as catalyst

while epoxidation of double bond was noticed in presence of peracids as shown in Scheme 1.7. Similarly, linalool gives one product in ca. 91 % selectivity as shown in Scheme 1.8. In the presence of TBHP, oxidation of $[\text{VO}(\text{acac})_2]$, through the breaking of acetylacetonato group, has been suggested which on reaction with TBHP in presence of allylic alcohol gives alkoxo-alkylperoxovanadium(V) complex.

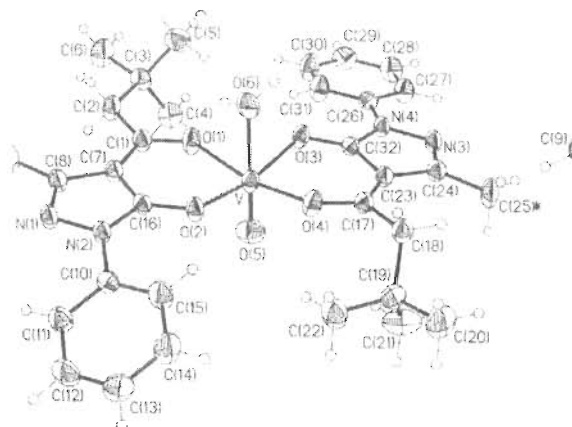


Scheme 1.7



Scheme 1.8

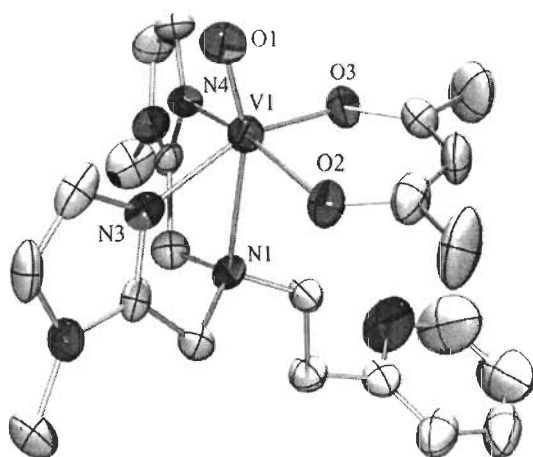
The catalytic activity of oxovanadium(IV) complexes, $\text{VO}(\text{Q})_2(\text{H}_2\text{O})$ (Figure 1.21) and related derivatives, have been exhaustively tested for the oxidation of styrene, α -methylstyrene and cis- β -methylstyrene, in the presence of H_2O_2 as primary oxidant. The effects of oxidant to substrate molar ratio, catalyst amount, solvent and temperature have been studied. Overall, the vanadium complexes showed high activity and high to moderate selectivity toward the benzaldehyde and acetophenone formation, depending from both the type of starting substrate and experimental reaction times [172].



83

Figure 1.21. Perspective view of complex with atomic numbering scheme (ellipsoids at the 40% level) [172].

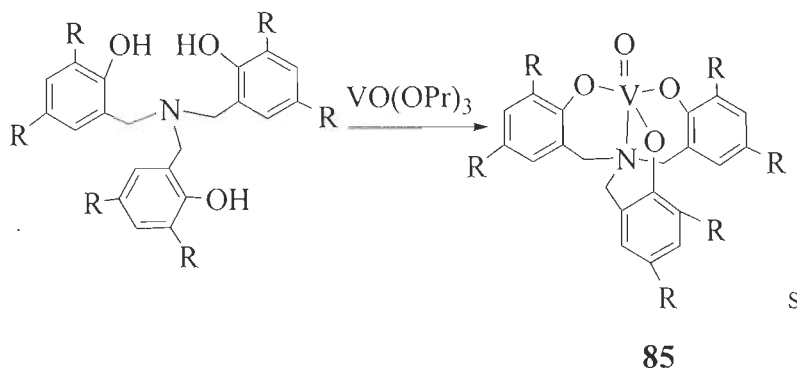
A bioinspired bromide and hydrocarbon oxidation catalyst [VOL] (Figure 1.22) ($\text{LH}_2 = (\text{bis}(1\text{-methylimidazol-2-yl)methyl})(2\text{-(pyridyl-2-yl)ethyl})\text{amine}$) has been prepared and characterized by various techniques including single crystal X-ray study. The complex oxidize bromide and catalyze the oxidation of benzene and cyclohexane in the presence of hydrogen peroxide [173].



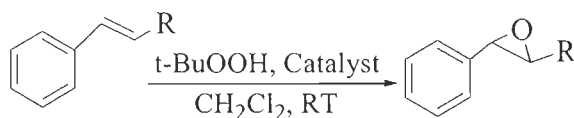
84

Figure 1.22. View of an ORTEP plot of complex with ellipsoids at the 50% level [173].

Vanadium(V) complexes (**85**), prepared from aminetris(phenolate) and $\text{VO}(\text{OPr})_3$ catalyse the epoxidation of styrene and cyclohexene in dichloromethane with TBHP in air atmosphere (Scheme 1.10) [174].



Scheme 1.9



R = H: styrene

R = Ph: *trans*-stilbene

Scheme 1.10

The mononuclear, binuclear and polynuclear oxovanadium(IV) complexes (Figure 1.23) were synthesized from the tetradentate ligand *N,N'*-bis(salicylidene) ethane-1,2-diamine (H_2salen) and tridentate ligands viz. salicylidene-3,3'-dihydroxy-4,4'-diaminobiphenyl ($\text{H}_4\text{sal}_2\text{-dhdabp}$) or *N*-(2-hydroxyphenyl) salicylideneamine ($\text{H}_2\text{sal-oap}$). These complexes catalyse sulfide oxidation and epoxidation of organic substrates. It was found that mononuclear homogenous complexes have significant catalytic properties as compared to polynuclear heterogenous complexes [175].

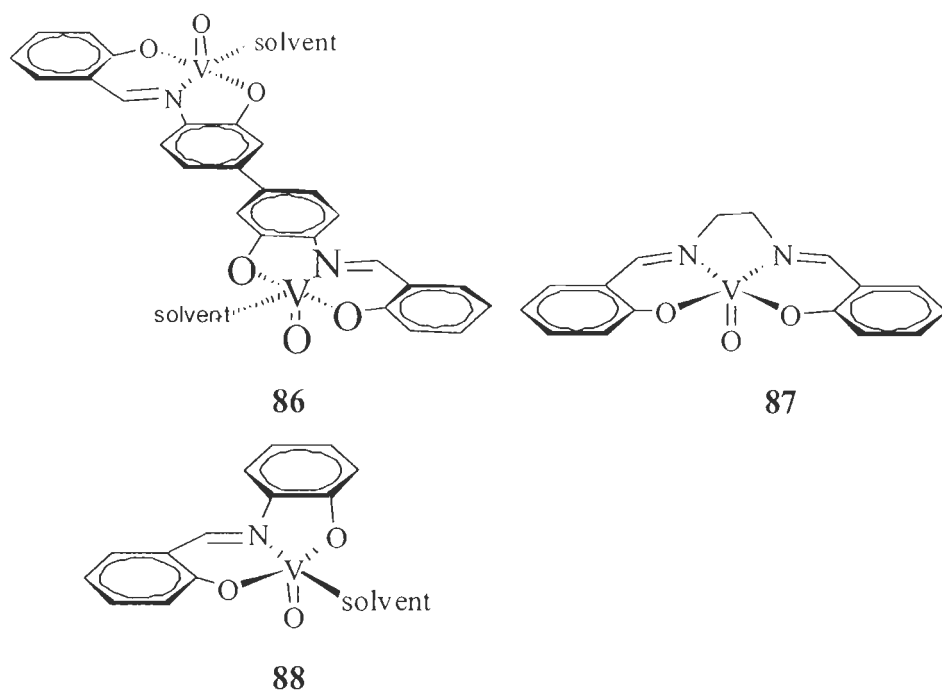
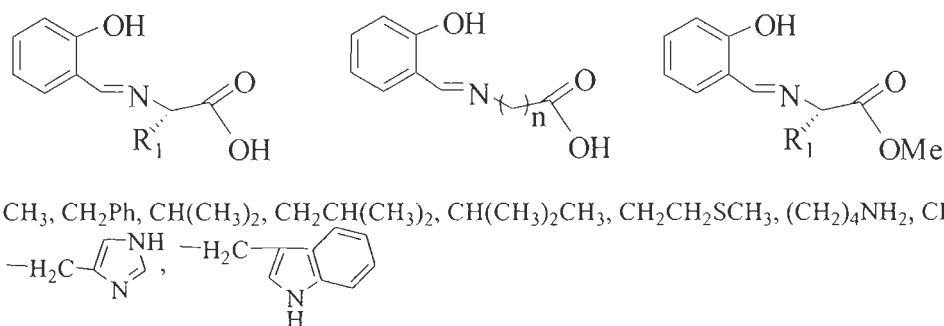


Figure 1.23. Complexes prepared by Ando *et al.* for catalytic activity.

Similarly, oxidation of methyl phenyl sulfide has also been catalysed by oxovanadium(IV) complexes of ligands (Figure 1.24) derived from salicylaldehyde or its derivatives and amino acids (eg. glycine, alanine, valine etc). All the oxovanadium(IV) complexes having L-conformational amino acids Schiff-bases convert sulfide to sulfoxide with R conformation in excess while D-conformational amino acids Schiff bases provide the sulfoxide with S-conformation in excess [176, 177].



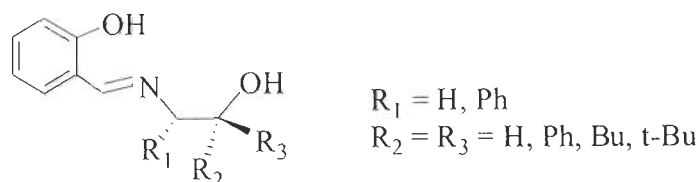
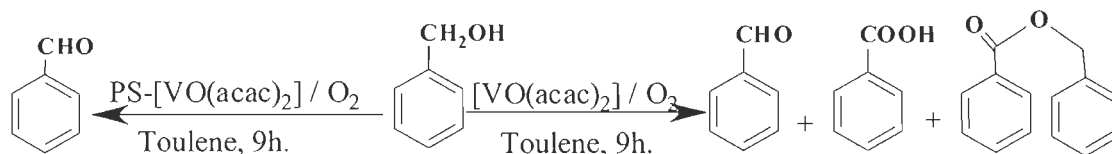


Figure 1.24. Ligands used to prepared oxovanadium(IV) complexes having catalytic potential.

Oxovanadium(V) complexes of dipicoline are able to catalyze the aerobic oxidative C-C bond cleavage of pinacol. Reaction under anaerobic conditions allowed the isolation of a V(III)- μ -oxo dimer, which provides strong support for the potential involvement of V(III) in aerobic oxidation reactions [178]

1.8. Catalytic activity of supported or encapsulated vanadium complexes

[VO(acac)₂] supported on polyaniline was able to catalyse oxidation of benzyl alcohol to benzaldehyde in 98 % yield in toluene at 100 °C. It was found that toluene was the best solvent for the oxidation of benzyl alcohol to benzaldehyde as compared to acetonitrile and *p*-xylene. Other aromatic and aliphatic alcohols were also oxidized using this catalyst to give corresponding aldehyde in good yield. [VO(acac)₂] also catalysed the oxidation of benzyl alcohol to give three oxidized products viz. benzoic acid, benzyl benzoate and benzaldehyde, Scheme 1.11 [179].



Scheme 1.11

Oxovanadium(IV) complex supported on polystyrene, PS-[VO(hmbmz)₂] (Hhmbmz = 2(α -hydroxymethyl)benzimidazole) **89** (Figure 1.25) has been used for the oxidation of styrene (Scheme 1.12) and ethylbenzene; oxidation of styrene gave at least four detectable products as shown in Scheme 1.5 [180] while ethylbenzene gave acetophenone as the major product. Oxidative bromination of salicylaldehyde, catalysed by this complex, using H₂O₂ /KBr gives 5-bromosalicylaldehyde in quantitative yield.

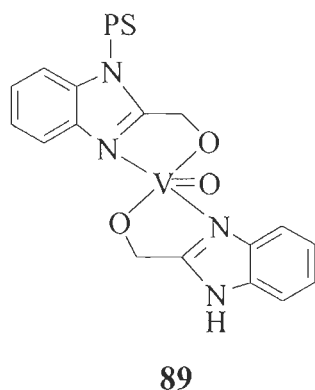
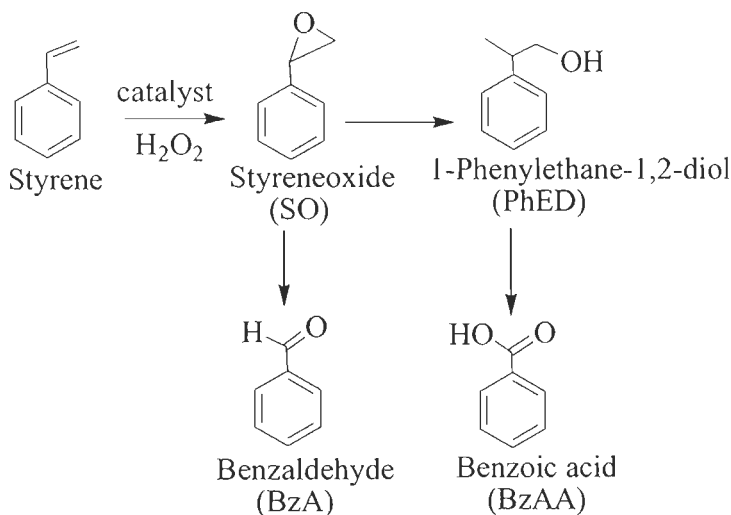


Figure 1.25. PS-[VO(hmbmz)₂], a polystyrene supported complex used for catalytic activity.



Scheme 1.12. Various oxidation products of styrene.

Similar polymeranchored oxovanadium(IV) complex, PS-[VO(pimin)_x] (Hpimin = 2-(2'-hydroxyphenyl)-1H-imidazoline, was also shown to catalyse the hydrogen peroxide-based oxidation of styrene, ethylbenzene and thioanisole. A maximum conversion of ethylbenzene (30.6%) and styrene (99.9%) was obtained by using 0.025 g of PS-[VO(pimin)_x] and 4 equiv. of hydrogen peroxide at 80 °C after 6 h. The oxidation of thioanisole proceeded quantitatively (99.6%) at room temperature within 4 h, with 0.025 g of PS-[VO(pimin)_x] and 2 equiv. of hydrogen peroxide [181].

Oxovanadium(IV) complexes of tridentate Schiff bases (derived from salicylaldehyde and 2-aminoethanol, L-histidine or L-phenylalanine) supported on Merrifield resin (Figure 1.26) [182] or oxovanadium(IV) complexes of pentadentate Schiff bases (derived from salicylaldehyde or its derivatives (e.g. 3-methoxysalicylaldehyde, 5-methoxysalicylaldehyde, 5-chlorosalicylaldehyde, 3,5-dichlorosalicylaldehyde and 3,5-dichlorosalicylaldehyde etc.) and 2,2'-bis(aminoethyl)amine) (Figure 1.26) [183] catalyze the oxidation of methyl phenyl sulfide to the corresponding sulfoxide in 80-90% yield by TBHP. It was found that the monomeric complexes show greater rate of reaction than the corresponding polymer supported complexes.

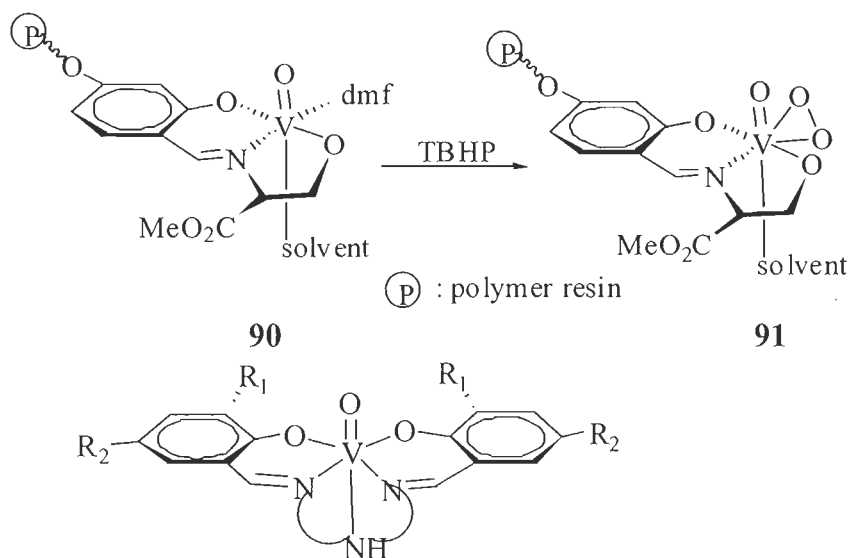


Figure 1.26. Complexes having catalytic potential for the oxidation of methyl phenyl sulfide.

Polymer-supported oxidovanadium(IV) complexes, PS-[VO(fsal-ea)·DMF] (**93**), PS-[VO(fsal-pa)·DMF] (**94**) and PS-[VO(fsal-amp)·DMF] (**95**) (fHsal = 3-formylsalicylaldehyde, ea = 2-aminoethanol, pa = 3-aminopropanol and amp = 2-amino-2-methylpropanol) (Figure 1.27) have been tested for the oxidation of styrene and cumene and were found to be efficient. Styrene gives five reaction products namely styrene epoxide, benzaldehyde, 1-phenylethane-1,2-diol, benzoic acid and phenylacetaldehyde, whereas cumene gives acetophenone, 2-phenylpropanal, α -methyl styrene epoxide, 2-phenyl-2-propanol, 2-isopropyl-1,4-benzoquinone and α -methyl styrene. The polymer-anchored heterogeneous catalysts are recyclable. The catalytic activities of the neat complexes have also been examined and compared with the corresponding anchored analogues [184].

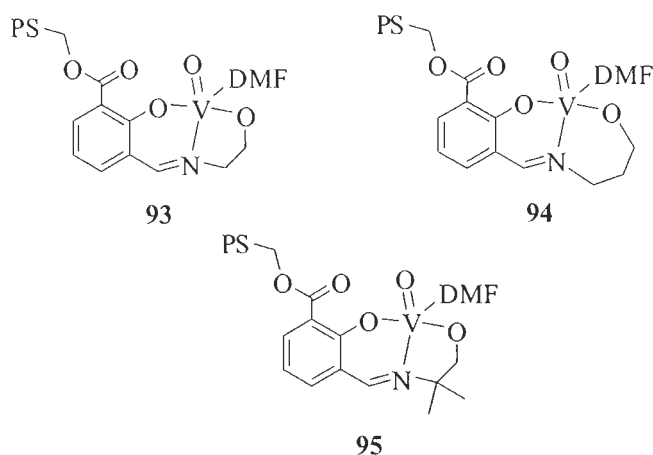
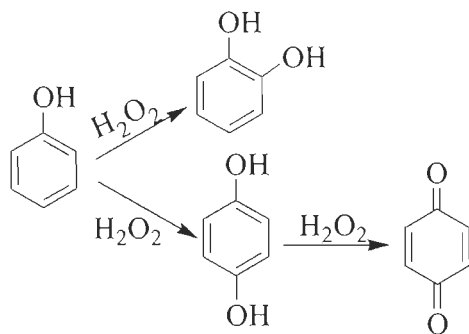


Figure 1.27. Polymer supported complexes.

Under optimised conditions, i.e. phenol (1.88 g, 20 mmol), H_2O_2 (4.56 g, 40 mmol), temperature (70 °C) and water (10 ml), PS-[VO(saldien)] (30 mg) ($\text{H}_2\text{saldien} = N,N'$ -bis(salicyledene)diethylenetriamine), exhibits only 3%

conversion of phenol in water with 100% selectivity towards *p*-benzoquinone. The catalyst became more selective towards catechol formation along with higher conversion in acetonitrile. The selectivity of *p*-benzoquinone was also found to be dependent on volume and nature of solvent, and temperature. Hydroquinone oxidation was also found to be pH dependent; carbonate buffer gives quantitative conversion within 30 min at 1:6 substrate to oxidant ratio [185].

Oxovanadium(IV) complexes have also been encapsulated in the cavity of zeolite-Y and studied for the oxidation reactions. Oxidative bromination of salicylaldehyde to 5-bromosalicylaldehyde and 3,5-dibromosalicylaldehyde catalysed by $[\text{VO}_2(\text{sal-inh})]^-$ ($\text{H}_2\text{sal-inh}$ = Schiff base derived from salicylaldehyde and isonicotinic acid hydrazide) and $\text{K}[\text{VO}_2(\text{sal-oap})]\text{-Y}$ ($\text{H}_2\text{sal-oap}$ = Schiff base derived from salicylaldehyde and *o*-aminophenol) encapsulated in the cavity of zeolite-Y has been reported by Maurya *et al.* [186]. Oxidation of phenol usually gives two products catechol and hydroquinone. In some cases a further oxidation of hydroquinone also occurs to form *para*-benzoquinone as shown in Scheme 1.13. These catalysts also catalyze the liquid phase hydroxylation of phenol with H_2O_2 to a mixture of catechol and hydroquinone in acetonitrile. [187]. A best-suited reaction condition has been optimized for both the catalysts by considering concentration of the oxidant, amount of catalyst and temperature. Styrene catalysed by very similar catalyst $[\text{VO}(\text{sal-oaba})(\text{H}_2\text{O})]\text{-Y}$ ($\text{H}_2\text{sal-oaba}$ = Schiff base derived from salicylaldehyde and *o*-aminobenzyl alcohol) under optimised reaction conditions gave five reaction products namely, styrene oxide, benzaldehyde, 1-phenylethane-1,2-diol, benzoic acid and phenylacetaldehyde. A maximum of 93.2% conversion of methyl phenyl sulfide has been achieved using H_2O_2 as oxidant, where selectivity of sulfoxide was 96.9%. Neat complex $[\text{VO}(\text{sal-oaba})]$ has also been found to be equally active [188].



Scheme 1.13. Oxidative product of phenol.

Oxovanadium(IV) picolinate, $[\text{VO}(\text{pic})_2]$ encapsulated in zeolite-Y has been studied for the oxidation of cyclohexane, isopropanol and benzene using H_2O_2 as an oxidant. Leaching of $[\text{VO}(\text{pic})_2]$ has, however, been noticed in the presence of H_2O_2 [189]. The monopero oxovanadium(V) monopicolinate complex has been isolated by the treatment of encapsulated complex with urea hydrogen peroxide in acetonitrile, the formation of which has been confirmed by UV-visible, Raman and XAFS studies. This novel catalyst retains the solution like activities in aliphatic and aromatic hydrocarbon oxidations as well as in alcohol oxidation [190].

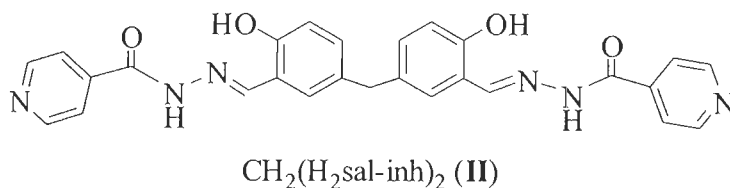
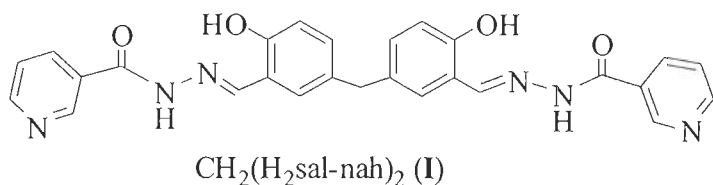
The encapsulation of $[\text{VO}(\text{salen})]$ (H_2salen = bis(salicylaldehyde) ethylenediimine) in zeolite Na-Y via the flexible ligand method has been described. NaY- $[\text{VO}(\text{salen})]$ was found to be an effective catalyst for the room temperature epoxidation of cyclohexene using *t*-butylhydroperoxide (*t*-BuOOH) as the oxidant [191]. Other oxovanadium(IV) complexes of Schiff bases (derived from salicylaldehyde and 1,2-diaminoethane, 1,3-diaminopropane, 1,2-diaminopropane or diethylenetriamine) encapsulated in zeolite also catalyse the oxidation of phenol in ca. 33 % yield. [192].

1.9. Objective of the present investigation

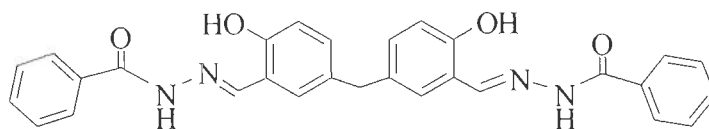
The literature reviewed clearly indicates that the coordination chemistry of vanadium is of increasing potential interest and it was considered desirable to study the coordination chemistry of vanadium that would provide: (i) structural and functional models of haloperoxidases, and (ii) medicinal as well as catalytic potentials. The present thesis is therefore, aimed to describe the coordination chemistry of vanadium considering biologically important ligands in biologically relevant oxidation states. Stability, structural and reactivity studies have been carried out to model the role of vanadium in vanadium based enzymes. The isolated complexes have been screened for their potential catalytic and medicinal applications.

The ligands selected to under take such studies and their abbreviations are presented below:

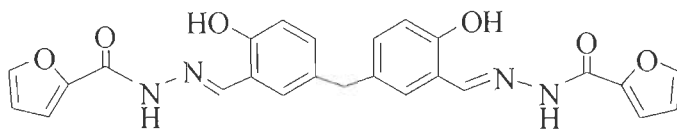
- (a) Binucleating hydrazones $\text{CH}_2(\text{H}_2\text{sal-nah})_2$ (**I**) and $\{\text{CH}_2(\text{H}_2\text{sal-inh})_2$ (**II**) derived from 5,5'-methylenebis(salicylaldehyde) $\{\text{CH}_2(\text{Hsal})_2\}$ and nicotinic acid hydrazide (nah) or isonicotinic acid hydrazide (inh).



- (b) Binucleating hydrazones $\text{CH}_2(\text{H}_2\text{sal-bhz})_2$ (**III**) and $\text{CH}_2(\text{H}_2\text{sal-fah})_2$ (**IV**), derived from 5,5'-methylbis(salicylaldehyde) and benzoylhydrazide (bhaz) or 2-furoylhydrazide (fah).

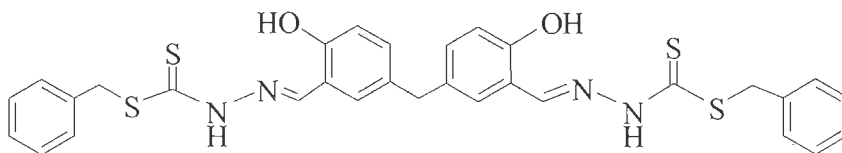


$\text{CH}_2(\text{H}_2\text{sal-bhz})_2$ (III)

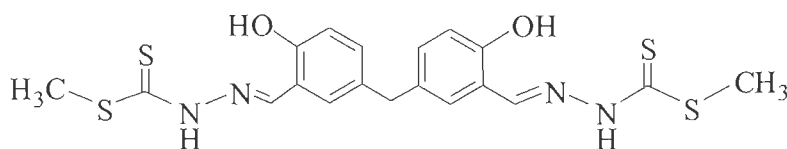


$\text{CH}_2(\text{H}_2\text{sal-fah})_2$ (IV)

(c) Binucleating thiohydrazones $\text{CH}_2(\text{H}_2\text{sal-sbdt})_2$ (V) and $\text{CH}_2(\text{H}_2\text{sal-smdt})_2$ (VI), derived from 5,5'-methylbis(salicylaldehyde) and S-benzyldithiocarbazate (sbdt) or S-methyldithiocarbazate (smdt).



$\text{CH}_2(\text{H}_2\text{sal-sbdt})_2$ (V)



$\text{CH}_2(\text{H}_2\text{sal-smdt})_2$ (VI)

Abstract of the work carried out is presented in the beginning of the thesis and details of the studies are presented in the following chapters.

Chapter-2

Binuclear oxidovanadium(IV) and dioxidovanadium(V) Complexes of 5, 5'-methylenebis(dibasic tridentate) ligands: Synthesis, spectral characterisation, reactivity, catalytic and antiamoebic activities

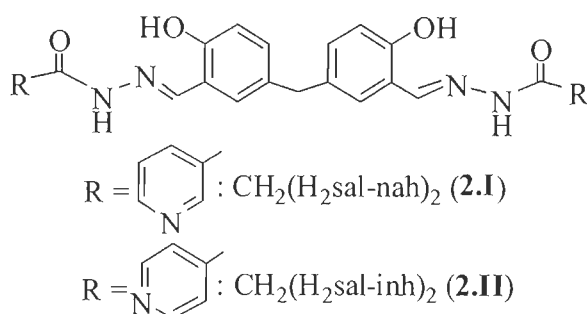
2.1. Introduction

The discovery of vanadium dependent haloperoxidase enzymes and the catalytic potential of several model vanadium complexes in oxidation and oxygen transfer reactions, including the oxidative halogenation of organic substrates [193–197] and oxidation of organic sulfides to sulfoxides, have stimulated the study of coordination chemistry of vanadium with multidentate ligands [198-202]. Several vanadium complexes have been shown to be active as insulin-mimetics *in vitro* and *in vivo*, and $[V^{IV}O(\text{ethylmaltolato})_2]$ has passed Phases I and II clinical tests [203, 204] demonstrating the usability of coordinating compounds of vanadium for the treatment of diabetes mellitus in human.

The intestinal protozoan parasite *Entamoeba histolytica*, has the capacity to invade intestinal mucosa resulting in intestinal amoebiasis. Around fifty million people also suffer from liver abscess caused by *E. histolytica* resulting in 50,000 to 100,000 deaths yearly [205]. Amoebiasis is the second leading cause of death among parasite diseases [206]. For the treatment of amoebiasis, metronidazole has been the drug of choice, but recent studies have shown that this drug has several toxic effects such as genotoxicity, gastric mucus irritation and spermatozoid damage [207-209]. Furthermore, failures in the treatment of several intestinal protozoan parasites may result from drug resistant to parasites [210, 211]. Therefore, research on the new drugs for the treatment is an important therapeutic demand. Metal ions are known to often accelerate drug action, and the efficacy of a therapeutic agent may be enhanced upon coordination with a metal ion [212]. Vanadium complexes show a variety of biological properties, and oxidovanadium(IV) complexes have been used to prevent and improve dexamethasone induced insulin resistance in 3T3-L1 adipocytes [213]. These compounds have also been used in receptor-mediated signals [214] and as anti-cancer agent [215, 216]. Recently antiamoebic activity of various vanadium

complexes have been reported which gave encouraging results in *in vitro* experiments [65, 59, 152, 153].

In this chapter, we describe the synthesis and characterization of dinuclear oxidovanadium(IV) and dioxidovanadium(V) complexes of hydrazones **2.I** and **2.II** derived from 5,5'-methylenebis(salicylaldehyde) $\{\text{CH}_2(\text{Hsal})_2\}$ and nicotinic acid hydrazide (nah) or isonicotinic acid hydrazide (inh), Scheme 2.1. The catalytic activity is demonstrated considering the oxidation, by peroxide, of methyl phenyl sulfide and diphenyl sulfide using the oxidovanadium(IV) complexes as catalyst precursors. In addition the haloperoxidase activity is confirmed as the dioxidovanadium(V) complexes are active in the oxidative bromination of salicylaldehyde. The dioxidovanadium(V) complexes have also been screened against HM1:1MSS strains of *Entamoeba histolytica*.



Scheme 2.1. Structures of ligands designated by **2.I** and **2.II** used in this work

2.2. Experimental section

2.2.1. Materials

V_2O_5 , isonicotinic acid hydrazide (Loba Chemie, India), nicotinic acid hydrazide, (Fluka Chemie, GmbH, Switzerland), acetylacetone (Aldrich, U.S.A.), methyl phenyl sulfide and diphenyl sulfide (Himedia, India), salicylaldehyde (Hsal), 30 % aqueous H_2O_2 and 70 % HClO_4 (Qualigens, India), were used as obtained. Other chemicals and solvents were of analytical reagent grade.

2.2.2. Characterization procedures

Elemental analyses of the compounds were carried out on an Elementar model Vario-El-III. IR spectra were recorded as KBr pellets on a Nicolet NEXUS Aligent 1100 series FT-IR spectrometer. Electronic spectra were measured in methanol or DMF with an UV-1601 PC UV-Vis spectrophotometer. ^1H NMR spectra were obtained on a Bruker 200, ^{13}C and ^{51}V NMR spectra on a Bruker Avance III 400 MHz spectrometer with the common parameter settings. NMR spectra were usually recorded in MeOH-d_4 or DMSO-d_6 , and $\delta(^{51}\text{V})$ values are referenced relative to neat VOCl_3 as external standard. Thermogravimetric analyses of the complexes were carried out under oxygen atmosphere using a TG Stanton Redcroft STA 780 instrument. The magnetic susceptibilities were measured by a Vibrating Sample Magnetometer model 155, using nickel as standard. Diamagnetic corrections were carried out using Pascal's constants [217]. EPR spectra were recorded with a Bruker ESP 300E X-band spectrometer. The spin Hamiltonian parameters were obtained by simulation of the spectra with the computer program of Rockenbauer and Korecz [218]. A Thermax Nicolet gas chromatograph fitted with a HP-1 capillary column ($30\text{ m} \times 0.25\text{ mm} \times 0.25\text{ }\mu\text{m}$) and FID detector was used to analyze the reaction products and their quantifications were made on the basis of the relative peak area of the respective product. The identity of the products was confirmed using a GC-MS model Perkin-Elmer, Clarus 500 and comparing the fragments of each product with the library available.



2.2.3. Preparations

$[\text{V}^{\text{IV}}\text{O}(\text{acac})_2]$

$[\text{V}^{\text{IV}}\text{O}(\text{acac})_2]$ and 5,5'-methylenebis(salicylaldehyde) was prepared according to the methods reported in the literature [219a, 219b].

CH₂(H₂sal-nah)₂ (2.I) and CH₂(H₂sal-inh)₂ (2.II)

Ligands CH₂(H₂sal-nah)₂ (2.I) and CH₂(H₂sal-inh)₂ (2.II) were prepared following the literature procedure with slight modifications [220]. A solution of 5, 5'-methylbis(salicylaldehyde) (2.65 g, 10 mmol) was prepared in hot methanol (40 mL) and was added to a solution of appropriate hydrazide (2.743 g, 20 mmol) dissolved in methanol (20 mL) with stirring. The obtained reaction mixture was refluxed on a water bath for 2 h. After reducing the solvent volume to ca. 30 mL and cooling to ca. 10 °C, the solid obtained was filtered, washed with methanol and dried in desiccator over silica gel.

Data for CH₂(H₂sal-nah)₂ (2.I)

Yield 5.67 g (91%). Found: C, 65.36; H, 4.41; N, 17.22 %. Calc for C₂₇H₂₂O₄N₆ - (494): C, 65.56; H, 4.49; N, 17.00 %.

Data for CH₂(H₂sal-inh)₂ (2.II)

Yield 5.76 g (92%). Found: C, 65.42; H, 4.44; N, 17.13 %. Calc for C₂₇H₂₂O₄N₆ (494): C, 65.56; H, 4.49; N, 17.00 %.

[CH₂{V^{IV}O(sal-nah)(H₂O)}₂] (2.1)

A solution of CH₂(H₂sal-nah)₂ (0.492 g, 1 mmol) was prepared by refluxing in dry methanol (80 mL) and filtered. A filtered solution of [V^{IV}O(acac)₂] (0.530 g, 2 mmol) in dry methanol (15 mL) was added to the above solution while stirring and the reaction mixture was refluxed on a water bath for 3 h. After reducing the volume to ca. 20 mL and keeping at room temperature for 10 h, the separated brown solid was filtered, washed with methanol and dried in a desiccator over silica gel. Yield: 0.451 g (72.3 %). μ_{eff} (293 K) = 1.71 μ_{B} . Found: C, 49.0; H, 3.41; N, 12.52 %. Calc for C₂₇H₂₂O₈N₆V₂ (660.39): C, 49.11; H, 3.36; N, 12.73 %.

[CH₂{V^{IV}O(sal-inh)(H₂O)}₂] (2.2)

Complex **2.2** was prepared from [V^{IV}O(acac)₂] (0.530 g, 2 mmol) and CH₂(H₂sal-inh)₂ (0.492 g, 1 mmol) by the method outlined for [CH₂{V^{IV}O(sal-nah)(H₂O)}₂] (**2.1**). Yield: 0.505 g. (80.9 %). μ_{eff} (293 K) = 1.70 μ_{B} . Found: C, 48.92; H, 3.46; N, 12.63 %. Calc for C₂₇H₂₂O₈N₆V₂ (660.39): C, 49.11; H, 3.36; N, 12.73 %.

K₂[CH₂{V^VO₂(sal-nah)}₂]·2H₂O (2.3)

Method A: A mixture of [CH₂{V^{IV}O(sal-nah)(H₂O)}₂] (0.312 g, 0.5 mmol) and KOH (0.068 g, 1.2 mmol) in 25 mL of methanol was refluxed for 2 h and then left for aerial oxidation as well as slow evaporation of the solvent at room temperature. Complex **2.3** slowly precipitated out in ca. 3 days. This was filtered off, washed with cold methanol and dried in a desiccator over silica gel. Yield: 0.265 g (72.0%).

Method B: A solution of CH₂(H₂sal-nah)₂ (0.612 g, 1 mmol) dissolved in aqueous KOH (0.224 g, 4 mmol) was added with stirring to a filtered aqueous solution of KVO₃ prepared in situ by dissolving vanadium(V) oxide (0.20 g, 2 mmol) in KOH (0.112 g, 2 mmol). The pH of the reaction mixture was adjusted to ~7.5 by adding 4 M HCl. The yellow solid of **2.3** started to separate and was filtered after 2 h of stirring, washed with water and dried. Yield 0.512 g (69.7 %). Found: C, 41.82; H, 2.73; N, 10.83 %. Calc for K₂C₂₇H₂₂O₁₀N₆V₂ (770.59): C, 42.08 ; H, 2.88 ; N, 10.91 %. ⁵¹V NMR (300 MHz, DMSO-d₆, 25 °C): δ = -533 ppm.

Cs₂[CH₂{V^VO₂(sal-nah)}₂]·2H₂O (2.4)

Method A: A filtered solution of [V^{IV}O(acac)₂] (0.463 g 1.75 mmol) in methanol (15 mL) was added while stirring to a solution of CH₂(H₂sal-nah)₂ (0.321 g, 0.65 mmol) prepared as reported for **2.1** in methanol (80 mL). After adding CsOH·H₂O

(0.300 g, 1.78 mmol), the reaction mixture was refluxed for 2 h. The dark red solution obtained was allowed to stand for aerial oxidation, and became yellow within 24 h. After reducing the volume to ca. 10 mL and keeping at room temperature, complex **2.4** separated within 24 h. This was filtered off, washed with cold methanol and dried in desiccator over silica gel. Yield 0.653 g (70.8 %). Found: C, 33.66; H, 2.37; N, 8.81 %. Calc for $\text{Cs}_2\text{C}_{27}\text{H}_{22}\text{O}_{10}\text{N}_6\text{V}_2$: C, 33.84; H, 2.31; N, 8.77 %. ^{51}V NMR (300 MHz, DMSO- d_6 , 25 °C): $\delta = -532$ ppm.

Method B: A mixture of $[\text{CH}_2\{\text{V}^{\text{IV}}\text{O}(\text{sal-nah})(\text{H}_2\text{O})\}_2]$ (0.312 g, 0.5 mmol) and $\text{CsOH}\cdot\text{H}_2\text{O}$ (0.202 g, 1.2 mmol) in 25 mL of methanol was refluxed for 2 h and then left for aerial oxidation as well as slow evaporation of the solvent at room temperature. Complex **2.4** slowly precipitated out in ca. 3 days. The rest of the procedure was the same as for method A. Yield 0.39 g (84.6) %.

$\text{Cs}_2[\text{CH}_2\{\text{V}^{\text{V}}\text{O}_2(\text{sal-inh})\}_2]\cdot 2\text{H}_2\text{O}$ (2.5)

This complex was prepared by the same procedures outlined for $\text{Cs}_2[\text{CH}_2\{\text{V}^{\text{V}}\text{O}_2(\text{sal-nah})_2\}]\cdot 2\text{H}_2\text{O}$. Yield 0.682 g (74.0 %). Found: C, 33.87; H, 2.34; N, 8.71 %. Calc for $\text{Cs}_2\text{C}_{27}\text{H}_{22}\text{O}_{10}\text{N}_6\text{V}_2$: C, 33.84; H, 2.31; N, 8.77%. ^{51}V NMR (300 MHz, DMSO- d_6 , 25 °C): $\delta = -532$ ppm.

2.2.4. Catalytic activity studies

Oxidation of Methyl phenyl sulfide and Diphenyl sulfide

Methyl phenyl sulphide (1.24 g, 10 mmol) or diphenyl sulfide (1.86 g, 10 mmol) and aqueous 30% H_2O_2 (2.27 g, 20 mmol) were suspended in petroleum ether (10 mL). After addition of catalyst precursors (oxidovanadium(IV) complexes $[\text{CH}_2\{\text{V}^{\text{IV}}\text{O}(\text{sal-nah})(\text{H}_2\text{O})\}_2]$ (**2.1**) or $[\text{CH}_2\{\text{V}^{\text{IV}}\text{O}(\text{sal-inh})(\text{H}_2\text{O})\}_2]$ (**2.2**), 0.020 g) to the above solution, the reaction mixture was stirred at room temperature for 7 h. During this period, the products formed were analyzed using

gas chromatography by withdrawing small aliquots at fixed time intervals, and the identity of the products confirmed using GC-MS.

Oxidative Bromination of Salicylaldehyde

Complexes $\text{K}_2[\text{CH}_2\{\text{V}^{\text{V}}\text{O}_2(\text{sal-nah})\}_2]\cdot 2\text{H}_2\text{O}$, $\text{Cs}_2[\text{CH}_2\{\text{V}^{\text{V}}\text{O}_2(\text{sal-nah})\}_2]\cdot 2\text{H}_2\text{O}$ and $\text{Cs}_2[\text{CH}_2\{\text{V}^{\text{V}}\text{O}_2(\text{sal-inh})\}_2]\cdot 2\text{H}_2\text{O}$ were used as catalyst to carry out oxidative bromination. In a typical reaction, salicylaldehyde (2.44 g, 20 mmol) was added to an aqueous solution (40 mL) of KBr (5.95 g, 50 mmol), followed by addition of aqueous 30 % H_2O_2 (13.62 g, 120 mmol) in a 100 mL reaction flask. The catalyst (0.02 g for $\text{Cs}_2[\text{CH}_2\{\text{V}^{\text{V}}\text{O}_2(\text{sal-nah})\}_2]\cdot 2\text{H}_2\text{O}$ (**2.4**) and $\text{Cs}_2[\text{CH}_2\{\text{V}^{\text{V}}\text{O}_2(\text{sal-inh})\}_2]\cdot 2\text{H}_2\text{O}$ (**2.5**), and 0.016 g for $\text{K}_2[\text{CH}_2\{\text{V}^{\text{V}}\text{O}_2(\text{sal-nah})\}_2]\cdot 2\text{H}_2\text{O}$ (**2.3**)) and 70 % HClO_4 (2.86 g, 20 mmol) were added, and the reaction mixture was stirred at room temperature. Three additional 20 mmol portions of 70 % HClO_4 were further added to the reaction mixture in three equal portions in half hour intervals under continuous stirring. After 7 h, the white product that had separated was filtered off, washed with water and dried. The crude mass was dissolved in CH_2Cl_2 ; insoluble material, if any, was removed by filtration, and the solvent evaporated. A CH_2Cl_2 solution of this material was subjected to gas chromatography and the identity of the products confirmed by GC-MS.

2.2.5. In vitro testing against E. Histolytica

The ligands and their dioxidovanadium(V) complexes $\text{K}_2[\text{CH}_2\{\text{V}^{\text{V}}\text{O}_2(\text{sal-nah})\}_2]\cdot 2\text{H}_2\text{O}$ (**2.3**), $\text{Cs}_2[\text{CH}_2\{\text{V}^{\text{V}}\text{O}_2(\text{sal-nah})\}_2]\cdot 2\text{H}_2\text{O}$ (**2.4**) and $\text{Cs}_2[\text{CH}_2\{\text{V}^{\text{V}}\text{O}_2(\text{sal-inh})\}_2]\cdot 2\text{H}_2\text{O}$ (**2.5**), were screened in vitro for antiamoebic activity against *HMI:1MSS* strain of *E. histolytica* by using a microplate method [221]. *E. histolytica* trophozoites were cultured in TYIS-33 growth medium in wells of 96 microtiter plate [222]. DMSO (40 μL) was added to all the samples (1 mg)

followed by enough culture medium to obtain concentration of 1 mg/mL. The maximum concentration of DMSO in the tests did not exceed 0.1%, at which level no inhibition of amoebal growth occurred [223, 224]. ^1H NMR spectra of all complexes in DMSO- d_6 were recorded to test whether the solvent induced any ligand solvolysis, but all were found to be stable at room temperature for several days. Samples were dissolved or suspended by mild sonication in a soniclearner bath for a few minutes and then further dilution with medium to a concentration of 0.1 mg/mL. Two fold serial dilutions were made in the wells of a 96-well microtiter plate (Costar) in 170 μL of the medium. Each test included metronidazole as the standard amoebicidal drug; control wells (culture medium plus amoebae) were prepared from a confluent culture by pouring off the medium, adding 2 mL of medium and chilling the culture on ice to detach the organisms from the side of the flask. The number of the amoeba per mL was estimated with a haemocytometer and trypan blue exclusion was used to confirm viability. The cell suspension used was diluted to 10^5 organism/mL by adding fresh medium and 170 μL of this suspension were added to the test and control well in the plate so that the wells were completely filled (total volume, 340 μL). An inoculum of 1.7×10^4 organisms/well was chosen so that confluent, but not excessive growth, took place in control wells. The plate was sealed with expanded polystyrene (0.5 mm). Secured with tape, placed in a modular incubating chamber (flow laboratories, High Wycombe, UK), and gassed for 10 min with nitrogen before incubation at 37 °C for 72 h.

Assessment of antiamoebic activity

After incubation, the growth of amoebae in the plate was checked with a low power microscope. The culture medium was removed by inverting the plate and shaking gently. The plate was then immediately washed once in NaCl (0.9%) at 37 °C. This procedure was completed quickly, and the plate was not allowed to cool in order to prevent the detachment of amoebae. The plate was allowed to dry

at room temperature, and the amoebae were fixed with methanol, when dry, stained with (0.5%) aqueous eosin for 15 min. The stained plate was washed once with tap water and then twice with distilled water and allowed to dry. A 200 μ L portion of 0.1 N NaOH solutions was added in each well to dissolve the protein and release the dye. The optical density of the resulting solution in each well was determined at 490 nm with a micro plate reader. The % inhibition of amoebal growth was calculated from the optical densities of the control and test wells and plotted against the logarithm of the dose of the drug tested. Linear regression analysis was used to determine the best-fitted straight line from which the IC₅₀ value was found.

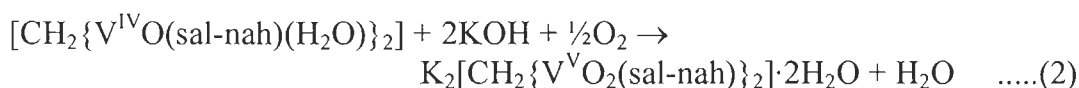
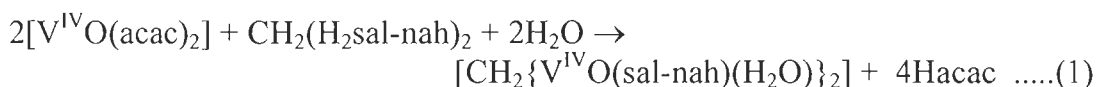
MTT toxicity

The human cervical (HeLa) cells were obtained from NCCS (Pune, India). The cells were cultured in DMEM (Invitrogen) with 10% fetal bovine serum, and 1% penicillin-streptomycin. The effect of active compounds $K_2[CH_2\{V^VO_2(sal-nah)\}_2]\cdot 2H_2O$ (**2.3**) and $Cs_2[CH_2\{V^VO_2(sal-inh)\}_2]\cdot 2H_2O$ (**2.5**), and the standard drug (metronidazole) on cell proliferation was measured by using an MTT-based assay [225]. Briefly, the cells (6000/well) were incubated in triplicate in a 96-well plate in the presence of various concentrations of compounds $K_2[CH_2\{V^VO_2(sal-nah)\}_2]\cdot 2H_2O$ (**2.3**) and $Cs_2[CH_2\{V^VO_2(sal-inh)\}_2]\cdot 2H_2O$ (**2.5**) as well as metronidazole or vehicle (DMSO) alone in a final volume of 200 μ l for different time lengths (24, 48 and 72h) at 37°C in a humidified chamber. At the end of each time point, 20 μ l of MTT solution (5 mg/mL in PBS) was added to each well and the cells were incubated for 4 h at 37°C in a humidified chamber. After 4 hours, the supernatant was removed from each well. The colored formazan crystal produced from MTT was dissolved in 200 μ L of DMSO and then the absorbance (*A*) value was measured at 570 nm by a multi scanner autoreader. The following

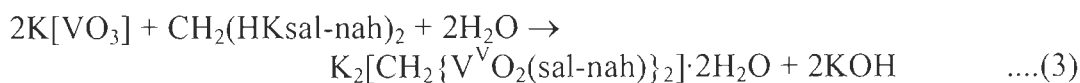
formula was used for the calculation of the percentage of cell viability (CV): CV (%) = (A of the experimental samples/A of the control) × 100.

2.3. Results and Discussion

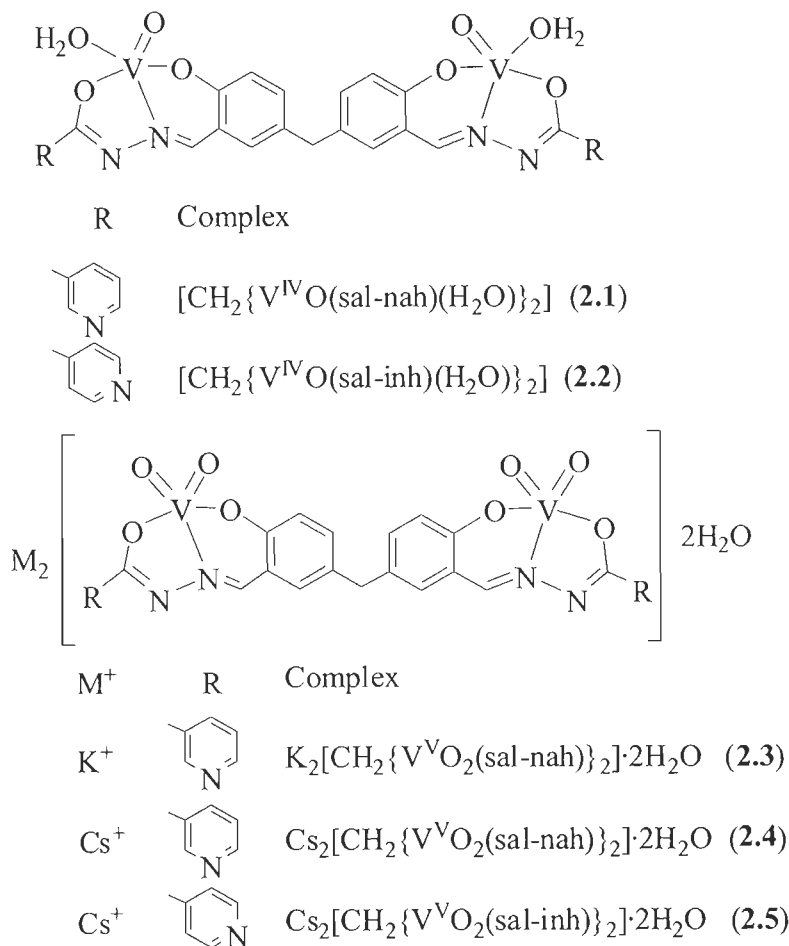
The reaction between $[\text{V}^{\text{IV}}\text{O}(\text{acac})_2]$ and $\text{CH}_2(\text{H}_2\text{sal-nah})_2$ or $\text{CH}_2(\text{H}_2\text{sal-inh})_2$ in 2:1 ratio in refluxing methanol leads to the formation of dinuclear oxidovanadium(IV) complexes $[\text{CH}_2\{\text{V}^{\text{IV}}\text{O}(\text{sal-nah})(\text{H}_2\text{O})\}_2]$ (**2.1**) and $[\text{CH}_2\{\text{V}^{\text{IV}}\text{O}(\text{sal-inh})(\text{H}_2\text{O})\}_2]$ (**2.2**), respectively. These complexes exhibit normal magnetic moment value of 1.71 and 1.70 μ_{B} , respectively, indicating only very weak or possibly no magnetic exchange interaction between the two vanadium(IV) centres. Aerial oxidation of these complexes in the presence of KOH or CsOH.H₂O in methanol results in the formation of the corresponding salt of dioxidovanadium(V) species $[\text{CH}_2\{\text{V}^{\text{V}}\text{O}_2(\text{sal-nah})\}_2]^{2-}$ and $[\text{CH}_2\{\text{V}^{\text{V}}\text{O}_2(\text{sal-inh})\}_2]^{2-}$, respectively. Alternatively, these complexes can also be isolated directly by the aerial oxidation of in situ generated $\text{V}^{\text{IV}}\text{O}$ -complexes in the presence of the corresponding hydroxide. Equations (1) and (2) present the whole synthetic procedure considering $\text{CH}_2(\text{H}_2\text{sal-nah})_2$ as a representative ligand.



Complex $\text{K}_2[\text{CH}_2\{\text{V}^{\text{V}}\text{O}_2(\text{sal-nah})\}_2] \cdot 2\text{H}_2\text{O}$ was also isolated by the reaction of potassium vanadate, generated in situ by dissolving V_2O_5 in an aqueous KOH solution, with the solution of the K^+ -salt of **2.I** and adjustment of the pH of the reaction mixture to ca. 7.0; equation (3). Under similar reaction conditions the complex of ligand **2.II** always gave an emulsified mixture from which the desired complex could not be isolated.



All complexes are soluble in methanol, ethanol, DMSO and DMF. Scheme 2.2 presents the structures proposed for these complexes which are supported by the spectroscopic characterisation (IR, electronic, ^1H , ^{13}C and ^{51}V NMR, and EPR), elemental analyses and thermogravimetric patterns. The coordination of the dianionic ligands involves their enolate tautomeric form (ONO^{2-}); cf. Scheme 2.1.



Scheme 2.2. Schematic structure of the $\text{V}^{\text{IV}}\text{O}$ - and $\text{V}^{\text{V}}\text{O}_2$ -complexes prepared. M corresponds to either K^+ or Cs^+ .

2.3.1. Thermogravimetric studies

The dioxidovanadium(V) complexes $\text{Cs}_2[\text{CH}_2\{\text{V}^{\text{V}}\text{O}_2(\text{sal-nah})\}_2]\cdot 2\text{H}_2\text{O}$ and $\text{Cs}_2[\text{CH}_2\{\text{V}^{\text{V}}\text{O}_2(\text{sal-inh})\}_2]\cdot 2\text{H}_2\text{O}$ lose weight in the temperature range 150–220 °C due to the loss of two water molecules. This loss indicates particularly the not strongly bound water. The water-free species $\text{Cs}_2[\text{CH}_2\{\text{V}^{\text{V}}\text{O}_2(\text{sal-nah})\}_2]$ further decomposes in two overlapping steps in the temperature range 280–440 °C, to form the vanadate $\text{Cs}[\text{VO}_3]$ (or $\text{V}_2\text{O}_5 + \text{Cs}_2\text{O}$). The total weight loss in both complexes corresponds to the loss of ligands minus two oxygen atoms. The initial part of the thermogram of $\text{K}_2[\text{CH}_2\{\text{V}^{\text{V}}\text{O}_2(\text{sal-nah})\}_2]\cdot 2\text{H}_2\text{O}$ is very similar to the above two complexes but water free species decomposes in multiple overlapping steps; the final residue corresponds to $\text{K}[\text{VO}_3]$ (or $\text{V}_2\text{O}_5 + \text{K}_2\text{O}$).

2.3.2. IR Spectral studies

The IR spectral data of ligand and complexes are presented in Table 2.1. The IR spectra of the ligands show bands at 1655 and 3204 cm^{-1} [$\text{CH}_2(\text{H}_2\text{sal-nah})_2$, **2.I**] and 1653 and 3250 cm^{-1} [$\text{CH}_2(\text{H}_2\text{sal-inh})_2$, **2.II**] due to $\nu(\text{C}=\text{O})$ and $\nu(\text{N-H})$ stretches, respectively. This is indicative of their ketonic nature in the solid state. Both bands disappear upon complex formation indicating the enolisation and dissociation of H^+ induced by the metal ion. A new band appearing in the region 1278–1287 cm^{-1} is assigned to the $\nu(\text{C-O}_{\text{enolic}})$ mode. The $\nu(\text{C}=\text{N}_{\text{azomethine}})$ stretch of the ligands appears at 1617 cm^{-1} , and this band is shifted to lower wave numbers by 20–24 cm^{-1} in the complexes, thereby indicating the coordination of the azomethine nitrogen. A ligand band appearing at 961 (in **2.I**) and 968 cm^{-1} (in **2.II**) due to the $\nu(\text{N-N})$ stretch which undergoes a blue shift of 95–98 cm^{-1} . This high frequency shift of the $\nu(\text{N-N})$ band is expected because of the decreased repulsion between the lone pairs of adjacent nitrogen atoms [226]. A medium intensity band of the free ligand, covering the region 2900–3400 cm^{-1} , is assigned to phenolic OH group involved in hydrogen bonding. In most complexes a broad

band in the range $3000 - 3400 \text{ cm}^{-1}$ is assigned to the $\nu(\text{OH})$ of the coordinated / non-coordinated H_2O involved in hydrogen bonding.

All dioxidovanadium(V) complexes exhibit one sharp band in the $921\text{--}927 \text{ cm}^{-1}$ region and one weak band at ca. 950 cm^{-1} due to $\nu_{\text{sym}}(\text{O}=\text{V}=\text{O})$ and $\nu_{\text{asym}}(\text{O}=\text{V}=\text{O})$ stretches. These bands confirm the *cis*- VO_2 structure in complexes. The O-atoms of the $\text{V}^{\text{V}}\text{O}_2$ -units are probably involved in binding to K^+/Cs^+ in the crystal structure; such oxygen coordination has been confirmed in anionic dioxidovanadium(V) complexes [65, 152]. Oxidovanadium(IV) complexes display only one sharp band each at $983\text{--}987 \text{ cm}^{-1}$ due to $\nu(\text{V}=\text{O})$ stretch.

Table 2.1. IR spectra of compounds (ν in cm^{-1})^a

Compounds	$\nu(\text{C}=\text{O})$	$\nu(\text{C}=\text{N})$	$\nu(\text{V}=\text{O})$	$\nu(\text{N}=\text{N})$
$\text{CH}_2(\text{H}_2\text{sal-nah})$ (2.I)	-	1617	-	961
$\text{CH}_2(\text{H}_2\text{sal-inh})$ (2.II)	-	1617	-	968
$[\text{CH}_2\{\text{V}^{\text{IV}}\text{O}(\text{sal-nah})(\text{H}_2\text{O})\}_2]$ (2.1)	1278	1594	983	1056
$\text{K}_2[\text{CH}_2\{\text{V}^{\text{V}}\text{O}_2(\text{sal-nah})\}_2] \cdot 2\text{H}_2\text{O}$ (2.3)	1283	1597	926, 950	1029
$\text{Cs}_2[\text{CH}_2\{\text{V}^{\text{V}}\text{O}_2(\text{sal-nah})\}_2] \cdot 2\text{H}_2\text{O}$ (2.4)	1278	1597	921, 950	1033
$[\text{CH}_2\{\text{V}^{\text{IV}}\text{O}(\text{sal-inh})(\text{H}_2\text{O})\}_2]$ (2.2)	1287	1593	987	1034
$\text{Cs}_2[\text{CH}_2\{\text{V}^{\text{V}}\text{O}_2(\text{sal-inh})\}_2] \cdot 2\text{H}_2\text{O}$ (2.5)	1286	1593	927, 950	1066

^a $\nu(\text{C}=\text{O})$ for $\text{CH}_2(\text{H}_2\text{sal-nah})$ at 1655; $\nu(\text{C}=\text{O})$ for $\text{CH}_2(\text{H}_2\text{sal-inh})$ at 1653.

2.3.3. Electronic spectral studies

Electronic spectral data of ligands and complexes are presented in Table 2.2. Ligands **2.I** and **2.II** exhibit four absorption bands at ca. 216, 243, 294 and 341 nm which are assigned to $\phi \rightarrow \phi^*$, $\pi \rightarrow \pi_1^*$, $\pi \rightarrow \pi_2^*$, and $n \rightarrow \pi^*$ transitions, respectively. In complexes, these bands generally are shifted towards lower wavelengths. In addition, a new band of medium intensity appears at 407 – 414

nm, which is assigned to a ligand to metal charge transfer (LMCT) band. The band at 565 nm, observed at higher concentration for complexes $[\text{CH}_2\{\text{V}^{\text{IV}}\text{O}(\text{sal-nah})(\text{H}_2\text{O})\}_2]$ (**2.1**) and $[\text{CH}_2\{\text{V}^{\text{IV}}\text{O}(\text{sal-inh})(\text{H}_2\text{O})\}_2]$ (**2.2**), is assigned to a d – d transition. For complexes $\text{K}_2[\text{CH}_2\{\text{V}^{\text{V}}\text{O}_2(\text{sal-nah})\}_2] \cdot 2\text{H}_2\text{O}$ (**2.3**), $\text{Cs}_2[\text{CH}_2\{\text{V}^{\text{V}}\text{O}_2(\text{sal-nah})\}_2] \cdot 2\text{H}_2\text{O}$ (**2.4**) and $\text{Cs}_2[\text{CH}_2\{\text{V}^{\text{V}}\text{O}_2(\text{sal-inh})\}_2] \cdot 2\text{H}_2\text{O}$ (**2.5**) no such bands were detected.

Table 2.2. Electronic spectral data of compounds

Compounds	λ (nm)
$\text{CH}_2(\text{H}_2\text{sal-nah})$ (2.I)	341, 294, 243, 216
$\text{CH}_2(\text{H}_2\text{sal-inh})$ (2.II)	342, 294, 244, 217
$[\text{CH}_2\{\text{V}^{\text{IV}}\text{O}(\text{sal-nah})(\text{H}_2\text{O})\}_2]$ (2.1)	565, 408, 325, 242, 207
$\text{K}_2[\text{CH}_2\{\text{V}^{\text{V}}\text{O}_2(\text{sal-nah})\}_2] \cdot 2\text{H}_2\text{O}$ (2.3)	408, 323, 292, 242
$\text{Cs}_2[\text{CH}_2\{\text{V}^{\text{V}}\text{O}_2(\text{sal-nah})\}_2] \cdot 2\text{H}_2\text{O}$ (2.4)	408, 325, 288, 240, 206
$[\text{CH}_2\{\text{V}^{\text{IV}}\text{O}(\text{sal-inh})(\text{H}_2\text{O})\}_2]$ (2.2)	565, 407, 328, 282, 239
$\text{Cs}_2[\text{CH}_2\{\text{V}^{\text{V}}\text{O}_2(\text{sal-inh})\}_2] \cdot 2\text{H}_2\text{O}$ (2.5)	414, 327, 283, 234

2.3.4. ^1H and ^{13}C NMR studies

^1H NMR spectra of the ligands and complexes were recorded to obtain further evidence for the coordinating mode of ligands. The relevant data are presented in Table 2.3. The ^1H NMR spectra of ligands exhibit signals at $\delta = 10.84$ ($\text{CH}_2(\text{H}_2\text{sal-nah})$, **2.I**) and at $\delta = 10.85$ ($\text{CH}_2(\text{H}_2\text{sal-inh})$, **2.II**) due to the –NH proton, indicating their existence in the ketonic form. The absence of these signals in V^{V} -complexes is in agreement with enolisation and subsequent replacement of H by the metal ion. Similarly, the absence of the signal for the phenolic OH (ca. 12.25 ppm in the ligands) indicates the coordination of phenolate oxygen. A significant downfield shift of the azomethine (–CH=N–) proton signal in V^{V} -

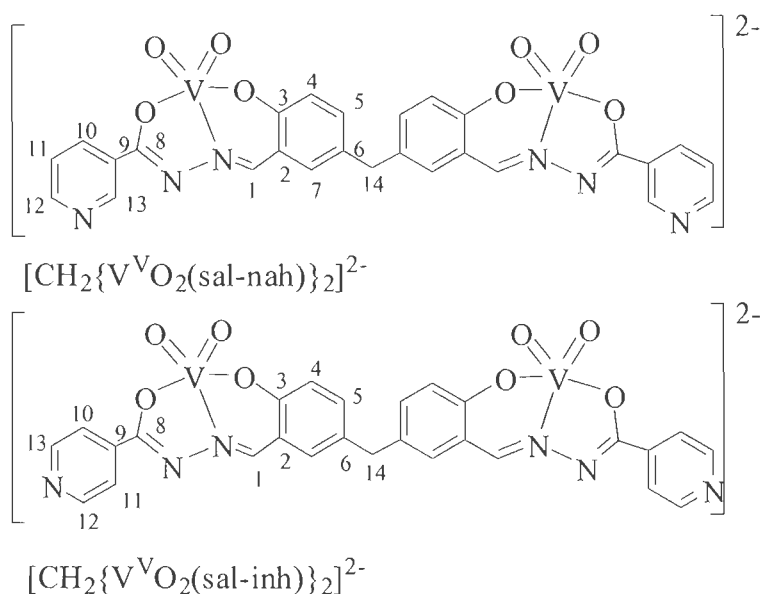
complexes, as compared with the corresponding free ligands, also indicates the coordination of the azomethine nitrogen. This and the other ^1H NMR data are thus consistent with the ONO dibasic tridentate binding mode of each unit of ligands and in agreement with the conclusions drawn from IR data.

We have also recorded ^{13}C NMR of complexes **2.3**, **2.4** and **2.5**. The ^{13}C spectra of complexes contain 13 signals corresponding to the 27 carbon atoms of the molecules owing to their symmetry. The assignment of the peaks (Table 2.4) was made with the help of the Chem Draw[®] software and all of them match within $\pm 2\%$ accuracy with the predicted values. The peaks of atoms C14 overlap those of DMSO so they cannot be properly assigned.

Table 2.3. ^1H NMR spectral data

Compound	$\delta(\text{OH})$	$\delta(\text{NH})$	$\delta(\text{CH}=\text{N})$	$\delta(-\text{CH}_2)$	$\delta(\text{aromatic})$
2.I	12.25	10.84	8.68	3.47	6.92-7.49
2.II	12.24	10.85	8.67	3.86	6.78-7.84, 8.80
2.3			8.25	3.81	6.68-8.90, 9.09
2.4			8.23	3.81	6.67-8.91, 9.00
2.5			8.60	3.82	6.67-8.93

Table 2.4. ^{13}C NMR chemical shifts observed; for the atom labelling see scheme below



Compound	C8	C3	C1	C12/C13	C10	C6
$[\text{K}]_2[\text{CH}_2\{\text{V}^{\text{V}}\text{O}_2(\text{sal-nah})\}_2]$	168.4	163.7	156.8	149.1	135.4	134.6
$[\text{Cs}]_2[\text{CH}_2\{\text{V}^{\text{V}}\text{O}_2(\text{sal-nah})\}_2]$	163.5	163.3	155.9	148.0	145.3	134.3
$[\text{Cs}]_2[\text{CH}_2\{\text{V}^{\text{V}}\text{O}_2(\text{sal-inh})\}_2]$	168.2	163.8	157.7	150.4	140.5	134.9
	C5	C7/C9		C11	C2	C4
$[\text{K}]_2[\text{CH}_2\{\text{V}^{\text{V}}\text{O}_2(\text{sal-nah})\}_2]$	132.4	130.3	128.9	123.9	120	119.8
$[\text{Cs}]_2[\text{CH}_2\{\text{V}^{\text{V}}\text{O}_2(\text{sal-nah})\}_2]$	132.1	130.2		119.9	113.9	112
$[\text{Cs}]_2[\text{CH}_2\{\text{V}^{\text{V}}\text{O}_2(\text{sal-inh})\}_2]$	132.5	130.3		121.9	120	119

2.3.5. Solution behaviour of $K_2[CH_2\{V^VO_2(sal-nah)\}_2]\cdot 2H_2O$ (**2.3**)

The ^{51}V NMR spectrum of $K_2[CH_2\{V^VO_2(sal-nah)\}_2]\cdot 2H_2O$ (**2.3**) dissolved in MeOH has resonances at -538 and a minor -545 ppm [Figure 2.1 (a)]. In DMSO a single peak is obtained at -533 ppm [Figure 2.2A (a)]. The assignment of these and other resonances was done by also considering the experiments described below.

Addition of methanol to a 4 mM solution of $K_2[CH_2\{V^VO_2(sal-nah)\}_2]\cdot 2H_2O$ (**2.3**) in DMSO shifts the -533 ppm resonances to -538 ppm, identical to the spectrum of **2.3** in MeOH only. The signal at -538 ppm is assigned to $[CH_2\{VO_2(sal-nah)(MeOH)\}_2]^{2-}$ (**CII**, S = MeOH) in Scheme 2.3 [227, 228]

Upon addition of acid (HCl/HClO₄) viz. 1, 2, 3, 4 equiv to a methanolic solution of **2.3** leads to the decrease in intensity of the -538 ppm peak and an increase at -545 ppm peak (see Figure 2.2B), the color of solution turns to red and the pH ~ 2.5 to 3.3. The addition of acid may protonate the ligand so the -545 ppm band may either be due to (**CII**, S = H₂O) or to free vanadate (V_I). As addition of H₂O to the 4 mM solution of **2.3** in DMSO shows an upfield shift to -539 ppm, this indicating the involvement of the solvent molecule, we assign the -539 ppm signal of Figure 2B to $[CH_2\{V^VO(sal-nah)(H_2O)\}_2]^{2-}$ (**CII**, S = H₂O).

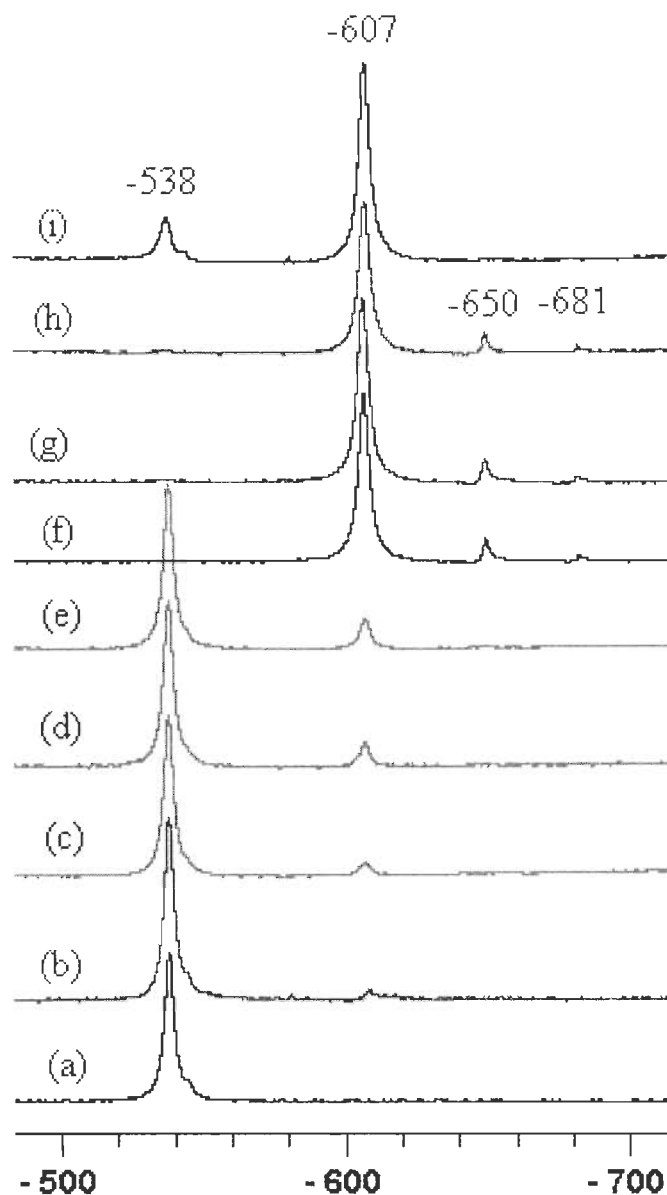


Figure 2.1. ^{51}V NMR spectra for solutions (ca. 4 mM) of $\text{K}_2[\text{CH}_2\{\text{V}^{\text{V}}\text{O}_2(\text{sal-nah})\}_2]\cdot 2\text{H}_2\text{O}$ (2.3): (a) in MeOH, and (b-h) after stepwise additions of an aqueous solution of 30% H_2O_2 ; (b) 0.5 equiv H_2O_2 added; (c) 2 equiv H_2O_2 (total) added; (d) 4.0 equiv H_2O_2 (total) added; (e) 6.0 equiv H_2O_2 (total) added; (f) 8.0 equiv H_2O_2 (total) added; (g) 10 equiv H_2O_2 (total) added; (h) solution of (g) after 2 h leaving tube open; (i) solution of (h) after 36 h leaving tube open.

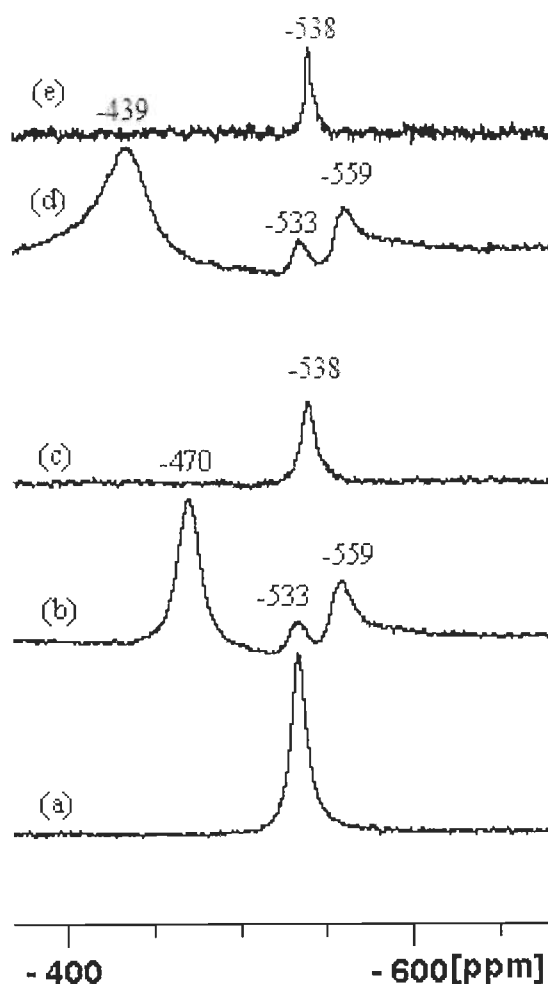


Figure 2.2A. ^{51}V NMR spectra for $\text{K}_2[\text{CH}_2\{\text{V}^{\text{V}}\text{O}_2(\text{sal-nah})\}_2]\cdot 2\text{H}_2\text{O}$ (**2.3**): (a) in DMSO (ca. 4 mM), (b) solution of (a) after addition of 3.0 equiv of an aqueous solution of HClO_4 (15.8 M), the pH being ~ 3.1 ; (c) solution of (b) after addition of MeOH, the solution now containing equal volumes of DMSO and MeOH; (d) solution of (a) after addition of 3.0 equiv of an aqueous solution of HCl (11.6 M), the pH being ~ 3.3 ; (e) solution of (d) after addition of MeOH, the solution now containing equal volumes of DMSO and of MeOH.

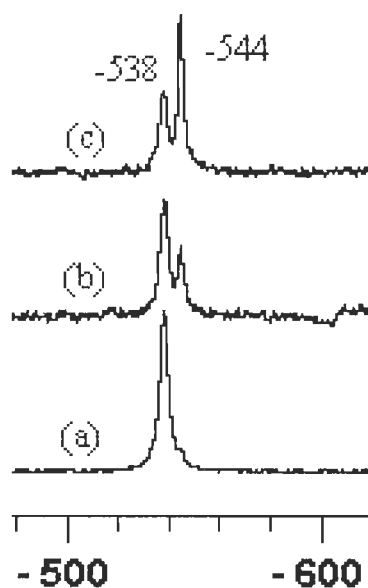


Figure 2.2B. ^{51}V NMR spectra for $\text{K}_2[\text{CH}_2\{\text{V}^{\text{V}}\text{O}_2(\text{sal-nah})\}_2]\cdot 2\text{H}_2\text{O}$ (**2.3**): (a) in MeOH, ca. 4 mM; (b) after addition of 2.0 equiv of an aqueous solution of HCl (11.6 M); (c) solution of spectrum (b) after standing for ca. 15h.

Upon the stepwise addition of an aqueous 30% solution of H_2O_2 to the methanolic solution of **2.3** (ca. 4 mM) the resonance at -538 ppm progressively disappears and resonances at -607 ppm are observed (Figure 1), which we tentatively assign as due to $[\text{CH}_2\{\text{V}^{\text{V}}\text{O}(\text{O}_2)(\text{sal-nah})\}_2]^{2-}$ (**CIII**). Upon further stepwise additions of H_2O_2 (8 equiv or higher) the resonance at -538 ppm totally disappears and two new signals are detected at $\delta = -651$ and -683 ppm, which we assign to inorganic peroxovanadates {tentatively $[\text{V}^{\text{V}}\text{O}(\text{O}_2)_2]^-$ (**CIV**)[229] and $[\text{V}^{\text{V}}\text{O}(\text{O}_2)_2(\text{H}_2\text{O})]^-$ (**CV**)[160, 230-235] (see Scheme 2.3). Leaving the NMR tube open for 36 h after recording the spectrum of Figure 1 (h), spectrum (i) was obtained, indicating the reversibility of the process.

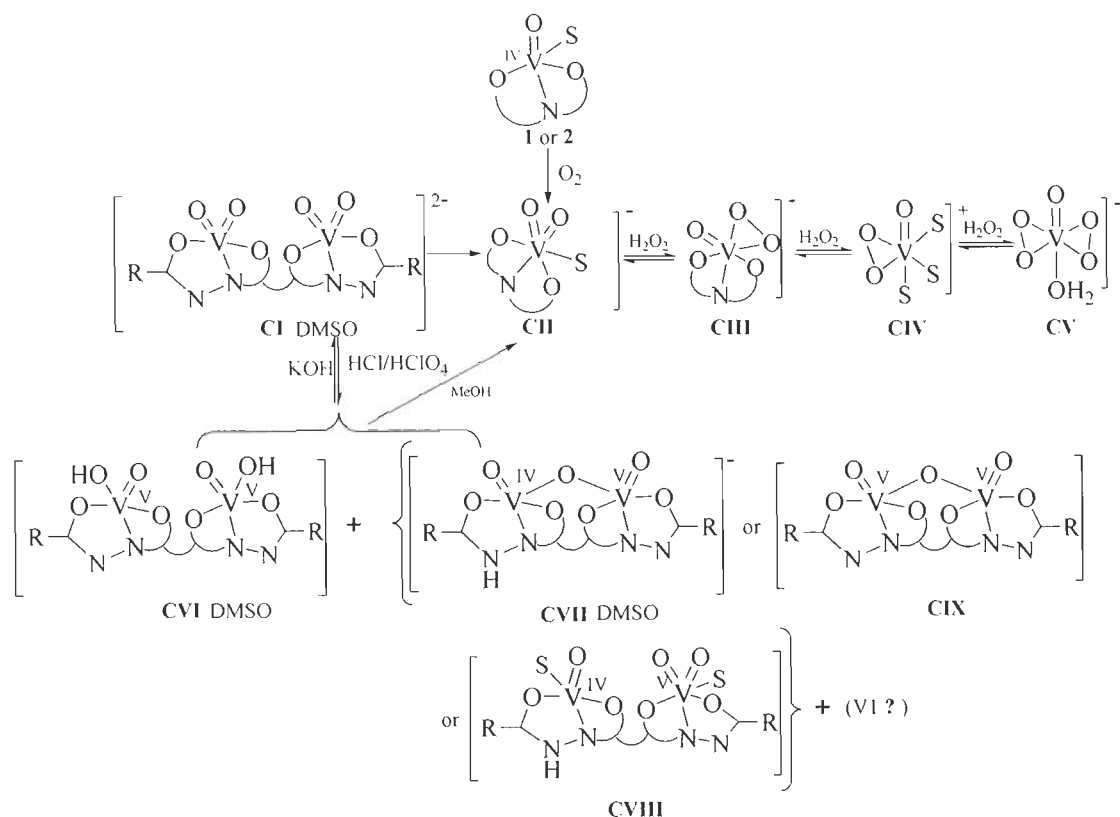
The behavior of $\text{K}_2[\text{CH}_2\{\text{V}^{\text{V}}\text{O}_2(\text{sal-nah})\}_2]\cdot 2\text{H}_2\text{O}$ (**2.3**) dissolved in DMSO differs from what was observed in methanol (Figure. 2.2). Upon addition of 3

equiv HClO_4 the ^{51}V NMR spectra shows two new signals at -470 (broad) (ca. 86 %) and -559 (ca. 9 %) ppm, as well as the original resonance at -533 (ca. 5%) ppm [Figure 2.2A (b), pH~ 3.1]. Similarly addition of 3 equiv HCl to the solution of **2.3** in DMSO yields two new signals at -439 (broad) (ca. 82%) and -559 (ca. 14%) ppm, as well as the original resonance at -533 (ca. 4%) ppm [Figure 2.2A (d)]. Similar results were obtained upon addition of H_2SO_4 instead of HCl or HClO_4 .

For further investigation both solutions of (b) and (d) in Figure 2.2A were divided in three parts. On addition of MeOH to one of these only the peak at -538 ppm [Figure 2.2 A (e)] is detected and this can be assigned to species (**CII**, S = MeOH). Addition of 4 equiv KOH to the second portion yields a resonance at -533 ppm indicating the reversibility of the reaction. The third portion of this solution was kept for 48 hr at room temperature and then showed a major resonance at -539 ppm corresponding to **CII**.

We assign the -559 ppm lower field resonances of Figure 2.2A (b) and (d) to the oxidohydroxo species (**CVI**). The partial protonation of the ligand is also a plausible possibility (see below).

Additionally the spectra of Figure 2.2A (b) and (d) show a global decrease and broadening of the ^{51}V NMR signals, indicating the presence of an oxidovanadium(IV) species in the solution, and this was confirmed by recording the EPR spectra for both solutions. The spectra are reasonably intense and the spin Hamiltonian parameters obtained are both similar to those of solutions of **2.1** in DMSO (see below) indicating a O_3N binding mode around the vanadium center, i.e. a binding mode identical to that of **2.1**.



Scheme 2.3.

To explain the peaks at ca. $-440/-475$ ppm, due to a V^{V} -species, we consider now three possibilities: (i) the formation of a mixed valence $\text{V}^{\text{IV}}\text{O}-\text{O}-\text{V}^{\text{V}}\text{O}$ complex (see structure **CVII** in Scheme 2.3), or (ii) a complex formulated as $[\text{CH}_2\{\text{V}^{\text{V}}\text{O}_2(\text{sal-fah})\}\{\text{V}^{\text{IV}}\text{O}_2(\text{sal-fah})\}]$ (see structure **CVIII**), (iii) the formation of a $\text{V}^{\text{V}}\text{O}-\text{O}-\text{V}^{\text{V}}\text{O}$ complex (see structure **CIX**), along with a V^{IV} -complex which corresponds to **2.1**. The ^{51}V NMR peaks in assignments (i) or (ii) correspond to the V^{V} -“half-part” of the molecule.

If a $\text{V}^{\text{IV}}\text{O}-\text{O}-\text{V}^{\text{V}}\text{O}$ complex such as represented in structure **CVII** is formed, the $\text{V}-\text{O}-\text{V}$ angle should not be close to 180° , so that the unpaired electron is localized on one of the V atoms of the $\text{V}-\text{O}-\text{V}$ dinuclear unit. To our knowledge there is no previous example of ^{51}V NMR signals being obtained for $\text{V}^{\text{IV}}\text{O}-\text{O}-\text{V}^{\text{V}}\text{O}$ complexes (or reports of attempts to measure it). In order that the $-440/-475$ ppm resonances may be assigned to the $\text{V}^{\text{V}}\text{O}_2$ -“half-part” of a species such as structure

CVIII, which correspond to significantly deshielded V^V -species, some electron density should have also been delocalized from the V^{IV} - to the V^V -centre and it is not clear if this is feasible in **CVIII**. Globally we consider structure **CIX** as a reasonable hypothesis of assignment for the $-440/-475$ ppm resonances; the different values recorded possibly resulting from some electrostatic influence of the counter-ions present (Cl^- , ClO_4^- or SO_4^{2-}) nearby.

The formation of $[CH_2\{V^V OL\}_2]$ complexes, containing the $V^V O^{3+}$ moiety, upon addition of acid, as reported for a few vanadium systems {e.g. salen and EHGS, ethylenebis[(o-hydroxyphenyl)glycine]} [236, 237] could be also a possibility to explain the ^{51}V NMR appearing at ca. -444 to -466 ppm. However, no strong CT band was observed in the 500-600 nm range for complexes with our ligands **2.I** and **2.II** (see below) as was found in the salen and EHGS systems, so we assume these high-field resonances are not due to the formation of $V^V OL$ -type complexes.

2.3.6. Solution behaviour of $Cs_2[CH_2\{V^V O_2(sal-nah)\}_2] \cdot 2H_2O$ (**2.4**)

Similar to $K_2[CH_2\{V^V O_2(sal-nah)\}_2] \cdot 2H_2O$ (**2.3**), complex **2.4** dissolved in MeOH shows two resonances at -537 and -544 ppm (Figure 2.3(a)), but the latter signal is more intense than the corresponding one in **2.3**. The major signal at -537 ppm is assigned to $[CH_2\{VO_2(sal-nah)(MeOH)\}_2]^{2-}$ (**CII**, $S = MeOH$) and the minor one is probably vanadate (V_I) or a complex resulting from protonation of the coordinated N-atom [238, 239]. Upon stepwise addition of 30% H_2O_2 (up to 8 equiv) resonances at -606 and -649 ppm are recorded, which we assign to **CIII** and **CIV**, respectively (Scheme 2.3). Leaving the solution of Figure 2.3(f) in contact with air spectrum (g) of Figure 2.3 was obtained after ca. 36 h indicating that the reactions are reversible. Addition of acid (HCl or $HClO_4$, e.g. 2 equiv) to a methanolic solution of **2.4** (see Figure 2.4) leads to the decrease in intensity of the -538 ppm peak and an increase of the -545 ppm peak. This may be due either to

protonation of the ligand, or to generation of **CII** ($S = H_2O$) or to free vanadate (V_I).

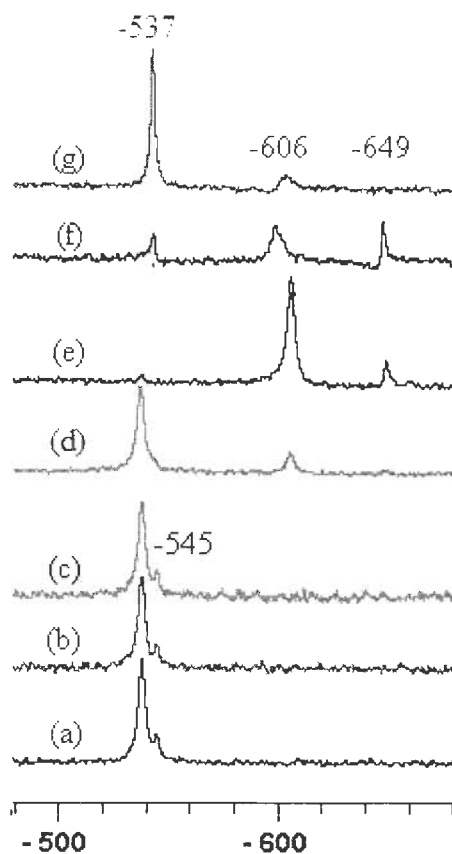


Figure 2.3. ^{51}V NMR spectra for $\text{Cs}_2[\text{CH}_2\{\text{V}^{\text{V}}\text{O}_2(\text{sal-nah})\}_2]\cdot 2\text{H}_2\text{O}$ (**2.4**): (a) in MeOH (ca. 4mM of **2.4**), and upon stepwise addition of aqueous 30% solution H_2O_2 : (b) 1.0 equiv H_2O_2 ; (c) 4.0 equiv H_2O_2 ; (d) 6.0 equiv H_2O_2 ; (e) 8.0 equiv H_2O_2 ; (f) solution of (e) after 24 h leaving the tube open (g) solution of (e) after 36 h of leaving the tube open.

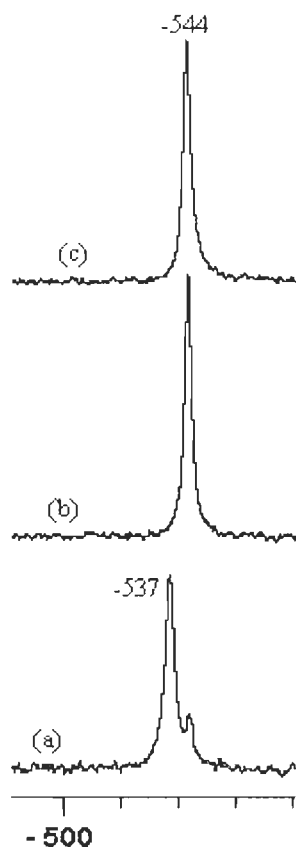


Figure 2.4. ^{51}V NMR spectra for $\text{Cs}_2[\text{CH}_2\{\text{V}^{\text{V}}\text{O}_2(\text{sal-nah})\}_2]\cdot 2\text{H}_2\text{O}$ (**2.4**): (a) in MeOH (ca. 4 mM of **2.4**), and after addition of an aqueous solution of HCl (11.6 M) (b) 1.0 equiv HCl and (c) 2.0 equiv HCl added.

In DMSO, complex **2.4** gives a resonance at ca. -532 ppm [Figure 2.5 (a) or (d)]. Addition of methanol and water yielded the up field resonances at -537 and -538 ppm, respectively, confirming the involvement of solvent molecules in these **CII**-species. Upon addition of 2 equiv of concentrated HCl solution two new resonances at -444 (ca. 35 %) and -559 (ca. 25 %) ppm appear along with the original resonance at -532 (ca. 30%) ppm. A similar behavior was observed upon addition of 2 equiv HClO_4 (or H_2SO_4). A broadening of the bands also occurs and rather intense EPR spectra could be recorded with the solutions of Figure 2.5 (b) and (d) confirming the formation of $\text{V}^{\text{IV}}\text{O}$ -complexes. The upfield resonance is assigned to the formation of an oxidohydroxovanadium(V) species at -559 ppm.

Addition of 4 equiv KOH to the solutions of Figure 2.5 (b) and (d) yielded only the resonance at -532 ppm, corresponding to **2.4** in DMSO, confirming the reversibility of reaction. Addition of methanol to the solutions of Figure 2.5 (b) and (d) yielded resonances at -539 ppm corresponding to the dioxido species (**CII**, $S = \text{MeOH}$). The EPR spectra of the solutions of Figure 2.5 (b) and (d) were simulated [218] and the data indicates that the binding mode of the $\text{V}^{\text{IV}}\text{O}$ -species present is identical to that of complex **2.1** in DMSO (see below). The broad downfield resonance is assigned as in the case of complex **2.3**, (see Scheme 2.3 and the above discussion regarding structures **CVII-CIX**).

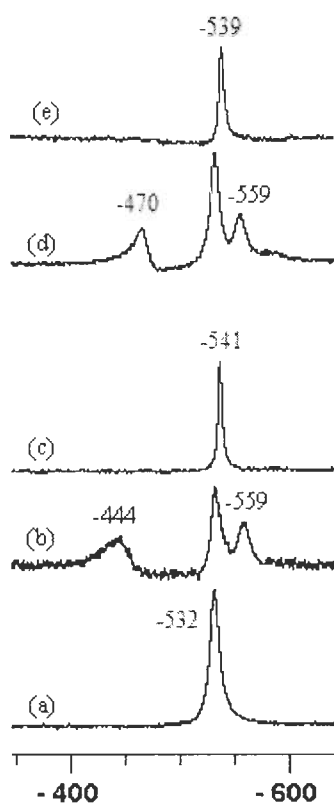


Figure 2.5. ^{51}V NMR spectra for $\text{Cs}_2[\text{CH}_2\{\text{V}^{\text{V}}\text{O}_2(\text{sal-nah})\}_2]\cdot 2\text{H}_2\text{O}$ (**2.4**): (a) in DMSO and after additions of aqueous acids: (b) 2.0 equiv HCl and (d) 2.0 equiv HClO_4 . Upon addition of MeOH to the solutions of spectra (b) and (d) so that the mixtures contain equal volumes of MeOH and DMSO, spectra (c) and (e), respectively, were recorded.

2.3.7. Solution behavior of $\text{Cs}_2[\text{CH}_2\{\text{V}^{\text{V}}\text{O}_2(\text{sal-inh})\}_2]\cdot 2\text{H}_2\text{O}$ (2.5)

Similarly to the previous observations with $\text{K}_2[\text{CH}_2\{\text{V}^{\text{V}}\text{O}_2(\text{sal-nah})\}_2]\cdot 2\text{H}_2\text{O}$ (2.3) $\text{Cs}_2[\text{CH}_2\{\text{V}^{\text{V}}\text{O}_2(\text{sal-nah})\}_2]\cdot 2\text{H}_2\text{O}$ (2.4), the ^{51}V NMR spectrum of $\text{Cs}_2[\text{CH}_2\{\text{V}^{\text{V}}\text{O}_2(\text{sal-inh})\}_2]\cdot 2\text{H}_2\text{O}$ (2.5) dissolved in MeOH [Figures 2.6(a) and 2.7(a)] shows signals at -539 and -545 ppm, assigned to [CII, S = MeOH and H_2O (and free vanadate)]. Upon addition of aqueous solutions of either HCl or HClO_4 [2 equiv of acid] a peak at -545 ppm was detected which at least partly may correspond to vanadate (Figure 2.7). Formation of the peroxo-complex (CIII) and bisperoxo species (CIV) at -606 and -649 ppm, respectively, was confirmed upon addition of aqueous solution of 30% H_2O_2 (1, 2, and 10 equiv).

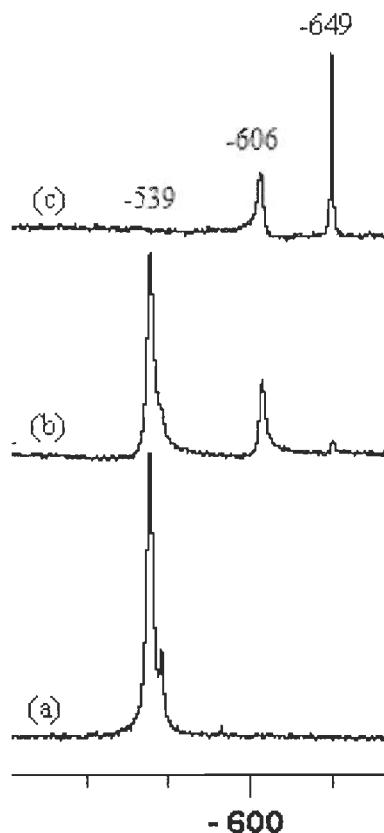


Figure 2.6. ^{51}V NMR spectra for $\text{Cs}_2[\text{CH}_2\{\text{V}^{\text{V}}\text{O}_2(\text{sal-inh})\}_2]$ (2.5): (a) in MeOH, and after addition of aqueous 30% solution of H_2O_2 : (b) 3.0 equiv H_2O_2 and (c) 5.0 equiv H_2O_2 .

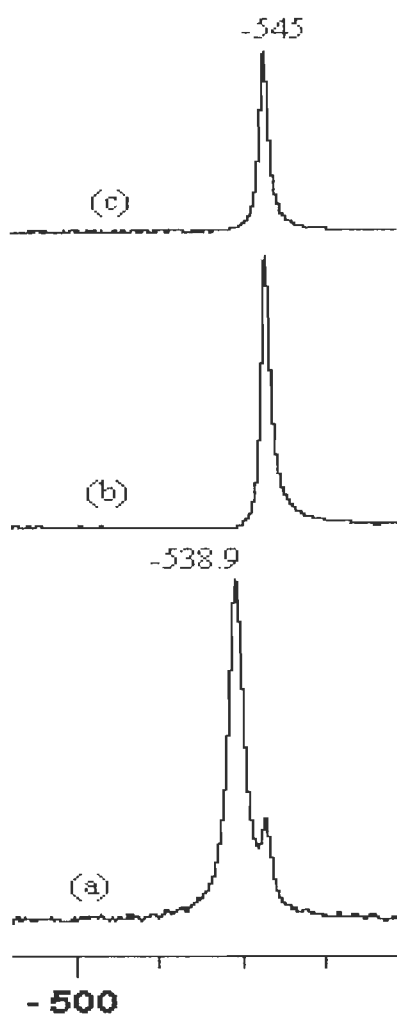


Figure 2.7. ^{51}V NMR spectra for $\text{Cs}_2[\text{CH}_2\{\text{V}^{\text{V}}\text{O}_2(\text{sal-inh})\}_2]$ (**2.5**): (a) in MeOH and after addition of an aqueous solution (11.6 M) of HCl; (b) 1.0 equiv HCl; (c) 2.0 equiv HCl.

In DMSO (Figure 2.8), complex **2.5** shows a resonance at -532 ppm. On addition of 2 equiv of HCl, resonances at -443 (ca. 13 %) and -557 (ca. 37 %) ppm appear. Similarly, addition of 2 equiv HClO_4 yields peaks at -466 (ca. 27 %) and -557 (ca. 24 %) ppm. The broadening of resonances indicates the presence of V^{IV} -species in solution. Upon addition of 4 equiv KOH only a resonance at -532

ppm is detected, corresponding to complexes **CII** (Scheme 2.3), confirming the reversibility of the processes. Upon addition of methanol to the solution of Figure 2.8 (b) only a resonance at -539 ppm is recorded, which corresponds to (**CII**, S = MeOH). Thus, in DMSO the behavior of complex **2.5** is very similar to what was recorded for complexes **2.3** and **2.4**.

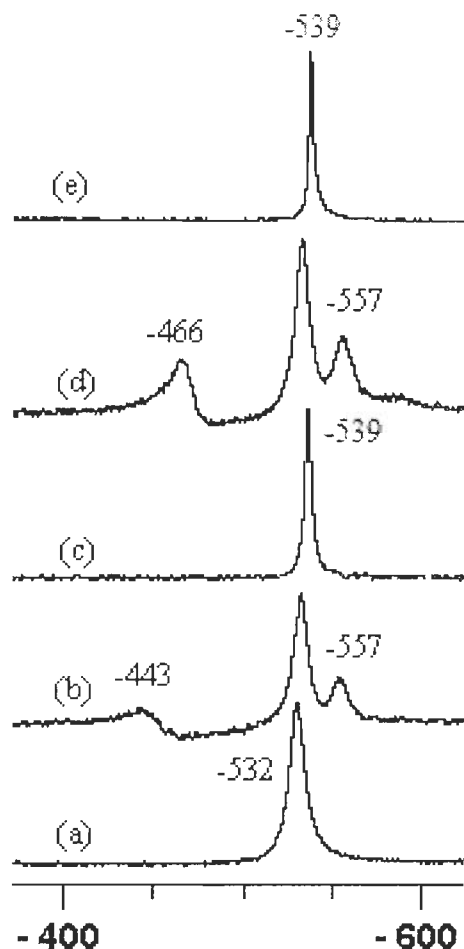


Figure 2.8. ^{51}V NMR spectra for $[\text{Cs}(\text{H}_2\text{O})]_2[\text{CH}_2\{\text{V}^{\text{V}}\text{O}_2(\text{sal-inh})\}_2]$ (**2.5**): (a) in DMSO and after additions of aqueous of either HCl or HClO_4 : (b) 2.0 equiv HCl and (d) 2.0 equiv HClO_4 . Upon addition of MeOH to the solutions of spectra (b) and of (d) so that the mixtures contain equal volumes of MeOH and DMSO, spectra (c) and (e), respectively, were recorded.

EPR and UV/Vis Study

The EPR spectra of “frozen” solutions (77 K) in DMSO of complexes $[\text{CH}_2\{\text{V}^{\text{IV}}\text{O}(\text{sal-nah})(\text{H}_2\text{O})\}_2]$ (**2.1**) and $[\text{CH}_2\{\text{V}^{\text{IV}}\text{O}(\text{sal-inh})(\text{H}_2\text{O})\}_2]$ (**2.2**) are depicted in Figure 2.9. Two sets of eight line spectra showing hyperfine splitting due to the ^{51}V nucleus are obtained, characteristic of square pyramidal complexes with an axially compressed d_{xy}^1 configuration. The spectra were simulated and the spin Hamiltonian parameters obtained [218] are included in Table 2.5.

The value of A_{\parallel} can be calculated using the additivity relationship [$A_{\parallel}^{\text{est}} = \sum A_{\parallel,i}$ ($i = 1$ to 4)] proposed by Wurthrich [240] and Chasteen [241], with estimated accuracy of $\pm 3 \times 10^{-4} \text{ cm}^{-1}$. The A_{\parallel} values obtained for **2.1** and **2.2** (Table 2.3) agree with the values calculated from the partial contributions of the equatorial donor groups: H_2O ($45.7 \times 10^{-4} \text{ cm}^{-1}$), $\text{O}_{\text{phenolate}}$ ($38.9 \times 10^{-4} \text{ cm}^{-1}$), N_{imine} , (38.1 to $43.7 \times 10^{-4} \text{ cm}^{-1}$), $\text{O-enolate}^{(1-)}$ ($37.6 \times 10^{-4} \text{ cm}^{-1}$), O_{DMSO} ($41.9 \times 10^{-4} \text{ cm}^{-1}$), O_{MeOH} ($45.7 \times 10^{-4} \text{ cm}^{-1}$) [242, 243].

Table 2.5. Spin Hamiltonian parameters obtained by simulation of the experimental EPR spectra recorded for DMSO solutions of complexes $[\text{CH}_2\{\text{V}^{\text{IV}}\text{O}(\text{sal-nah})(\text{H}_2\text{O})\}_2]$ (**2.1**) and $[\text{CH}_2\{\text{V}^{\text{IV}}\text{O}(\text{sal-inh})(\text{H}_2\text{O})\}_2]$ (**2.2**) at 77K.

Complex	Solvent	g_{\parallel}	$A_{\parallel} \times 10^4 / \text{cm}^{-1}$	g_{\perp}	$A_{\perp} \times 10^4 / \text{cm}^{-1}$
$[\text{CH}_2\{\text{V}^{\text{IV}}\text{O}(\text{sal-nah})(\text{H}_2\text{O})\}_2]$	DMSO	1.951	163.3	1.980	56.7
	MeOH	1.948	166.4	1.979	57.5
0.5 equiv H_2O_2	MeOH	1.936	177.8	1.977	66.0
$[\text{CH}_2\{\text{V}^{\text{IV}}\text{O}(\text{sal-inh})(\text{H}_2\text{O})\}_2]$	DMSO	1.951	162.3	1.981	56.8
	MeOH	1.949	165.9	1.979	57.4
0.5 equiv H_2O_2	MeOH	1.935	178.0	1.977	66.2

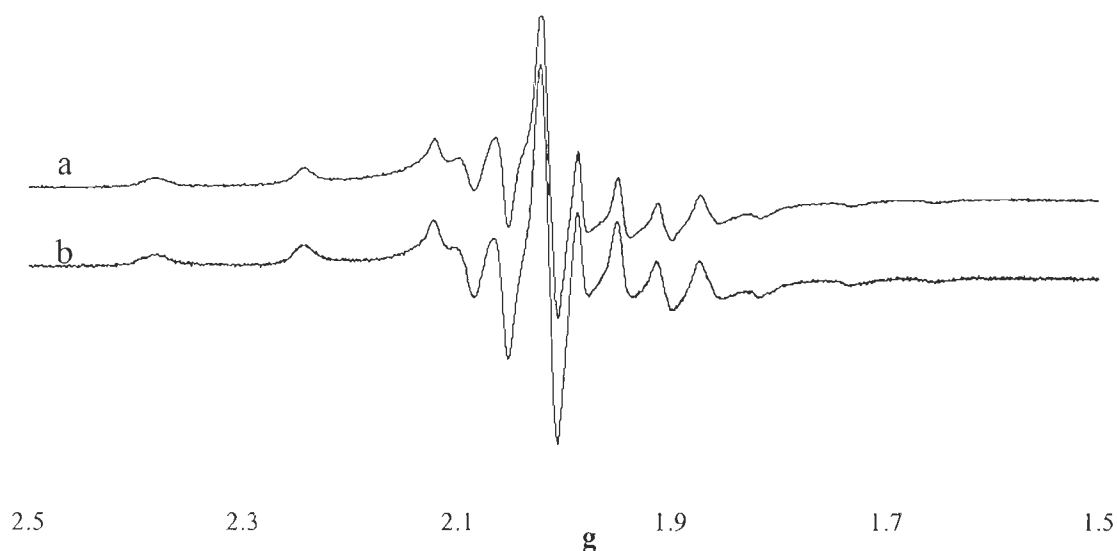


Figure 2.9. EPR spectra of frozen solution (4 mM) samples of $[\text{CH}_2\{\text{V}^{\text{IV}}\text{O}(\text{sal-nah})(\text{H}_2\text{O})\}_2]$ (**2.1**) (a) and $[\text{CH}_2\{\text{V}^{\text{IV}}\text{O}(\text{sal-inh})(\text{H}_2\text{O})\}_2]$ (**2.2**) (b) in DMSO.

The EPR spectra of both complexes in DMSO are in good agreement with an O_3N binding mode, one of the equatorial donor atoms being O_{DMSO} . The effect of solvent on EPR parameters was examined by also measuring the spectra in MeOH (e.g. Figure 2.10). As indicated in Table 2.5 for **2.1** the g_{\parallel} decrease from 1.951 to 1.948 and A_{\parallel} increase from 163.3 to 166.4, this being compatible with the substitution of one coordinated O_{DMSO} by O_{MeOH} [243]. Similar data was obtained for **2.2** (Table 2.5).

Addition of H_2O_2 portions to solutions of $[\text{CH}_2\{\text{V}^{\text{IV}}\text{O}(\text{sal-nah})(\text{H}_2\text{O})\}_2]$ (**2.1**) or $[\text{CH}_2\{\text{V}^{\text{IV}}\text{O}(\text{sal-inh})(\text{H}_2\text{O})\}_2]$ (**2.2**) in MeOH acidifies the solutions and different $\text{V}^{\text{IV}}\text{O}$ -species form with EPR parameters ($g_{\parallel} = 1.936$, $A_{\parallel} = 177.8 \times 10^{-4}$

cm^{-1} for **2.1**, and $g_{\parallel} = 1.935$, $A_{\parallel} = 178.0 \times 10^{-4} \text{ cm}^{-1}$ for **2.2**); the $\text{V}^{\text{IV}}\text{O}$ is also progressively oxidized to V^{V} (Figures 2.11 and 2.12). According to the g_{\parallel} and A_{\parallel} values obtained for these partially oxidized solutions, in these $\text{V}^{\text{IV}}\text{O}$ -species the binding mode is probably O_4 , the $\text{V}^{\text{IV}}\text{O}$ -complexes being extensively hydrolyzed.

Upon leaving solutions of $[\text{CH}_2\{\text{V}^{\text{IV}}\text{O}(\text{sal-nah})(\text{H}_2\text{O})\}_2]$ (**2.1**) or $[\text{CH}_2\{\text{V}^{\text{IV}}\text{O}(\text{sal-inh})(\text{H}_2\text{O})\}_2]$ (**2.2**) in DMSO in contact with air, after ca. 3 – 4 days ^{51}V NMR resonances were recorded at ca. -532 ppm (Figure 2.12). $\text{V}^{\text{V}}\text{O}_2$ -complexes therefore form with signals similar to those recorded for DMSO solutions of **2.3**, **2.4** and **2.5**. The stepwise addition of aqueous H_2O_2 solution (1, 2, 3, 4, 5 equiv) peaks at ca. -597 and -648 ppm were obtained, corresponding to the peroxo-complex (**CIII**) and the bisperoxo species (**CIV**), respectively. Subsequent addition of 10 equiv methyl phenyl sulfide produced after ca. 12 hr the resonance at -539 ppm corresponding to dioxido species (**CII**, $\text{S} = \text{MeOH}$) supporting the reversibility of the processes

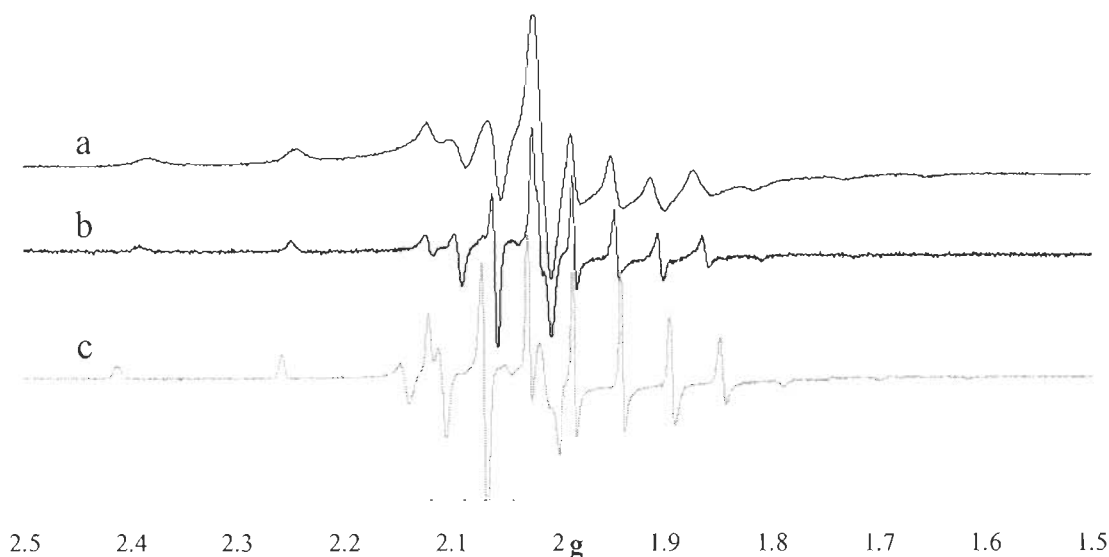


Figure 2.10. 1st derivative EPR spectra (at 77 K) of a solution of $[\text{CH}_2\{\text{VO}(\text{sal-nah})(\text{H}_2\text{O})\}_2]$ (**2.1**): (a) in DMSO (ca. 4 mM); (b) after addition of an equal volume of MeOH; (c) after addition of 0.5 equiv of an aqueous 30% H_2O_2 solution.

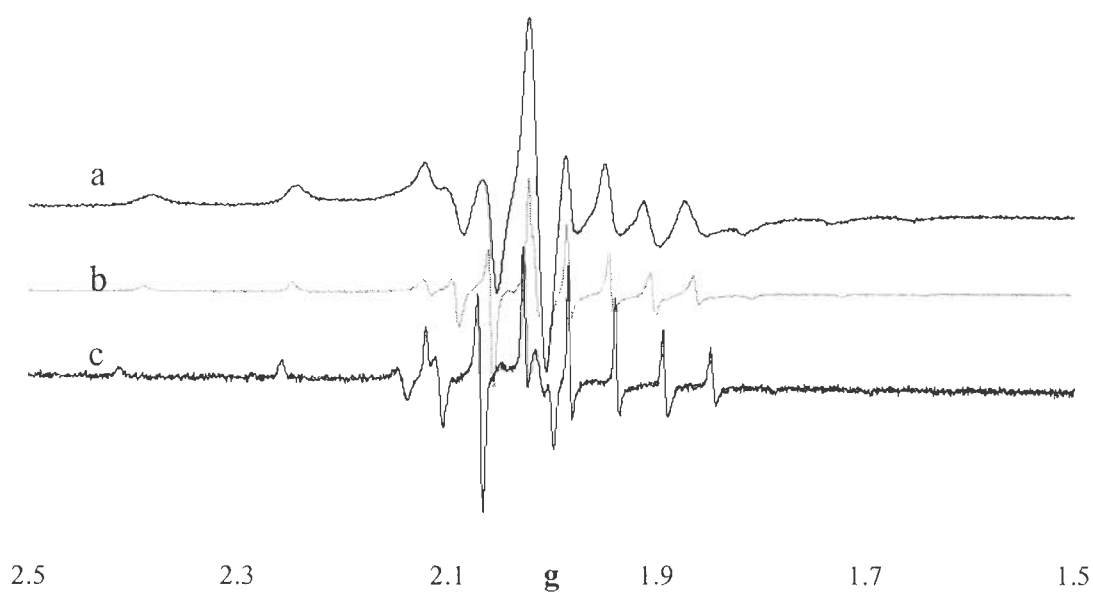


Figure 2.11. 1st derivative EPR spectra (at 77 K) of a solution of $[\text{CH}_2\{\text{V}^{\text{IV}}\text{O}(\text{salinh})(\text{H}_2\text{O})\}_2]$ (**2.2**): (a) in DMSO (ca. 4 mM); (b) after addition of an equal volume of MeOH; (c) after addition of 0.5 equiv of an aqueous 30% H_2O_2 solution (see text).

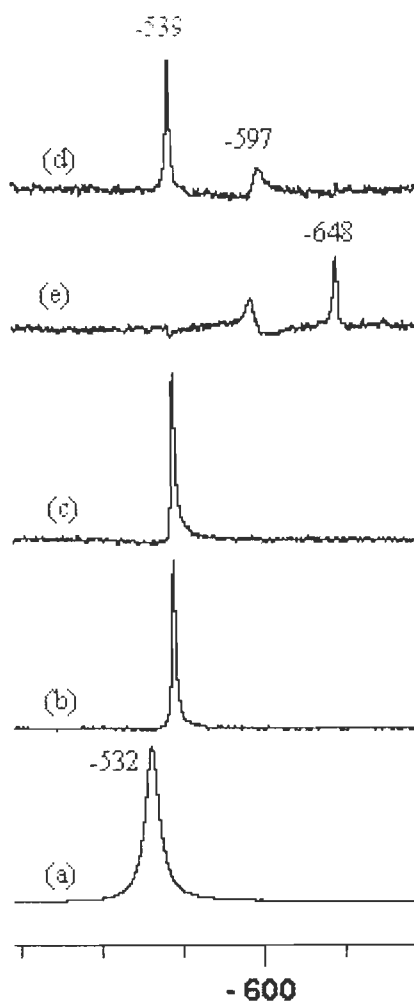


Figure 2.12. ^{51}V NMR spectra for $[\text{CH}_2\{\text{V}^{\text{IV}}\text{O}(\text{sal-inh})(\text{H}_2\text{O})\}_2]$ (**2.2**): (a) in DMSO after standing in air for 3 days, (b) upon adding 2.0 equiv H_2O_2 ; (c) upon adding 3.0 equiv H_2O_2 (total); (e) upon adding 5.0 equiv H_2O_2 ; (d) after 12 h of adding 10 equiv methyl phenyl sulfide addition to solution of (e).

The formation of peroxo complexes in methanol by treatment of the respective dioxido complexes with H_2O_2 could be also established by electronic absorption. Thus, the addition of 30 % aqueous H_2O_2 (30 drops, 18.04 mmol) to 20 mL of ca. 4.135×10^{-5} M solution of $\text{Cs}_2[\text{CH}_2\{\text{V}^{\text{V}}\text{O}_2(\text{sal-inh})\}_2] \cdot 2\text{H}_2\text{O}$ (**2.5**), and recording the spectral changes after every 25 min resulted in the spectra

presented in Figure 2.13. The band at 412 nm slowly shifted to 415 nm along with a decrease in intensity. The two UV bands appearing at 232 and 282 nm (not within the scale in the figure) increase in intensity while the 328 nm band becomes a shoulder. A band at ca. 470 nm slightly increases its intensity. This change in spectra is interpreted as the formation of a peroxo compound. Similar spectral changes were recorded with solutions of **2.3** and **2.4** upon similar treatment (see Figures 2.14 and 2.15).

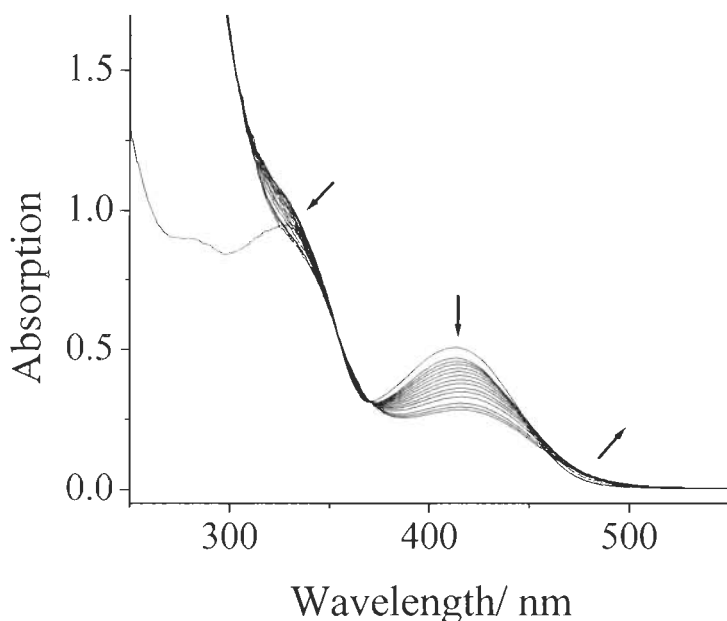


Figure 2.13. UV-Vis spectrum of 20 mL of ca. 4.135×10^{-5} M methanolic solution of $\text{Cs}_2[\text{CH}_2\{\text{V}^{\text{V}}\text{O}_2(\text{sal-inh})\}_2] \cdot 2\text{H}_2\text{O}$ (**2.5**) and spectral changes observed with time after addition of 30 % aqueous H_2O_2 (30 drops, 18.04 mmol). Each spectrum was recorded with 25 min interval.

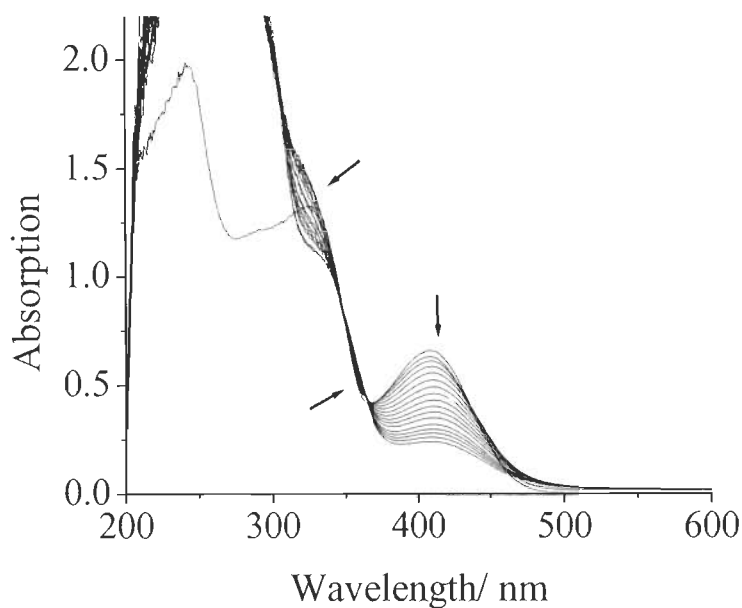


Figure 2.14. UV-Vis spectrum of 20 mL of ca. 5×10^{-5} M methanolic solution of ca. 5×10^{-5} M of $\text{K}_2[\text{CH}_2\{\text{V}^{\text{V}}\text{O}_2(\text{sal-nah})\}_2] \cdot 2\text{H}_2\text{O}$ (**2.3**) and spectral changes observed with time after addition of 30 % aqueous H_2O_2 (30 drops, 18.04 mmol). Each spectrum was recorded with 25 min interval.

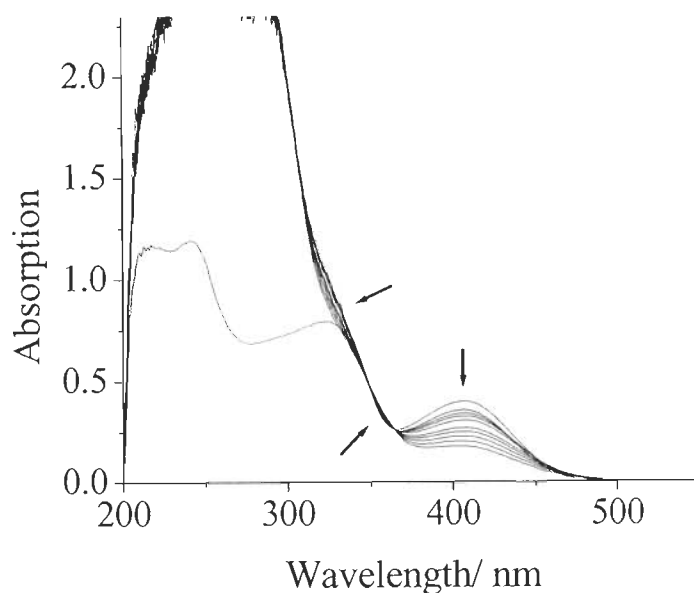


Figure 2.15. UV-Vis spectrum of 20 mL of ca. 5×10^{-5} M methanolic solution of $\text{Cs}_2[\text{CH}_2\{\text{V}^{\text{V}}\text{O}_2(\text{sal-nah})\}_2] \cdot 2\text{H}_2\text{O}$ (**2.4**) and spectral changes observed with time after addition of 30 % aqueous H_2O_2 (30 drops, 18.04 mmol). Each spectrum was recorded after every 25 min interval.

The reactivity of methanolic solutions of dioxidovanadium(V) complexes with HCl was also monitored by electronic absorption spectroscopy. Thus the drop-wise addition of HCl gas saturated in methanol to a 20 mL of 6.535×10^{-5} M solution of Cs $[\text{CH}_2\{\text{V}^{\text{V}}\text{O}_2(\text{sal-inh})\}_2] \cdot 2\text{H}_2\text{O}$ (**2.5**) caused the darkening of the solution along with an increase in intensity of the 279 nm band and its transformation into a shoulder (Figure 2.16). The other UV bands at 274 and 298 nm only gain intensity. The band appearing at 412 nm apparently progressively broadens with decrease in its intensity, while the band at ca. 470 nm increases intensity. Very similar features have been observed with **2.3** and **2.4** upon similar treatment (Figures 2.17 and 2.18).

As done by other authors for other systems [231, 244-246], we interpret these results in terms of the formation of an oxido-hydroxo species $[\text{CH}_2\{\text{VO}(\text{OH})(\text{L})\}_2]$. It is possible that the ligand might also protonate, complexes $[\text{CH}_2\{\text{VO}_2(\text{HL})(\text{S})\}_2]$ being formed. Protonation of the hydrazone nitrogen has been reported, e.g. for the structurally characterized complex $[\text{VO}(\text{Hsal-bhz})]$ ($\text{H}_2\text{sal-bhz}$ derives from salicylaldehyde and benzoylhydrazide), which forms on treatment of the corresponding anionic dioxido complex with HCl [238], as well as for complex $[\text{VO}(\text{salim})(\text{acac})]$ (salim = a Schiff base ligand also containing imidazole), where the EPR and ESEEM spectra recorded upon addition of acid were explained by the protonation of the imine N-atom [239].

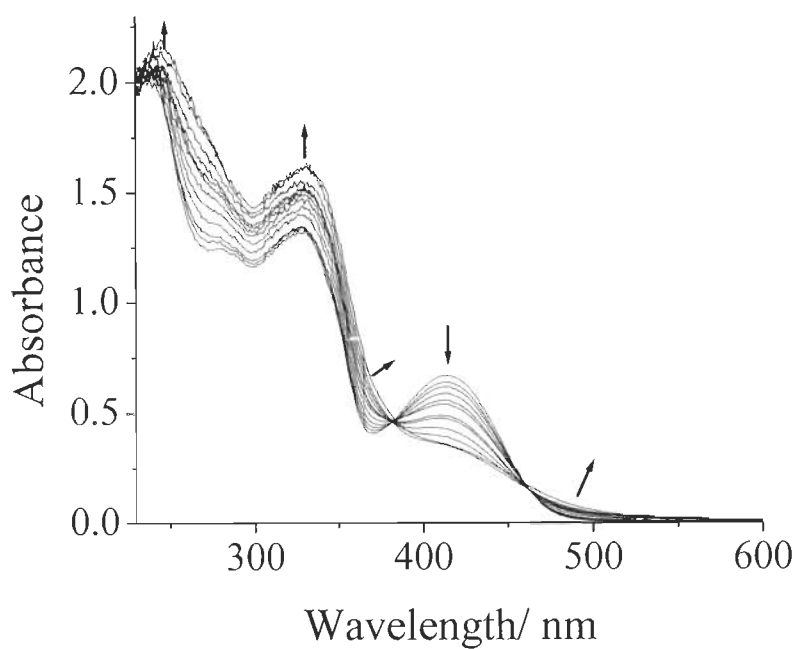


Figure 2.16. Spectral changes obtained during titration of 20 mL of 6.535×10^{-5} M methanolic solution of $\text{Cs}_2[\text{CH}_2\{\text{V}^{\text{V}}\text{O}_2(\text{sal-inh})\}_2] \cdot 2\text{H}_2\text{O}$ (**2.5**) with HCl gas saturated in methanol; the spectra were recorded after the successive additions of 1-drop portions.

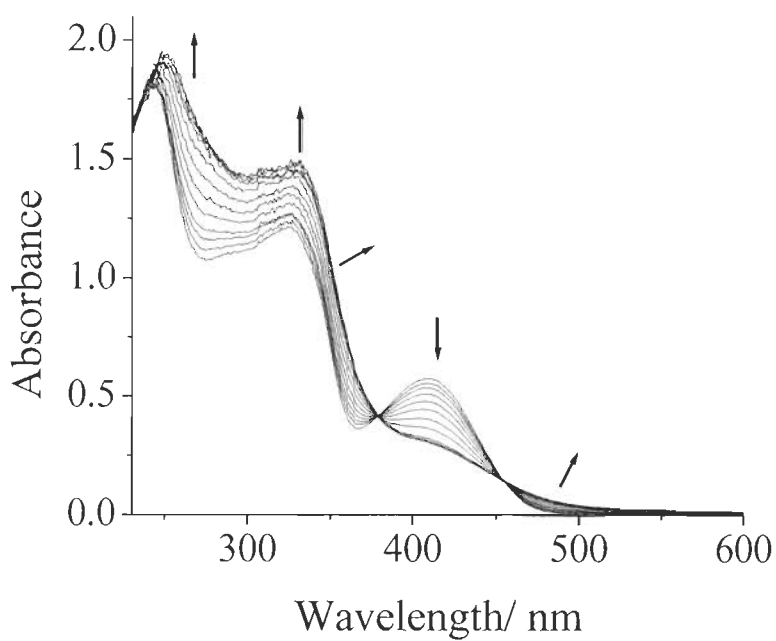


Figure 2.17. Spectral changes obtained during titration of 20 mL of 5×10^{-5} M methanolic solution of $\text{K}_2[\text{CH}_2\{\text{V}^{\text{V}}\text{O}_2(\text{sal-nah})\}_2] \cdot 2\text{H}_2\text{O}$ (**2.3**) with HCl gas saturated in methanol; the spectra were recorded after the successive addition of 1-drop portions

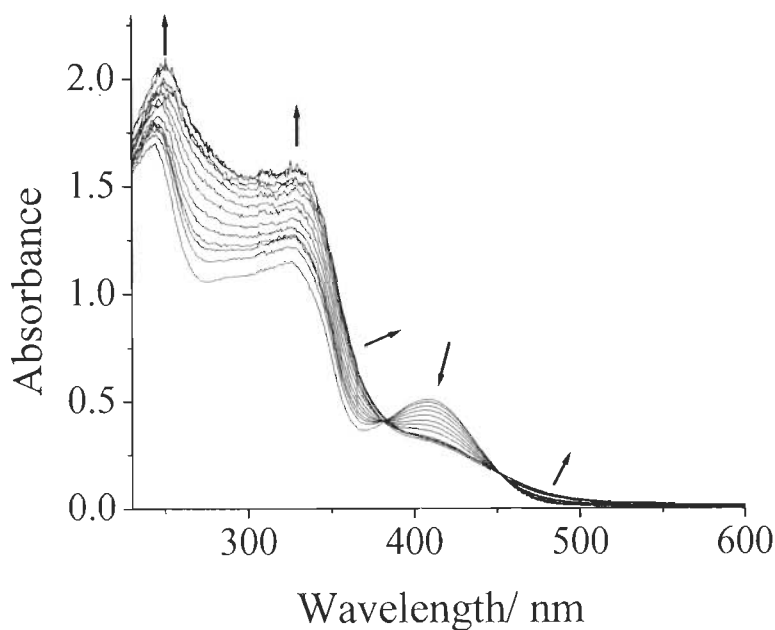


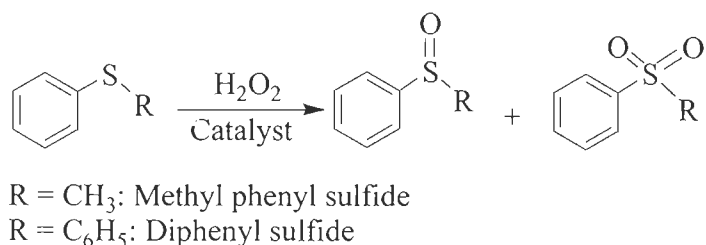
Figure 2.18. Spectral changes obtained during titration of 20 mL of 5×10^{-5} M methanolic solution of $\text{Cs}_2[\text{CH}_2\{\text{V}^{\text{V}}\text{O}_2(\text{sal-nah})\}_2] \cdot 2\text{H}_2\text{O}$ (**2.4**) with HCl gas saturated in methanol; the spectra were recorded after the successive addition of 1-drop portions.

2.3.8. Catalytic activity studies

Oxidation of Methyl phenyl sulfide and Diphenyl sulfide

It is known that several vanadium dependent haloperoxidases also catalyze sulfoxidations [242, 247, 248]. We tested complexes $[\text{CH}_2\{\text{V}^{\text{IV}}\text{O}(\text{sal-nah})(\text{H}_2\text{O})\}_2]$

(**2.1**) and $[\text{CH}_2\{\text{V}^{\text{IV}}\text{O}(\text{sal-inh})(\text{H}_2\text{O})\}_2]$ (**2.2**) as catalyst precursors taking methyl phenyl sulfide and diphenyl sulfide to model these reactions using aqueous 30% H_2O_2 as oxidant (Scheme 2.4). Among the two complexes studied, **2.1** was chosen as a representative one and the amount of catalyst precursor and oxidant were varied to obtain maximum conversion (based on substrate consumption). The effect of H_2O_2 was studied (Figure 2.19) considering substrate to oxidant ratios of 1:1, 1:2 and 1:3 for the fixed amount of catalyst (0.015 g) and substrate (1.24 g 10 mmol) in petroleum ether (10 mL), and the reaction was monitored at room temperature. Thus, in 7 h of contact time, on increasing the substrate to oxidant ratios from 1:1 to 1:2 the conversion increases from 11.4 % to 99.6 %. Increasing this ratio to 1:3 did not improve conversion except the completion of the reaction within 6 h and slight change in the selectivity of products.



Scheme 2.5. Oxidation of Organic sulfides.

Similarly four different amounts of catalyst precursor viz. 0.005, 0.015, 0.025, 0.035 g were taken at fixed reaction conditions optimized as above {i.e. substrate (1.24 g, 10 mmol), H_2O_2 (2.27 g, 20 mmol) and petroleum ether (10 mL)} to see the effect of amount of catalyst on the reaction and results are presented in Figure 2.20. It is clear from the figure that 0.015 g of catalyst was sufficient enough to give 99.6% conversion with a turn over frequency of 57.1 h^{-1} . Higher amount of catalyst only reduced the time in achieving the steady state of the reaction.

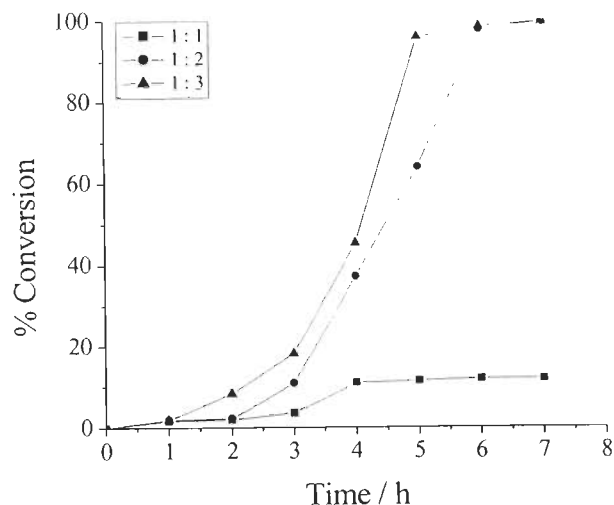


Figure 2.19. Effect of oxidant on the oxidation of methyl phenyl sulfide. Reaction conditions: methylphenyl sulfide (1.24 g, 10 mmol), catalyst $[\text{CH}_2\{\text{V}^{\text{IV}}\text{O}(\text{sal-nah})(\text{H}_2\text{O})\}_2]$ (**2.1**) (0.015 g) and petroleum ether (10 ml).

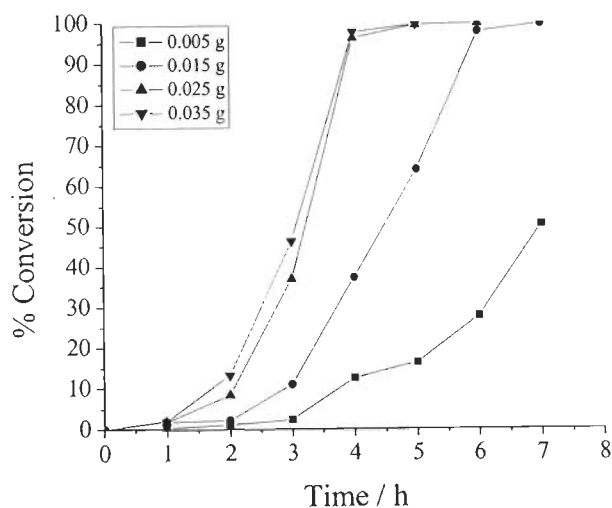


Figure 2.20. Effect of catalyst $[\text{CH}_2\{\text{V}^{\text{IV}}\text{O}(\text{sal-nah})(\text{H}_2\text{O})\}_2]$ (**2.1**) on the oxidation of methyl phenyl sulfide. Reaction conditions: methyl phenyl sulfide (1.24 g, 10 mmol), H_2O_2 (2.27 g, 20 mmol) and petroleum ether (10 ml).

Therefore, from these experiments, the best reaction conditions for the maximum oxidation of methyl phenyl sulfide are considered to be: substrate (1.24

g, 10 mmol), catalyst (0.015 g), H₂O₂ (2.27 g, 20 mmol) and petroleum ether (10 mL). The other substrate (diphenyl sulfide) using [CH₂{V^{IV}O(sal-nah)(H₂O)}₂](**2.1**) as catalyst precursor under the above reaction conditions, as well as the other catalyst precursor [CH₂{V^{IV}O(sal-inh)(H₂O)}₂](**2.2**) for both substrates were also tested and the corresponding results are summarized in Table 2.6.

From the Table, it is clear that more than 99 % methyl phenyl sulfide was converted into products using both catalysts, while diphenyl sulfide was only converted by 62.8 – 68.4 % under the conditions used. Normally, two major products, sulfoxide and sulfone, were obtained in major yield along with only small amounts (<0.4 %) of an unidentified product. The selectivity of the major product (sulfone) is ca. 85% while that of sulfoxide is ca. 15 % in all cases. In the absence of the catalyst, the reaction mixture gave 35.3% conversion of methyl phenyl sulfide with 65.5 % selectivity towards sulfoxide, 34.2% towards sulfone and ca. 0.3 % an unidentified product. Blank reaction with diphenyl sulfide under the above reaction conditions gave ca. 5 % conversion with selectivity sulfoxide : sulfone of 57 : 43. Thus, catalysts not only improve the conversion of substrates, they alter the selectivity of the products as well.

The conversion of methyl phenyl sulfide and the selectivity of different reaction products using [CH₂{V^{IV}O(sal-nah)(H₂O)}₂](**2.1**) as catalyst under the optimised reaction conditions have been analysed as a function of time and are presented in Figure 2.21. It is clear from the plot that the formation of methyl phenyl sulfoxide is good (75.6%) at the beginning but decreases considerably with time being 16.8 % after 7 h of reaction time. The selectivity of methyl phenyl sulfone is 24.2 % after 1h of reaction time and reaches to 83.0 % after 7 h. The unidentified product which is only in minor amount remains nearly constant throughout.

Table 2.6. Percent conversion^a of methyl phenyl sulfide and diphenyl sulfide along with the turn over frequency and selectivity of the reaction products after 7 h of reaction time.

Entry No.	Catalyst	Substrate ^b	% Conv.	TOF (h ⁻¹)	Selectivity %		
					Sulfoxide	Sulfone	others
1	1	mps	99.6	62.6	16.8	82.5	0.2
2	1	dps	68.4	45.0	15.4	84.5	0.2
3	2	mps	99.2	62.4	13.3	86.3	0.4
4	2	dps	62.8	39.4	14.3	85.4	0.4
5	-	mps	35.5	-	65.5	34.2	0.3
6	-	dps	5.0	-	57.0	43.0	-

^aReaction conditions: substrate (10 mmol), catalyst (0.015 g), H₂O₂ (2.27 g, 20 mmol) and petroleum ether (10 mL), room temperature. ^bmps = methyl phenyl sulfide, dps = diphenyl sulfide

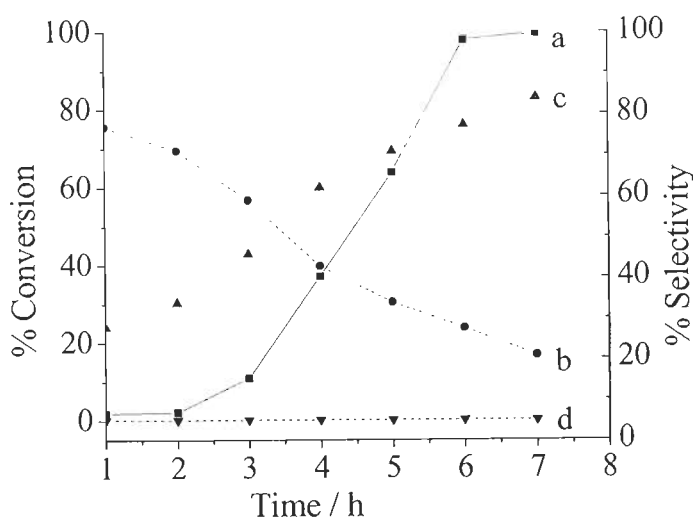


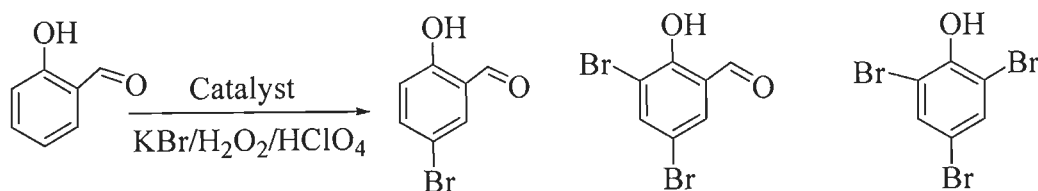
Figure 2.21. Conversion of methyl phenyl sulfide and variation in the selectivity of different reaction products as a function of time using [CH₂{V^{IV}O(sal-nah)(H₂O)}₂] (**2.1**) as catalyst: (a) conversion of methyl phenyl sulfide, (b) selectivity of methyl phenyl sulfoxide, (c) selectivity of methyl phenyl sulfone and (d) other unidentified product.

Oxidative Bromination of Salicylaldehyde

It is known that vanadium(V) complexes can also act as functional models of vanadium dependent haloperoxidases catalyzing the oxidative bromination of organic substrates in the presence of H_2O_2 and bromide ion [241, 242, 249]. During oxidation vanadium coordinates with 1 or 2 equivalents of H_2O_2 , forming oxido-monoperoxido, $[\text{CH}_2\{\text{V}^{\text{V}}\text{O}(\text{O}_2)(\text{L})\}_2]^{2-}$ **CIII** or oxido-diperoxido, $[\text{V}^{\text{V}}\text{O}(\text{O}_2)]^-$ **CIV/CV** species (*vide supra*). Species **CIII** (Scheme 2.3) or its protonated form ultimately oxidizes bromide species (to Br_2 , Br_3^- and/or HOBr), the bromination of the substrate then proceeding with the liberation of a proton [245]. We have found that the dioxidovanadium(V) complexes reported here satisfactorily catalyze the oxidative bromination of salicylaldehyde to give 5-bromosalicylaldehyde, 3,5-dibromosalicylaldehyde and 2,4,6-tribromophenol using $\text{H}_2\text{O}_2/\text{KBr}$ in presence of HClO_4 in aqueous solution at room temp.; cf. Scheme 2.5 .

After several trials the best suited reaction conditions obtained for the maximum conversion of salicylaldehyde in 7 h of reaction time were: salicylaldehyde (2.44 g, 20 mmol), KBr (5.95 g, 50 mmol), aqueous 30 % H_2O_2 (15 g, 120 mmol), catalyst (0.020 g for $\text{Cs}_2[\text{CH}_2\{\text{V}^{\text{V}}\text{O}_2(\text{sal-nah})\}_2]\cdot 2\text{H}_2\text{O}$ (**2.4**) and $\text{Cs}_2[\text{CH}_2\{\text{V}^{\text{V}}\text{O}_2(\text{sal-inh})\}_2]\cdot 2\text{H}_2\text{O}$ (**2.5**) or 0.016 g for $\text{K}_2[\text{CH}_2\{\text{V}^{\text{V}}\text{O}_2(\text{sal-nah})\}_2]\cdot 2\text{H}_2\text{O}$ (**2.3**)), aqueous 70 % HClO_4 (4.02 g, 80 mmol) and water (40 mL); the addition of HClO_4 , however, in four equal portions during the first two hours of reaction time was necessary to improve the conversion of the substrate and to avoid decomposition of catalyst. Under the above conditions, a maximum of 89.4 % conversion was achieved with $\text{Cs}_2[\text{CH}_2\{\text{V}^{\text{V}}\text{O}_2(\text{sal-inh})\}_2]\cdot 2\text{H}_2\text{O}$ (**2.5**) and at least three products were identified (see Table 2.7). Increasing the amount of oxidant improves the conversion of salicylaldehyde. However, the selectivity of 5-bromosalicylaldehyde decreases considerably, while that of 3,5-dibromosalicylaldehyde and 2,4,6-tribromophenol increase. The presence of

excess H_2O_2 facilitates the formation of more and more HOBr which ultimately helps in the further oxidative bromination of salicylaldehyde to other position(s). Catalysts **2.3** and **2.4** gave very similar results. The counter ions (Cs^+ or K^+) did not much affect the conversion. In the absence of the catalyst, the reaction mixture gave ca. 4 % conversion of salicylaldehyde.



Scheme 2.5. Oxidation products of salicylaldehyde

Table 2.7. Conversion of salicylaldehyde and selectivity of oxidative brominated products data after 7 h of contact time^a

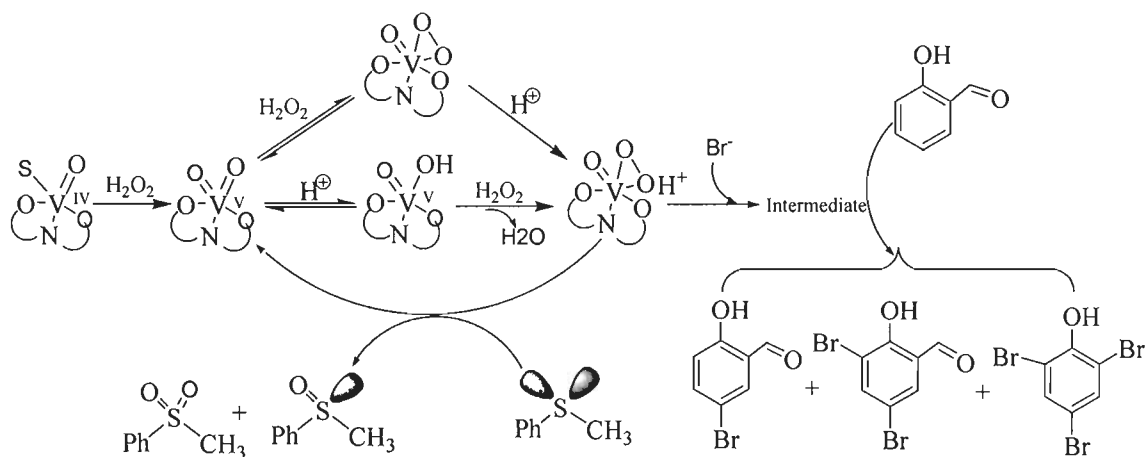
Entry No.	Catalyst	Substr : H_2O_2	Conv. %	TOF (h^{-1})	Selectivity of products		
					Mono	dibromo	tribromo
1	2.5	1 : 2	89.4	122	71.5	26.3	2.1
2	2.5	1 : 3	88.7	121	69.3	27.9	2.8
3	2.5	1 : 4	91.0	125	51.7	42.8	5.5
4	2.5	1 : 5	92.7	127	28.8	59.4	11.8
5	2.5	1 : 6	94.5	129	12.9	64.9	22.2
6	2.3	1 : 2	87.2	120	78.1	19.8	2.1
7	2.3	1 : 4	93.1	128	50.4	41.3	8.3
8	2.4	1 : 2	86.8	119	76.3	19.1	4.6
9	2.4	1 : 4	91.8	126	57.3	39.2	3.5

^aOther reaction conditions: salicylaldehyde (2.44 g, 20 mmol), KBr (5.95 g, 50 mmol), catalyst (0.020 g for $\text{Cs}_2[\text{CH}_2\{\text{V}^{\text{V}}\text{O}_2(\text{sal-nah})\}_2] \cdot 2\text{H}_2\text{O}$ (**2.4**) and

$\text{Cs}_2[\text{CH}_2\{\text{V}^{\text{V}}\text{O}_2(\text{sal-inh})\}_2]\cdot 2\text{H}_2\text{O}$ (2.5) or 0.016 g for $\text{K}_2[\text{CH}_2\{\text{V}^{\text{V}}\text{O}_2(\text{sal-nah})\}_2]\cdot 2\text{H}_2\text{O}$ (2.3)), aqueous 70 % HClO_4 (11.44 g, 80 mmol) and water (40 mL).

Mechanism of Bromination and Sulfide Oxidation

The $\text{Cs}_2[\text{CH}_2\{\text{V}^{\text{V}}\text{O}_2(\text{sal-nah})\}_2]\cdot 2\text{H}_2\text{O}$ (2.4), $\text{Cs}_2[\text{CH}_2\{\text{V}^{\text{V}}\text{O}_2(\text{sal-inh})\}_2]\cdot 2\text{H}_2\text{O}$ (2.5) and $\text{K}_2[\text{CH}_2\{\text{V}^{\text{V}}\text{O}_2(\text{sal-nah})\}_2]\cdot 2\text{H}_2\text{O}$ (2.3) were used as catalysts to carry out oxidative brominations and a global outline of the reaction is presented in Scheme 5. The formation of intermediates proposed in the catalytic cycles, *i.e.* oxido-hydroxo complexes such as $[\text{CH}_2\{\text{V}^{\text{V}}\text{O}(\text{OH})(\text{L})\}_2]$ **CVI** and oxido-peroxo complexes $[\text{CH}_2\{\text{V}^{\text{V}}\text{O}(\text{O}_2)(\text{L})\}_2]^{2-}$ **CIII** and bisperoxo $[\text{V}^{\text{V}}\text{O}(\text{O}_2)_2]^-$ **CIV** were confirmed on the basis of ^{51}V NMR and characteristics in the UV-Vis spectra of the anionic dioxidovanadium precursor compounds $[\text{CH}_2\{\text{V}^{\text{V}}\text{O}_2(\text{L})\}_2]^{2-}$ **CI**, treated with acid and hydrogen peroxide which ultimately oxidise bromide, possibly *via* a hydroperoxo intermediate. The oxidized bromine species (Br_2 , Br_3^- and/or HOBr) then brominates the substrate [249, 250].



Scheme 2.6. Outline of the catalytic processes.

Complexes $[\text{CH}_2\{\text{V}^{\text{IV}}\text{O}(\text{sal-nah})(\text{H}_2\text{O})\}_2]$ (2.1) and $[\text{CH}_2\{\text{V}^{\text{IV}}\text{O}(\text{sal-inh})(\text{H}_2\text{O})\}_2]$ (2.2) were used for sulfoxidations, and we tried to investigate the intermediate species by EPR and ^{51}V NMR. Upon titration with H_2O_2 , complexes

are oxidized and generate signals at $\delta = -538$, -597 and -649 ppm (dioxido-complex **CII**, peroxo-complex **CIII**, bisperoxo **CIV/CV**). The addition of sulfide consumes the intermediates formed and yield only one ^{51}V NMR signal at -539 ppm corresponding to the dioxidovanadium(V) complex **CII**. This supports the involvement of these intermediate species during the catalytic process, namely the hydroperoxo form of **CIII**. The catalytic cycle for oxidation of methyl phenyl sulfide (as a model reaction), proposed previously by several authors [162, 250, 251], is also given in Scheme 2.6.

2.3.9. Antiamoebic activity study

Dioxidovanadium (V) complexes along with ligands **2.I** and **2.II** were screened for antiamoebic activity in vitro against *HMI:IMSS* strain of *E.histolytica*. The IC_{50} values are in the micro molar range and are shown in Table 2.8. The data are presented in terms of percentage growth inhibition related to untreated controls, and plotted as % Inhibition Vs logarithm of the dose concentration. The IC_{50} values were obtained by interpolation in the corresponding dose response curves. Complexes $\text{K}_2[\text{CH}_2\{\text{V}^{\text{V}}\text{O}_2(\text{sal-nah})\}_2]\cdot 2\text{H}_2\text{O}$ (**2.3**) ($\text{IC}_{50} = 0.47 \mu\text{M}$) and $\text{Cs}_2[\text{CH}_2\{\text{V}^{\text{V}}\text{O}_2(\text{sal-inh})\}_2]\cdot 2\text{H}_2\text{O}$ (**2.5**) ($\text{IC}_{50} = 0.32 \mu\text{M}$) cause a marked inhibition, while ligands **2.I** ($\text{IC}_{50} = 8.97 \mu\text{M}$) and **2.II** ($\text{IC}_{50} = 7.61 \mu\text{M}$) are less active than metronidazole. This shows that complexation of the organic ligands to vanadium substantially enhances the activity. It is plausible that complexation directly or indirectly favours permeation of the complexes through the lipid layer of cell membrane [252]. The significance of the statistical difference between the IC_{50} values of the metronidazole and the most active complexes **2.3** and **2.5** was evaluated by a *T* test. The values of the calculated *T* were found to be higher than the table value of *T* at the 4% level [253], thus clearly demonstrating that the vanadium complexes are potent inhibitors of the

development of *E. histolytica* *in vitro* and that they are more active than the standard drug metronidazole.

Toxicity of compounds accessed by the MTT Assay

The cells were treated with various concentrations of the compounds $\text{K}_2[\text{CH}_2\{\text{V}^{\text{V}}\text{O}_2(\text{sal-nah})\}_2]\cdot 2\text{H}_2\text{O}$ (**2.3**) and $\text{Cs}_2[\text{CH}_2\{\text{V}^{\text{V}}\text{O}_2(\text{sal-inh})\}_2]\cdot 2\text{H}_2\text{O}$ (**2.5**) or vehicle (DMSO) alone for 24 h, 48 h and 72 h (as indicated in the Figures 2.22 and 2.23). Cell survival was determined by MTT assay. Cell viability was calculated as described in the Materials and methods. *Columns*, mean from three independent experiments in which each treatment was done in triplicate. To assess the survival effects of the compounds, human cervical (HeLa) cells were used. 6000 cells per well in 200 μL complete DMEM medium were plated. Different concentrations of the different compounds were added in the wells as indicated in the Figures 2.22 and 2.23. The concentration range for compound **2.3** was 0.47 to 250 $\mu\text{M/L}$ and for compound **2.5** 0.32 to 250 $\mu\text{M/L}$. The viable cells were measured after 24 h, 48 h, and 72 h., by MTT assay. At 72 h, the IC_{50} of the compounds **2.3** and **2.5** are 150 $\mu\text{M/L}$ and 50 $\mu\text{M/L}$ respectively. The cell survival assay was also performed in the presence of metronidazole and the IC_{50} value was found to be more than 750 μM as given in Table 2.8. This shows that compounds **2.3** and **2.5** are more toxic as compared to metronidazole.

Table 2.8. Vanadium Complexes, antiamoebic activity against HM1 : IMSS strain of *E. histolytica* and toxicity profile of compound $K_2[CH_2\{V^VO_2(sal-nah)\}_2]\cdot 2H_2O$ (**2.3**) and $Cs_2[CH_2\{V^VO_2(sal-inh)\}_2]\cdot 2H_2O$ (**2.5**).

S. No.	Compound	Antiamoebic		Toxicity profile	
		IC ₅₀ (μM) ^a	S.D. ^b	IC ₅₀ (μM) ^a	S.D. ^b
1	CH ₂ (H ₂ sal-nah) ₂	8.97	0.01	N.D.	N.C.
2	CH ₂ (H ₂ sal-inh) ₂	7.61	0.02	N.D.	N.C.
3.	$K_2[CH_2\{V^VO_2(sal-nah)\}_2]\cdot 2H_2O$	0.47	0.01	150	0.045
4	$Cs_2[CH_2\{V^VO_2(sal-nah)\}_2]\cdot 2H_2O$	4.34	0.05	N.D.	N.C.
5.	$Cs_2[CH_2\{V^VO_2(sal-inh)\}_2]\cdot 2H_2O$	0.32	0.03	50	0.015
6	Metronidazole	1.89	0.03	> 750	0.050

^aThe values were obtained from at least three separate assays done in duplicate.

^bStandard deviation; N.D.= Not Done; N.C.= Not Calculated.s

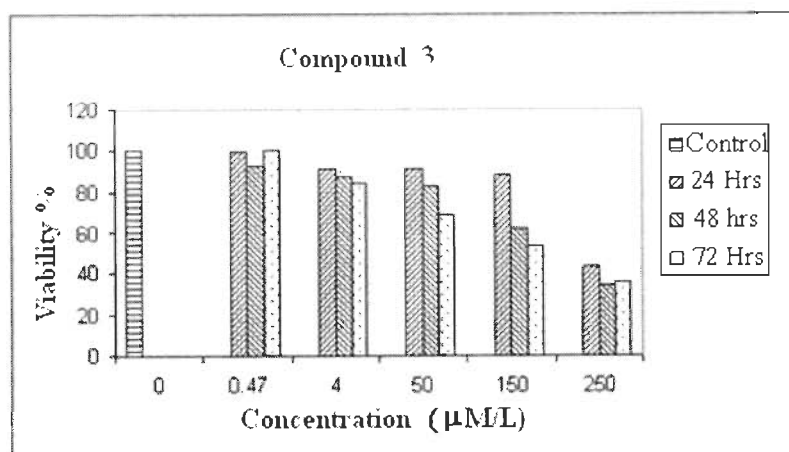


Figure 2.22. Percentage of viable cells after 24 h, 48 h and 72 h on human cervical (HeLa) cells on incubation with various concentrations of compound $K_2[CH_2\{V^VO_2(sal-nah)\}_2]\cdot 2H_2O$ (**2.3**) or vehicle (DMSO). Cell survival was determined by the MTT assay.

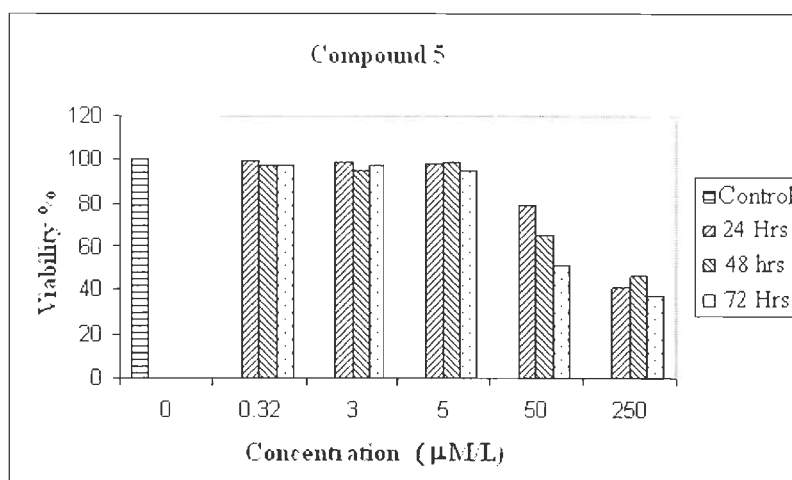


Figure 2.23. Percentage of viable cells after 24 h, 48 h and 72 h on human cervical (HeLa) cells on incubation with various concentrations of compound $\text{Cs}_2[\text{CH}_2\{\text{V}^{\text{V}}\text{O}_2(\text{sal-inh})\}_2]\cdot 2\text{H}_2\text{O}$ (**2.5**) or vehicle (DMSO). Cell survival was determined by the MTT assay.

2.4. Conclusions

The hydrazones $\{\text{CH}_2(\text{H}_2\text{sal-nah})_2\}$ (**2.I**) and $\{\text{CH}_2(\text{H}_2\text{sal-inh})_2\}$ (**2.II**) derived from 5,5'-methylenebis(salicylaldehyde) $\{\text{CH}_2(\text{Hsal})_2\}$ and nicotinic acid hydrazide (nah) or isonicotinic acid hydrazide (inh) and their $\text{V}^{\text{IV}}\text{O}$ - and $\text{V}^{\text{V}}\text{O}_2$ -complexes were synthesized and characterized. The complexes are dinuclear in the solid state and in solution, but no significant interactions are detected between the vanadium centres.

Compounds $[\text{CH}_2\{\text{V}^{\text{V}}\text{O}_2(\text{sal-nah})\}_2]^{2-}$ and $[\text{CH}_2\{\text{V}^{\text{V}}\text{O}_2(\text{sal-inh})\}_2]^{2-}$ were shown to be functional models of vanadium dependent haloperoxidases, satisfactorily catalyzing the oxidative bromination of salicylaldehyde to give 5-bromosalicylaldehyde, 3,5-dibromosalicylaldehyde and 2,4,6-tribromophenol using $\text{H}_2\text{O}_2/\text{KBr}$ in the presence of HClO_4 in aqueous solution at room temperature. The complexes $[\text{CH}_2\{\text{V}^{\text{IV}}\text{O}(\text{sal-nah})(\text{H}_2\text{O})\}_2]$ and $[\text{CH}_2\{\text{V}^{\text{IV}}\text{O}(\text{sal-}$

inh)(H₂O)}₂] were shown to be catalyst precursors for the catalytic oxidation, by peroxide, of methyl phenyl sulfide and diphenyl sulfide, yielding the corresponding sulfoxide and sulfone at room temperature.

The reactivity in methanol and DMSO of the V^{IV}O- and V^VO₂-complexes of {CH₂(H₂sal-nah)₂} (**2.I**) and {CH₂(H₂sal-inh)₂} (**2.II**) was studied by UV-Vis, EPR and ⁵¹V NMR spectroscopy, by either adding H₂O₂ or acid (HCl or HClO₄) or both, the formation of several species being established, some of them probably being intermediates in the catalytic processes studied, namely [CH₂{V^VO(O₂)(L)}₂]²⁻ and [CH₂{V^VO(OH)(L)}₂]. On addition of acid (HCl or HClO₄) the V^V-species present are partly reduced yielding V^{IV}O-species containing the {V^{IV}O(sal-nah)(S)} and {V^{IV}O(sal-inh)(S)} moieties (S = solvent), the oxidohydroxocomplex and a ⁵¹V NMR active species whose nature is suggested.

Amoebiasis is caused by *Entamoeba histolytica*, the second leading cause of death among parasite diseases. For the treatment of amoebiasis metronidazole has been till now the drug of choice. The V^V-complexes of {CH₂(H₂sal-nah)₂} (**2.I**) and {CH₂(H₂sal-inh)₂} (**2.II**) were also screened against HM1:IMSS strains of *Entamoeba histolytica*, the results showing that they are significantly more active than metronidazole. The MTT assay results showed that the compounds K₂[CH₂{V^VO₂(sal-nah)}₂]·2H₂O (**2.3**) and Cs₂[CH₂{V^VO₂(sal-inh)}₂]·2H₂O (**2.5**) are toxic against human cervical (HeLa) cells line.

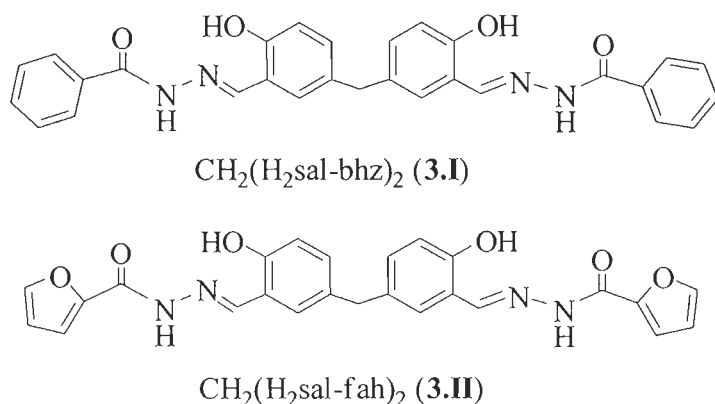
Chapter-3

Vanadium complexes having $[V^{IV}O]^{2+}$ and $[VO_2]^+$ cores with binucleating dibasic tetradentate ligands: Synthesis, characterization, catalytic and antiamoebic activities

3.1. Introduction

Vanadium is a biologically relevant metal and is incorporated in several natural products e.g. amavadin in *Amanitae* mushrooms, [254] blood cells of sea-squirts (*Ascidiaeae*) and fan worms [255, 256]. With the discovery and characterization of vanadate-dependent heloperoxidases [19, 22, 54, 80, 156, 257] the coordination chemistry of vanadium has acquired renewed interest. The prospective therapeutic applications of vanadium compounds, particularly in the treatment of *Diabetes mellitus* in human [139, 258, 261], their potency as inhibitors of phosphoryl transfer enzymes [262] and their catalytic potential in the organic transformations [45, 57, 59, 65, 160, 169, 184, 186, 263 - 267] have further stimulated studies on the vanadium coordination chemistry.

N-Salicylidenehydrazides are versatile tridentate ligands and several types of $V^{IV}O$ -, V^VO - and V^VO_2 -complexes have been obtained [15, 16]. Some of these complexes have been reported as structural as well as functional mimics of vanadium-bromoperoxidases [231, 271] and also as structural models for vanadium(V)-transferrin binding [272]. In this work we report the synthesis and characterization of the binucleating hydrazones $CH_2(H_2sal-bhz)_2$ (**3.I**) and $CH_2(H_2sal-fah)_2$ (**3.II**) (Scheme 3.1), of their oxidovanadium(IV) and dioxidovanadium(V) complexes as well as their catalytic and reactivity patterns modeling reactions of vanadium-haloperoxidases.



Scheme 3.1. Structures of ligands used in this work.

Among all parasites, the protozoan parasite *Entamoeba histolytica* is the etiologic agent of amoebiasis, affecting millions of people worldwide, especially in tropical developing countries. Approximately 90% of patients having mild to moderate amoebic dysentery respond to metronidazole (MNZ), an important drug [273 - 275]. However, several side effects have been noticed by patients. MNZ also induces certain tumors in rodents and is mutagenic towards bacteria [276 - 280]. In the last years our research group have been interested in investigating the antiamoebic activity of vanadium complexes and reported encouraging results on the in vitro activity of dioxidovanadium(V) complexes of ONO, ONN and ONS donor ligands against *Entamoeba histolytica* [59, 152, 153, 154, 281]. In the present work the dioxidovanadium(V) complexes prepared were also screened for their antiamoebic activity against HM1:1MSS strains of the protozoan parasite *Entamoeba histolytica*.

Cation π -interactions can play an important role in biological systems [282]. The attraction between a hard cation and a simple π system can determine the assembly between the components of supramolecular entities. Only a limited group of systems present cation π -interactions with alkali metals, e.g. the recognition by uranyl complexes with unusual Cs^+ -halide coordination has been investigated where cation- π interactions are established between the aromatic pendants and the counter ion [283, 284]. Other examples involve calixanions [285, 286], and the phosphorous atom in tertiary phosphines [287]. Ligands presenting extensive π -delocalization can be stabilized as carbonium ions, radical, or carbanions [288, 289]. In the present work we found that in the $CH_2(sal-bhz)_2$ “carbanion” present in complex $Cs_2[CH_2\{V^VO_2(sal-bhz)\}_2] \cdot 2H_2O$ (**3.3**), both weak and reasonably strong Cs-C π -interactions exists.

3.2. Experimental

3.2.1. Materials

V₂O₅, ethyl benzoate, hydrazine hydrate (Loba Chemie, India), 2-furoylhydrazide, CsOH.H₂O (Across Organics, Belgium), acetylacetone (Aldrich, U.S.A.), 30 % aqueous H₂O₂ and 70 % HClO₄ (Qualigens, India) were used as obtained. Benzoyl hydrazide was prepared by the reaction of a two fold excess of hydrazine hydrate with ethyl benzoate in ethanol. Details of other chemicals and solvents are reported in Chapter 2.

3.2.2. Characterization Procedures

Instrumentation and analyses details are reported in Chapter 2.

3.3.3. Preparations

Preparation of ligands

Ligands CH₂(H₂sal-bhz)₂ (**3.I**) and CH₂(H₂sal-fah)₂ (**3.II**) were prepared following the literature procedure with slight modifications [220]. A solution of 5,5'-methylbis(salicylaldehyde) (2.65 g, 10 mmol) in hot methanol (40 mL) was added to a solution of the appropriate hydrazide (20 mmol) dissolved in methanol (20 mL) with stirring. The reaction mixture was refluxed for 2 h. After reducing the solvent volume to ca. 30 mL and cooling to ca. 10 °C, the solid obtained was filtered, washed with methanol and dried in desiccator over silica gel.

CH₂(H₂sal-bhz)₂ (3.I**)**

Yield 3.146 g (64 %). Found: C, 70.8; H, 4.8; N, 11.3 %. Calc for C₂₉H₂₄N₄O₄ (492.53): C, 70.7; H, 4.9; N, 11.4 %.

CH₂(H₂sal-fah)₂ (3.II**)**

Yield 3.38 g (72%). Found: C, 63.4; H, 4.4; N, 11.8 %. Calc for $C_{25}H_{20}N_4O_6$ (472.14): C, 63.5; H, 4.3; N, 11.9%.

Preparation of $[CH_2\{V^{IV}O(sal-bhz)(H_2O)\}_2]$ (3.1)

A solution of $CH_2(H_2sal-bhz)_2$ (0.492 g, 1 mmol) was prepared by refluxing in methanol (80 mL) and filtering the resulting mixture. A filtered solution of $[V^{IV}O(acac)_2]$ (0.530 g, 2 mmol) in methanol (15 mL) was then added while stirring, and this reaction mixture was refluxed for 3 h. After reducing the volume of solvent to ca. 20 mL and keeping at room temperature for 10 h, the brown solid was filtered, washed with methanol and dried in desiccator over silica gel. Yield 0.417 g (68 %). Found: C, 52.7; H, 3.9; N, 8.6 %. Calc for $C_{29}H_{24}N_4O_8V_2$ (658.41): C, 52.9; H, 3.9; N, 8.5 %.

Preparation of $K_2[CH_2\{V^VO_2(sal-bhz)\}_2] \cdot 2H_2O$ (3.2)

A solution of $CH_2(H_2sal-bhz)_2$ (0.492 g, 1 mmol) dissolved in aqueous KOH (0.224 g, 4 mmol) was added with stirring to a filtered aqueous solution of KVO_3 prepared in situ by dissolving vanadium(V) oxide (0.20 g, 2 mmol) in KOH (0.112 g, 2 mmol). The pH of the reaction mixture was adjusted to ~7.5 by adding 4 M HCl. The yellow solid of **3.2** started to separate and after 2 h of stirring it was filtered, washed with water and dried. Yield 0.715 g (77.7%). Found: C, 45.4; H, 3.2; N, 7.3 %. Calc for $C_{29}H_{24}N_4O_{10}V_2K_2$ (768.6): C, 45.3; H, 3.2; N, 7.3 %.

Preparation of $Cs_2[CH_2\{V^VO_2(sal-bhz)\}_2] \cdot 2H_2O$ (3.3)

Method A. A filtered solution of $[V^{IV}O(acac)_2]$ (0.464 g 1.75 mmol) in methanol (15 mL) was added while stirring to a solution of $CH_2(sal-bhz)_2$ (0.320 g, 0.65 mmol) prepared as reported for $[CH_2\{V^{IV}O(sal-bhz)(H_2O)\}_2]$ (**3.1**) in methanol (80 mL). $CsOH \cdot H_2O$ (0.300 g, 1.78 mmol) was then added and the reaction mixture was refluxed for 2 h. The obtained dark red solution was allowed to stand for aerial oxidation and became yellow within 24 h. After reducing the volume of

the solvent to ca. 10 mL and keeping at room temperature, complex **3.3** separated within 24 h. This was filtered off washed with cold methanol and dried in a desiccator over silica gel. Yield 0.750 g (81.5%). Found: C, 36.4; H, 2.6; N, 5.9%. Calc for $Cs_2C_{29}H_{24}O_7N_4V_2$ (956.22): C, 36.4; H, 2.5; N, 5.9%.

Method B. Complex **3.3** was also prepared by refluxing a mixture of $[CH_2\{V^{IV}O(sal-bhz)(H_2O)\}_2]$ (**3.1**) (0.329 g, 0.5 mmol) and $CsOH \cdot H_2O$ (0.200 g, 1.2 mmol) in methanol (20 mL) for 2 h followed by aerial oxidation for ca. 24 h. The rest of the work up procedure followed was as reported for method A. Yield 0.782 g, (84.9%).

Preparation of $[CH_2\{V^{IV}O(sal-fah)(H_2O)\}_2]$ (3.4**)**

This complex was prepared from $CH_2(sal-fah)_2$ (0.472 g, 1 mmol) and $[V^{IV}O(acac)_2]$ (0.530 g, 2 mmol) in methanol as outlined for $[CH_2\{V^{IV}O(sal-bhz)(H_2O)\}_2]$ (**3.1**). Yield 0.425 g (70.6 %). Found: C, 46.9; H, 3.2; N, 8.8 %. Calc for $C_{25}H_{20}N_4O_{10}V_2$ (638.0): C, 47.0; H, 3.2; N, 8.9 %.

Preparation of $K_2[CH_2\{V^VO_2(sal-fah)\}_2] \cdot 2H_2O$ (3.5**)**

This complex was prepared following the procedure outlined for $K_2[CH_2\{V^VO_2(sal-bhz)\}_2] \cdot 2H_2O$ (**3.2**) . Yield 0.605 g (85%). Found: C, 40.0; H, 2.7; N, 7.6 %. Calc for $C_{25}H_{20}N_4O_{12}V_2K_2$ (748.53): C, 40.1; H, 2.7; N, 7.5 %.

$Cs_2[CH_2\{V^VO_2(sal-fah)\}_2] \cdot 2H_2O$ (3.6**)**

Complex **3.6** was prepared considering both methods outlined for $Cs_2[CH_2\{V^VO_2(sal-bhz)\}_2] \cdot 2H_2O$ (**3.3**) . Yield 0.648 g (72%). (Found: C, 32.1; H, 2.2; N, 5.9 %. Calc for $C_{25}H_{20}N_4O_{12}V_2Cs_2$ (936.15): C, 32.1; H, 2.2; N, 6.0 %.

3.2.4. Catalytic activity studies

Oxidation of methyl phenyl sulfide and diphenyl sulfide

Methyl phenyl sulphide (1.24 g, 10 mmol) or diphenyl sulfide (1.86 g, 10 mmol) and aqueous 30% H_2O_2 (2.27 g, 20 mmol) were dissolved in petroleum ether (10 mL). After addition of catalyst (oxidovanadium(IV) complexes $[CH_2\{V^{IV}O(sal-bhz)(H_2O)\}_2]$ (**3.1**) or $[CH_2\{V^{IV}O(sal-fah)(H_2O)\}_2]$ (**3.4**) 0.020 g) to the above solution, the reaction mixture was stirred at room temperature for 7 h. During this period, the reaction products formed were analyzed using gas chromatography by withdrawing small aliquots after fixed time intervals. The identities of the reaction products were confirmed by GC-MS and comparing the fragments of each product with the library available.

Oxidative bromination of salicylaldehyde

Complexes $K_2[CH_2\{V^VO_2(sal-bhz)_2\}]\cdot 2H_2O$ (**3.2**), $K_2[CH_2\{V^VO_2(sal-fah)_2\}]\cdot 2H_2O$ (**3.5**), $Cs_2[CH_2\{V^VO_2(sal-bhz)_2\}]\cdot 2H_2O$ (**3.3**) and $Cs_2[CH_2\{V^VO_2(sal-fah)_2\}]\cdot 2H_2O$ (**3.6**), were used as catalysts to carry out oxidative brominations. In a typical reaction, salicylaldehyde (2.44 g, 20 mmol) was added to an aqueous solution (40 mL) of KBr (5.95 g, 50 mmol), followed by addition of aqueous 30 % H_2O_2 (15 g, 120 mmol) in a 100 mL reaction flask. The catalyst (0.02 g for **3.3** and **3.6**, or 0.016 g for **3.2** and **3.5**) and 70 % $HClO_4$ (4.02 g, 20 mmol) were added, and the reaction mixture was stirred at room temperature. Three additional 20 mmol portions of 70 % $HClO_4$ were further added to the reaction mixture in three equal portions in half hour intervals under continuous stirring. After 7 h, the white product that had separated was filtered off, washed with water and dried. The crude mass was dissolved in CH_2Cl_2 ; insoluble material, if any, was removed by filtration, and the solvent evaporated. A CH_2Cl_2 solution of this material was subjected to gas chromatography, and the identity of the products confirmed by GC-MS.

3.2.5. In vitro testing against *E. histolytica*

The ligands $(CH_2(H_2sal-bhz)_2)$ (**3.I**) and $(CH_2(H_2sal-fah)_2)$ (**3.II**) and their dioxido vanadium(V) complexes $(K_2[CH_2\{V^VO_2(sal-bhz)\}_2] \cdot 2H_2O)$ (**3.2**), $Cs_2[CH_2\{V^VO_2(sal-bhz)\}_2] \cdot 2H_2O$ (**3.3**), $K_2[CH_2\{V^VO_2(sal-fah)\}_2] \cdot 2H_2O$ (**3.5**) and $Cs_2[CH_2\{V^VO_2(sal-fah)\}_2] \cdot 2H_2O$ (**3.6**) were screened in vitro for antiamoebic activity against *HMI:IMSS* strain of *E. histolytica* by using a microplate method [221]. Details of the method are described in Chapter 2.

MTT Assay

The human cervical (HeLa) cells were obtained from NCCS (Pune, India). The cells were cultured in DMEM (Invitrogen) with 10% fetal bovine serum, and 1% penicillin-streptomycin. The effect of active compounds $Cs_2[CH_2\{V^VO_2(sal-bhz)\}_2] \cdot 2H_2O$ (**3.3**) and $Cs_2[CH_2\{V^VO_2(sal-fah)\}_2] \cdot 2H_2O$ (**3.6**), and the standard drug (metronidazole) on cell proliferation was measured by using an MTT-based assay [225]. Briefly, the cells (6000/well) were incubated in triplicate in a 96-well plate in the presence of various concentrations of compounds **3.3**, **3.6** and metronidazole or vehicle (DMSO) alone in a final volume of 200 μ L for different periods of time (24, 48 and 72 h) at 37 °C in a humidified chamber. At the end of each time interval, 20 μ L of MTT solution (5 mg/ml in PBS) was added to each well and the cells were incubated for 4 h at 37°C in a humidified chamber. After 4 h, the supernatant was removed from each well. The colored formazan crystal produced from MTT was dissolved in 200 μ L of DMSO and then the absorbance (*A*) value was measured at 570 nm by a multi scanner autoreader. The following formula was used for the calculation of the percentage of cell viability (CV): $CV (\%) = (A \text{ of the experimental samples} / A \text{ of the control}) \times 100$.

3.2.6. X-Ray crystal structure determination of $Cs_2[CH_2\{V^VO_2(sal-bhz)\}_2]\cdot 2H_2O$ (3.3)

Single crystals of $Cs_2[CH_2\{V^VO_2(sal-bhz)\}_2]\cdot 2H_2O$ (**3.3**), obtained from a methanol/ethanol solution, were mounted in inert oil and transferred to the cold gas stream of the diffractometer. Three-dimensional X-ray data for $Cs_2[CH_2\{V^VO_2(sal-bhz)\}_2]\cdot 2H_2O$ (**3.3**) was collected on a Bruker Kappa X8 Apex CCD diffractometer by the ϕ - ω scan method. Data was collected at low temperature. Reflections were measured from a hemisphere of data collected of frames each covering 0.3 degrees in ω . Complex scattering factors were taken from the program package SHELXTL [290]. The structures were solved using the SHELXS Program for Crystal Structure Determination and refined with SHELXL Program for Crystal Structure Refinement [290]. The non-hydrogen atoms were refined with anisotropic thermal parameters in all cases. The hydrogen atoms were included in calculated positions and refined by using a riding mode for all the atoms except for C(4), C(8), C(10) and C(12). The hydrogen atoms for the water molecules O(1W) and O(2W) were not located. The absolute configuration has been established by refinement of the enantiomorph polarity parameter [$x = 0.00(2)$] [291]. A final difference Fourier map showed no residual density outside: 0.947, -1.202 e.Å⁻³. Crystal data and structure refinement parameters for complex **3.3** are presented in Table 3.1.

Table 3.1. Crystal data and structure refinement parameters for $Cs_2[CH_2\{VO_2(sal-bhz)\}_2] \cdot 2H_2O$ **3.3**

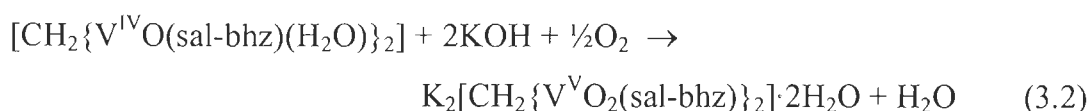
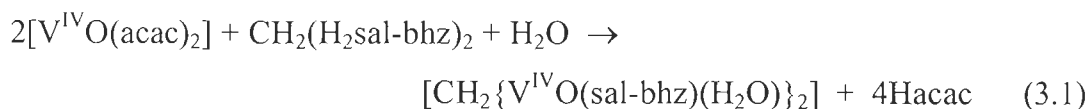
	3
Empirical formula	$C_{29}H_{19}Cs_2N_4O_{10}V_2$
Formula weight	951.18
Temperature	293(2) K
Wavelength	0.71073 Å
Crystal system	Orthorhombic
Space group	P212121
Unit cell dimensions	$a = 6.7107(3)$ Å $\alpha = 90^\circ$. $b = 14.8288(5)$ Å $\beta = 90^\circ$. $c = 31.5966(13)$ Å $\gamma = 90^\circ$.
Volume	$3144.2(2)$ Å ³
Z	4
Density (calculated)	2.009 Mg/m ³
Absorption coefficient	2.940 mm ⁻¹
F(000)	1828
Crystal size	$0.10 \times 0.08 \times 0.04$ mm ³
Theta range for data collection	1.29 to 28.27° .
Index ranges	$-8 \leq h \leq 8$, $-13 \leq k \leq 19$, $-41 \leq l \leq 41$
Reflections collected	30945
Independent reflections	7746 [R(int) = 0.0559]
Completeness to theta = 28.27°	99.6 %
Absorption correction	Semi-empirical from equivalents
Max. and min. transmission	0.8865 and 0.7516
Refinement method	Full-matrix least-squares on F ²
Data / restraints / parameters	7746 / 0 / 441
Goodness-of-fit on F ²	1.108
Final R indices [I > 2sigma(I)] ^a	R1 = 0.0413, wR2 = 0.0962
R indices (all data) ^b	R1 = 0.0582, wR2 = 0.1156
Absolute structure parameter	1.00(2)
Largest diff. peak and hole	0.947 and -1.202 e.Å ⁻³

^a $R_1 = \sum ||F_o| - |F_c|| / \sum |F_o|$.

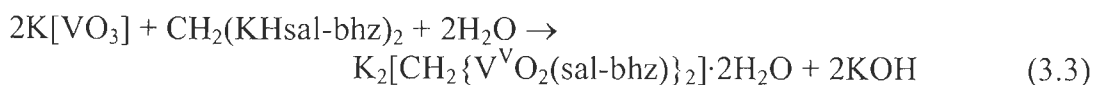
^b $wR_2 = \{ \sum [w(|F_o|^2 - |F_c|^2)^2] / \sum [w(F_o^4)] \}^{1/2}$.

3.3. Results and discussion

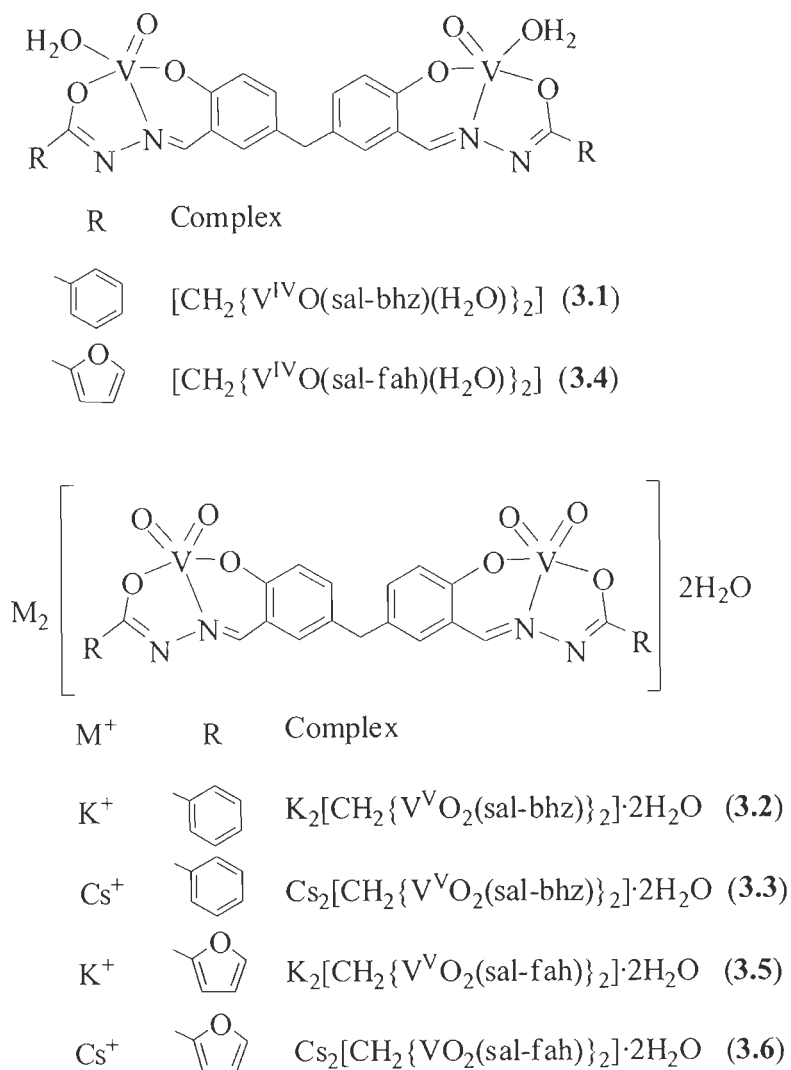
The reaction between $CH_2(H_2sal-bhz)_2$ or $CH_2(H_2sal-fah)_2$ and $[V^{IV}O(acac)_2]$ in 1:2 molar ratio in refluxing methanol resulted in the formation of dinuclear oxidovanadium(IV) complexes $[CH_2\{V^{IV}O(sal-bhz)(H_2O)\}_2]$ (**3.1**) and $[CH_2\{V^{IV}O(sal-fah)(H_2O)\}_2]$ (**3.4**), respectively. In the presence of KOH or CsOH.H₂O, aerial oxidation of these complexes in methanol yielded the corresponding salt of dioxidovanadium(V) species $[CH_2\{V^VO_2(sal-bhz)\}_2]^{2-}$ (**3.2** and **3.3**) and $[CH_2\{V^VO_2(sal-fah)\}_2]^{2-}$ (**3.5** and **3.6**). These complexes were also isolated directly by the reaction of $[V^{IV}O(acac)_2]$ with $CH_2(H_2sal-bhz)_2$ and $CH_2(H_2sal-fah)_2$ in 2:1 ratio in refluxing methanol followed by aerial oxidation in the presence of KOH/CsOH.H₂O. Here, reaction probably proceeds through the formation of the oxidovanadium(IV) complexes $[CH_2\{V^{IV}O(sal-bhz)(H_2O)\}_2]$ (**3.1**) and $[CH_2\{V^{IV}O(sal-fah)(H_2O)\}_2]$ (**3.4**). Equations (3.1) and (3.2) present the whole synthetic procedures considering $CH_2(H_2sal-bhz)_2$ as a representative ligand.



A solution of potassium vanadate, generated *in situ* by dissolving V₂O₅ in aqueous KOH, reacts with the potassium salts of **3.I** and **3.II** at pH ca. 7.5 to give the potassium salts of the dioxidovanadium(V) anions, $[CH_2\{V^VO_2(sal-bhz)\}_2]^{2-}$ and $[CH_2\{V^VO_2(sal-fah)\}_2]^{2-}$; equation (3.3).



All complexes are soluble in methanol, ethanol, DMSO and DMF. Scheme 3.2 presents the structures proposed for these complexes and are based on the spectroscopic characterization (IR, electronic, EPR, 1H , ^{13}C and ^{51}V NMR), elemental analyses, thermogravimetric patterns and single crystal X-ray analysis of $Cs_2[CH_2\{V^V O_2(sal-bhz)\}_2] \cdot 2H_2O$ (**3.3**). The coordination of the ligands involves their dianionic (ONO^{2-}) enolate tautomeric form.



Scheme 3.2. Vanadium complexes prepared in the present work.

3.3.1. Crystal and molecular structure of $Cs_2[CH_2\{V^VO_2(sal-bhz)\}_2]\cdot 2H_2O$ (3.3)

The molecular structure of $Cs_2[CH_2\{V^VO_2(sal-bhz)\}_2]\cdot 2H_2O$ (3.3) was determined by single-crystal X-ray diffraction. This compound crystallized in an orthorhombic lattice with four molecules in the unit cell. One of the $Cs_2[CH_2\{V^VO_2(sal-bhz)\}_2]$ units is shown in Figure 3.1 and the bond lengths and bond angles are presented in Table 3.2. Compound 3.3 adopts a polymeric structure in the solid state and there are four $Cs_2[CH_2\{V^VO_2(sal-bhz)\}_2]\cdot 2H_2O$ moieties in the asymmetric unit which contains a Cs_4O_{18} cluster (Figure 3.2), bridging three chains. These moieties lie on pseudo-inversion centres halfway along the $Cs(1)\cdots Cs(1A)$ and $Cs(2)\cdots Cs(2A)$ vectors [292].

Each $Cs_2[CH_2\{V^VO_2(sal-bhz)\}_2]\cdot 2H_2O$ moiety contains two cis-dioxidovanadium(V) units, thus forming a dinuclear compound. The geometry is characterized by τ values of 0.260 for V(1), square pyramidal distorted towards a trigonal bipyramid, and 0.075 for V(2) coordination ($\tau = 0$ for ideal tetragonal pyramid; $\tau = 1$ for ideal trigonal bipyramid). The vanadium V(1) atom is displaced by about 0.4852 Å from the plane N(3)-O(5)-O(6)-O(8), and V(2) by 0.4791 Å from the plane N(2)-O(1)-O(2)-O(4). The V=O distances are V(1)-O(6): 1.639(5) Å; V(1)-O(7): 1.622(5) Å; V(2)-O(2): 1.644(5) Å; V(2)-O(3): 1.616(5) Å, in the range reported for other cis-dioxidovanadium centres. A tridentate N-salicylinenehydrazide group is bound to each metal ion through the O-carbonyl and the deprotonated O-phenolic atoms [V-O distances of V(1)-O(5): 1.895(5) Å and V(2)-O(4): 1.907(5) Å] and the N-atom of the hydrazone group [V(1)-N(3): 2.145(6) Å and V(2)-N(2): 2.144(6) Å], consistent with the values reported for other complexes [293]. The Cs^+ ions are coordinated by O-atoms coming from cis- $[V^VO_2]^+$ unit and from an oxo bridge, and by carbon atoms from sal-bhz ligands. These features make this structure an interesting example of Cs-C π -bonds, namely for Cs(2). Indeed, the Cs(1) is coordinated by the “carbanion” (sal-

bhz) by η^2 cation π -interactions and by two oxygen atoms, O(1) and O(3) of the same $[\text{CH}_2\{\text{V}^{\text{V}}\text{O}_2(\text{sal-bhz})\}_2]^{2-}$ complex, by other O-atoms of two other $[\text{CH}_2\{\text{V}^{\text{V}}\text{O}_2(\text{sal-bhz})\}_2]^{2-}$ moieties O(2A) and O(6B), and one O(2W). The oxygen atoms and Cs^+ ions form a cluster which connect the $[\text{CH}_2\{\text{V}^{\text{V}}\text{O}_2(\text{sal-bhz})\}_2]^{2-}$ moieties, the distances with the O-atoms being in the range 2.9-3.3 Å. The Cs^+ cations also interact with the carbanion through the two carbon atoms of the chain, C(23) and C(24). The Cs-C distances, [Cs(1)-C(23): 3.703(6) Å and Cs(1)-C(24): 3.901(6) Å] correspond to weak interactions with this part of the molecule. Cs(2) is coordinated by the “carbanion” (sal-bhz) centre by η^2 cation lateral π -interaction with two carbon atoms of the phenyl ring (Figure 3.1). The distances Cs-C [Cs(2)-C(27): 3.519(8) Å and Cs(2)-C(28): 3.384(8) Å] show stronger interactions to C-atoms than Cs(1), and the Cs(2)-C(28) distance is even comparable to Cs-C σ -bonds [294-297]; therefore these lateral interactions are rather strong. The coordination sphere of the Cs(2) ion is completed by O-atoms of another $[\text{CH}_2\{\text{V}^{\text{V}}\text{O}_2(\text{sal-bhz})\}_2]^{2-}$ complex and by O(2W). The Cs(2) – O-atoms internuclear distances are similar to those of Cs(1).

The distances [N(1)-C(23): 1.313(9) Å, N(2)-C(22): 1.298(10) Å, N(3)-C(8): 1.295(10) Å and N(4)-C(7): 1.289(10) Å] in $[\text{CH}_2\{\text{V}^{\text{V}}\text{O}_2(\text{sal-bhz})\}_2]^{2-}$ units are typical of double bonds [298]. The distances [O(1)-C(23) and O(8)-C(7): 1.321(8) Å] reflect the partial double character of these bonds [299, 300]. The space filling view of $\text{Cs}_2[\text{CH}_2\{\text{V}^{\text{V}}\text{O}_2(\text{sal-bhz})\}_2]\cdot 2\text{H}_2\text{O}$ (3.3) (see Figure 3.3) along the a-axis show a porous 3D metal organic framework architecture formed by supramolecular interactions between neighbouring moieties and cluster of oxygen atoms and Cs^+ ions.

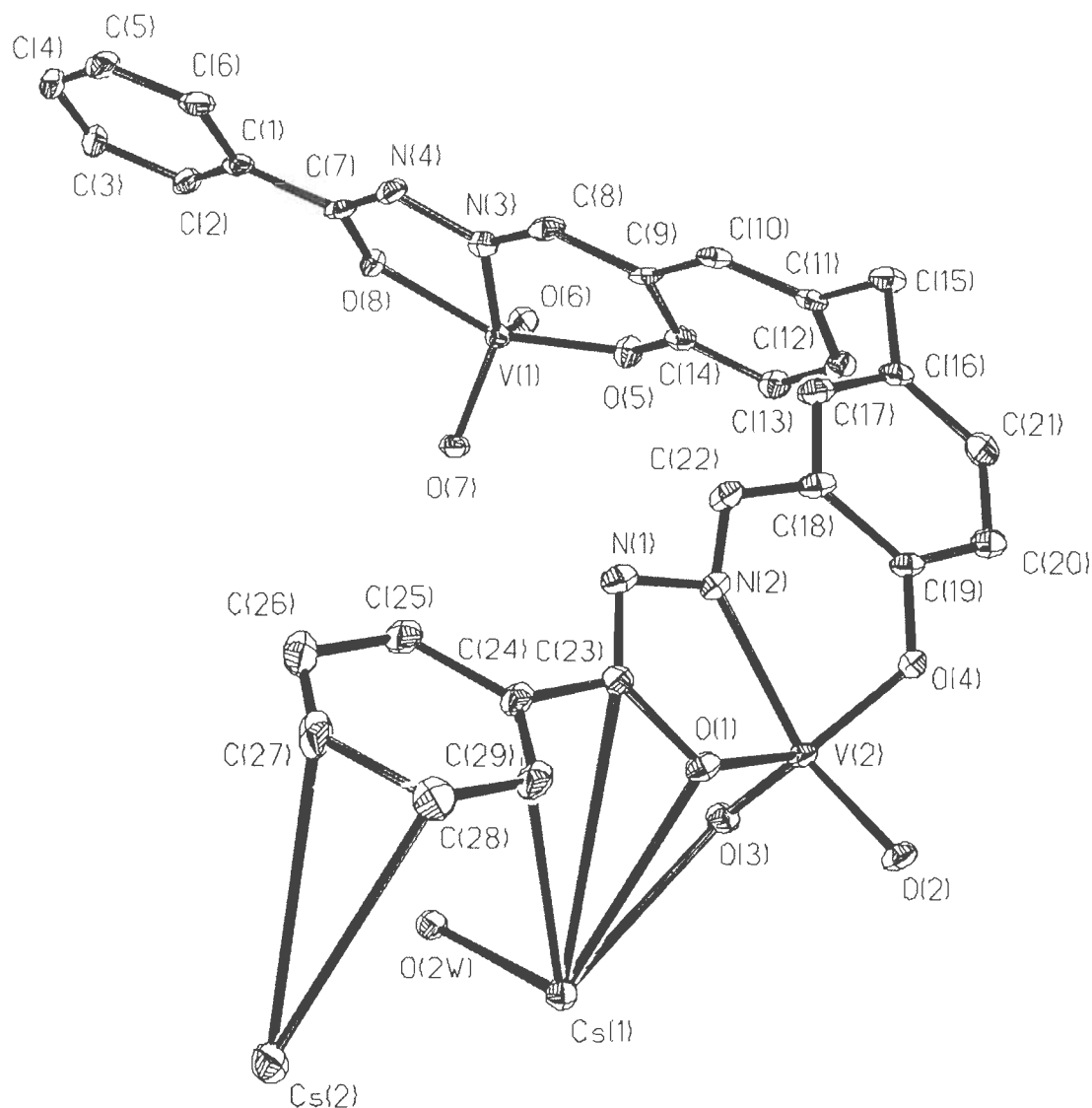


Figure 3.1. ORTEP diagram with the thermal ellipsoids of the non-hydrogen atoms drawn at the 30% probability level representing one of the four moieties of the asymmetric unit of $Cs_2[CH_2\{V^V O_2(sal-bhz)\}_2] \cdot 2H_2O$ (**3.3**).

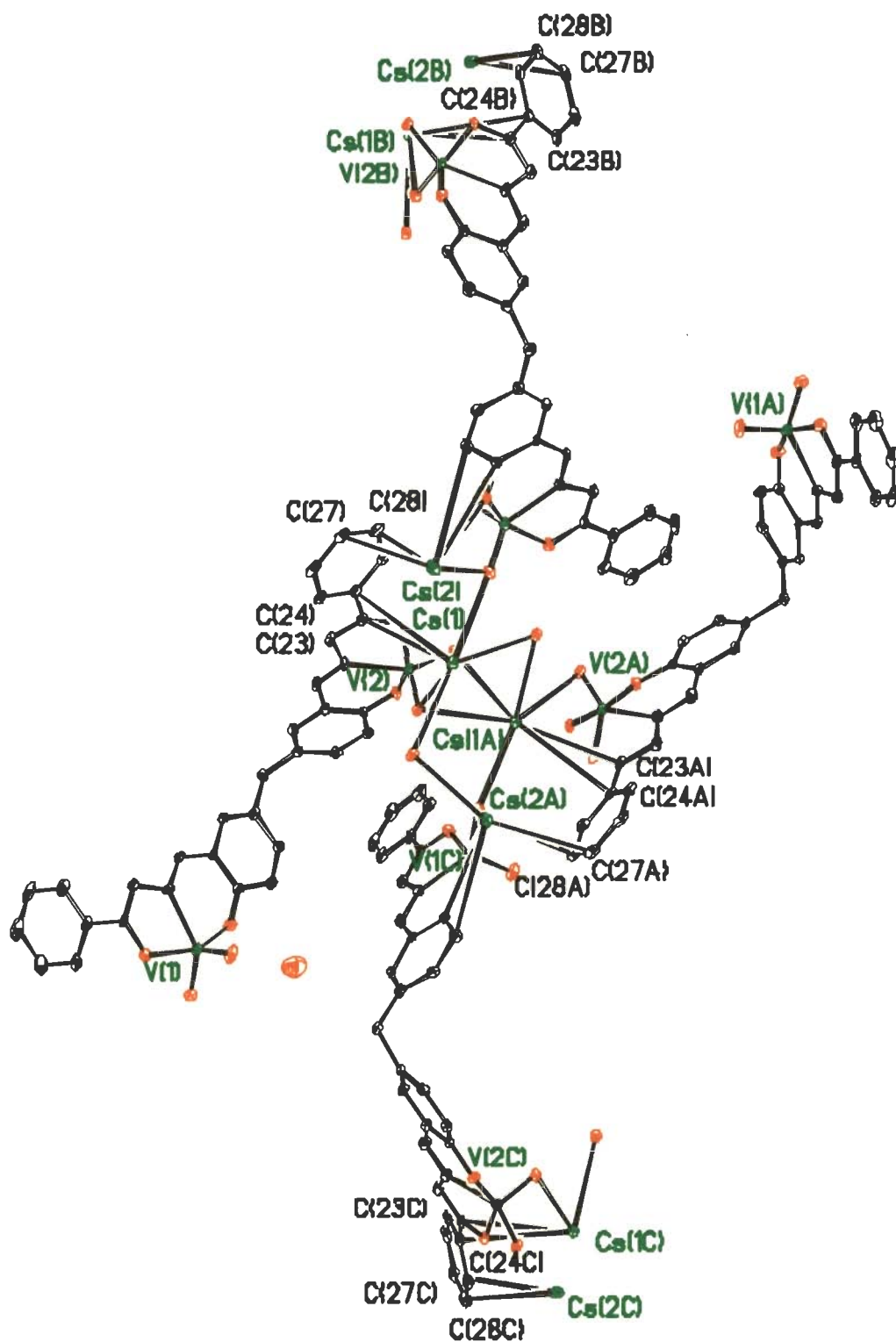


Figure 3.2. The four dinuclear molecules present in the unit cell of compound $Cs_2[CH_2\{V^VO_2(sal-bhz)\}_2] \cdot 2H_2O$ (3.3).

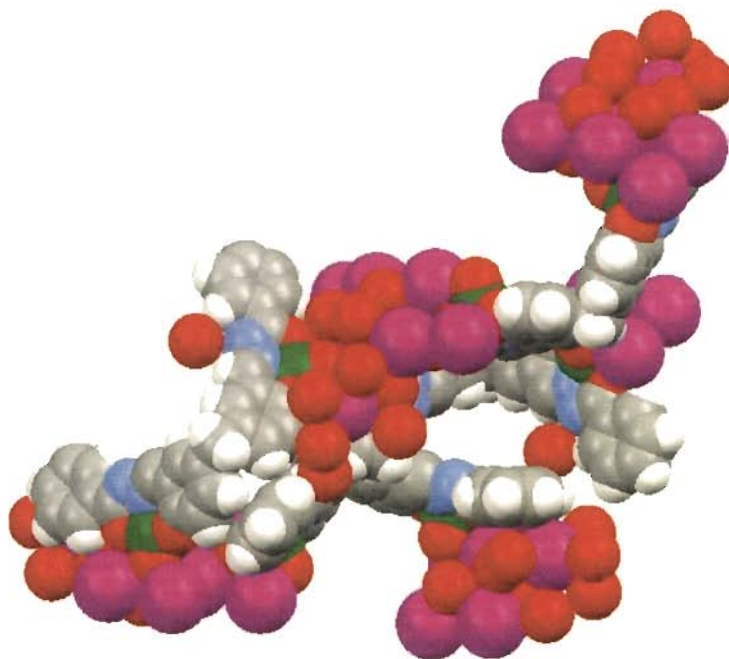


Figure 3.3. Space filling representation of the crystal packing of compound $Cs_2[CH_2\{V^VO_2(sal-bhz)\}_2] \cdot 2H_2O$ (**3.3**), showing cation π -interactions. In red: oxygen, pink: caesium, gray: carbon, green: vanadium, dark blue: nitrogen and white: hydrogen atoms.

Table 3.2. Selected bond lengths (Å) and angles (°) for $[Cs]_2[CH_2\{V^VO_2(salbh_z)\}_2]$ (3.3)

Cs(1)-O(2)#1	2.944(4)	V(1)-O(7)	1.622(5)
Cs(1)-O(6)#2	3.081(5)	V(1)-O(6)	1.639(5)
Cs(1)-O(2W)#3	3.118(5)	V(1)-O(5)	1.895(5)
Cs(1)-O(1)	3.131(5)	V(1)-O(8)	2.001(5)
Cs(1)-O(3)#3	3.164(5)	V(1)-N(3)	2.145(6)
Cs(1)-O(3)	3.170(5)	Cs(1)-V(2)#3	3.8426(12)
Cs(1)-O(2)#3	3.177(5)	Cs(1)-V(2)	3.8457(12)
Cs(1)-O(2W)#1	3.242(5)	V(1)-Cs(2)#4	3.7818(12)
Cs(1)-C(23)	3.703(6)	V(1)-Cs(2)#5	4.0020(12)
Cs(1)-C(24)	3.901(6)	V(2)-O(3)	1.616(5)
Cs(2)-O(2)#1	2.955(5)	V(2)-O(2)	1.644(5)
Cs(2)-O(5)#2	3.070(5)	V(2)-O(4)	1.907(5)
Cs(2)-O(8)#7	3.073(5)	V(2)-N(2)	2.144(6)
Cs(2)-O(7)#7	3.155(6)	V(2)-Cs(1)#9	3.8426(12)
Cs(2)-O(6)#2	3.192(5)	V(2)-Cs(2)#6	4.1059(12)
Cs(2)-O(2W)#8	3.261(5)	V(2)-Cs(1)#6	4.2578(11)
Cs(2)-C(28)	3.384(8)	Cs(2)-V(1)#7	3.7818(12)
Cs(2)-O(1)#1	3.430(5)	O(1)-V(2)	1.973(5)
Cs(2)-C(27)	3.519(8)	O(1)-C(23)	1.321(8)
Cs(2)-C(14)#2	3.842(6)	N(1)-C(23)	1.313(9)
Cs(2)-C(13)#2	3.851(7)	N(1)-N(2)	1.386(8)
O(2)-Cs(1)#6	2.944(4)	N(2)-C(22)	1.298(10)
O(2)-Cs(2)#6	2.955(5)	N(3)-C(8)	1.295(10)
O(2)-Cs(1)#9	3.177(5)	N(3)-N(4)	1.404(8)
O(2W)-Cs(1)#9	3.118(5)	N(4)-C(7)	1.289(10)
O(2W)-Cs(1)#6	3.242(5)	O(5)-C(14)	1.323(8)
O(2W)-Cs(2)#10	3.261(5)	C(7)-O(8)	1.321(8)
O(3)-Cs(1)#9	3.164(5)		
O(6)-Cs(1)#5	3.081(5)	O(2)#1-Cs(1)-C(23)	86.94(15)
O(6)-Cs(2)#5	3.192(5)	O(6)#2-Cs(1)-C(23)	91.48(14)
O(7)-Cs(2)#4	3.155(6)	O(2W)#3-Cs(1)-C(23)	109.59(13)
O(8)-Cs(2)#4	3.073(5)	O(1)-Cs(1)-C(23)	20.13(13)
C(13)-Cs(2)#5	3.851(7)	O(3)#3-Cs(1)-C(23)	166.13(14)
C(14)-Cs(2)#5	3.842(6)	O(3)-Cs(1)-C(23)	60.04(14)
		O(2)#3-Cs(1)-C(23)	144.03(14)
O(2)#1-Cs(1)-O(6)#2	89.29(14)	O(2W)#1-Cs(1)-C(23)	99.35(13)
O(2)#1-Cs(1)-O(2W)#3	145.29(13)	O(2)#1-Cs(1)-V(2)#3	105.87(9)
O(6)#2-Cs(1)-O(2W)#3	60.91(13)	O(6)#2-Cs(1)-V(2)#3	92.45(10)
O(2)#1-Cs(1)-O(1)	106.56(12)	O(2W)#3-Cs(1)-V(2)#3	61.76(8)
O(6)#2-Cs(1)-O(1)	87.29(13)	O(1)-Cs(1)-V(2)#3	147.56(8)

O(2W)#3-Cs(1)-O(1)	90.41(12)	O(3)#3-Cs(1)-V(2)#3	24.28(9)
O(2)#1-Cs(1)-O(3)#3	88.22(13)	O(3)-Cs(1)-V(2)#3	108.68(8)
O(6)#2-Cs(1)-O(3)#3	75.46(13)	O(2)#3-Cs(1)-V(2)#3	24.84(8)
O(2W)#3-Cs(1)-O(3)#3	68.37(12)	O(2W)#1-Cs(1)-V(2)#3	82.69(8)
O(1)-Cs(1)-O(3)#3	157.26(12)	C(23)-Cs(1)-V(2)#3	166.64(11)
O(2)#1-Cs(1)-O(3)	121.61(13)	O(7)-V(1)-O(6)	108.2(3)
O(6)#2-Cs(1)-O(3)	133.50(13)	O(7)-V(1)-O(5)	101.4(3)
O(2W)#3-Cs(1)-O(3)	92.86(13)	O(6)-V(1)-O(5)	97.0(2)
O(1)-Cs(1)-O(3)	52.90(12)	O(7)-V(1)-O(8)	98.9(2)
O(3)#3-Cs(1)-O(3)	132.92(9)	O(6)-V(1)-O(8)	92.5(2)
O(2)#1-Cs(1)-O(2)#3	117.65(13)	O(5)-V(1)-O(8)	153.6(2)
O(6)#2-Cs(1)-O(2)#3	113.19(13)	O(7)-V(1)-N(3)	112.8(2)
O(2W)#3-Cs(1)-O(2)#3	65.75(12)	O(6)-V(1)-N(3)	138.0(2)
O(1)-Cs(1)-O(2)#3	130.51(12)	O(5)-V(1)-N(3)	83.4(2)
O(3)#3-Cs(1)-O(2)#3	48.79(12)	O(8)-V(1)-N(3)	73.2(2)

Symmetry transformations used to generate equivalent atoms:

#1 $x+1, y, z$ #2 $-x+3/2, -y+1, z-1/2$ #3 $x+1/2, -y+1/2, -z$

#4 $-x+5/2, -y+1, z+1/2$ #5 $-x+3/2, -y+1, z+1/2$ #6 $x-1, y, z$

#7 $-x+5/2, -y+1, z-1/2$ #8 $x+3/2, -y+1/2, -z$ #9 $x-1/2, -y+1/2, -z$

#10 $x-3/2, -y+1/2, -z$

3.3.2. IR spectral studies

Selected IR spectral data of ligand and complexes are presented in Table 3.3. The IR spectra of the ligands show bands at 1655 and 3270 $[\text{CH}_2(\text{H}_2\text{sal-nah})_2, \mathbf{3.I}]$ and 1653 and 3250 cm^{-1} $[\text{CH}_2(\text{H}_2\text{sal-inh})_2, \mathbf{3.II}]$ due to $\nu(\text{C}=\text{O})$ and $\nu(\text{N-H})$ stretches, respectively. This is indicative of their ketonic nature in the solid state. The disappearance of both bands on complex formation indicates the enolisation and replacement of H by the metal ion. New bands appearing in the region 1269–1285 cm^{-1} are assigned to the $\nu(\text{C}-\text{O}_{\text{enolic}})$ mode. The $\nu(\text{C}=\text{N}_{\text{azomethine}})$ stretch of the ligands appear at 1620 (in $\mathbf{3.I}$) and 1622 cm^{-1} (in $\mathbf{3.II}$), and this band is shifted to lower wave numbers by 21–32 cm^{-1} in the complexes, indicating the coordination of the azomethine nitrogen. A band appearing at 964 (in $\mathbf{3.I}$) and 966 cm^{-1} (in $\mathbf{3.II}$) due to the $\nu(\text{N-N})$ stretch undergoes a shift to higher wavenumbers by 49–83 cm^{-1} upon complex formation. A high frequency shift of the $\nu(\text{N-N})$ band is expected

because of the diminished repulsion between the lone pairs of adjacent nitrogen atoms [48]. A medium intensity band of the free ligand, covering the region 2900–3400 cm^{-1} , is assigned to intramolecular hydrogen bond involving the phenolic OH group, while the broad band appearing in the range 3000 – 3400 cm^{-1} in complexes is assigned to the $\nu(\text{OH})$ of the coordinated/non-coordinated H_2O involved in hydrogen bonding.

Both oxido vanadium(IV) complexes exhibit a band at 926 (in $[\text{CH}_2\{\text{V}^{IV}\text{O}(\text{sal-bhz})(\text{H}_2\text{O})\}_2]$ (3.1)) and 927 cm^{-1} (in $[\text{CH}_2\{\text{V}^{IV}\text{O}(\text{sal-fah})(\text{H}_2\text{O})\}_2]$ (3.4)) due $\nu(\text{V}=\text{O})$ while dioxido vanadium(V) complexes exhibit two sharp bands in the 911–952 cm^{-1} range due to $\nu_{\text{asym}}(\text{O}=\text{V}=\text{O})$ and $\nu_{\text{sym}}(\text{O}=\text{V}=\text{O})$ stretches corresponding to the $\text{cis-}[V^VO_2]^+$ unit.

Table 3.3. Summary of IR spectra of compounds (ν in cm^{-1})^a

Compounds	$\nu(\text{C-O})$	$\nu(\text{C=N})$	$\nu(\text{V=O})$	$\nu(\text{N-N})$
$\text{CH}_2(\text{sal-bhz})_2$ I	-	1622	-	964
$\text{CH}_2(\text{sal-fah})_2$ II	-	1620	-	966
$[\text{CH}_2\{\text{V}^{IV}\text{O}(\text{sal-bhz})(\text{H}_2\text{O})\}_2]$	1273	1590	926	1043
$\text{K}_2[\text{CH}_2\{\text{V}^VO_2(\text{sal-bhz})_2\}]\cdot 2\text{H}_2\text{O}$	1269	1593	918, 952	1032
$\text{Cs}_2[\text{CH}_2\{\text{V}^VO_2(\text{sal-bhz})_2\}]\cdot 2\text{H}_2\text{O}$	1274	1595	918, 950	1024
$[\text{CH}_2\{\text{V}^{IV}\text{O}(\text{sal-fah})(\text{H}_2\text{O})\}_2]$	1279	1594	927	1021
$\text{K}_2[\text{CH}_2\{\text{V}^VO_2(\text{sal-fah})_2\}]\cdot 2\text{H}_2\text{O}$	1281	1598	911, 934	1024
$\text{Cs}_2[\text{CH}_2\{\text{V}^VO_2(\text{sal-fah})_2\}]\cdot 2\text{H}_2\text{O}$	1285	1599	913, 931	1015

^a $\nu(\text{C=O})$ for $\text{CH}_2(\text{H}_2\text{sal-bhz})_2$ at 1648; $\nu(\text{C=O})$ for $\text{CH}_2(\text{H}_2\text{sal-fah})_2$ at 1645.

3.3.3. Electronic spectral studies

Electronic spectral data of ligands and complexes are presented in Table 3.4. Ligands $\text{CH}_2(\text{H}_2\text{sal-nah})_2$ (3.I) and $\text{CH}_2(\text{H}_2\text{sal-inh})_2$ (3.II) exhibit four absorption bands at ca. 205, 240, 290, 300 and 335 nm which are assigned to $\phi \rightarrow$

φ^* , $\pi \rightarrow \pi_1^*$, $\pi \rightarrow \pi_2^*$, $n \rightarrow \pi_1^*$ and $n \rightarrow \pi_2^*$, transitions, respectively. In the complexes with ligand **3.I**, the $\varphi \rightarrow \varphi^*$ band shifted towards higher wavelength, while the bands due to $\pi \rightarrow \pi_1^*$ and $\pi \rightarrow \pi_2^*$ shift towards lower wavelengths. The splitted $n \rightarrow \pi^*$ bands in are now merged and appeared at ca. 325 nm. Other complexes present similar trend except the $\pi \rightarrow \pi_1^*$ band, which shifts towards higher wavelengths, and $\pi \rightarrow \pi_2^*$ shows no systematic trend. In addition, new bands of medium intensity appear at 404 – 414 nm, which are assigned to a ligand to metal charge transfer (LMCT) band. The oxido vanadium(IV) complexes also present a medium intensity band at ca. 560 nm due to d – d transitions.

Table 3.4. Electronic spectral data of compounds recorded in methanol.

Compounds	λ (nm)
$CH_2(H_2sal-bhz)_2$ (3.I)	337, 300, 290, 237, 206
$CH_2(H_2sal-fah)_2$ (3.II)	336, 305, 294, 244, 207
$[CH_2\{V^{IV}O(sal-bhz)(H_2O)\}_2]$ (3.1)	561, 408, 328, 258, 223, 206
$K_2[CH_2\{V^VO_2(sal-bhz)\}_2] \cdot 2H_2O$ (3.2)	404, 323, 243, 228, 209
$Cs_2[CH_2\{V^VO_2(sal-bhz)\}_2] \cdot 2H_2O$ (3.3)	405, 325, 243, 223, 208
$[CH_2\{V^{IV}O(sal-fah)(H_2O)\}_2]$ (3.4)	568, 407, 331, 276, 247, 213
$K_2[CH_2\{V^VO_2(sal-fah)\}_2] \cdot 2H_2O$ (3.5)	404, 325, 306, 293, 215
$Cs_2[CH_2\{V^VO_2(sal-fah)\}_2] \cdot 2H_2O$ (3.6)	406, 327, 271, 244, 217

3.3.4. 1H NMR studies

The relevant 1H NMR data are summarized in Table 3.5. The 1H NMR spectra of the ligands exhibit signals at $\delta = 10.98$ ($CH_2(H_2sal-nah)_2$ (**3.I**)) and at $\delta = 10.94$ ($CH_2(H_2sal-inh)_2$ (**3.II**)) due to the –NH proton, indicating their existence in the ketonic form. The absence of this signal in the complexes is in agreement with enolisation and subsequent replacement of H by the metal ion. Similarly, the absence of the 12.09 ppm signal of the ligands, due to phenolic OH, indicates the deprotonation/coordination of the O-phenolate. A significant downfield shift

$[\text{CIS}(\Delta\delta) = 0.19 - 0.35 \text{ ppm}]$ (CIS = Chemical induced shift) of the azomethine ($-\text{CH}=\text{N}-$) proton signal in the complexes in respect to the corresponding free ligands confirms the coordination of the azomethine nitrogen. The ^1H NMR data are thus consistent with the ONO dibasic tridentate binding mode of each unit of ligands. The aromatic protons of ligands and complexes appear as complex multiplets in the expected region. The signal due to the methylene group attached to the two aromatic rings in ligands as well as in complexes, appears at nearly the same position ($\Delta\delta = 0.0 - 0.14 \text{ ppm}$) Thus, the ^1H NMR data is in agreement with the conclusions from IR data and with the structures proposed.

Table 3.5. ^1H NMR spectral data (δ in ppm) for ligands **3.I** and **3.II** and the V^{VO_2} -complexes recorded in $\text{DMSO}-d_6$

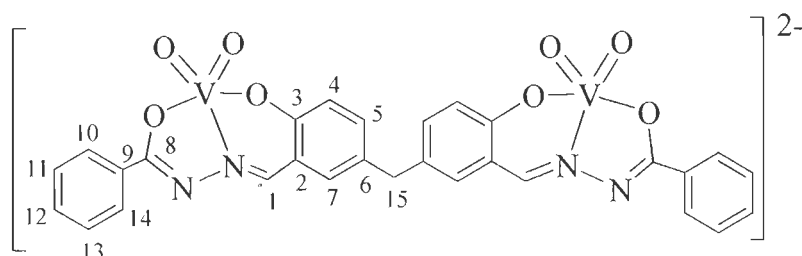
Compound ^{a,b,c}	$-\text{CH}=\text{N}-$	Aromatic H	$-\text{CH}_2-$
$\text{CH}_2(\text{H}_2\text{sal-bhz})_2$	8.64(s, 2H)	6.70-7.94(m, 16H)	3.85(s, 1H)
$\text{K}_2[\text{CH}_2\{\text{VO}_2(\text{sal-bhz})\}_2]$ ($\Delta\delta$)	8.97(s, 2H) (0.33)	6.73-8.02(m, 16H)	3.86(s, 1H) 0.01
$\text{Cs}_2[\text{CH}_2\{\text{VO}_2(\text{sal-bhz})\}_2]$ ($\Delta\delta$)	8.94(s, 2H) (0.30)	6.74-8.02(m, 16H)	3.86(s, 1H) (0.01)
$\text{CH}_2(\text{H}_2\text{sal-fah})_2$	8.63(s, 2H)	6.87-7.95(m, 12H)	3.85(s, 1H)
$\text{K}_2[\text{CH}_2\{\text{VO}_2(\text{sal-fah})\}_2]$ ($\Delta\delta$)	8.87(s, 2H) (0.24)	6.62-7.96(m, 12H)	3.85(s, 1H) (0.00)
$\text{Cs}_2[\text{CH}_2\{\text{VO}_2(\text{sal-fah})\}_2]$ ($\Delta\delta$)	8.89(s, 2H) (0.26)	6.35-7.81(m, 12H)	3.85(s, 1H) (0.00)

^aLetters given in parentheses indicate the signal structure: s = singlet, m = multiplet. ^b $\Delta\delta = \delta(\text{complex}) - \delta(\text{ligand})$. ^c δ ($-\text{OH}$) for $\text{CH}_2(\text{H}_2\text{sal-bhz})_2$ and $\text{CH}_2(\text{H}_2\text{sal-fah})_2$ at 12.09 (s, 2H). δ ($-\text{NH}$) for $\text{CH}_2(\text{H}_2\text{sal-bhz})_2$ and $\text{CH}_2(\text{H}_2\text{sal-fah})_2$ at 11.09(b, 2H) and 10.94(b, 2H), respectively.

3.3.5. ^{13}C NMR studies

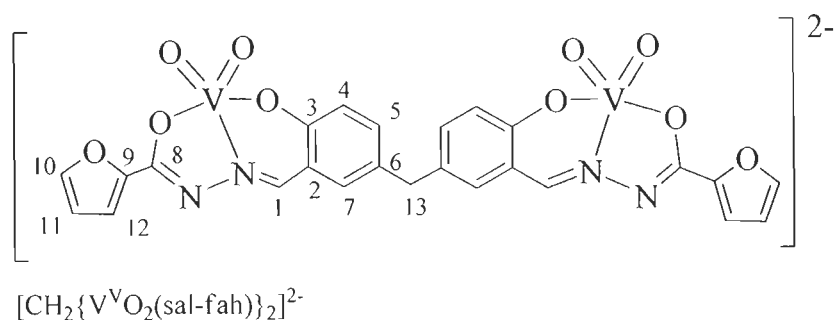
The ^{13}C spectra of complexes $\text{K}_2[\text{CH}_2\{\text{V}^{\text{V}}\text{O}_2(\text{sal-bhz})\}_2]\cdot 2\text{H}_2\text{O}$ (**3.2**) and $\text{Cs}_2[\text{CH}_2\{\text{V}^{\text{V}}\text{O}_2(\text{sal-bhz})\}_2]\cdot 2\text{H}_2\text{O}$ (**3.3**) contain 13 signals corresponding to the 27 carbon atoms of the molecules owing to their symmetry. The assignment of the peaks (Table 3.6) was made with the help of the Chem Draw[®] software and all of them match within $\pm 2\%$ accuracy with the predicted values. The peaks of atoms C14 overlap those of DMSO so they cannot be properly assigned. For compounds $\text{K}_2[\text{CH}_2\{\text{V}^{\text{V}}\text{O}_2(\text{sal-fah})\}_2]\cdot 2\text{H}_2\text{O}$ (**3.5**) and $\text{Cs}_2[\text{CH}_2\{\text{V}^{\text{V}}\text{O}_2(\text{sal-fah})\}_2]\cdot 2\text{H}_2\text{O}$ (**3.6**), 10 and 9 distinct signals, respectively, were recorded (see Table 3.7)

Table 3.6. ^{13}C NMR chemical shifts observed; for the atom labelling see scheme below



Compound	C8	C1	C3	C10/11	C12/13
$\text{K}_2[\text{CH}_2\{\text{V}^{\text{V}}\text{O}_2(\text{sal-bhz})\}_2]$	163.5	148	147.9	145	134
$\text{Cs}_2[\text{CH}_2\{\text{V}^{\text{V}}\text{O}_2(\text{sal-bhz})\}_2]$	163	147	142	134.9	132.3
	C14	C7/9	C5	C2	C4
$\text{K}_2[\text{CH}_2\{\text{V}^{\text{V}}\text{O}_2(\text{sal-bhz})\}_2]$	132	130	120	113.7	112
$\text{Cs}_2[\text{CH}_2\{\text{V}^{\text{V}}\text{O}_2(\text{sal-bhz})\}_2]$	130.4	121.9	120	119.7	

Table 3.7. ^{13}C NMR chemical shifts observed; for the atom labelling see scheme below

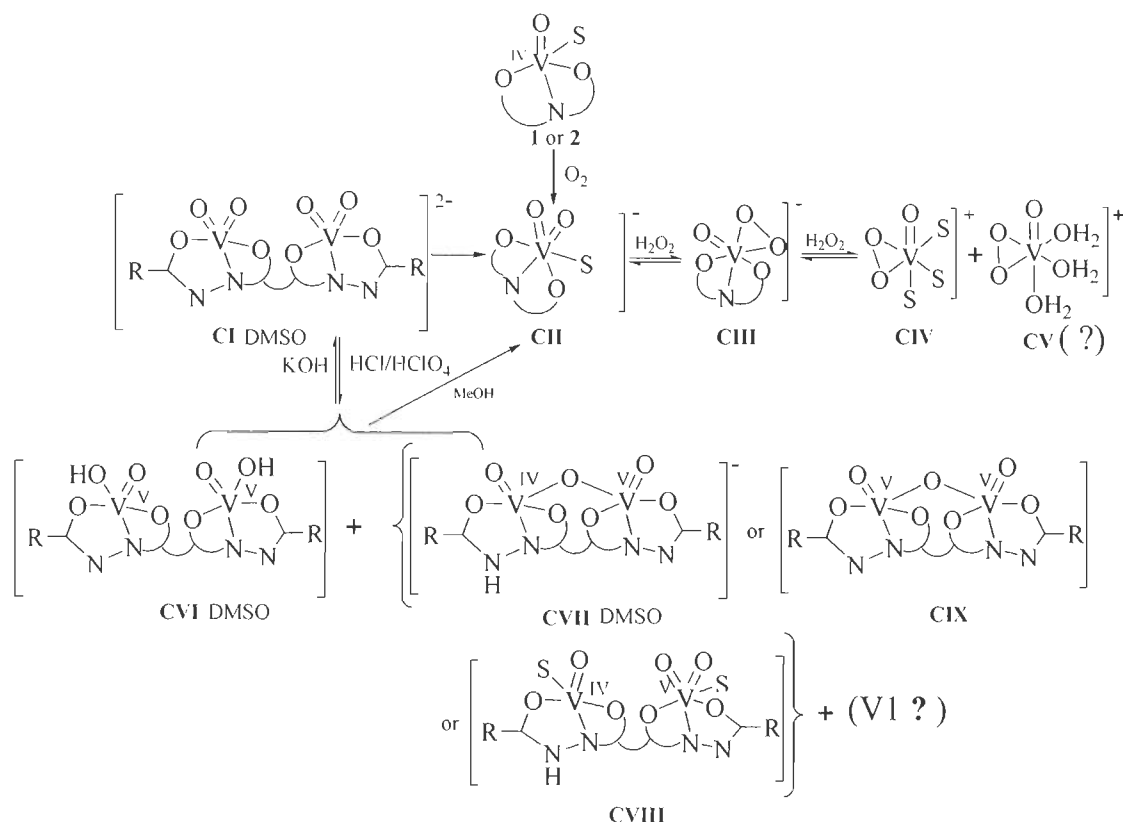


Compound	C8	C1	C3	C9	C7/ 6/ 4/ 5
$K_2[CH_2\{V^VO_2(sal-fah)\}_2]$	163.5	156	147.9	145	134 132 130
$Cs_2[CH_2\{V^VO_2(sal-fah)\}_2]$	163.5	156	147	145	134 132
	C10/ 11/ 12				
$K_2[CH_2\{V^VO_2(sal-fah)\}_2]$	120	113.7	112		
$Cs_2[CH_2\{V^VO_2(sal-fah)\}_2]$	119	113	112		

3.3.6. ^{51}V NMR studies

Further characterization of the complexes was obtained from the ^{51}V NMR spectra and the ^{51}V NMR spectral data of complexes $K_2[CH_2\{V^VO_2(sal-bhz)\}_2] \cdot 2H_2O$ (**3.2**), $Cs_2[CH_2\{V^VO_2(sal-bhz)\}_2] \cdot 2H_2O$ (**3.3**), $K_2[CH_2\{V^VO_2(sal-fah)\}_2] \cdot 2H_2O$ (**3.5**) and $Cs_2[CH_2\{V^VO_2(sal-fah)\}_2] \cdot 2H_2O$ (**3.6**) are collected in Table 3.8. The line widths are approximately 200 Hz, which may be considered comparatively narrow. The ^{51}V NMR spectra of $[CH_2\{V^VO_2(ONO)\}_2]^{2-}$ (4 mM) in DMSO shows resonances at $-532/ -534$ ppm, and upon addition of 0.5 M methanol there is a slight upfield shift to $-537/ -540$ ppm, the spectra becoming identical to those recorded in MeOH, Figure 3.4. The resonances are assigned to $[CH_2\{V^VO_2(ONO)(S)\}_2]^{2-}$ (**CII**, S = DMSO or MeOH in Scheme 3.3). On the other hand addition of H_2O (the solvent becoming MeOH: H_2O 95:5 v/v)

resonances at -540 ppm are obtained suggesting the coordination of H_2O {i.e. formation of $[CH_2\{V^VO_2\}(ONO)(H_2O)\}_2]^{2-}$.



Scheme 3.3. Summary of speciation of vanadium species in solution.

Table 3.8. Summary of the ^{51}V NMR data (ppm) and assignment of the vanadium complexes studied in this work (see text and Scheme 3.3).

Compounds	CII, S = DMSO	CII, S = MeOH	CIII	$[\text{VO}(\text{O}_2)(\text{S})]^+$	$[\text{VO}(\text{O})_2/\text{H}_2\text{O}]^+ (?)$
3.2	-533	-537	-604	-616	-640
3.3	-532	-538	-606	-622	-640
3.5	-533	-538	-608	-618	-638
3.6	-534	-540	-607	-625	-640

Upon the stepwise addition of an aqueous 30% solution of H_2O_2 to the methanolic solution of **3.5** (ca. 4 mM) the resonance at -538 ppm progressively

disappears and resonances at -608 ppm are observed (Figure 3.5(b)), which we tentatively assign as due to $[CH_2\{V^VO(O_2)(ONO)\}_2]^{2-}$ (**CIII**). Upon further stepwise additions of H_2O_2 (8 equiv or higher) the resonance at -538 ppm totally disappears and two new signals are detected at $\delta = -618$ and -638 ppm, which we assign to inorganic peroxovanadates {tentatively $[V^VO(O_2)(S)_n]^+$ (**CIV**) [229] and $[V^VO(O_2)(H_2O)_n]^+$, (**CV**) [293-300] (see Scheme 3.3). Leaving the NMR tube open for 36 h after recording the spectrum of Figure 3.5 (d), a spectrum identical to (a) was obtained, indicating the reversibility of the process.

The addition of acid (HCl/HClO₄) viz. 1, 2, 3, 4 equiv to a methanolic solution of $[CH_2\{V^VO_2(ONO)\}_2]^{2-}$ leads to the decrease in intensity of the -538 ppm peak and an increase at -545 ppm (Figure 3.6), the color of solution turns to red and the pH ~ 2.5 to 3.3. The addition of acid may protonate the ligand so the -545 ppm band may either be due to (**CII**, $S = H_2O$) or to free vanadate (V_1). As addition of H_2O to the 4 mM solution of **3** in DMSO yields an upfield shift to -540 ppm, this indicating the involvement of the solvent molecule, we assign the -540 ppm signal in these solutions to $[CH_2\{V^VO(ONO)(H_2O)\}_2]^{2-}$ (**CII**, $S = H_2O$).

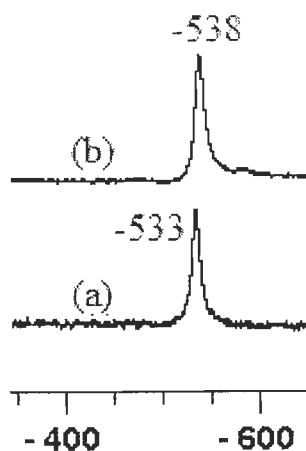


Figure 3.4. (a) ^{51}V NMR spectrum of a 4 mM solution of $K_2[CH_2\{V^VO_2(sal-fah)\}_2]$ (**3.5**) in DMSO; (b) addition of 0.5 M methanol to the solution of (a).

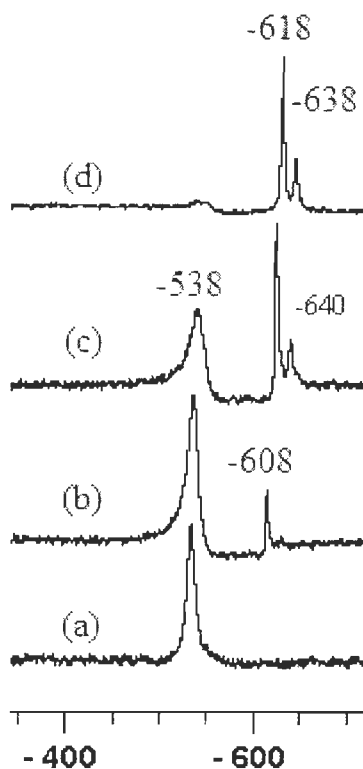


Figure 3.5. ^{51}V NMR spectra for $\text{K}_2[\text{CH}_2\{\text{V}^{\text{VO}}\text{O}_2(\text{sal-fah})\}_2]$ (**3.5**): (a) in MeOH, (b) after addition of 3.0 equiv H_2O_2 (30%) to the solution of (a); (c) after addition of a total of 5 equiv H_2O_2 (30%) to the solution of (a); (d) after addition of a total of 8.0 equiv H_2O_2 (30%) to the solution of (a).

The behavior of $\text{K}_2[\text{CH}_2\{\text{V}^{\text{VO}}\text{O}_2(\text{sal-fah})\}_2]$ (**3.5**) dissolved in DMSO differs from what is observed in methanol. Upon addition of 3 equiv HClO_4 the ^{51}V NMR spectrum at $\text{pH} \sim 3.1$ shows two new signals at -470 (broad) (ca. 96 %) and -560 (ca. 2 %) ppm, as well as the original resonance at -533 (ca. 2%) ppm [Figure 3.6(d)]. Similarly addition of 3 equiv HCl to the solution of **3.5** in DMSO yields two new signals at -447 (broad with a shoulder) (ca. 98%) [Figure 3.6(b)].

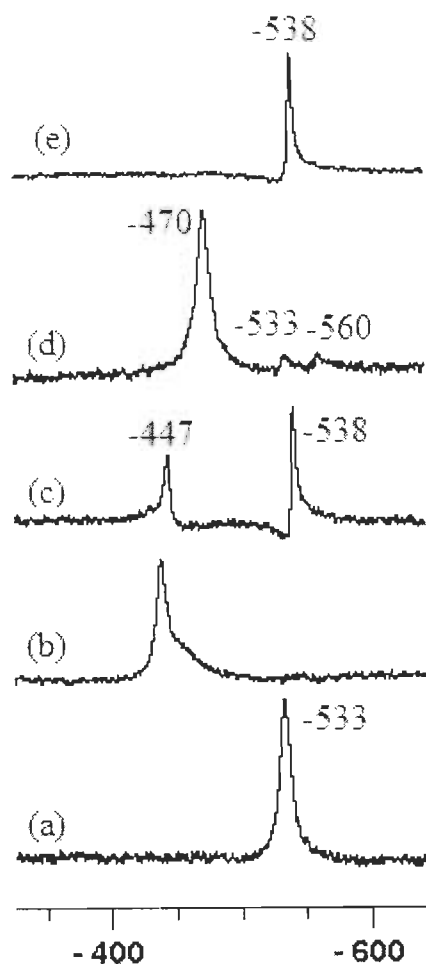


Figure 3.6. ^{51}V NMR spectra for $\text{K}_2[\text{CH}_2\{\text{V}^{\text{VO}}\text{O}_2(\text{sal-fah})\}_2]$ (**3.5**): (a) in DMSO, (b) 3.0 equiv HCl to the solution (a); (c) addition of methanol to solution of (b) [final MeOH ca. 50% v/v] ; (d) 3.0 equiv HClO_4 to the solution (a); (e) addition of methanol to solution of (d) [final MeOH ca. 50% v/v].

For further investigation both solutions of (b) and (d) in Figure 3.6 were divided in three parts. On addition of MeOH to one of these only the peak at -538 ppm [Figure 3.3(c, e)] is detected and this can be assigned to species (**CII**, $S = \text{MeOH}$). Addition of 4 equiv KOH to the second portion yields a resonance at -533 ppm indicating the reversibility of the reaction. The third portion of this solution was kept for 48 hr at room temperature and then showed a major resonance at -539 ppm corresponding to **CII**.

Additionally the spectra of Figure 3.6(b) and (d) shows broadening of ^{51}V NMR signals, indicating the possible presence of an oxido vanadium(IV) species in the solution. This was confirmed by recording the EPR spectra for both solutions. The spectra are reasonably intense and the spin Hamiltonian parameters obtained are $g_{\perp} = 1.972$; $g_{\parallel} = 1.953$; $A_{\perp} = 58.7 \times 10^4 \text{ cm}^{-1}$ and $A_{\parallel} = 167 \times 10^4 \text{ cm}^{-1}$ [for solution of (d)] and $g_{\perp} = 1.974$; $g_{\parallel} = 1.954$; $A_{\perp} = 59 \times 10^4 \text{ cm}^{-1}$ and $A_{\parallel} = 168 \times 10^4 \text{ cm}^{-1}$ [for solution of (b)]. The parameters are similar to those of solutions of **3.1** in DMSO (see below) indicating a O_3N binding mode around the vanadium center, i.e. a binding mode identical to that of **3.4**.

We assign the -560 ppm lower field resonances of Figure 3.6(d) to the oxido hydroxo species (**CVI**). The partial protonation of the ligand is also a plausible possibility.

As mentioned, in the conditions of Figure 3.6 (b, d) a $\text{V}^{\text{IV}}\text{O}$ -species forms from partial reduction of the V^{V} present. This is reflected in the global decrease of the ^{51}V NMR signals recorded and by the reasonably intense EPR spectra recorded. Moreover, for the solution of e.g. Figure 3.6 (b) the EPR spectrum recorded is compatible with the formation of a $\text{V}^{\text{IV}}\text{O}$ -species with a binding mode including a tridentate ONO ligand and a solvent molecule. To explain the peaks at ca. $-447/-470$ ppm, due to a V^{V} -species, we consider now three possibilities: (i) the formation of a mixed valence $\text{V}^{\text{IV}}\text{O}-\text{O}-\text{V}^{\text{V}}\text{O}$ complex (see structure **CVII** in Scheme 3.6), or (ii) a complex formulated as $[\text{CH}_2\{\text{V}^{\text{V}}\text{O}_2(\text{sal-fah})\}\{\text{V}^{\text{IV}}\text{O}_2(\text{sal-fah})\}]$ (see structure **CVIII**), (iii) the formation of a $\text{V}^{\text{V}}\text{O}-\text{O}-\text{V}^{\text{V}}\text{O}$ complex (see structure **CIX**), along with a V^{IV} -complex which corresponds to **3.4**. The ^{51}V NMR peaks in assignments (i) or (ii) correspond to the V^{V} -“half-part” of the molecule.

If a $\text{V}^{\text{IV}}\text{O}-\text{O}-\text{V}^{\text{V}}\text{O}$ complex is formed as in structure **CVII**, the V-O-V angle should not be close to 180° , so that the unpaired electron is localized on one of the V atoms of the V-O-V dinuclear unit. To our knowledge there is no previous

example of ^{51}V NMR signals being obtained for $\text{V}^{\text{IV}}\text{O}-\text{O}-\text{V}^{\text{V}}\text{O}$ complexes (or reports of attempts to measure it). In order that the $-440/-475$ ppm resonances may be assigned to the $\text{V}^{\text{V}}\text{O}_2$ -“half-part” of structure **CVIII**, which correspond to significantly deshielded V^{V} -species, some electron density should also have been delocalized from the V^{IV} - to the V^{V} -centre and it is not clear if this is feasible in **CVIII**. Globally we consider structure **CIX** as the most plausible assignment for the $-447/-470$ ppm resonances, the different values recorded possibly resulting from some electrostatic influence of the counter-ions present (Cl^- , ClO_4^-) nearby.

The formation of $[\text{CH}_2\{\text{V}^{\text{V}}\text{OL}\}_2]$ complexes, containing the $\text{V}^{\text{V}}\text{O}^{3+}$ moiety, upon addition of acid, as reported for a few vanadium systems {e.g. salen [236], EHGS, ethylenebis[*o*-hydroxyphenyl]glycine [237] and HSHED [301]} could be also a possibility to explain the ^{51}V NMR appearing at ca. -447 to -470 ppm. However, no strong LMCT band was observed in the 500-600 nm range for complexes with our ligands **3.I** and **3.II** (see below) as was found in the salen, HSHED and EHGS systems, so we assume these high-field resonances are not due to the formation of $\text{V}^{\text{V}}\text{OL}$ -type complexes.

3.3.7. EPR and UV/Vis studies

The EPR spectra of “frozen” solutions (77 K) in DMSO of compounds $\text{CH}_2\{\text{V}^{\text{IV}}\text{O}(\text{sal-bhz})(\text{H}_2\text{O})\}_2$ (**3.1**) and $[\text{CH}_2\{\text{V}^{\text{IV}}\text{O}(\text{sal-fah})(\text{H}_2\text{O})\}_2]$ (**3.4**) are depicted in Figures 3.7 and 3.8. Two sets of eight lines showing hyperfine splitting due to the ^{51}V nucleus are obtained, characteristic of square pyramidal complexes with an axially compressed d_{xy}^1 configuration. The value of A_{\parallel} can be calculated using the additivity relationship $[A_z^{\text{est}} = \sum A_{z,i} \text{ (} i = 1 \text{ to } 4\text{)}]$ proposed by Würthrich [240] and Chasteen [241], with estimated accuracy of $\pm 3 \times 10^{-4} \text{ cm}^{-1}$. The A_{\parallel} values obtained for $\text{CH}_2\{\text{V}^{\text{IV}}\text{O}(\text{sal-bhz})(\text{H}_2\text{O})\}_2$ (**3.1**) and $[\text{CH}_2\{\text{V}^{\text{IV}}\text{O}(\text{sal-fah})(\text{H}_2\text{O})\}_2]$ (**3.4**) (Table 3.9) agree with the values calculated from the partial contributions of the equatorial donor groups relevant in the present case [241]:

H_2O ($45.7 \times 10^{-4} \text{ cm}^{-1}$), $O_{\text{phenolate}}$ ($38.9 \times 10^{-4} \text{ cm}^{-1}$), N_{imine} , (38.1 to $43.7 \times 10^{-4} \text{ cm}^{-1}$), $O\text{-enolate}^{(1-)}$ ($37.6 \times 10^{-4} \text{ cm}^{-1}$), O_{DMSO} ($41.9 \times 10^{-4} \text{ cm}^{-1}$) [243]. The EPR spectra of both complexes in DMSO are in good agreement with the calculated and experimental data corresponding to O_3N binding mode, one of the equatorial donor atoms being O_{DMSO} .

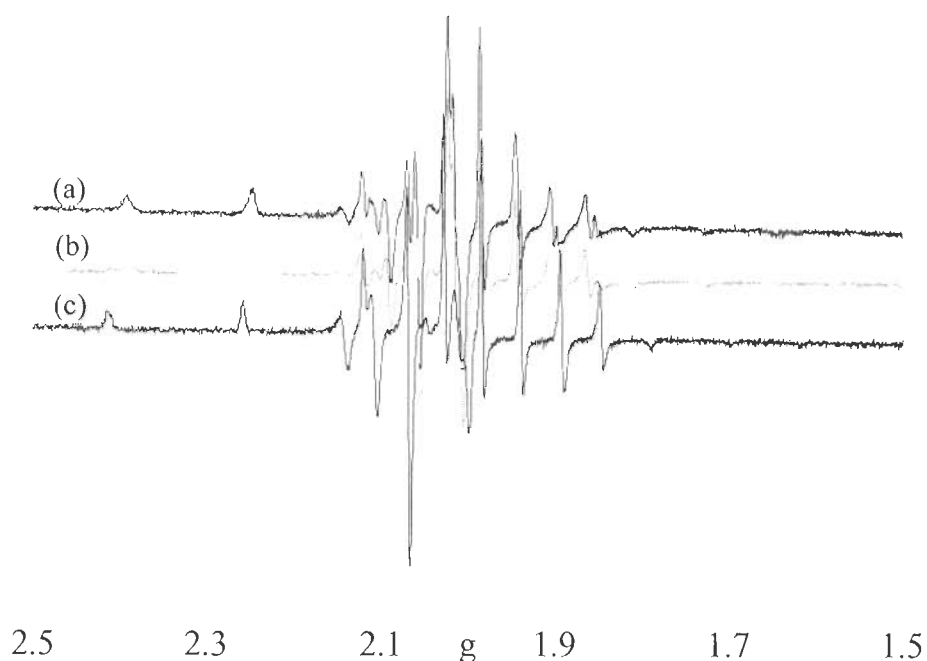


Figure 3.7. EPR spectra for 4 mM $[CH_2\{V^{IV}O(\text{sal-bhz})\}_2]$ (3.1) (a) in DMSO; (b) after addition of 1.0 equiv. of HCl [aqueous solution (11.6 M)] (c) after addition of a total of 2.0 equiv. of HCl [aqueous solution (11.6 M)].

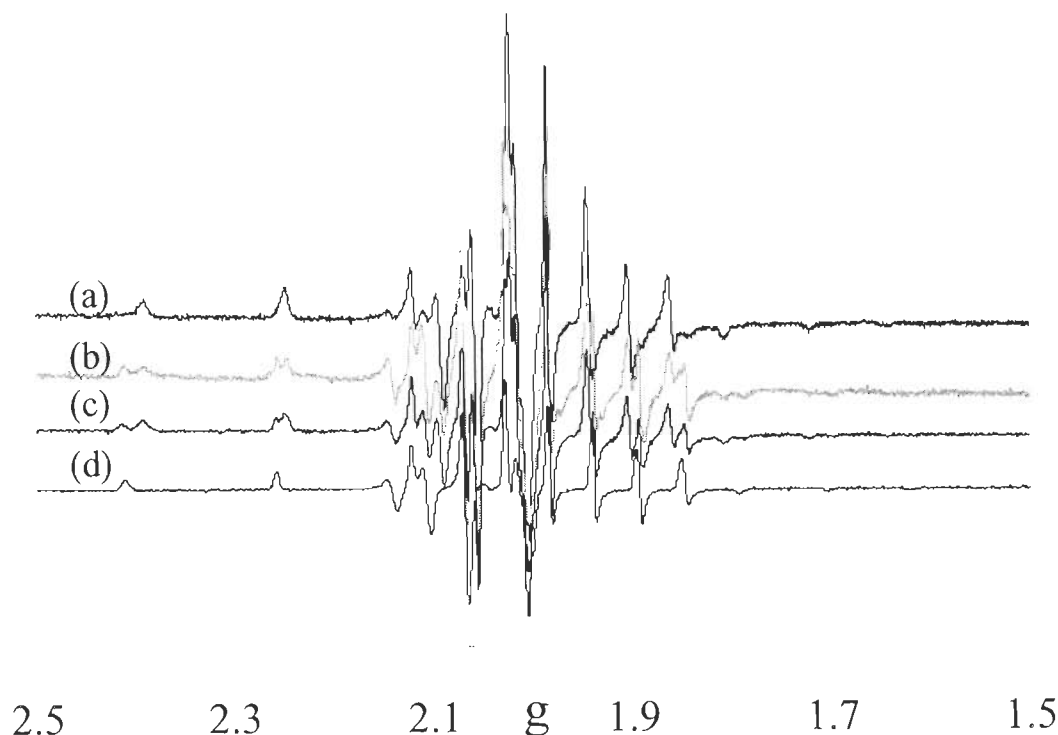


Figure 3.8. EPR spectra for 4 mM $[CH_2\{V^{IV}O(sal-fah)\}]_2$ (3.5) (a) in DMSO; (b) after addition of 1.0 equiv. of HCl [aqueous solution (11.6 M)] (c) after addition of a total of 2.0 equiv. of HCl [aqueous solution (11.6 M)], (d) after addition of a total of 3.0 equiv. of HCl [aqueous solution (11.6 M)].

The progressive addition of 1, 2 and 3 equiv of aqueous HCl to either $CH_2\{V^{IV}O(sal-bhz)(H_2O)\}_2$ (3.1) or $[CH_2\{V^{IV}O(sal-fah)(H_2O)\}_2]$ (3.4) led to the generation of a second complex species with EPR parameters (ca. $g_{||} = 1.937$ and $A_{||} = 176.5 \times 10^{-4} \text{ cm}^{-1}$). In this latter complex the binding mode appears to be either NO3 or O4, this indicating the substitution of the ligand by DMSO and/or H_2O molecules in the coordination sphere. Upon addition of 2 equiv portion of 30% aqueous H_2O_2 the intensity of EPR spectrum decreases, indicating the oxidation of the $V^{IV}O$ -complexes present. This solution shows the ^{51}V NMR resonance at -533 ppm as observed in DMSO solutions, i.e. the corresponding V^{VO_2} -complexes were formed.

Table 3.9. Spin Hamiltonian parameters obtained by simulation of the experimental EPR spectra recorded for solutions of complexes $CH_2\{V^{IV}O(sal-bhz)(H_2O)\}_2$ (**3.1**) and $[CH_2\{V^{IV}O(sal-fah)(H_2O)\}_2]$ (**3.4**) at 77K.

Complex	Solvent	g_{\parallel}	A_{\parallel} ($\times 10^4 \text{ cm}^{-1}$)	g_{\perp}	A_{\perp} ($\times 10^4 \text{ cm}^{-1}$)
$[CH_2\{VO(sal-bhz)\}_2]$	DMSO	1.949	166.7	1.979	58.5
1.0 equiv HCl ^a	Species 1	1.949	166.1	1.976	58.0
	Species 2	1.937	175.6	1.981	65.5
2.0 equiv HCl ^a		1.937	176.4	1.978	65.5
$[CH_2\{VO(sal-fah)\}_2]$	DMSO	1.948	167.3	1.977	59.0
1.0 equiv HCl ^a	Species 1	1.954	167.4	1.973	59.3
	Species 2	1.936	176.1	1.978	59.0
2.0 equiv HCl ^a	Species 1	1.955	167.3	1.979	58.6
	Species 2	1.935	176.7	1.978	65.8
3.0 equiv HCl ^a		1.938	176.7	1.978	65.7

^a Addition of aqueous HCl (11.6 M) solution.

The peroxo complexes of these ligands could not be isolated in the solid state. However, the formation of peroxo complexes in methanol by treatment of the respective dioxido complexes with H_2O_2 could also be established by electronic absorption spectroscopy. Thus, the treatment of 20 mL of 2.86×10^{-5} M (0.655 mM) solution of $Cs_2[CH_2\{V^VO_2(sal-bhz)\}_2 \cdot 2H_2O]$ (**3.2**) with the stepwise addition of 30 % aqueous H_2O_2 (total of 2.405 g, 18.04 mmol), recording the spectra after 25 min of each addition, resulted in the spectra presented in Figure 3.9. Initially, the two UV bands appearing at 232 and 282 nm (not shown in figure) experience a considerable increase in intensity while the band at 328 nm becomes a shoulder. Further addition of H_2O_2 results in the broadening of 405 nm along with slow

decrease in intensity, while the shoulder appearing at ca. 328 nm shifts to 325 nm along with sharpness. This change in spectra has been interpreted as the formation of peroxo compound [59, 65, 160, 169, 186, 263].

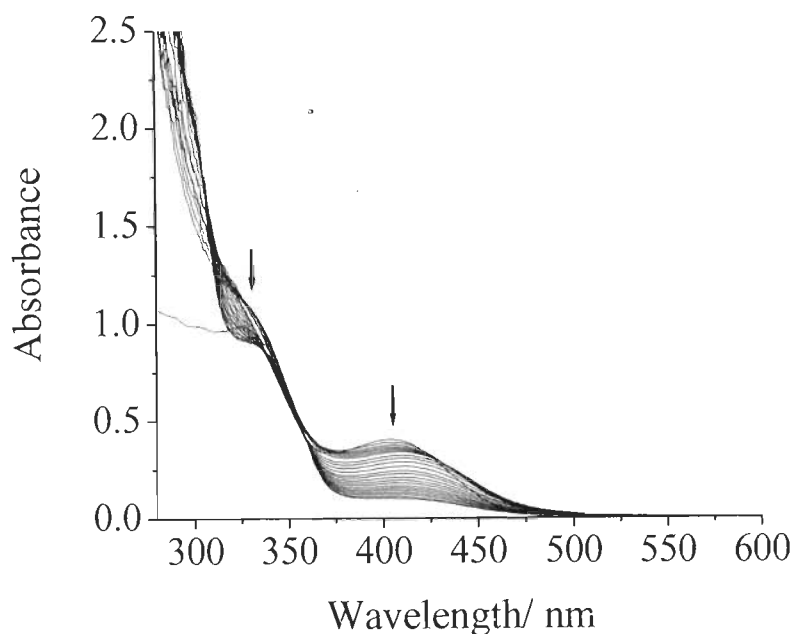


Figure 3.9. Spectral changes obtained during titration of 20 mL of 2.86×10^{-5} M methanolic solution of $Cs_2[CH_2\{V^VO_2(sal-bhz)\}_2] \cdot 2H_2O$ with dilute solution of 30% aqueous H_2O_2 (0.401 g, 3.01 mmol in 20 mL MeOH). Spectra were recorded after 25 min of each stepwise addition of dilute H_2O_2 solution up to a total of ca. 18 mmol (see text).

The behavior of the methanolic solutions of dioxidovanadium(V) complexes with HCl added was also monitored by electronic absorption spectroscopy. Thus the drop-wise addition of a saturated solution of HCl gas in methanol to 20 mL of ca. 4.183×10^{-5} M solution of $Cs_2[CH_2\{V^VO_2(sal-bhz)\}_2] \cdot 2H_2O$ (**3.3**) causes the darkening of the solution along with the decrease in intensity of the 236 nm band, and the appearance of a new band at 264 nm with increase in intensity; Figure 3.10. Simultaneously the UV bands at 328 nm and

304 nm gain intensity. The LMCT band appearing at 404 nm slowly broadens with decrease in its intensity. Similar features have been observed with the other three complexes $K_2[CH_2\{V^VO_2(sal-bhz)\}_2]\cdot 2H_2O$ (3.2), $K_2[CH_2\{V^VO_2(sal-fah)\}_2]\cdot 2H_2O$ (3.5) and $Cs_2[CH_2\{V^VO_2(sal-fah)\}_2]\cdot 2H_2O$ (3.6) (see Figures. 3.11, 3.12 and 3.13). We interpret these results in terms of the formation of the species mentioned above while explaining the ^{51}V NMR peaks at $-447/ -470$ ppm and at ca. -560 ppm (see Scheme 3.3).

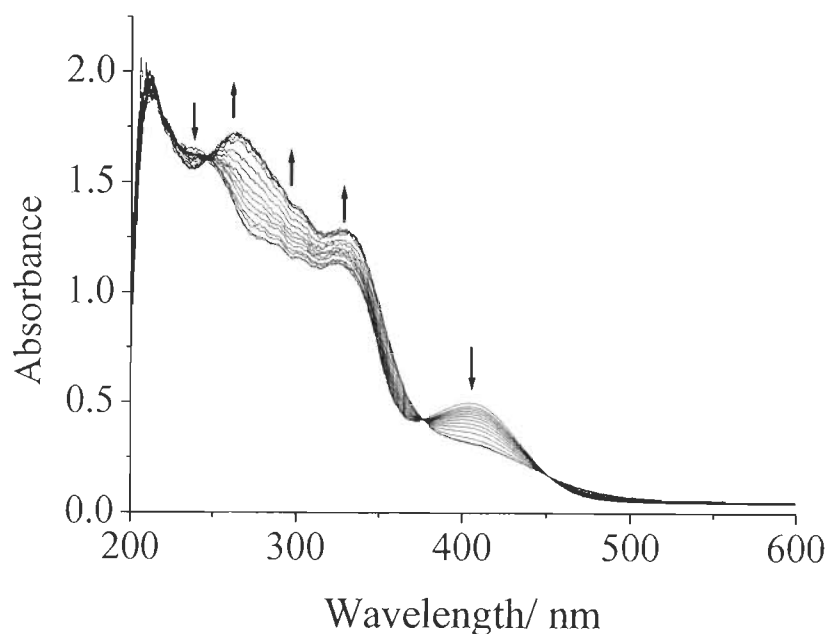


Figure 3.10. Spectral changes obtained during titration of 20 mL of 4.2×10^{-5} M methanolic solution of $Cs_2[CH_2\{V^VO_2(sal-bhz)\}_2]\cdot 2H_2O$ with a methanolic solution saturated with HCl gas. The spectra were recorded after the successive addition of 1-drop portions.

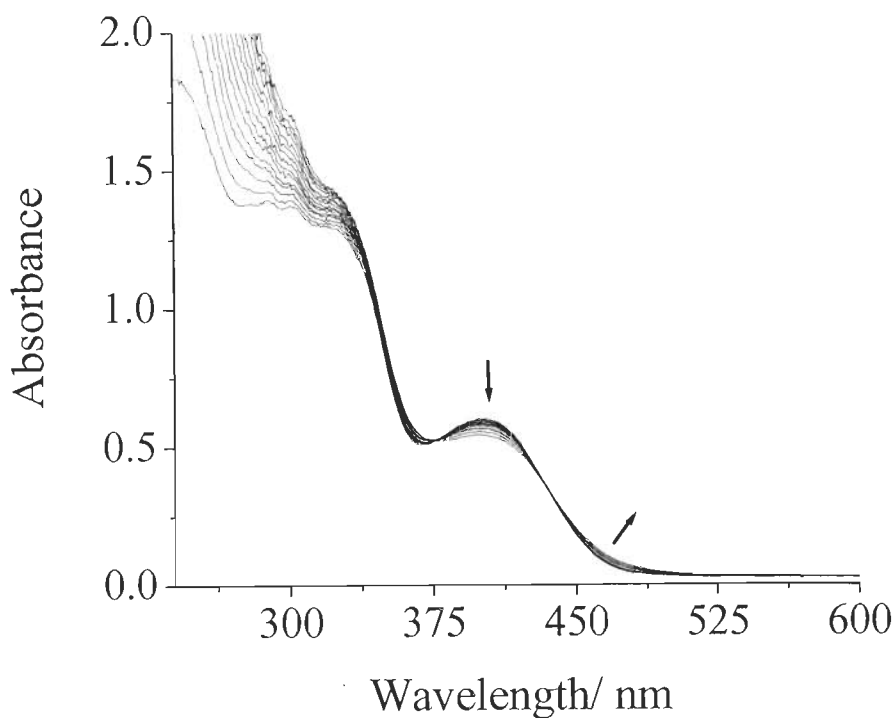


Figure 3.11. Spectral changes obtained during titration of 20 mL of 3.3×10^{-5} M methanolic solution of $K_2[CH_2\{V^V O_2(\text{sal-bhz})\}_2] \cdot 2H_2O$ with dilute solution of 30% aqueous H_2O_2 (0.401 g, 3.01 mmol in 20 mL MeOH). Spectra were recorded after 25 min of every addition of dilute H_2O_2 .

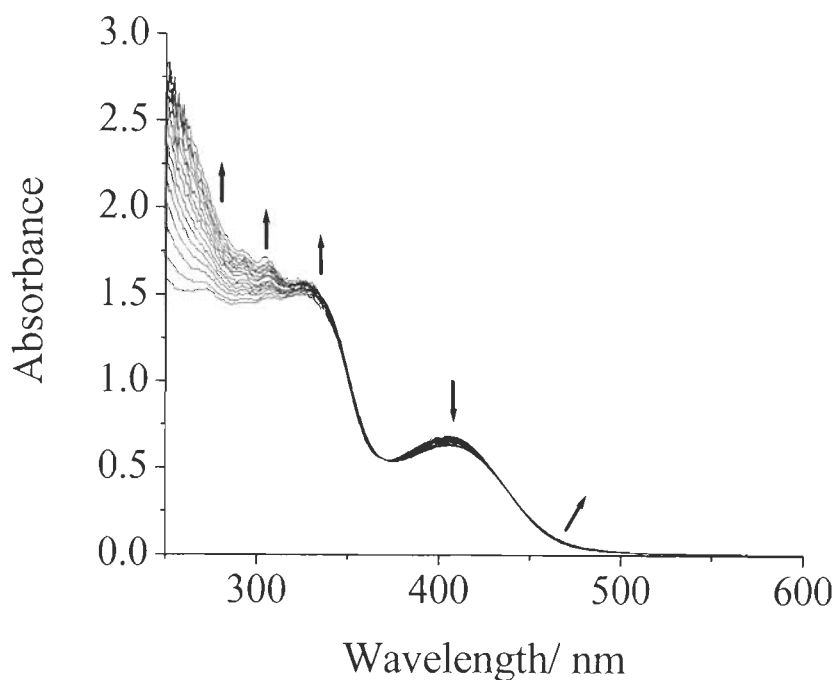


Figure 3.12. Spectral changes obtained during titration of 20 mL of 4.7×10^{-5} M methanolic solution of $K_2[CH_2\{V^VO_2(\text{sal-fah})\}_2] \cdot 2H_2O$ with dilute solution of 30% aqueous H_2O_2 (0.401 g, 3.01 mmol in 20 mL MeOH). Spectra were recorded after 25 min of every addition of dilute H_2O_2 .

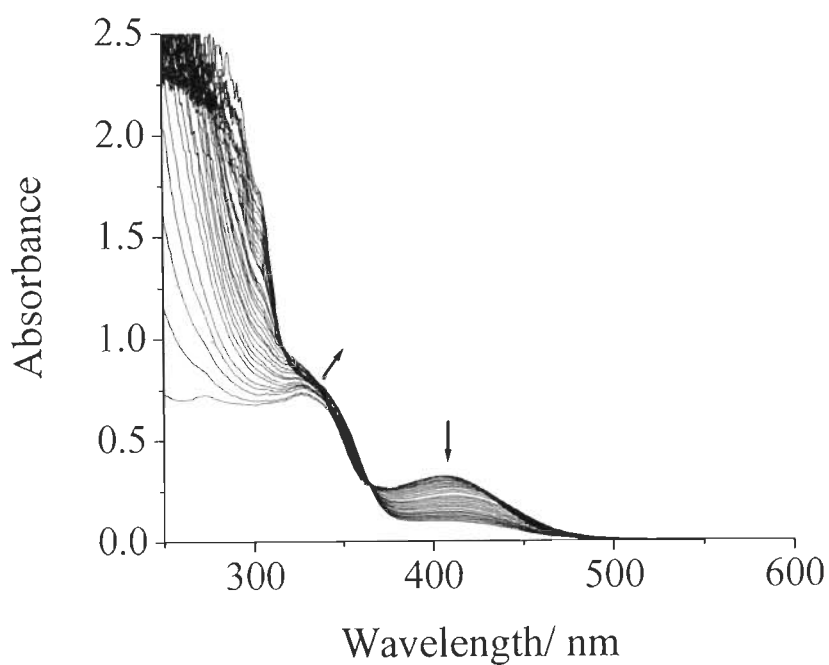


Figure 3.13. Spectral changes obtained during titration of 20 mL of 3.3×10^{-5} M methanolic solution of $Cs_2[CH_2\{V^VO_2(sal-fah)\}_2] \cdot 2H_2O$ with dilute solution of 30% aqueous H_2O_2 (0.401 g, 3.01 mmol in 20 mL MeOH). Spectra were recorded after 25 min of every addition of dilute H_2O_2 .

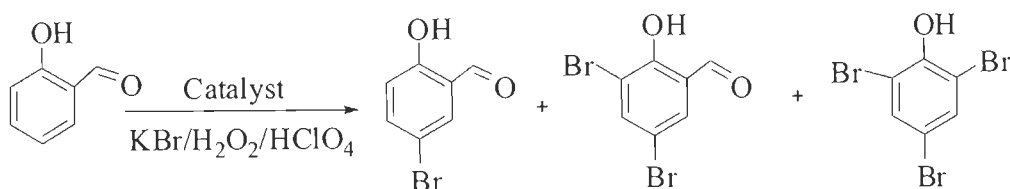
3.3.8. Catalytic activity studies

Oxidative bromination of salicylaldehyde

Vanadium(V) complexes catalyze the oxidative bromination of organic substrates in the presence of H_2O_2 and bromide ion. During oxidation vanadium coordinates with 1 or 2 equivalents of H_2O_2 , forming oxo-monoperoxo, $[VOL(O_2)^+]$ or oxo-diperoxo, $[VO(O_2)_2]^+$ species (*vide supra*), which ultimately oxidize bromide species (most likely to HOBr) then brominates the substrate. We have found that the dioxidovanadium(V) systems reported here satisfactorily catalyze the oxidative bromination of salicylaldehyde to give 5-bromosalicylaldehyde, 3,5-dibromosalicylaldehyde and 2,4,6-tribromophenol using H_2O_2 /KBr in presence of $HClO_4$ in aqueous solution at room temp.; cf. Scheme 3.4.

After several trials the best suited reaction conditions obtained for the maximum conversion of salicylaldehyde were: salicylaldehyde (2.44 g, 20 mmol), KBr (5.95 g, 50 mmol), aqueous 30 % H_2O_2 (15 g, 120 mmol), catalyst (0.02 g for Cs^+ salt and 0.016 for K^+ salt), aqueous 70 % $HClO_4$ (4.02 g, 80 mmol) and water (40 mL); the addition of $HClO_4$, however, in four equal portions during the first two hours of reaction time was necessary to improve the conversion of the substrate and to avoid decomposition of catalyst. Under the above conditions, a maximum of 95.7% conversion was achieved with $Cs_2[CH_2\{V^VO_2(sal-bhz)\}_2] \cdot 2H_2O$ and at least three products were identified, Table 3.10. Increasing the amount of oxidant improves the conversion of salicylaldehyde. However, the selectivity of 5-bromosalicylaldehyde decreases considerably while that of 3,5-dibromosalicylaldehyde and 2,4,6-tribromophenol increase. The presence of an excess of H_2O_2 facilitates the formation of more and more HOBr which ultimately helps in the further oxidative bromination of salicylaldehyde to the other position(s). Other catalysts gave similar results. The counter ions (Cs^+ or K^+) did

not much affect the conversions. In the absence of the catalyst, the reaction mixture gave only ca. 4 % conversion of salicylaldehyde.



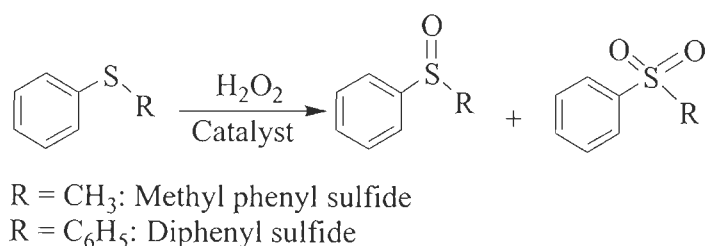
Scheme 3.4. Products obtained upon the catalytic oxidative bromination of salicylaldehyde.

Table 3.10. Results of oxidative bromination of salicylaldehyde catalyzed by $V^V O_2$ -complexes ($K_2[CH_2\{V^V O_2(sal-bhz)\}_2] \cdot 2H_2O$ (**3.2**), $Cs_2[CH_2\{V^V O_2(sal-bhz)\}_2] \cdot 2H_2O$ (**3.3**), $K_2[CH_2\{V^V O_2(sal-fah)\}_2] \cdot 2H_2O$ (**3.5**) and $Cs_2[CH_2\{V^V O_2(sal-fah)\}_2] \cdot 2H_2O$ (**3.6**). Conversion and products obtained after 7 h of contact time.

Entry No.	Catalyst	Substr : H ₂ O ₂	Conv. %	TOF (h ⁻¹)	% Selectivity		
					Mono	dibromo	tribromo
1	3.3	1:2	82.4	108.3	78.3	20.4	1.3
2	3.3	1:3	84.9	111.6	69.1	28.8	2.1
3	3.3	1:4	87.0	114.4	54.6	41.1	4.3
4	3.3	1:5	94.5	124.2	26.8	60.5	12.7
5	3.3	1:6	95.7	125.8	11.6	64.5	23.9
6	3.2	1:2	86.1	90.1	77.6	20.6	1.8
7	3.2	1:4	91.7	96.0	52.6	42.3	5.1
8	3.5	1:2	84.6	86.1	72.4	25.3	2.3
9	3.5	1:4	89.7	91.3	51.6	42.3	6.1
10	3.6	1:2	83.2	107.0	76.3	21.1	2.6
11	3.6	1:4	87.3	112.3	57.3	39.1	4.6

Oxidation of sulfides

Many vanadium complexes catalyse the oxidation of organic sulfides to sulfoxides [158, 162, 250, 251] a reaction also promoted by vanadium haloperoxidases. The oxidation of two sulfides by peroxide using the oxidovanadium(IV) complexes $[CH_2\{V^V O(sal-bhz)(H_2O)\}_2]$ (3.1) and $[CH_2\{V^V O(sal-fah)(H_2O)\}_2]$ (3.4) as catalyst precursors was also studied here; Scheme 3.5.



Scheme 3.5. Oxidation of Organic sulfides.

The catalytic activity of $[CH_2\{V^V O(sal-bhz)(H_2O)\}_2]$ (3.1) and $[CH_2\{V^V O(sal-fah)(H_2O)\}_2]$ (3.4) was tested for the oxidation of methyl phenyl sulfide and diphenyl sulfide using aqueous 30% H₂O₂. Among the catalyst precursors studied, 3.1 was taken as a representative one and amount of complex and concentration of oxidant were varied to obtain maximum conversion. The effect of H₂O₂ was studied considering substrate to oxidant ratios of 1:1, 1:2 and 1:3 for a fixed amount of catalyst (0.015 g) and substrate (1.24 g 10 mmol) in petroleum ether (10 mL), and the reaction was monitored at room temperature. Thus, the conversion increases from ca. 11 % to 100 % in 7 h of contact time on increasing the substrate to oxidant ratios from 1:1 to 1:2. Increasing this ratio to 1:3 did not improve conversion, except the completion of the reaction within 6 h and slight change in the selectivity of products. However, the relative amount of sulfone formed is much higher for 1:2 and 1:3 ratios.

Similarly, four different amount of complex viz. 0.005, 0.015, 0.025, 0.035 g were taken at a fixed reaction condition optimized as above {i.e. substrate (1.24 g, 10 mmol), H_2O_2 (2.27 g, 20 mmol) and petroleum ether (10 mL)} to see the effect of amount of catalyst on the reaction. It was observed that 0.015 g of catalyst was sufficient enough to give 99.7% conversion with a turn over frequency value of $57\ h^{-1}$. Higher amount of catalyst only reduced the time in acquiring the steady state of the reaction. From these experiments, the best reaction conditions for the maximum oxidation of methyl phenyl sulfide are: substrate (1.24 g, 10 mmol), catalyst (0.015 g), H_2O_2 (2.27 g, 20 mmol) and petroleum ether (10 mL).

The results for both substrates (methyl phenyl sulfide and diphenyl sulfide) and catalyst precursors $\{[CH_2\{V^{IV}O(sal-bhz)(H_2O)\}_2]$ (3.1) and $[CH_2\{V^{IV}O(sal-fah)(H_2O)\}_2]$ (3.4)}, under the above reaction conditions are summarized in Table 3.11. From the table it is clear that conversion of methyl phenyl sulfide using both catalysts is more than 99%, while that of diphenyl sulfide is ca. 60 – 64 %. Normally two major products, sulfoxide and sulfone, were obtained along with only small amounts (<0.4 %) of an unidentified product. The selectivity for the major product, sulfone, is ca. 85% while that of sulfoxide is ca. 15 % in all cases. Blank reaction with methyl phenyl sulfide under the above reaction conditions gave 35.3% conversion of methyl phenyl sulfide with 65.5 % selectivity towards sulfoxide, 34.2% towards sulfone and ca. 0.3 % an unidentified product. In the absence of the catalyst, diphenyl sulfide gave ca. 5 % conversion with selectivity towards sulfoxide : sulfone of 57 : 43. Thus, catalysts not only improve the conversion of substrates, they alter the selectivity of the products as well.

Table 3.11. Percent conversion^a of methyl phenyl sulfide and diphenyl sulfide along with the turn over frequency and selectivity of the reaction products after 7 h of reaction time. $[CH_2\{V^{IV}O(sal-bhz)(H_2O)\}_2]$ (**3.1**) and $[CH_2\{V^{IV}O(sal-fah)(H_2O)\}_2]$ (**3.4**).

Entry No.	Catalyst precursor	Substrate ^b	% Conv.	TOF (h ⁻¹)	% Selectivity		
					sulfoxide	sulfone	others
1	3.1	mps	99.7	57	15.7	84.1	0.2
2	3.1	dps	64.3	37	18.4	81.4	0.2
3	3.4	mps	99.8	58	14.3	85.3	0.4
4	3.4	dps	60.5	35	19.8	79.9	0.3

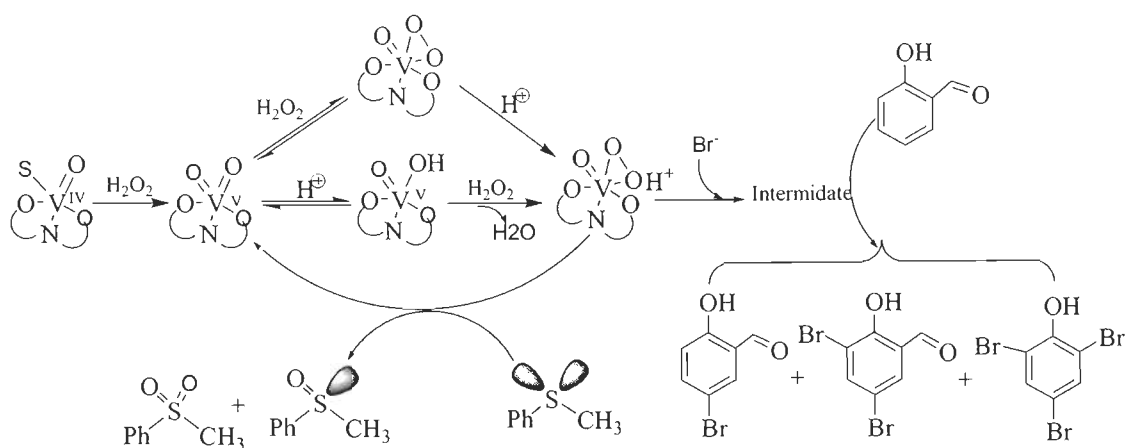
^aReaction conditions: substrate (10 mmol), catalyst (0.015 g), H₂O₂ (2.27 g, 20 mmol) and petroleum ether (10 mL). ^bmps = methyl phenyl sulfide, dps = diphenyl sulfide.

The understanding of the main features of the mechanism of these reactions is important from both practical and fundamental standpoints. As described above the complexes were studied in DMSO/MeOH/aqueous solution by ⁵¹V NMR, EPR and UV-Vis absorption spectroscopy. Most of the signals observed are in the typical range for complexes with similar ligand donor sets. Both V^V-inorganic-peroxo-compounds and V^V-peroxo-complexes have been reported to mediate oxygen-transfer reactions including the oxidation of sulfides to sulfoxides and sulfones, and the epoxidation of alkenes and allylic alcohols [59, 65, 160, 169, 186, 263].

The oxidation of a variety of organic sulfides in the presence of hydrogen peroxide catalyzed by vanadium(V) species to sulfoxides and sulfones in organic solvents have also been studied [158, 162, 250, 251]. We demonstrated that, on treatment with H₂O₂, complexes **3.1** and **3.4** are able to generate monoperoxo complexes and for higher H₂O₂ amounts even bisperoxovanadium(V) species. The

sulfur atom of the sulfides is electron rich; therefore, under the conditions used the formation of hydroperoxo complexes is plausible, enhancing the electrophilicity of the coordinated peroxo ligand and facilitating the nucleophilic attack by the sulfide yielding the sulfoxide and also the sulfone. The reaction may proceed as outlined in Scheme 3.6, but the participation of inorganic peroxo compounds cannot be ruled out.

The peroxo-complexes being stable and detectable, it is feasible that hydroperoxovanadium(V) complexes also form as aqueous acid is being added and the pH decreases. As described above upon addition of acid several species form namely V^{IV} -complexes. We do not expect that V^{IV} -complexes catalyze the bromination of salicylaldehyde, but as also shown above V^V -peroxo (inorganic- and organic ligand containing-) complexes, hydroxo species and possibly simple monovanadate (V_1) may also be present. Therefore the halogenations may indeed proceed involving the intermediates outlined in Scheme 3.6 or also involving other vanadium-containing species.



Scheme 3.6. Overall catalytic schemes for the oxidative bromination of salicylaldehyde and sulfoxidation of organic sulfides.

3.3.9. Antiamoebic activity study

The *in vitro* antiamoebic activity of the hydrazone based ligand ($CH_2(H_2sal-bhz)_2$ (**3.I**) and $CH_2(H_2sal-fah)_2$ (**3.II**)) and their dioxidovanadium(V) complexes (Table 3.12) were carried out against the *HMI:IMSS* strain of *E. histolytica*. The maximum concentration of DMSO in the test did not exceed 0.1%, at which level no inhibition of amoebal growth occurred [302]. Metronidazole was used as the reference drug with $IC_{50} = 1.89 \mu M$, also included in the table. The results were estimated as the percentage of growth inhibition compared with the inhibited controls and plotted as probit values as a function of the drug concentration. IC_{50} and 95% confidence limits were interpolated in the corresponding dose response curve. The biological data suggests that the free ligands **3.I** ($IC_{50} = 9.08 \mu M$) and **3.II** ($IC_{50} = 7.97 \mu M$) showed no activity against the trophozoites of *E. histolytica* as compared to metronidazole whereas complexes of these ligands showed much better results. The IC_{50} values of other metal precursors ($9.02 \mu M$ for K^+ ion and $8.1 \mu M$ for Cs^+ ion) suggest that counter cation of complexes has no contribution to the antiamoebic activity. A possible explanation is that, by coordination, the polarity of the ligand and central metal ion are reduced through the charge equilibration, which favors permeation of the complexes through the lipid layer of the cell membrane [252]. Out of the four V^V -complexes, complexes $Cs_2[CH_2\{V^VO_2(sal-bhz)\}_2] \cdot 2H_2O$ (**3.3**) ($IC_{50} = 0.54 \mu M$; entry no. 4) and $Cs_2[CH_2\{V^VO_2(sal-fah)\}_2] \cdot 2H_2O$ (**3.6**) ($IC_{50} = 0.36 \mu M$; entry no. 6) showed the most promising activity, which may be due to the presence of Cs^+ to balance the charge. The null hypothesis was tested using t-test and the significance of the difference between the IC_{50} value of metronidazole vs. active complexes **3.3** and **3.6** was evaluated. The values of the calculated t were found higher than the table value of t at 4% level. This means that the complexes under study do contribute to the activity [253]. Moreover, these results indicate that the presence

of the vanadium ion not only enhances the activity of the ligands but also modifies it from amoebostatic to amoebicidal.

Toxicity of compounds accessed by the MTT assay

The cells were treated with various concentrations of compounds $Cs_2[CH_2\{V^V O_2(sal-bhz)\}_2] \cdot 2H_2O$ (**3.3**) and $Cs_2[CH_2\{V^V O_2(sal-fah)\}_2] \cdot 2H_2O$ (**3.6**) or vehicle (DMSO) alone for 24 h, 48 h and 72 h (as indicated in the Figures. 3.14 and 3.15). Cell survival was determined by the MTT assay. Cell viability was calculated as described in the section of Materials and methods. To assess the survival effects / toxicity of the compounds, human cervical (HeLa) cancer cells were used. 6000 cells per well in 200 μ L complete DMEM medium were plated. Different concentrations of the two compounds were added in the wells as indicated in the Figures. 3.14 and 3.15. The bars correspond to the mean values of three independent experiments in which each treatment was done in triplicate. The concentration range tested for compound **3.3** was from 0.54 to 250 μ M and for compound **3.6** from 0.36 to 25 μ M. The viable cells were measured after 24 h, 48 h, and 72 h., by the MTT assay. At 72 h, the IC_{50} of compounds **3.3** and **3.6** are 100 μ M and 25 μ M, respectively. The cell survival assay was also performed in the presence of metronidazole and the IC_{50} value was found to be higher than 750 μ M as also specified in Table 3.12. This shows that although compounds **3.3** and **3.6** are more toxic than metronidazole for the HeLa cell line, their IC_{50} values indicate their toxicity is relatively low. The cell viability assay of K^+ and Cs^+ ions (Figure 3.16) clearly shows that the cell survival is not affected by these ions and the toxicity is entirely due to the compounds.

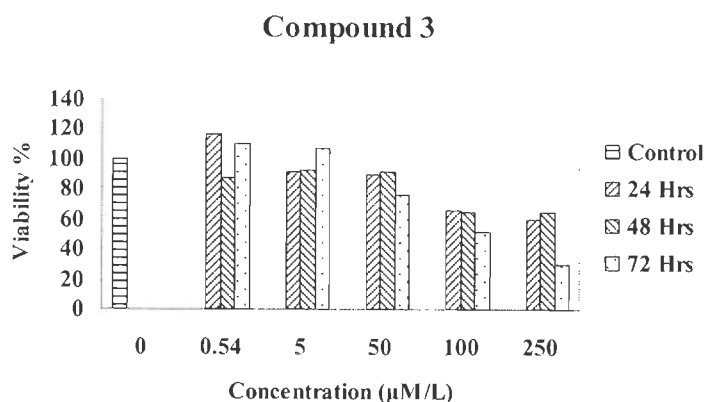


Figure 3.14. Percentage of viable cells after 24 h, 48 h and 72 h on human cervical (HeLa) cells on incubation with various concentrations of compound $Cs_2[CH_2\{V^VO_2(sal-bhz)\}_2] \cdot 2H_2O$ (**3.3**) or vehicle (DMSO). Cell survival was determined by the MTT assay.

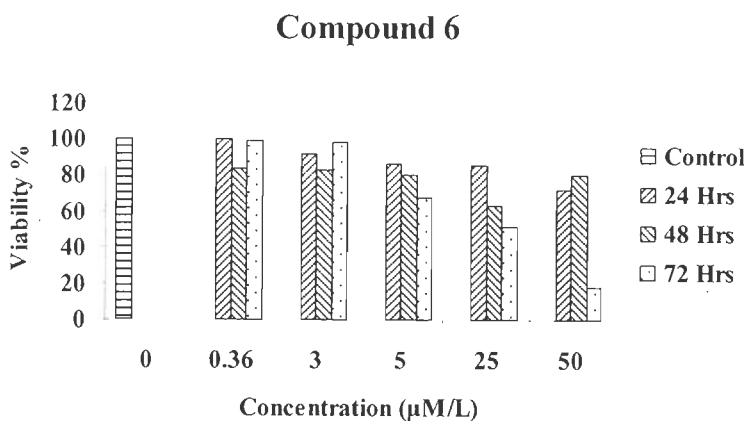


Figure 3.15. Percentage of viable cells after 24 h, 48 h and 72 h on human cervical (HeLa) cells on incubation with various concentrations of compound $Cs_2[CH_2\{V^VO_2(sal-fah)\}_2] \cdot 2H_2O$ (**3.6**) or vehicle (DMSO). Cell survival was determined by MTT assay.

Table 3.12. Antiamoebic activity against HM1:IMSS strain of *E. histolytica* and toxicity profile of vanadium Complexes.

S. No.	Compound	Antiamoebic		Toxicity profile	
		IC ₅₀ (μ M) ^a	S.D. ^b	IC ₅₀ / (μ M) ^a	S.D. ^b
1.	CH ₂ (H ₂ sal-bhz)	9.08	0.01	N.D	N.C
2.	CH ₂ (H ₂ sal-fah)	7.97	0.01	N.D	N.C
3.	K ₂ [CH ₂ {V ^V O ₂ (sal-bhz)} ₂].2H ₂ O	2.21	0.02	N.D	N.C
4.	Cs ₂ [CH ₂ {V ^V O ₂ (sal-bhz)} ₂].2H ₂ O	0.54	0.01	100	0.008
5.	K ₂ [CH ₂ {V ^V O ₂ (sal-fah)} ₂].2H ₂ O	2.32	0.04	N.D	N.C
6.	Cs ₂ [CH ₂ {V ^V O ₂ (sal-fah)} ₂].2H ₂ O	0.36	0.02	25	0.015
7.	KCl ^c	9.02	-	0.04	-
8.	CsOH ^c	8.1	-	0.04	-
9.	Metronidazole (MNZ)	1.89	0.03	>750	0.050

^a The values were obtained from at least three separate assays done in duplicate.

^b Standard deviation; N.D = Not Done; N.C = Not Calculated. ^c The values were obtained from one assay only.

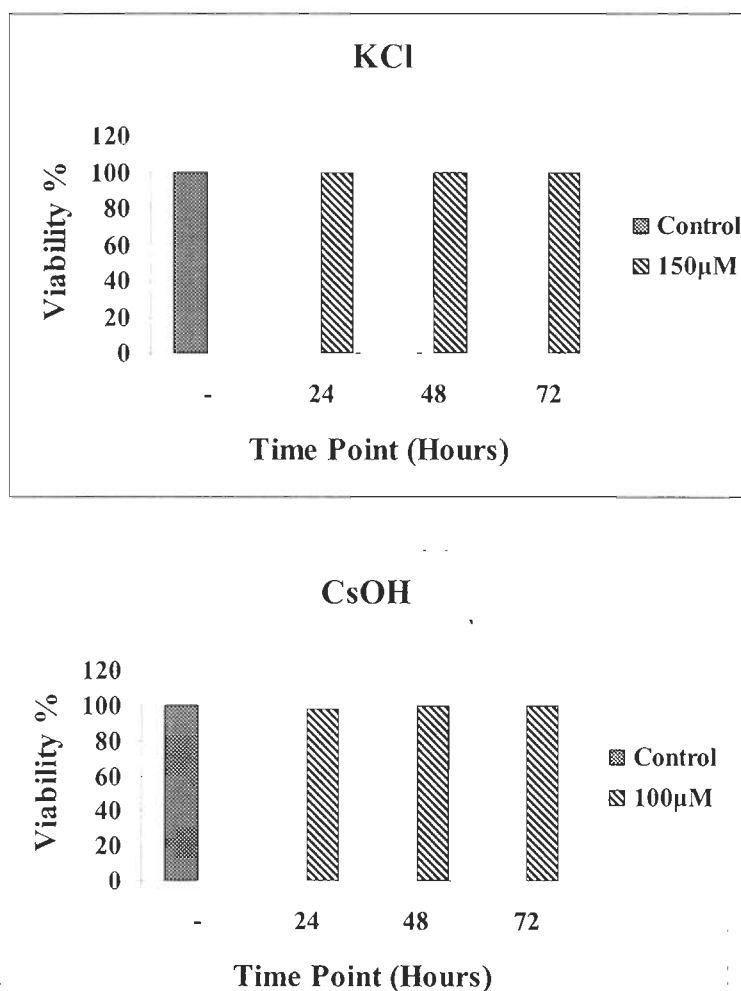


Figure 3.16. Percentage of viable cells after 24 h, 48 h and 72 h on human cervical (HeLa) cells on incubation with KCl (150 μM, above) and CsOH (100 μM, below) or vehicle (DMSO). Cell survival was determined by MTT assay. \pm SD bars are not visible as most of them are less than 0.04.

3.4. Conclusions

The hydrazones $\{CH_2(H_2sal-bhz)_2\}$ (**3.I**) and $\{CH_2(H_2sal-fah)_2\}$ (**3.II**) derived from methylenebis(salicylaldehyde) $\{CH_2(Hsal)_2\}$ and benzoylhydrazide (bhz) or 2-furoylhydrazide (fah) and their $V^{IV}O$ - and V^VO_2 -complexes were synthesized and characterized. The complexes are dinuclear in the solid state and in solution, but no significant interactions are detected between the vanadium centres. For one of the V^VO_2 -complexes, $Cs_2[CH_2\{V^VO_2(sal-bhz)\}_2] \cdot 2H_2O$ the crystal and molecular structure was determined. Each $Cs_2[CH_2\{V^VO_2(sal-bhz)\}_2] \cdot 2H_2O$ moiety contains two cis-dioxidovanadium(V) units, forming a dinuclear compound with no relevant interactions between the V^V -centres. A tridentate N-salicylinenehydrazide group is bound to each metal ion through the O-carbonyl, the deprotonated O-phenolic atoms and the N-atom. The Cs^+ ions are coordinated by O-atoms coming from the cis- $[V^VO_2]^+$ unit and from an oxo bridge, and by carbon atoms from the sal-bhz ligands, this structure being an interesting example of Cs-C π -bonds.

Species $[CH_2\{V^VO_2(sal-bhz)\}_2]^{2-}$ and $[CH_2\{V^VO_2(sal-fah)\}_2]^{2-}$ were shown to be functional models of vanadium dependent haloperoxidases, satisfactorily catalyzing the oxidative bromination of salicylaldehyde to give 5-bromosalicylaldehyde, 3,5-dibromosalicylaldehyde and 2,4,6-tribromophenol using H_2O_2/KBr in the presence of $HClO_4$ in aqueous solution at room temperature. The complexes $[CH_2\{V^{IV}O(sal-bhz)(H_2O)\}_2]$ and $[CH_2\{V^{IV}O(sal-fah)(H_2O)\}_2]$ were also shown to be catalyst precursors for the catalytic oxidation, by peroxide, of methyl phenyl sulfide and diphenyl sulfide, yielding the corresponding sulfoxide and sulfone at room temperature.

The reactivity in methanol and DMSO of the $V^{IV}O$ - and V^VO_2 -complexes of $\{CH_2(H_2sal-bhz)_2\}$ and $\{CH_2(H_2sal-fah)_2\}$ was studied by UV-Vis, EPR and ^{51}V NMR spectroscopy, by either adding H_2O_2 or acid (HCl or $HClO_4$) or both, the formation of several species being established, some of them probably being

intermediates in the catalytic processes studied, namely $[CH_2\{V^VO(O_2)(L)\}_2]^{2-}$ and $[CH_2\{V^VO(OH)(L)\}_2]$. On addition of acid (HCl or HClO₄) the V^V-species present are partly reduced yielding V^{IV}O-species containing the $\{V^{IV}O(sal-bhz)(S)\}$ and $\{V^{IV}O(sal-fah)(S)\}$ moieties (S = solvent), the oxohydroxocomplex and a ⁵¹V NMR active species whose nature is suggested.

Amoebiasis is caused by *Entamoeba histolytica*, the second leading cause of death among parasite diseases. For the treatment of amoebiasis metronidazole has been till now the drug of choice. The V^V-complexes of $\{CH_2(H_2sal-nah)_2\}$ and $\{CH_2(H_2sal-inh)_2\}$ were also screened against HM1:IMSS strains of *Entamoeba histolytica*, the results and determined IC₅₀ values showing that they are significantly more active than metronidazole, suggesting that these vanadium compounds may be promising drugs for the treatment of this disease. Moreover, toxicity tests carried out with the HeLa cell line showed that compounds Cs₂[CH₂{V^VO₂(sal-bhz)}₂].2H₂O (**3.3**) and Cs₂[CH₂{V^VO₂(sal-fah)}₂].2H₂O (**3.6**) offered remarkable viability (>90%), further supporting that these vanadium compounds may be promising drugs for the treatment of Amoebiasis.

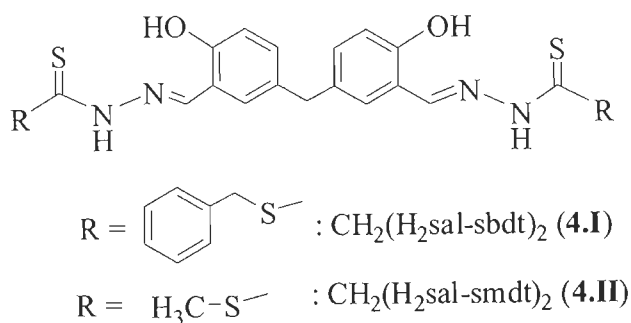
Chapter-4

Synthesis, characterisation, catalytic and antiamoebic activities of vanadium complexes with 5,5'-methylenebis(dibasic tridentate ONS donor) system

4.1. Introduction

In previous chapters we have described dinuclear oxidovanadium(IV) and dioxidovanadium(V) complexes of binucleating, bis(dibasic tridentate ONO donor) ligands and have studied their reactivity, catalytic and antiamoebic activity. Their good reactivity patterns, catalytic and antiamoebic activity encouraged to consider binucleating, bis(dibasic tridentate ONS donor) ligands. In this chapter, therefore, we describe the synthesis and characterization of dinuclear oxidovanadium(IV) and dioxidovanadium(V) complexes of ligands **4.I** and **4.II** derived from 5,5'-methylenebis(salicylaldehyde) $\{\text{CH}_2(\text{Hsal})_2\}$ and S-benzylthiocarbamate (sbd) or S-methyldithiocarbamate (smdt); Scheme 4.1.

The haloperoxidase activity is confirmed considering oxidative bromination of salicylaldehyde and styrene using dioxidovanadium(V) complexes as catalyst. In addition, the catalytic activity is demonstrated considering the oxidation, by peroxide, of styrene using dioxidovanadium(V) complexes as catalyst. These complexes (oxidovanadium(IV) and dioxidovanadium(V)) have also been screened against HM1:1MSS strains of *Entamoeba histolytica*.



Scheme 4.1.

4.2. Experimental

4.2.1. Materials

V_2O_5 (Loba Chemie, India), acetylacetone (Hacac, E. Merck, India), salicylaldehyde, (S.D. fine chemicals, India), styrene (Acros, USA), 30% aqueous

H₂O₂ and 70 % HClO₄ (Qualigens, India) were used as obtained. Other chemicals and solvents were of analytical reagent grade. S-Benzyldithiocarbazate[303] and S-methyldithiocarbazate [304] were prepared as reported in the literature. Details of other chemicals and solvents are presented in Chapters 2 and 3.

4.2.2. Characterization Procedures

Instrumentation and analyses details are reported in Chapter 2.

4.2.3. Preparations

Preparation of ligands

Ligands, CH₂(H₂sal-sbdt)₂ (**4.I**) and CH₂(H₂sal-smdt)₂ (**4.II**) were prepared according to methods reported in the literature [305]. Preparation of a representative ligand CH₂(H₂sal-sbdt)₂ (**4.I**) is given here. 5,5'-methylbis(salicylaldehyde) (2.65 g, 10 mmol) was dissolved in 30 mL methanol. A solution of S-benzyldithiocarbazide (3.966 g, 20 mmol) in 10 mL of methanol was added to the above and the reaction mixture was refluxed for 3 h on a water bath and allowed to stand in refrigerator for 12 h. Deposited yellow solid was filtered, washed with methanol and dried in desiccator. Finally, it was recrystallised from methanol to give a fine needle like solid.

Data for CH₂(H₂sal-sbdt)₂ (4.I**):** Yield 4.03 g (65.3 %). Found: C, 60.10; H, 4.56; N, 8.94 %. Calc for C₃₁H₂₈O₂N₄S₄ (616.83): C, 60.36; H, 4.58; N, 9.08 %.

Data for CH₂(H₂sal-smdt)₂ (4.II**):** Yield 3.38 g (72.8 %). Found: C, 49.20; H, 4.36; N, 12.14 %. Calc for C₁₉H₂₀O₂N₄S₄ (464.63): C, 49.12; H, 4.34; N, 12.06 %.

[CH₂{V^{IV}O(sal-sbdt)(H₂O)}₂](4.1**)**

A filtered solution of [V^{IV}O(acac)₂] (0.530 g, 2 mmol) in dry methanol (10 mL) was added to a filtered solution of CH₂(H₂sal-sbdt)₂ (0.464 g, 1 mmol)

prepared in dry hot methanol (225 mL) while shaking the reaction flask and the reaction mixture was refluxed on a water bath for 4 h. After reducing the volume of the solvent to ca. 20 mL and keeping at room temperature for 10 h, the separated brown solid was filtered, washed with methanol and dried in desiccator over silica gel. Yield: 0.568 g (72.6 %). μ_{eff} (293 K) = 1.73 μ_{B} . Found: C, 47.68; H, 3.53; N, 7.24 %. Calc for $\text{C}_{31}\text{H}_{28}\text{O}_6\text{N}_4\text{S}_4\text{V}_2$ (782.68): C, 47.57; H, 3.61; N, 7.16 %.

$[\text{CH}_2\{\text{V}^{\text{IV}}\text{O}(\text{sal-smdt})(\text{H}_2\text{O})\}_2](4.2)$

Complex **4.2** was prepared from $[\text{VO}(\text{acac})_2]$ (0.530 g, 2 mmol) and $\text{CH}_2(\text{H}_2\text{sal-smdt})_2$ (0.464 g, 1 mmol) by the method outlined for **4.1**. Yield: 0.431 g (68.4 %). μ_{eff} (293 K) = 1.71 μ_{B} . Found: C, 36.37; H, 3.02; N, 8.94 %. Calc for $\text{C}_{19}\text{H}_{20}\text{O}_6\text{N}_4\text{S}_4\text{V}_2$ (630.48): C, 36.19; H, 3.20; N, 8.89 %.

$\text{K}_2[\text{CH}_2\{\text{V}^{\text{V}}\text{O}_2(\text{sal-sbdt})\}_2] \cdot 2\text{H}_2\text{O}$ (4.3)

Method A: A filtered solution of $[\text{V}^{\text{IV}}\text{O}(\text{acac})_2]$ (0.530 g, 2 mmol) in methanol (15 mL) was added while stirring to a solution of $\text{CH}_2(\text{H}_2\text{sal-sbdt})_2$ (0.616 g, 1 mmol) in methanol (450 mL) and refluxed for 4 h. After adding KOH (0.224 g, 4 mmol) to the above, the reaction mixture was further refluxed for 2 h. The obtained light brown solution was allowed to oxidize aerielly along with slow evaporation at room temperature. After 2 days solution changed to yellow and complex **4.3** separated out after reducing the volume of the solvent to ca. 10 mL and keeping over night at room temperature. This was filtered off, washed with methanol and dried in desiccator over silica gel. Yield 0.786 g (72.8 %). Found: C, 41.82; H, 2.96; N, 6.34 %. Calc for $\text{K}_2\text{C}_{31}\text{H}_{28}\text{N}_4\text{O}_8\text{S}_4\text{V}_2$ (892.90): C, 41.70; H, 3.16; N, 6.27 %.

Method B: A mixture of $[\text{CH}_2\{\text{V}^{\text{IV}}\text{O}(\text{sal-sbdt})(\text{H}_2\text{O})\}_2]$ (0.391 g, 0.5 mmol) and KOH (0.068 g, 1.2 mmol) in 25 mL of methanol was refluxed for 2 h and then left for aerial oxidation as well as slow evaporation of the solvent at room

temperature. Complex **4.3** slowly precipitated out in ca. 3 days. This was filtered off, washed with cold methanol and dried in a desiccator over silica gel. Yield: 0.358 g (84.7%). ^{51}V NMR (300 MHz, DMSO- d_6 , 25 °C): $\delta = -462$ ppm (major) and -524 ppm (minor) .

$\text{Cs}_2[\text{CH}_2\{\text{V}^{\text{V}}\text{O}_2(\text{sal-sbdt})\}_2]\cdot 2\text{H}_2\text{O}$ (4.4**)**

Method A: A filtered solution of $[\text{V}^{\text{IV}}\text{O}(\text{acac})_2]$ (0.530 g, 2 mmol) in methanol (15 mL) was added while stirring to a solution of $\text{CH}_2(\text{H}_2\text{sal-sbdt})_2$ (0.616 g, 1 mmol) in methanol (450 mL) and refluxed for 4 h. After adding $\text{CsOH}\cdot\text{H}_2\text{O}$ (0.403 g, 2.4 mmol) to the above, the reaction mixture was further refluxed for 2 h. The obtained light green solution was allowed to oxidize aerielly while slow evaporation at room temperature. After 2 days the green solution changed to yellow and complex **4.4** separated out after reducing the volume of solvent to ca. 10 mL and keeping over night at room temperature. This was filtered off, washed with methanol and dried in desiccator over silica gel. Yield 0.786 g (72.8 %). Found: C, 34.33; H, 2.52; N, 5.32 %. Calc for $\text{Cs}_2\text{C}_{31}\text{H}_{28}\text{O}_8\text{N}_4\text{S}_4\text{V}_2$ (1080.49): C, 34.46; H, 2.61; N, 5.19 %.

Method B: A mixture of $[\text{CH}_2\{\text{V}^{\text{IV}}\text{O}(\text{sal-sbdt})(\text{H}_2\text{O})\}_2]$ (**4.1**) (0.782 g, 1 mmol) and $\text{CsOH}\cdot\text{H}_2\text{O}$ (0.404 g, 2.4 mmol) in 25 mL of methanol was refluxed for 2 h and then left for slow evaporation of the solvent as well as aerial oxidation at room temperature. Complex **4.4** slowly precipitated out in ca. 3 days. Rest procedure was same as stated above. Yield 0.965 g (89.3%). ^{51}V NMR (300 MHz, DMSO- d_6 , 25 °C): $\delta = -463$ ppm.

$\text{K}_2[\text{CH}_2\{\text{V}^{\text{V}}\text{O}_2(\text{sal-smdt})\}_2]\cdot 2\text{H}_2\text{O}$ (4.5**)**

This complex was prepared by the procedures outlined for $\text{Cs}_2[\text{CH}_2\{\text{VO}_2(\text{sal-sbdt})_2\}]\cdot 2\text{H}_2\text{O}$ (**4.3**) using both method A and B. Yield from method A: 0.513 g (73.9 %) and from B 0.602 g (86.7 %). Found: C, 30.92; H,

2.68; N, 7.54 %. Calc for $\text{K}_2\text{C}_{19}\text{H}_{20}\text{N}_4\text{O}_8\text{S}_4\text{V}_2$ (740.71) : C, 30.81; H, 2.72; N, 7.56 %. ^{51}V NMR (300 MHz, DMSO-d_6 , 25 °C): $\delta = -462$ ppm (major) and -524 ppm (minor).

$\text{Cs}_2[\text{CH}_2\{\text{V}^{\text{V}}\text{O}_2(\text{sal-smdt})\}_2]\cdot 2\text{H}_2\text{O}$ (4.6)

This complex was prepared by the procedure outlined as method A and B for $\text{Cs}_2[\text{CH}_2\{\text{VO}_2(\text{sal-sbdt})\}_2]\cdot 2\text{H}_2\text{O}$. Yield from method A: 0.591 g (63.7 %) and from B 0.735 g (79.2 %). Found: C, 24.47; H, 2.14; N, 6.17 %. Calc for $\text{Cs}_2\text{C}_{19}\text{H}_{20}\text{O}_8\text{N}_4\text{S}_4\text{V}_2$ (928.29): C, 24.58; H, 2.17; N, 6.04 %. ^{51}V NMR (300 MHz, DMSO-d_6 , 25 °C): $\delta = -463$ ppm.

4.2.4. Catalytic activity studies

Oxidation of styrene

In a typical procedure, styrene (1.04 g, 10 mmol) and 30 %, w/v H_2O_2 (1.13 g, 10 mmol) were taken in 7 mL of methanol and the flask was maintained at the specified temperature (80 °C) using an electrically heated oil bath. The catalyst $\text{Cs}_2[\text{CH}_2\{\text{VO}_2(\text{sal-smdt})\}_2]\cdot 2\text{H}_2\text{O}$ (0.001 g, 0.0012 mmol) or $\text{Cs}_2[\text{CH}_2\{\text{VO}_2(\text{sal-sbdt})\}_2]\cdot 2\text{H}_2\text{O}$ (0.003 g, 0.0028 mmol) to be examined was added and the reaction mixture was stirred for 8 h. The products were extracted in n-heptane and analysed quantitatively by a Thermo trace gas chromatograph having HP-1 column (30 m \times 0.25 mm) and FID detector. The products were identified by GC–MS (Perkin-Elmer Clarus 500 column; 30 m \times 60 mm).

Oxidative bromination of salicylaldehyde

Complexes $\text{K}_2[\text{CH}_2\{\text{V}^{\text{V}}\text{O}_2(\text{sal-sbdt})\}_2]\cdot 2\text{H}_2\text{O}$, $\text{Cs}_2[\text{CH}_2\{\text{V}^{\text{V}}\text{O}_2(\text{sal-sbdt})\}_2]\cdot 2\text{H}_2\text{O}$, $\text{Cs}_2[\text{CH}_2\{\text{V}^{\text{V}}\text{O}_2(\text{sal-smdt})\}_2]\cdot 2\text{H}_2\text{O}$ and $\text{K}_2[\text{CH}_2\{\text{V}^{\text{V}}\text{O}_2(\text{sal-smdt})\}_2]\cdot 2\text{H}_2\text{O}$ were used as catalyst to carry out oxidative bromination. In a typical reaction, salicylaldehyde (2.44 g, 20 mmol) was added to an aqueous solution (40 mL) of KBr (5.95 g, 50 mmol), followed by addition of aqueous 30 % H_2O_2 (15.0 g, 120

mmol) in a 100 mL reaction flask. The catalyst (0.007 g) and 70 % HClO₄ (4.02 g, 20 mmol) were added, and the reaction mixture was stirred at room temperature. Three additional 20 mmol portions of 70 % HClO₄ were further added to the reaction mixture in three equal portions in half hour intervals under continuous stirring. After 7 h, the white product that had separated was filtered off, washed with water and dried. The crude mass was dissolved in CH₂Cl₂; insoluble material, if any, was removed by filtration, and the solvent evaporated. A CH₂Cl₂ solution of this material was subjected to gas chromatography, and the identity of the products confirmed by GC-MS.

Oxidative bromination of styrene

Complexes Cs₂[CH₂{V^VO₂(sal-sbdt)}₂].2H₂O and Cs₂[CH₂{V^VO₂(sal-smdt)}₂].2H₂O were used as catalyst to carry out oxidative bromination of styrene. Styrene (1.04 g, 10 mmol), KBr (2.50 g, 21 mmol), aqueous 30 % H₂O₂ (7.5 g, 60 mmol) catalyst (0.007 g for Cs₂[CH₂{VO^V(sal-sbdt)}₂].2H₂O, 0.005 g for Cs₂[CH₂{VO^V(sal-smdt)}₂].2H₂O and aqueous 70% HClO₄ (2.01 g, 10 mmol) were taken in a mixture of water (20 mL) and dichloromethane (20 mL). The reaction mixture was stirred at room temperature for 4 h. Three additional 10 mmol portions of 70 % HClO₄ were further added to the reaction mixture in three equal portions in half hour intervals under continuous stirring. At the end of reaction, dichloromethane layer was separated by separatory funnel and reaction products were analyzed by gas chromatography and their identity confirmed by GC-MS and comparing the data with electronic library.

4.2.5. In Vitro Testing against *E. histolytica*

The Ligands **4.I** and **4.II** and their complexes **4.1** to **4.6** were screened in vitro for antiamebic activity against the HM1:1MSS strain of *E. histolytica* by using a microplate method. *E. histolytica* trophozoites were cultured in TYIS-33 growth medium. DMSO (40 µL) was added to all the samples (1 mg) followed by

enough fresh culture medium to obtain a concentration of 1 mg/mL. The maximum concentration of DMSO in the tests did not exceed 0.1%, at which level no inhibition of amoebal growth occurred. Samples were dissolved or suspended by mild sonication for a few minutes to obtain a clear solution, then further dilution with medium to obtain a concentration of 0.1 mg/mL. Two fold serial dilutions were made in the wells of a 96-well microtitre plate (costar) in the medium (170 μ L). Each test included metronidazole as the standard amoebicidal drug; control wells (culture medium plus amoebae) were prepared from a confluent culture by pouring off the medium, adding medium (2 mL) and chilling the culture on ice for 8 min to detach the organisms from the side of the flask. The number of the amoeba per mL was estimated with a haemocytometer, and trypan blue exclusion was used to confirm viability. The cell suspension used was diluted to 10^5 organism/mL by adding fresh medium, and 170 μ L of this suspension was added to the test and control well in the plate with multichannel pipette so that the wells were completely filled (total volume, 340 μ L). An inoculum of 1.7×10^4 organisms/well was chosen so that confluent, but not excessive, growth took place in control wells. The plate was sealed with expanded polystyrene (0.5 mm), secured with tape, placed in a modular incubating chamber (flow laboratories, High Wycombe, UK) and gassed for 10 min with nitrogen before incubation at 37 °C for 72 h.

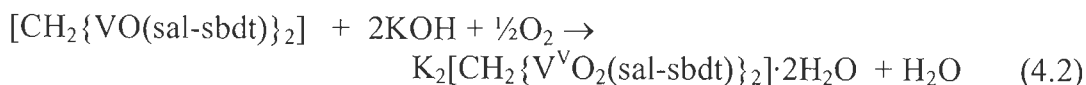
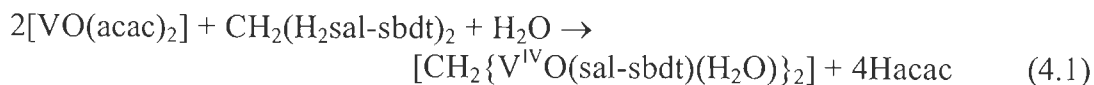
Assessment of Antiamoebic Activity

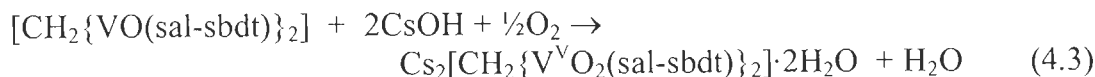
After incubation, the growth of amoebae in the plate was checked with a low-power microscope. The culture medium was removed by inverting the plate and shaking gently. The plate was then immediately washed once in 0.9% NaCl at 37 °C. This procedure was completed quickly, and the plate was not allowed to cool in order to prevent the detachment of amoebae. The plate was allowed to dry at room temperature and the amoebae were fixed with chilled (–20 °C) methanol for 15 min, when dry, stained with 0.5% aqueous eosin for 15 min. The stained

plate was washed once with tap water and then twice with distilled water and allowed to dry. A 200- μ L portion of 0.1 NaOH solutions was added in each well to dissolve the protein and release the dye. The optical density of the resulting solution in each well was determined at 490 nm with a microplate reader. The percentage of inhibition of amoebal growth was calculated from the optical densities of the control and test wells and plotted against the logarithm of the dose of the drug tested. Linear regression analysis was used to determine the best fit straight line from which the IC₅₀ value was found.

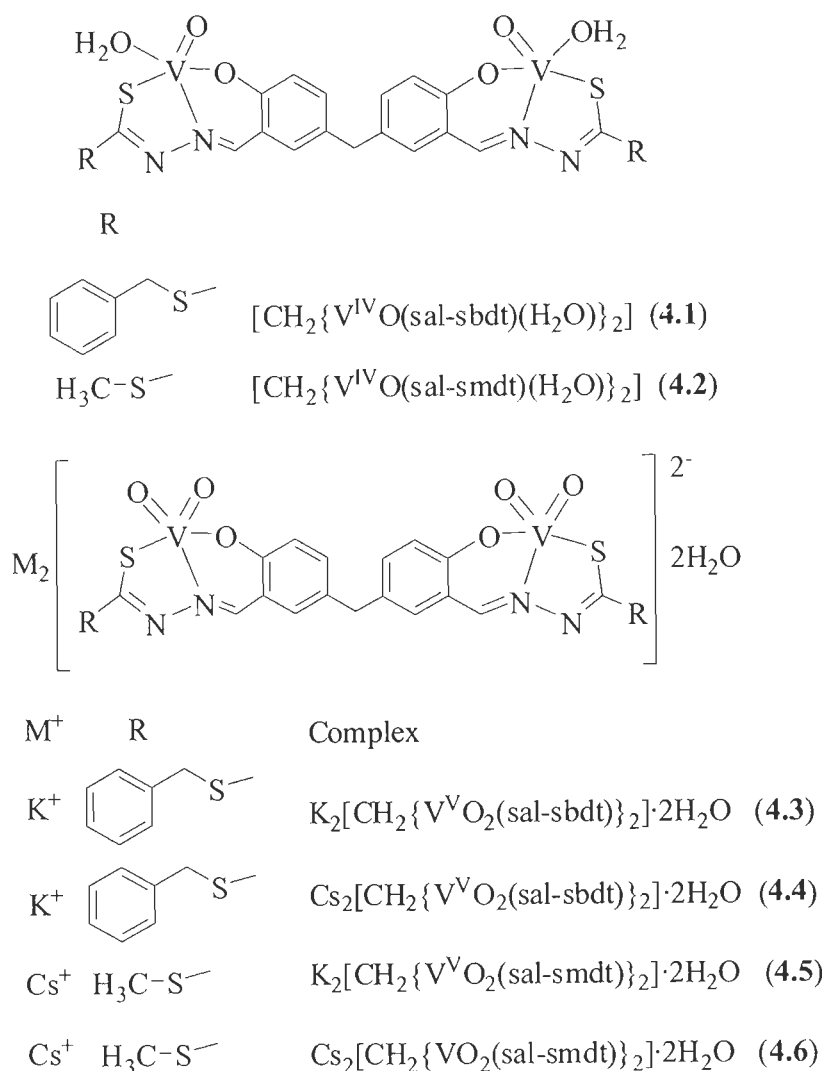
4.3. Results and discussion

[VO(acac)₂] reacts with binucleating ligands CH₂(H₂sal-sbdt)₂ or CH₂(H₂sal-smdt)₂ in 2:1 molar ratio in refluxing methanol and give dinuclear oxidovanadium(IV) complexes, [CH₂{V^{IV}O(sal-sbdt)(H₂O)}₂] (4.1) and [CH₂{V^{IV}O(sal-smdt)(H₂O)}₂] (4.2), respectively. Oxidation of [CH₂{V^{IV}O(sal-sbdt)(H₂O)}₂] and [CH₂{V^{IV}O(sal-smdt)(H₂O)}₂] in the presence KOH or CsOH.H₂O gave the corresponding dioxidovanadium(V) species K₂[CH₂{V^VO₂(sal-sbdt)}₂].2H₂O (4.3), Cs₂[CH₂{V^VO₂(sal-sbdt)}₂].2H₂O (4.4), Cs₂[CH₂{V^VO₂(sal-smdt)}₂].2H₂O (4.5) and Cs₂[CH₂{V^VO₂(sal-smdt)}₂].2H₂O (4.6), respectively. These complexes can also be isolated directly by the reaction of [VO(acac)₂] with CH₂(H₂sal-sbdt)₂ or CH₂(H₂sal-smdt)₂ in 2:1 ratio in refluxing methanol followed by aerial oxidation in the presence of corresponding hydroxides. Here, reaction proceeds, ultimately, through the formation of oxidovanadium(IV) complexes 4.1 and 4.2. Equations (4.1) to (4.3) present the whole synthetic procedures considering CH₂(H₂sal-sbdt)₂ as a representative ligand.





All complexes are soluble in methanol, ethanol, DMSO and DMF. Scheme 4.2 presents the structures proposed for these complexes and are based on the spectroscopic characterization (IR, electronic, ^1H and ^{51}V NMR) and elemental analyses. The ligands coordinate through each of their dianionic (ONS(2-)) thioenolate tautomeric form.



Scheme 4.2.

4.3.1. IR spectral studies

A partial list of IR spectral data of ligands and complexes are presented in Table 4.1. Both ligands exhibit a sharp band at 1030 (**4.I**) and 1039 cm^{-1} (**4.II**) due to $\nu(\text{C}=\text{S})$ and a broader weak band in the region 3090 - 3250 cm^{-1} due to $\nu(\text{NH})$. The disappearance of these bands in the spectra of complexes indicates the thioenolisation of $>\text{C}=\text{S}$ group and coordination of sulfur to the vanadium. A broad band appearing at ca. 3400 cm^{-1} due to $\nu(\text{OH})$ mode is found absent in oxidovanadium(IV) complexes and this suggests the coordination of phenolic oxygen after deprotonation. However, presence of such band in dioxidovanadium(V) complexes is likely due to the coordinated/non-coordinated H_2O involved in hydrogen bonding. The $\nu(\text{C}=\text{N}_{\text{azomethine}})$ stretch of the ligands appear at 1624 (in **4.I**) and 1625 cm^{-1} (in **4.II**), and shifts of this band to lower frequency region (1578 – 1594 cm^{-1}) suggests the coordination of azomethine nitrogen. A band appearing at 948 (in **4.I**) and 939 cm^{-1} (in **4.II**) due to the $\nu(\text{N-N})$ stretch undergoes a shift to higher wavenumbers upon complex formation. A high frequency shift of the $\nu(\text{N-N})$ band is expected because of the diminished repulsion between the lone pairs of adjacent nitrogen atoms [226].

Both oxidovanadium(IV) complexes exhibit a band at 926 (in $[\text{CH}_2\{\text{V}^{\text{IV}}\text{O}(\text{sal-sbdt})(\text{H}_2\text{O})\}_2]$ (**4.1**)) and 956 cm^{-1} (in $[\text{CH}_2\{\text{V}^{\text{IV}}\text{O}(\text{sal-smdt})(\text{H}_2\text{O})\}_2]$ (**4.2**)) due to $\nu(\text{V}=\text{O})$ stretch. The dioxidovanadium(V) complexes exhibit one sharp band in the 887–968 cm^{-1} region and one weak band at ca. 926–987 cm^{-1} due to $\nu_{\text{sym}}(\text{O}=\text{V}=\text{O})$ and $\nu_{\text{asym}}(\text{O}=\text{V}=\text{O})$ stretches. These bands confirm the cis- VO_2 structure in complexes [270]. The O-atoms of the $\text{V}^{\text{V}}\text{O}_2$ -units are probably involved in binding to K^+/Cs^+ in the crystal structure; such oxygen coordination has been confirmed in anionic dioxidovanadium(V) complexes [65, 152].

Table 4.1. IR spectra of compounds (ν in cm^{-1})

Compounds	$\nu(\text{C}=\text{S})$	$\nu(\text{C}=\text{N})$	$\nu(\text{V}=\text{O})$	$\nu(\text{N}-\text{N})$
$\text{CH}_2(\text{H}_2\text{sal-sbdt})_2$	1030	1624	-	948
$\text{CH}_2(\text{H}_2\text{sal-smdt})_2$	1039	1625	-	939
$[\text{CH}_2\{\text{V}^{\text{IV}}\text{O}(\text{sal-sbdt})(\text{H}_2\text{O})\}_2]$	-	1582	926	994
$\text{K}_2[\text{CH}_2\{\text{V}^{\text{V}}\text{O}_2(\text{sal-sbdt})\}_2]\cdot 2\text{H}_2\text{O}$	-	1578	943, 987	1030
$\text{Cs}_2[\text{CH}_2\{\text{V}^{\text{V}}\text{O}_2(\text{sal-sbdt})\}_2]\cdot 2\text{H}_2\text{O}$	-	1588	887, 926	989
$[\text{CH}_2\{\text{V}^{\text{IV}}\text{O}(\text{sal-smdt})(\text{H}_2\text{O})\}_2]$	-	1594	956	997
$\text{K}_2[\text{CH}_2\{\text{V}^{\text{V}}\text{O}_2(\text{sal-smdt})\}_2]\cdot 2\text{H}_2\text{O}$	-	1583	968, 980	1037
$\text{Cs}_2[\text{CH}_2\{\text{V}^{\text{V}}\text{O}_2(\text{sal-smdt})\}_2]\cdot 2\text{H}_2\text{O}$	-	1587	888, 930	995

Table 4.2. Electronic spectral data of compounds

Compounds	λ (nm)
$\text{CH}_2(\text{H}_2\text{sal-sbdt})_2$	355, 324, 256, 206
$\text{CH}_2(\text{H}_2\text{sal-smdt})_2$	352, 323, 257, 206
$[\text{CH}_2\{\text{V}^{\text{IV}}\text{O}(\text{sal-sbdt})(\text{H}_2\text{O})\}_2]$	845, 680, 575, 405, 350, 300, 240, 210
$\text{K}_2[\text{CH}_2\{\text{V}^{\text{V}}\text{O}_2(\text{sal-sbdt})\}_2]\cdot 2\text{H}_2\text{O}$	410, 352, 302, 244, 207
$\text{Cs}_2[\text{CH}_2\{\text{V}^{\text{V}}\text{O}_2(\text{sal-sbdt})\}_2]\cdot 2\text{H}_2\text{O}$	410, 351, 300, 290, 210
$[\text{CH}_2\{\text{V}^{\text{IV}}\text{O}(\text{sal-smdt})(\text{H}_2\text{O})\}_2]$	875, 675, 565, 405, 352, 305, 248, 213
$\text{K}_2[\text{CH}_2\{\text{V}^{\text{V}}\text{O}_2(\text{sal-smdt})\}_2]\cdot 2\text{H}_2\text{O}$	404, 337, 292, 233, 215
$\text{Cs}_2[\text{CH}_2\{\text{V}^{\text{V}}\text{O}_2(\text{sal-smdt})\}_2]\cdot 2\text{H}_2\text{O}$	408, 348, 299, 238, 208

4.3.2. Electronic spectral studies

Electronic spectral data of ligands and complexes are presented in Table 4.2. Ligands **4.I** and **4.II** exhibit four absorption bands at ca. 210, 240, 300 and 350 nm which are assigned to $\phi \rightarrow \phi^*$, $\pi \rightarrow \pi_1^*$, $\pi \rightarrow \pi_2^*$, and $n \rightarrow \pi^*$ transitions, respectively. These bands are also observed in complexes with slight shifting. In addition, a new band of medium intensity appears at ca. 405 nm, which is assigned to a ligand to metal charge transfer (LMCT) band. Three bands at 575, 680 and 845 nm (in $[\text{CH}_2\{\text{V}^{\text{IV}}\text{O}(\text{sal-sbdt})\}_2]$) and at 565, 675 and 875 nm (in $[\text{CH}_2\{\text{VO}^{\text{IV}}(\text{sal-smtdt})\}_2]$, observed at higher concentration are assigned to $d - d$ transitions. For dioxidovanadium(V) complexes no such bands were detected.

4.3.3. ^1H NMR studies

Table 4.3 presents the ^1H NMR spectra of the ligands and complexes. The ^1H NMR spectra of ligands exhibit a singlet at $\delta = 13.35$ (**4.I**) and at $\delta = 13.30$ (**4.II**) due to phenolic protons. The absence of this signal in the complexes indicates the coordination of phenolate oxygen. Similarly, the disappearance of the signal appearing at $\delta = 10.10$ (**4.I**) and at $\delta = 10.05$ (**4.II**) due to $-\text{NH}$ proton is in accord with the thioenolisation of the existed thione group in ligands and subsequent replacement of H by the metal ion. A significant downfield shift [CIS ($\Delta\delta$) = 0.51 – 0.53 ppm] (CIS = Chemical induced shift) of the azomethine ($-\text{CH}=\text{N}-$) proton signal of the complexes with respect to the corresponding free ligands confirms the coordination of the azomethine nitrogen. The signal, due to $-\text{CH}_2-$ group attached to two aromatic rings in ligands as well as in complexes, appears at nearly same position ($\Delta\delta = 0.08 - 0.14$ ppm) and this suggests that the two Schiff base units are attached in solution as well. Other resonances due to $-\text{SCH}_2-$ protons (singlet), $-\text{SCH}_3$ protons (singlet) and aromatic protons (complex multiplets) in the complexes also appear in almost the same positions as in the respective ligands. The ^1H NMR data are thus consistent with the ONS dibasic tridentate binding mode of each unit of ligands.

Table 4.3. ^1H NMR spectral data (δ in ppm) of ligands and complexes.

Compound ^{a,b}	–CH=N–	Aromatic H		–CH ₂ –
CH ₂ (H ₂ sal-sbdt) ₂	8.50(s, 2H)	6.80 (d, 2H), 7.50 (d, 2H), 7.35 (m, 12H)		3.75(s, 2H)
K ₂ [CH ₂ {VO ₂ (sal-sdbt)} ₂].2H ₂ O (Δδ)	9.02(s, 2H) (0.52)	6.78(d, 2H), 7.0- 7.80(m, 14H)		3.89(s, 2H) (0.14)
Cs ₂ [CH ₂ {VO ₂ (sal-sbdt)} ₂].2H ₂ O (Δδ)	9.03(s, 2H) (0.53)	6.77 (d, 2H), 7.35-7.75(m, 14H)		3.89(s, 2H) (0.14)
CH ₂ (H ₂ sal-smdt) ₂	8.45(s, 2H)	6.75(d, 2H), 7.13(d, 2H), 7.55(d, 2H)		3.80(s, 2H)
K ₂ [CH ₂ {VO ₂ (sal-smdt)} ₂].2H ₂ O (Δδ)	8.96(s, 2H) (0.51)	6.77(d, 2H), 7.26 (d, 2H), 7.51(d, 2H)		3.87(s, 1H) (0.07)
Cs ₂ [CH ₂ {VO ₂ (sal-smdt)} ₂].2H ₂ O (Δδ)	8.97(s, 2H) (0.52)	6.84(d, 2H), 7.26(d, 2H), 7.50(d, 2H)		3.88(s, 1H) (0.08)
	–OH	–NH	–SCH ₂ –	–CH ₃
CH ₂ (H ₂ sal-sbdt) ₂	13.35(s, 2H)	10.10(s, 2H)	4.50(s, 4H)	
K ₂ [CH ₂ {VO ₂ (sal-sdbt)} ₂].2H ₂ O (Δδ)			4.39(s, 4H) (-0.11)	
Cs ₂ [CH ₂ {VO ₂ (sal-sbdt)} ₂].2H ₂ O (Δδ)			4.39(s, 4H) (-0.11)	
CH ₂ (H ₂ sal-smdt) ₂	13.30(s, 2H)	10.05(s, 2H)		2.47(s, 6H)
K ₂ [CH ₂ {VO ₂ (sal-smdt)} ₂].2H ₂ O (Δδ)				2.50(s, 6H) (0.03)
Cs ₂ [CH ₂ {VO ₂ (sal-smdt)} ₂].2H ₂ O (Δδ)				2.50(s, 6H) (0.03)

^aLetters given in parentheses indicate the signal structure: s = singlet, b = broad (unresolved), m = multiplet.

^b $\Delta\delta = \delta(\text{complex}) - \delta(\text{ligand})$.

4.3.4. ^{51}V NMR studies

Complexes **4.3**, **4.4**, **4.5** and **4.6** were further characterized in solution by recording their ^{51}V NMR spectra in DMSO-d_6 . The resonances are somewhat broadened due to quadrupolar interaction (^{51}V : nuclear spin = $7/2$, quadrupole moment = $-0.05 \times 10^{-28} \text{ m}^2$), the line widths at half height are around 200 Hz, which is still considered comparatively narrow in ^{51}V NMR spectroscopy [306]. The ^{51}V NMR spectral data of these complexes show one strong resonance at $\delta = -462$ (**4.3** and **4.4**) and at $\delta = -463$ ppm (**4.5** and **4.6**), an expected value for vanadium(V) complexes where a soft S atom participates in coordination in addition to the O and N donor atoms [152, 307]. A minor peak at -524 ppm indicates the interaction of solvent DMSO with the metal centre.

4.3.5. Reaction H_2O_2

The formation of peroxo complexes in methanol by treatment of $[\text{CH}_2\{\text{V}^{\text{IV}}\text{O}(\text{sal-sbdt})(\text{H}_2\text{O})\}_2]$ and $[\text{CH}_2\{\text{V}^{\text{IV}}\text{O}(\text{sal-smtdt})(\text{H}_2\text{O})\}_2]$ with H_2O_2 has been established by electronic absorption spectroscopy. Thus, the addition of two drops dilute solution of 30% aqueous H_2O_2 (3.214 g, 28.35 mmol dissolved in 30 mL MeOH) to ca. 20 mL of $6.429 \times 10^{-5} \text{ M}$ methanolic solution of $[\text{CH}_2\{\text{V}^{\text{IV}}\text{O}(\text{sal-sbdt})(\text{H}_2\text{O})\}_2]$ and recording the spectra after every 15 min interval resulted in the spectral changes presented in Figure 4.1. The band at 405 nm slowly shifted to 400 nm along with a slightly decrease in intensity and flattening. Simultaneously, a new shoulder starts to appear at ca. 350 which finally becomes relatively sharper and appears at ca. 350 nm. The band at 300 nm band gains intensity while maintaining the position and bands at 210 and 240 nm sharply gain intensity and finally disappear. The three visible bands appearing at 575, 680 and 845 nm in more concentrated solution, slowly decrease their intensity and finally become flat (Fig. 4.2). The change in spectra has been interpreted as the oxidation of oxidovanadium(IV) species followed by formation of oxidoperoxidovanadium(V) compound [160, 169 184, 186, 263 - 267].

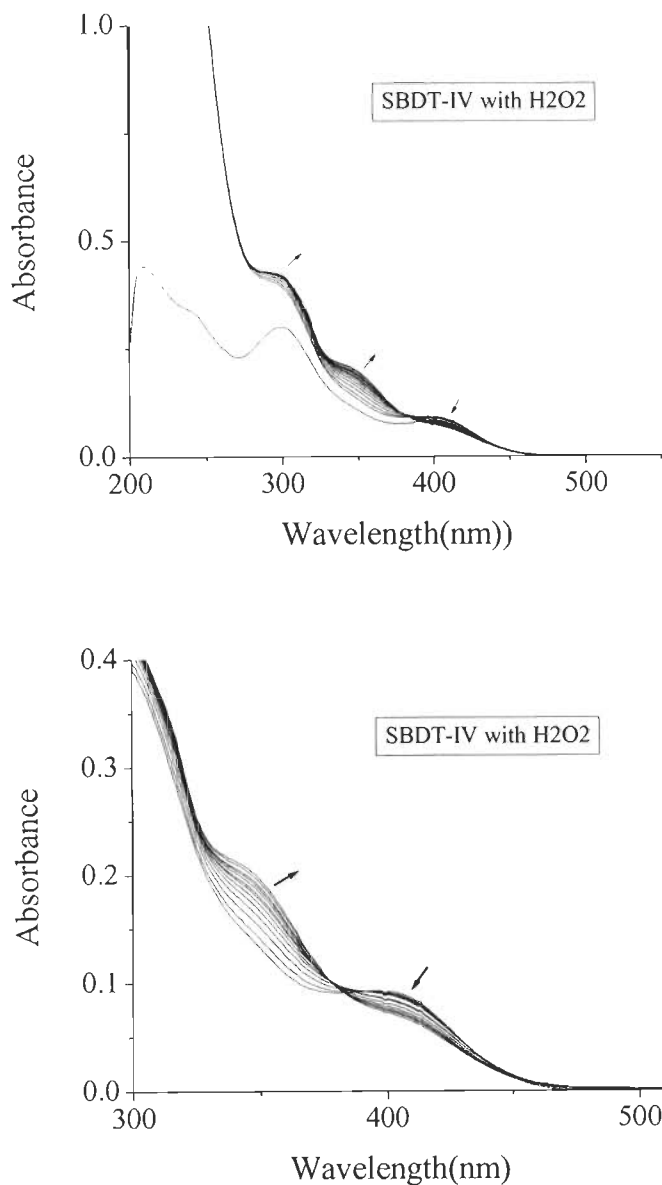


Figure 4.1. Spectral changes obtained after adding two drop dilute solution of 30% aqueous H_2O_2 (3.214 g, 28.35 mmol dissolved in 30 mL MeOH) to 20 mL of ca. 20 mL of 6.429×10^{-5} M methanolic solution of $[\text{CH}_2\{\text{V}^{\text{IV}}\text{O}(\text{sal-sbdt})(\text{H}_2\text{O})\}_2](\mathbf{4.1})$. Spectra were recorded at every 15 min. interval. Bottom plots are expanded region of 300 to 500 nm of top.

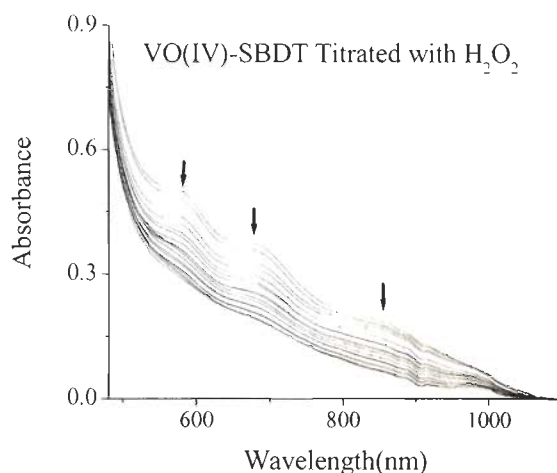


Figure 4.2. Spectral changes obtained during titration of 20 mL of 5.76×10^{-3} M DMSO solution of $[\text{CH}_2\{\text{V}^{\text{IV}}\text{O}(\text{sal-sbdt})(\text{H}_2\text{O})\}_2]$ (**4.1**) with a dilute solution of 30% aqueous H_2O_2 (1.256 g, 11.1 mmol in 5 mL DMSO). Spectra were recorded after the successive addition of 1-drop portions.

A very similar results was obtained with $[\text{CH}_2\{\text{V}^{\text{IV}}\text{O}(\text{sal-smdt})(\text{H}_2\text{O})\}_2]$ (**4.2**) when 20 mL of 8.76×10^{-3} M solution of complex in DMSO was treated with one drop portions of a solution of 30% aqueous H_2O_2 (1.256 g, 11.085 mmol dissolved in 5 mL DMSO). Here, the shoulder bands appearing at ca. 565, 675 and 875 nm slowly disappeared; Figure 4.3. The changes in the UV region could be visualized only in the lower concentration of the complex; Figure 4.4. Thus, after adding two drops dilute solution of 30% aqueous H_2O_2 (3.214 g, 28.36 mmol dissolved in 30 mL MeOH) to 20 mL of ca. 20 mL of 6.327×10^{-5} M solution of $[\text{CH}_2\{\text{V}^{\text{IV}}\text{O}(\text{sal-smdt})(\text{H}_2\text{O})\}_2]$ in methanol resulted in the sharp gain in the intensity of 213 nm band while only small gain in the intensity of 305 nm band along with marginal shift towards lower wave number and the appearance of a weak shoulder band at ca. 350 nm. Further addition of H_2O_2 resulted in slow decrease in intensity of 405 nm band along with broadening, while the shoulder appearing at ca. 350 nm shifted to 345 nm along with sharpness. The 213 and 305 nm bands show marginal increase in intensity.

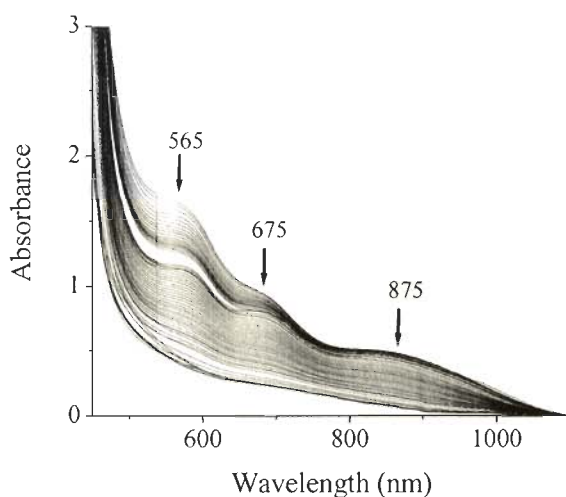


Figure 4.3. Spectral changes obtained during titration of 20 mL of 8.76×10^{-3} M DMSO solution of $[\text{CH}_2\{\text{V}^{\text{IV}}\text{O}(\text{sal-smdt})(\text{H}_2\text{O})\}_2]$ with a dilute solution of 30% aqueous H_2O_2 (1.256 g, 11.085 mmol in 5 mL DMSO). Spectra were recorded after the successive addition of 1-drop portions.

Reactivity of $\text{Cs}_2[\text{CH}_2\{\text{V}^{\text{V}}\text{O}_2(\text{sal-sbdt})\}_2] \cdot 2\text{H}_2\text{O}$ and $\text{Cs}_2[\text{CH}_2\{\text{V}^{\text{V}}\text{O}_2(\text{sal-smdt})\}_2] \cdot 2\text{H}_2\text{O}$ with H_2O_2 were also tested and spectral changes were monitored by electronic absorption spectroscopy. The spectral changes obtained upon adding successive one drop portions of 30 % aqueous H_2O_2 (3.214 g, 28.36 mmol dissolved in 30 mL MeOH) to a 20 mL solution of $\text{Cs}_2[\text{CH}_2\{\text{V}^{\text{V}}\text{O}(\text{sal-sbdt})\}_2] \cdot 2\text{H}_2\text{O}$ (ca. 5.631×10^{-5} M in methanol) are presented in Figures 4.5 and 4.6. Only considerable increase in the intensity of 210 nm band and increase in the intensity followed by disappearance of 290 nm band was noted in the beginning i.e. after addition of about 20 drops of H_2O_2 while the band at 410 nm remains nearly constant. Simultaneously, a weak shoulder starts to appear at ca. 350 and on further addition of H_2O_2 resulted in the appearance of a new band at 345 nm and further weakening of charge transfer band at 410 nm; Figure 4.6. Very similar spectral changes has been obtained for complex $\text{Cs}_2[\text{CH}_2\{\text{V}^{\text{V}}\text{O}_2(\text{sal-smdt})\}_2] \cdot 2\text{H}_2\text{O}$; Figures 4.7 and 4.8. The final spectra of both the complexes are

very are similar to the one obtained by the reaction of the corresponding oxidovanadium(IV) complexes with H_2O_2 .

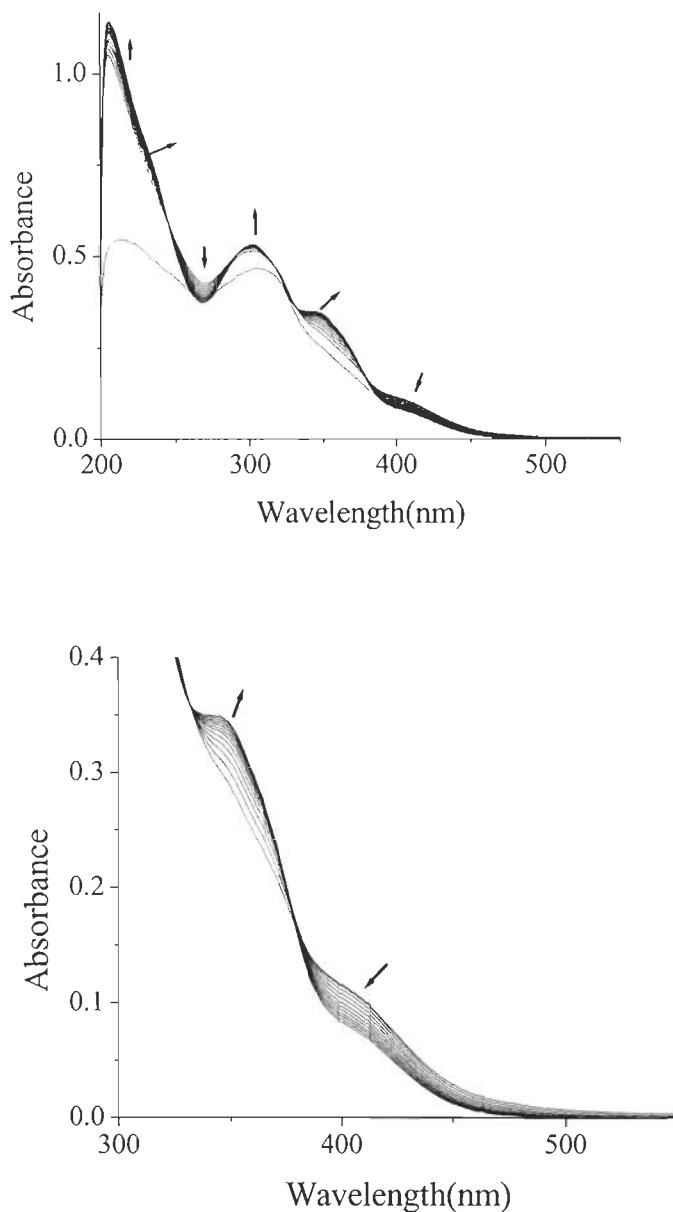


Figure 4.4. Spectral changes obtained after adding two drop dilute solution of 30% aqueous H_2O_2 (3.214 g, 28.36 mmol dissolved in 30 mL MeOH) to 20 mL of ca. 20 mL of 6.327×10^{-5} M methanolic solution of $[\text{CH}_2\{\text{V}^{\text{IV}}\text{O}(\text{sal-smdt})(\text{H}_2\text{O})\}_2](\mathbf{4.2})$. Spectra were recorded at every 10 min. Bottom plots are expanded region of 300 to 500 nm of top.

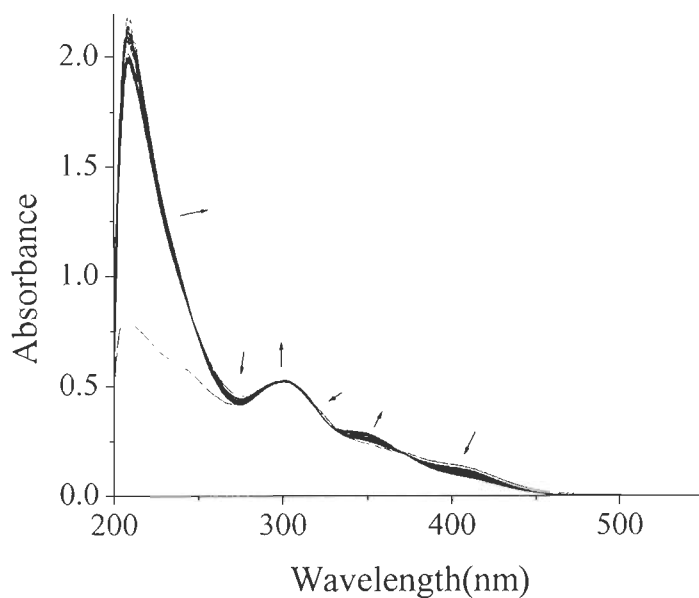


Figure 4.5. Spectral changes obtained after adding one drop dilute solution of 30% aqueous H_2O_2 (3.214 g, 28.358 mmol dissolved in 30 mL MeOH) to 20 mL of ca. 3.124×10^{-5} M methanolic solution of $\text{Cs}_2[\text{CH}_2\{\text{V}^{\text{V}}\text{O}_2(\text{sal-sbdt})\}_2] \cdot 2\text{H}_2\text{O}$ (4.4). Spectra were recorded at every 10 min.

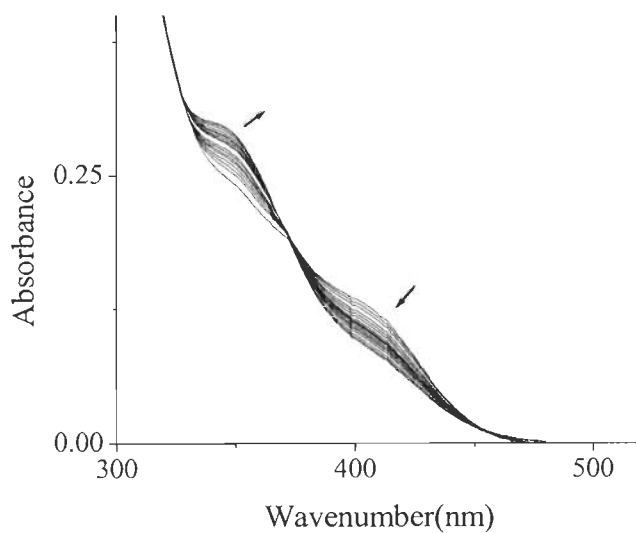


Figure 4.6. Expanded spectra (300 – 500 nm) of Figure 4.5.

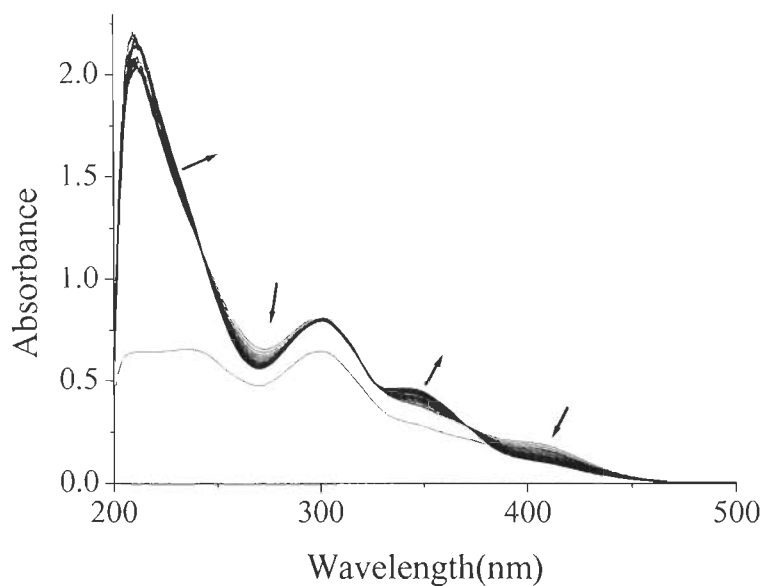


Figure 4.7. Spectral changes obtained after adding one drop dilute solution of 30% aqueous H_2O_2 (3.214 g, 28.358 mmol dissolved in 30 mL MeOH) to 20 mL of ca. 3.326×10^{-5} M methanolic solution of $\text{Cs}_2[\text{CH}_2\{\text{V}^{\text{V}}\text{O}_2(\text{sal-smdt})\}_2] \cdot 2\text{H}_2\text{O}$. Spectra were recorded at every 13 min.

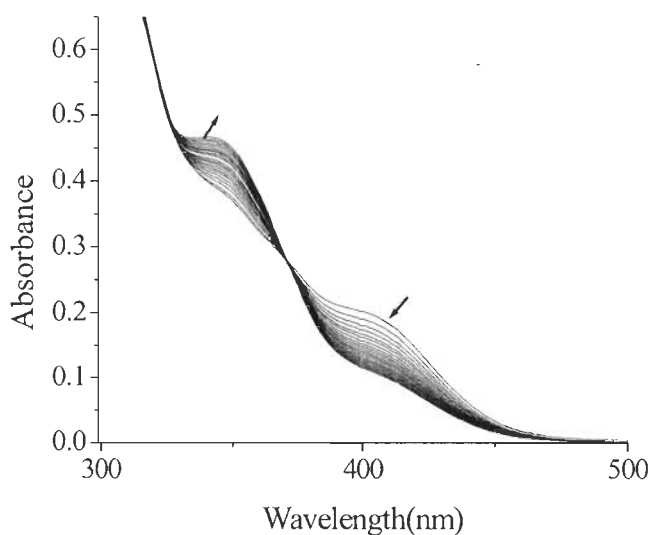


Figure 4.8. Expanded spectrum (300 – 500 nm) of Figure 4.7.

4.3.6. Reaction with HCl

Reactivity of the methanolic solutions of dioxidovanadium(V) complexes with HCl was also monitored by electronic absorption spectroscopy. Thus the drop-wise addition of a saturated solution of HCl gas in methanol to 20 mL of ca. 2.851×10^{-5} solution of $\text{Cs}_2[\text{CH}_2\{\text{V}^{\text{V}}\text{O}_2(\text{sal-sbdt})\}_2] \cdot 2\text{H}_2\text{O}$ (**4.4**) causes the darkening of the solution along with slow broadening with decrease in intensity of LMCT band appearing at 410 nm; Figure 4.9. Simultaneously, the UV bands at 210 nm gains intensity without change in its position while 300 nm gains intensity with shift to 312 nm. A very weak new band also appears at 280 nm.

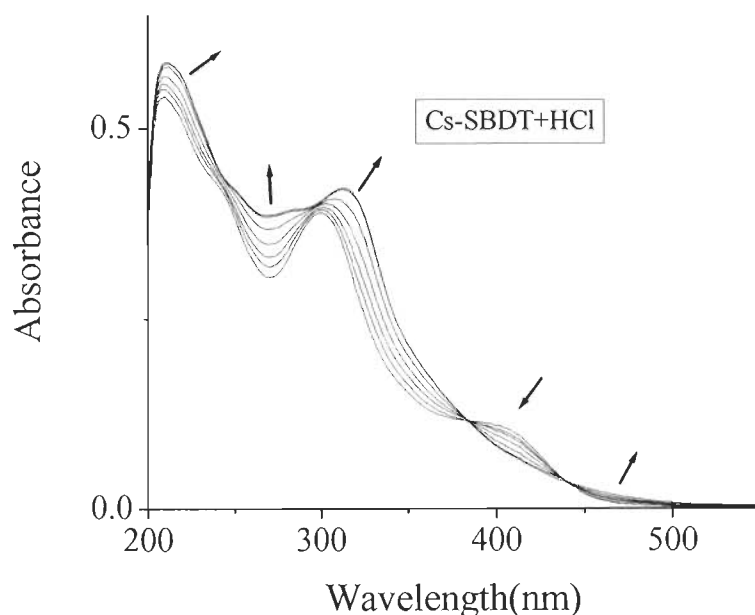


Figure 4.9. Spectral changes obtained during titration of 20 mL of ca. 2.851×10^{-5} M methanolic solution of $\text{Cs}_2[\text{CH}_2\{\text{V}^{\text{V}}\text{O}_2(\text{sal-sbdt})\}_2] \cdot 2\text{H}_2\text{O}$ with drop wise addition of HCl (3.877×10^{-3} M) dissolved in MeOH. The spectra were recorded after the successive addition of 1-drop portions.

Exactly similar features have also been observed with other three complexes, $\text{K}_2[\text{CH}_2\{\text{V}^{\text{V}}\text{O}_2(\text{sal-sbdt})\}_2] \cdot 2\text{H}_2\text{O}$ (**4.3**), $\text{K}_2[\text{CH}_2\{\text{V}^{\text{V}}\text{O}_2(\text{sal-smtdt})\}_2]$

$\cdot 2\text{H}_2\text{O}$ (4.5) and $\text{Cs}_2[\text{CH}_2\{\text{V}^{\text{V}}\text{O}_2(\text{sal-smdt})\}_2]\cdot 2\text{H}_2\text{O}$ (4.6) and spectral changes in case of $\text{Cs}_2[\text{CH}_2\{\text{V}^{\text{V}}\text{O}_2(\text{sal-smdt})\}_2]\cdot 2\text{H}_2\text{O}$ (4.6) is presented in Figure 4.10.

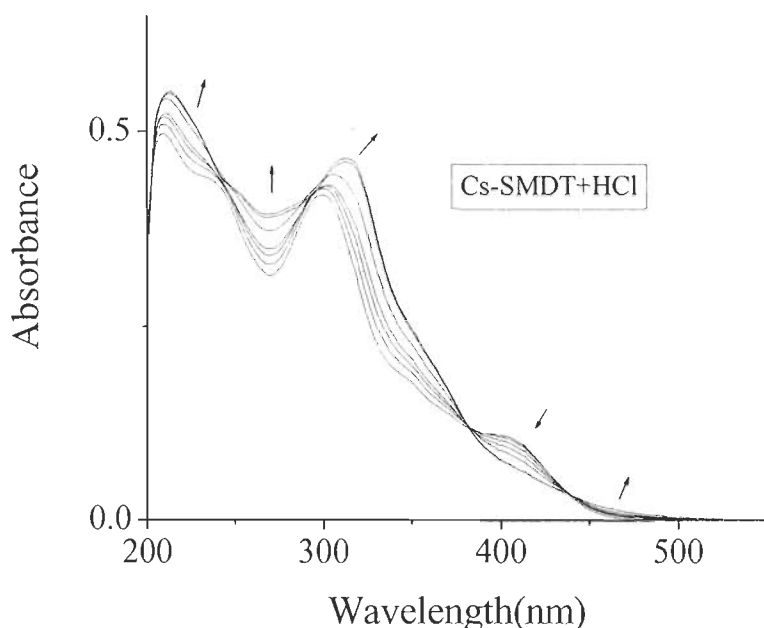
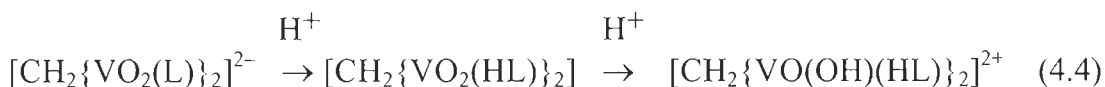


Figure 4.10. Spectral changes obtained during titration of 20 mL of ca. 2.643×10^{-5} M methanolic solution of $\text{Cs}_2[\text{CH}_2\{\text{V}^{\text{V}}\text{O}_2(\text{sal-smdt})\}_2]\cdot 2\text{H}_2\text{O}$ with drop wise addition of HCl (3.877×10^{-3} M) dissolved in MeOH. The spectra were recorded after the successive addition of 1-drop portions.

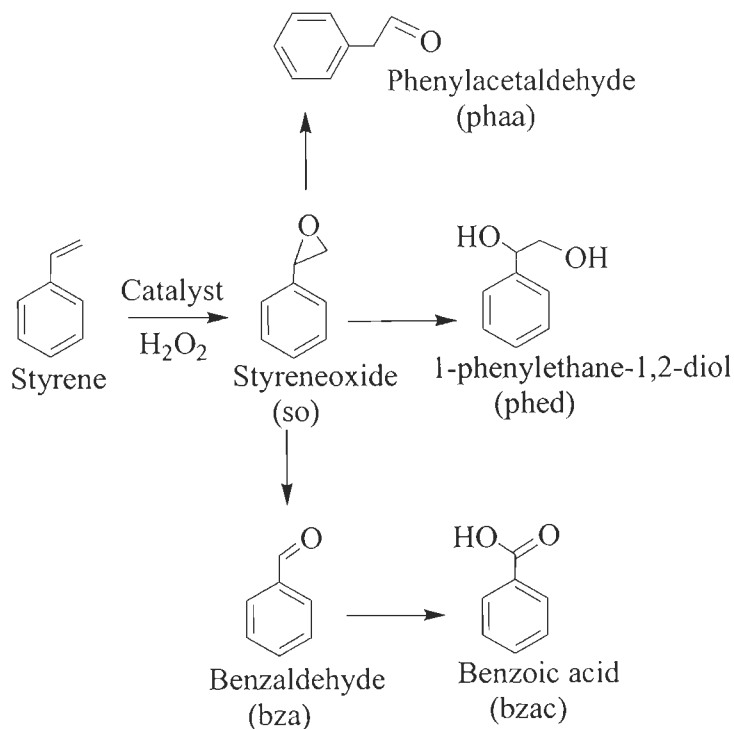
We interpret these result in terms of the formation of oxidohydroxido species of composition $[\text{CH}_2\{\text{VO}(\text{OH})(\text{HL})\}_2]^{2+}$ via $[\text{CH}_2\{\text{VO}_2(\text{HL})\}_2]$ (equation (4.4), with one of the $=\text{N}-\text{N}=\text{}$ nitrogens being the site of protonation. Protonation of the hydrazone nitrogen has been reported, e.g. for the structurally characterised complex $[\text{VO}(\text{Hsal-bhz})]$ ($\text{H}_2\text{sal-bhz}$ derives from salicylaldehyde and benzoylhydrazide), which forms on treatment of the corresponding anionic dioxido complex with HCl [238]. EPR and ESEEM spectra recorded for $[\text{VO}(\text{salim})(\text{acac})]$ (salim = a Schiff base ligand containing imidazole) upon addition of acid were explained by the protonation of the imine N-atom [239].



4.3.7. Catalytic activity studies

Oxidation of styrene

Oxidation of styrene has been carried out by several workers using homogeneous as well as heterogeneous catalysts and major oxidation products generally obtained are styrene oxide, benzaldehyde, benzoic acid, phenyl acetaldehyde and 1-phenylethane-1,2-diol; Scheme 4.3 [161, 162, 184, 188, 264]. We have carried out the oxidation of styrene, catalysed by $\text{Cs}_2[\text{CH}_2\{\text{V}^{\text{V}}\text{O}_2(\text{sal-sbdt})\}_2] \cdot 2\text{H}_2\text{O}$ and $\text{Cs}_2[\text{CH}_2\{\text{V}^{\text{V}}\text{O}_2(\text{sal-smdt})\}_2] \cdot 2\text{H}_2\text{O}$ using hydrogen peroxide as an oxidant to give all expected products as mentioned above along with minor amount of unidentified products.



Scheme 4.3. Various oxidation products of styrene.

In order to get the maximum oxidation of styrene, following parameters were studied in detail considering $\text{Cs}_2[\text{CH}_2\{\text{V}^{\text{V}}\text{O}_2(\text{sal-smdt})\}_2]\cdot 2\text{H}_2\text{O}$ as a representative catalyst:

- (i) amount of catalyst,
- (ii) amount of oxidant and
- (iii) amount of solvent.

The effect of amount of catalyst on the oxidation of styrene was studied as a function of time and the results are presented in Figure 4.11. Three different amount viz. 0.001 g, 0.0035 g and 0.005 g of $\text{Cs}_2[\text{CH}_2\{\text{V}^{\text{V}}\text{O}_2(\text{sal-smdt})\}_2]\cdot 2\text{H}_2\text{O}$ were taken for which styrene (10 mmol) to aqueous 30% H_2O_2 (10 mmol) of ratio 1:1 were taken in 5 mL of methanol and the reaction was carried out at 80 °C. As shown in figure, 0.001 g of catalyst gave 99.5 % conversion of styrene in 8 h of reaction time. Increasing this amount of catalyst lowers the conversion. Thus, 0.001 g catalyst may be considered sufficient enough to run the reaction under above conditions.

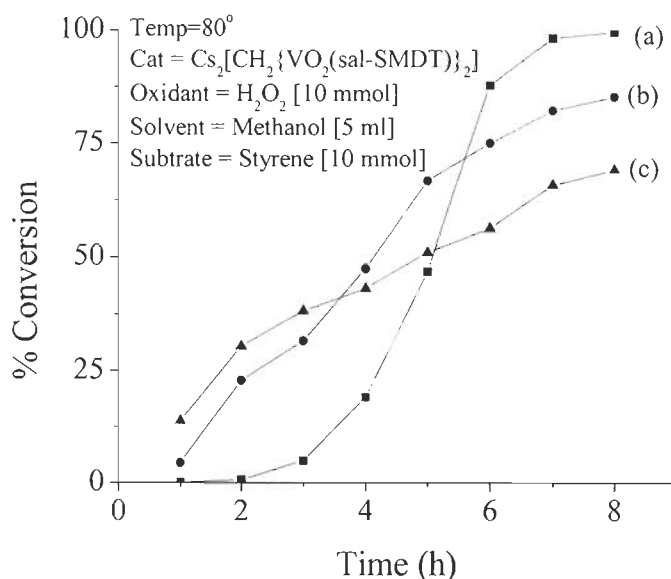


Figure 4.11. Effect of amount of catalyst per unit weight of styrene. (a) 0.001 g, (b) 0.0035 g and (c) 0.005 g. For other reaction conditions see text.

Similarly three different molar ratios of aqueous 30 % H_2O_2 to styrene (e.g. 2:1, 1:1 and 1:2) were considered under above reaction conditions i.e. $\text{Cs}_2[\text{CH}_2\{\text{V}^{\text{V}}\text{O}_2(\text{sal-smdt})\}_2]\cdot 2\text{H}_2\text{O}$ (0.001 g) in 5 mL of methanol and the reaction was carried out at 80 °C for 8 h. The increment of H_2O_2 to styrene ratio from 2:1 to 1:1 improved the conversion from 66.4 % to 99.5 % while the 1:2 ratio gave almost same conversion to that of 1:1 ratio (99.8 %); Figure 4.12. Volume of solvent also affects on the net conversion of styrene. Thus, varying the methanol amount from 5 mL to 7 mL improved the rate of conversion and reaction acquires steady state in shorter period of time (6 h), though it does not affect on the overall conversion of styrene; Figure 4.13. Taking 10 mL methanol causes the dilution of the reactants and thus reaction takes more time to acquire the steady state.

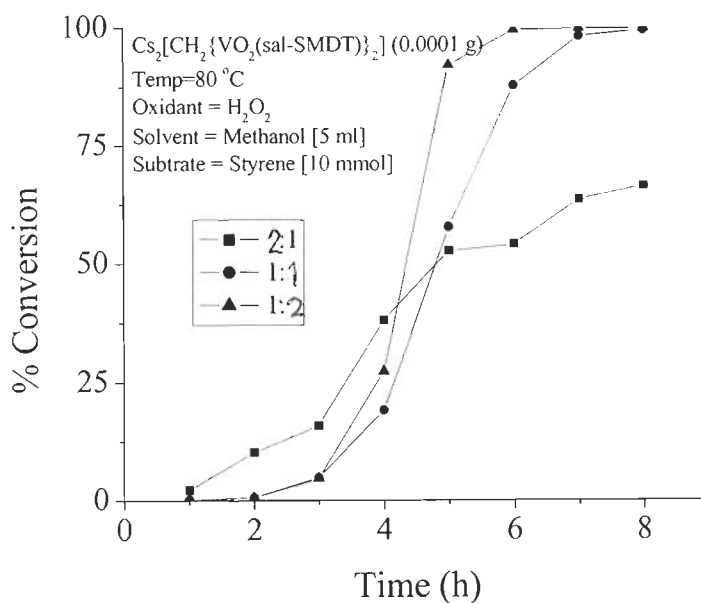


Figure 4.12. Effect of H_2O_2 concentration (H_2O_2 : styrene molar ratio) on oxidation of styrene. For reaction conditions see text.

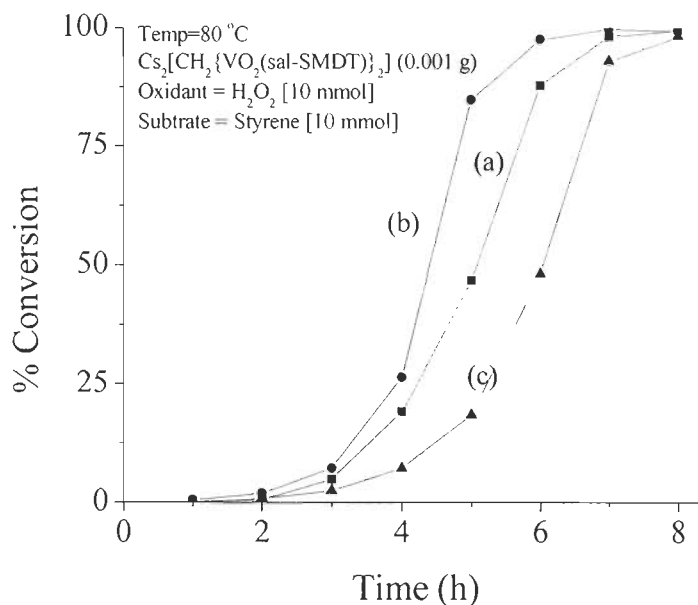


Figure 4.13. Effect of solvent (methanol) on oxidation of styrene. (a) 5 mL, (b) 7 mL and (c) 10 mL. For reaction conditions see text.

After acquiring the optimized reaction conditions for $\text{Cs}_2[\text{CH}_2\{\text{V}^{\text{V}}\text{O}_2(\text{sal-smdt})\}_2] \cdot 2\text{H}_2\text{O}$, other catalyst $\text{Cs}_2[\text{CH}_2\{\text{V}^{\text{V}}\text{O}_2(\text{sal-sbdt})\}_2] \cdot 2\text{H}_2\text{O}$ was also tested under the same reaction conditions. Thus, for 10 mmol of styrene, 10 mmol of 30 % H_2O_2 and 0.001 g of $\text{Cs}_2[\text{CH}_2\{\text{V}^{\text{V}}\text{O}_2(\text{sal-sbdt})\}_2] \cdot 2\text{H}_2\text{O}$ were taken in 7 mL of methanol and the reaction was carried out at 80 °C. A maximum of 31.8 % conversion was only obtained after 8 h of reaction time. However, increasing this amount increases the conversion and as high as 88.5 % conversion of styrene was achieved with 0.003 g of catalyst in 6 h of reaction time. The reaction completed in ca. 5 h on increasing catalysts amount to 0.004 g but the over all conversion is almost same (89.8%); Figure 4.14. The conversion and selectivity of different products are presented in Table 4.4.

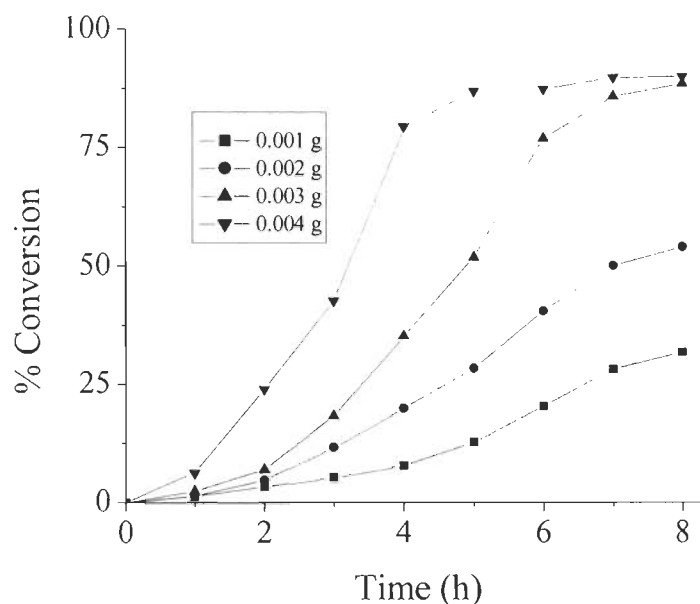


Figure 4.14. Effect of amount of catalyst, $\text{Cs}_2[\text{CH}_2\{\text{V}^{\text{V}}\text{O}_2(\text{sal-sbdt})\}_2]\cdot 2\text{H}_2\text{O}$ per unit weight of styrene. For reaction conditions see text.

Table 4.4. Products selectivity and percent conversion of styrene after 6 h of reaction time

Catalyst	Conv. %	TOF (h^{-1})	% Selectivity ^a					
			so	bza	Phed	bzac	phaa	Other
4.4	88.5	397.9	4.4	10.8	40.3	30.4	13.8	0.3
4.6	99.5	1153.7	3.7	4.6	11.2	77.2	3.0	0.3

^a so: Styrene oxide, bza: Benzaldehyde, phed: 1-phenylethane-1,2-diol, bza: Benzoic acid, phaa: Phenyl acetaldehyde.

Under the optimized reaction conditions, the selectivity of the products formed using $\text{Cs}_2[\text{CH}_2\{\text{V}^{\text{V}}\text{O}_2(\text{sal-sbdt})\}_2]\cdot 2\text{H}_2\text{O}$ as catalyst follows the order: 1-phenylethane-1,2-diol > benzoic acid > phenyl acetaldehyde > benzaldehyde >

styrene oxide. In case of $\text{Cs}_2[\text{CH}_2\{\text{V}^{\text{V}}\text{O}_2(\text{sal-smdt})\}_2]\cdot 2\text{H}_2\text{O}$, the order is: benzoic acid > 1-phenylethane-1,2-diol > benzaldehyde > styrene oxide > phenyl acetaldehyde. Formation of styrene in very poor yield suggests the conversion of styrene oxide to other products.

Oxidative bromination of salicylaldehyde

Dioxidovanadium(V) complexes also catalyze the oxidative bromination of salicylaldehyde in presence of H_2O_2 . In this reaction vanadium complexes react with one or 2 equivalents of H_2O_2 , forming oxidomonoperoxido, $[\text{VO}(\text{O}_2)]^+$ or oxidodiperoxido $[\text{VO}(\text{O}_2)_2]^-$ which ultimately oxidizes bromide species (to Br_2 , Br_3^- and/or HOBr), the bromination of the substrate then proceeding with the liberation of a proton [245]. Oxidative bromination of salicylaldehyde gave 5-bromosalicylaldehyde, 3,5-dibromosalicylaldehyde and 2,4,6-tribromophenol. These are the same products obtained considering dioxidovanadium(V) complexes of ONO donor ligands in Chapters 2 and 3. After several trials, the optimized reaction conditions have been obtained and are: salicylaldehyde (2.44 g, 20 mmol), KBr (5.95 g, 50 mmol), aqueous 30 % H_2O_2 (15.0 g, 120 mmol) catalyst (0.007 g for $\text{Cs}_2[\text{CH}_2\{\text{VO}^{\text{V}}(\text{sal-sbdt})\}_2]\cdot 2\text{H}_2\text{O}$, 0.006 g for $\text{Cs}_2[\text{CH}_2\{\text{VO}^{\text{V}}(\text{sal-smdt})\}_2]\cdot 2\text{H}_2\text{O}$, 0.006 g for $\text{K}_2[\text{CH}_2\{\text{VO}^{\text{V}}(\text{sal-sbdt})\}_2]\cdot 2\text{H}_2\text{O}$, and 0.005 g for $\text{K}_2[\text{CH}_2\{\text{VO}^{\text{V}}(\text{sal-smdt})\}_2]\cdot 2\text{H}_2\text{O}$), aqueous 70% HClO_4 (4.02 g, 80 mmol) and water (40 mL). It was observed that the addition of HClO_4 in four equal portions in first two hours were necessary to obtained better conversion. Conversion of salicylaldehyde, selectivity of different products after 7 h of reaction time are presented in Table 4.5.

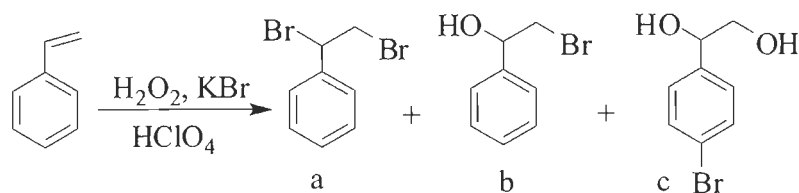
Oxidative bromination of styrene

bromination of styrene, catalysed by $\text{Cs}_2[\text{CH}_2\{\text{VO}^{\text{V}}(\text{sal-sbdt})\}_2]\cdot 2\text{H}_2\text{O}$ and $\text{Cs}_2[\text{CH}_2\{\text{VO}^{\text{V}}(\text{sal-smdt})\}_2]\cdot 2\text{H}_2\text{O}$ in the presence of KBr, HClO_4 and H_2O_2 gave mainly three products namely, (a) 1,2-dibromo-1-phenylethane, (b) (2-bromo-1-

phenylethane-1-ol and (c) 1-(4-bromophenyl)ethane-1,2-diol; Scheme 4.5. Some minor products (benzaldehyde, styrene epoxide, benzoic acid and 4-bromostyrene) with a total selectivity of ca. 7 % have also been detected; most of them are as observed during the oxidation of styrene in the presence of H_2O_2 . The obtained products are similar to the one observed by Conte et al. [171]

Table 4.5. Results of oxidative bromination of salicylaldehyde catalysed by $\text{K}_2[\text{CH}_2\{\text{VO}^{\text{V}}(\text{sal-sbdt})\}_2]\cdot 2\text{H}_2\text{O}$ (**4.3**), $\text{Cs}_2[\text{CH}_2\{\text{VO}^{\text{V}}(\text{sal-sbdt})\}_2]\cdot 2\text{H}_2\text{O}$ (**4.4**), $\text{K}_2[\text{CH}_2\{\text{VO}^{\text{V}}(\text{sal-smdt})\}_2]\cdot 2\text{H}_2\text{O}$ (**4.5**) and $\text{Cs}_2[\text{CH}_2\{\text{VO}^{\text{V}}(\text{sal-smdt})\}_2]\cdot 2\text{H}_2\text{O}$ (**4.6**). Conversion and products obtained in after 7 h.

Entry no	Catalyst	Subst. : H_2O_2	Conv. %	TOF (h^{-1})	Selectivity of product		
					mono	dibromo	tribromo
1	4.6	1 : 2	88.94	393.3	81.3	17.4	1.3
2	4.6	1 : 3	87.25	385.9	76.2	21.9	1.9
3	4.6	1 : 4	87.67	387.7	68.4	28.5	3.1
4	4.6	1 : 5	88.13	389.8	55.2	39.6	5.2
5	4.6	1 : 6	88.48	391.3	40.3	51.8	7.9
6	4.5	1 : 6	86.27	365.1	38.8	59.3	6.9
7	4.4	1 : 6	91.34	402.7	36.2	55.3	8.5
8	4.3	1 : 6	89.01	378.4	28.8	61.4	9.8



Scheme 4.5. Oxidative bromination of styrene. (a) 1,2-dibromo-1-phenylethane, (b) 2-bromo-1-phenylethanol and (c) 1-(4-bromophenyl)ethane-1,2-diol.

Table 4.6 presents conversion of styrene and selectivity of major products obtained after 4 h of reaction time. Increasing the reaction time increases the formation of 2-bromo-1-phenylethane-1-ol and decreases of 1,2-dibromo-1-phenylethane. Reaction conditions for this reaction could not been optimized due to certain constraints but initial results are very encouraging.

Table 4.6. Results of oxidative bromination of styrene catalysed by $\text{Cs}_2[\text{CH}_2\{\text{VO}^{\text{V}}(\text{sal-sbdt})\}_2]\cdot 2\text{H}_2\text{O}$ (**4.4**) and $\text{Cs}_2[\text{CH}_2\{\text{VO}^{\text{V}}(\text{sal-smdt})\}_2]\cdot 2\text{H}_2\text{O}$ (**4.6**). Conversion and products obtained after 4 h.

Entry no	Catalyst	Subst. : H_2O_2	Conv. %	TOF (h^{-1})	Selectivity of product ^a			
					a	b	c	others
1	4.4	1 : 6	99.4	383.5	46.1	4.5	42.9	6.5
2	4.6	1 : 6	99.3	384.3	49.5	3.3	39.6	7.6

^a(a) 1,2-dibromo-1-phenylethane, (b) 2-bromo-1-phenylethane-1-ol and (c) 1-(4-bromophenyl)ethane-1,2-diol.

4.3.8. Antiamoebic activity study

Ligands **4.I** and **4.II** along with their Vanadium complexes **4.1** to **4.6** were screened for antiamoebic activity in vitro against the HM1:IMSS strain of *E. histolytica*. The IC₅₀ values are in the micromolar range and are shown in Table 4.7 below. The data are presented in terms of percentage growth inhibition related to untreated controls and plotted as percentage inhibition versus logarithm of the dose concentration. The IC₅₀ values were obtained by interpolation in the corresponding dose response curves. Complexes $\text{K}_2[\text{CH}_2\{\text{V}^{\text{V}}\text{O}_2(\text{sal-sbdt})\}_2]\cdot 2\text{H}_2\text{O}$ (**4.3**) (IC₅₀ = 0.47 μM) $\text{Cs}_2[\text{CH}_2\{\text{V}^{\text{V}}\text{O}_2(\text{sal-sbdt})\}_2]\cdot 2\text{H}_2\text{O}$ (**4.4**) (IC₅₀ = 0.16 μM),

$K_2[CH_2\{V^VO_2(sal-smdt)\}_2]\cdot 2H_2O$ (**4.5**) ($IC_{50} = 0.56 \mu M$) and $Cs_2[CH_2\{V^VO_2(sal-smdt)\}_2]\cdot 2H_2O$ (**4.6**) ($IC_{50} = 0.22 \mu M$), caused remarkable inhibition more than the standard drug metronidazole, whereas ligands $CH_2(Hsal-sbdt)_2$ (**4.I**) ($IC_{50} = 8.21$) and $CH_2(Hsal-smdt)_2$ (**4.II**) ($IC_{50} = 9.17$) showed comparatively less activity. The moderate activity exhibited by complexes $[CH_2\{V^{IV}O(sal-sbdt)(H_2O)\}_2]$ (**4.1**) ($IC_{50} = 3.45 \mu M$) and $[CH_2\{V^{IV}O(sal-smdt)(H_2O)\}_2]$ (**4.2**) ($IC_{50} = 3.13 \mu M$), showed that complexation of the organic ligands to vanadium substantially enhances the activity. It is apparent that complexation directly or indirectly favours the permeation of the complexes through the lipid layer of the cell membrane [252].

Table 4.7. Vanadium complexes, Antiamoebic activity against HM1:IMSS strain of *E. histolytica*.

Entry No.	Compound	Antiamoebic activity	
		$IC_{50} [\mu M]^a$	S.D ^b
1	$CH_2(H_2sal-sbdt)_2$ (4.I)	8.21	0.02
2	$[CH_2\{V^{IV}O(sal-sbdt)(H_2O)\}_2]$ (4.1)	3.45	0.01
3	$K_2[CH_2\{V^VO_2(sal-sbdt)\}_2]\cdot 2H_2O$ (4.3)	0.47	0.04
4	$Cs_2[CH_2\{V^VO_2(sal-sbdt)\}_2]\cdot 2H_2O$ (4.4)	0.16	0.02
5	$CH_2(H_2sal-smdt)_2$ (4.II)	9.17	0.01
6	$[CH_2\{V^{IV}O(sal-smdt)(H_2O)\}_2]$ (4.2)	3.13	0.03
7	$K_2[CH_2\{V^VO_2(sal-smdt)\}_2]\cdot 2H_2O$ (4.5)	0.56	0.03
8	$Cs_2[CH_2\{V^VO_2(sal-smdt)\}_2]\cdot 2H_2O$ (4.6)	0.22	0.01
9	Metronidazole	1.25	0.03

^a The values were obtained from at least three separate assays done in duplicate.

^b Standard deviation.

4.4. Conclusions

Vanadium complexes with binucleating ligands having ONS functional groups have been synthesized and characterized. Dioxidovanadium(V) complexes retain their structure in the solid as well as in solution as evidenced by ^1H NMR. Dioxidovanadium(V) complexes, $[\text{CH}_2\{\text{V}^{\text{V}}\text{O}_2(\text{sal-sbdt})\}_2]^{2-}$ and $[\text{CH}_2\{\text{V}^{\text{V}}\text{O}_2(\text{sal-smdt})\}_2]^{2-}$ were shown to be functional models of vanadium dependent haloperoxidases, satisfactorily catalyzing the oxidative bromination of styrene and salicylaldehyde using $\text{H}_2\text{O}_2/\text{KBr}$ in the presence of HClO_4 in aqueous solution at room temperature. These complexes also catalyse the oxidation of styrene in the presence of oxidant H_2O_2 , giving five products, styrene oxide, benzaldehyde, benzoic acid, phenyl acetaldehyde and 1-phenylethane-1,2-diol. Thus, these complexes exhibit good catalytic activity and their catalytic potentials are comparable to that of the corresponding complexes having ONO donor ligands reported in chapters 2 and 3. Reactivity of these complexes with H_2O_2 and HCl has been studied. Oxidovanadium(IV) complexes oxidize to the corresponding oxidoperoxidovanadium(V) complexes. These peroxido complexes can also be obtained by the reaction of dioxidovanadium(V) complexes with H_2O_2 . Reaction of HCl with dioxidovanadium(V) complexes produces oxidohydroxo species, an intermediate proposed during catalytic turn over. The V^{V} -complexes of $\{\text{CH}_2(\text{H}_2\text{sal-sbdt})_2\}$ and $\{\text{CH}_2(\text{H}_2\text{sal-smdt})_2\}$ were also screened against HM1:1MSS strains of *Entamoeba histolytica*, the determined IC_{50} values showing that they are significantly more active than metronidazole, suggesting that these vanadium compounds may be promising drugs for the treatment of this disease.

References

1. N. G. Sefström, “Ueber das Vanadin, ein neues Metall, gefunden im Stangeneisen von Eckersholm, einer Eisenhütte, die ihr Erz von Taberg in Småland bezieht”, *Annalen der Physik und Chemie*, **97**, 43, (1831); Source Wikipedia}.
2. F. Betz, *Managing Technological Innovation: Competitive Advantage from Change*. Wiley-IEEE, pp. 158–159, (2003). ISBN 0471225630.
3. L.L.Hopkins Jr., H.L. Cannon, A.T. Miesch, R.M. Welch and F.H. Nielsen, Trace elements related to health and disease: Vanadium, *Geochem. Environ.*, **2**, 93–107, (1977).
4. F.H. Nielsen, “Evidence of the essentiality of arsenic, nickel, and vanadium and their possible nutritional significance”, *Adv. Nutr. Res.*, 1980, **3**, 157–172.
5. N. N. Greenwood and A. Earnshaw, “Chemistry of elements, Second Edition, Butterworth–Heinemann”, 2001.
6. S. Gambarotta, M. Mazzanti, C. Floriani, A. Chiesi–Villa and C. Guastini, “Organometallic derivatives of N,N'–ethylenebis(acetylacetoniminato) vanadium(III) containing a vanadium–carbon σ –bond”, *J. Chem. Soc., Chem. Commun.*, 829–830, (1985).
7. M. Mazzanti, C. Floriani, A. Chiesi–Villa and C. Guastini, “N,N'–ethylenebis(acetylacetoniminato)vanadium(III) derivatives: Syntheses and substitution reactions at the vanadium–chlorine bond”, *Inorg. Chem.*, **25**, 4158–4164 (1986).
8. L. M. Berreau, J. A. Hays, V. G. Young Jr. and L. K. Woo, “Synthesis of early transition metal porphyrin halide complexes: First structural characterization of a vanadium(III) porphyrin complex”, *Inorg. Chem.*, **33**, 105–108 (1994).
9. K. Kanamori, “Structures and properties of multinuclear vanadium(III) complexes: Seeking a clue to understand the role of vanadium(III) in ascidians”, *Coord. Chem. Rev.*, **237**, 147–161 (2003).
10. J.-Q. Wu, L. Pan, Y.-G. Li, S.-R. Liu and Y.-S. Li, “Synthesis, structural characterization, and olefin polymerization behavior of vanadium(III) complexes bearing tridentate Schiff base ligands”, *Organometallics*, **28**, 1817–1825 (2009).

11. A. Butler and J.V. Walker, Marine haloperoxidases, *Chem. Rev.*, **93**, 1937–1944 (1993).
12. O. Kirk and L.S. Conrad, “Metal-free haloperoxidases: Fact or artifact”, *Ang. Chem., Inter. Ed.*, **38**, 977–979 (1999).
13. A. Butler, and J.N. Carter-Franklin, “The role of vanadium bromoperoxidase in the biosynthesis of halogenated marine natural products”, *Natural Product Reports*, **21**, 180–188 (2004).
14. C. Dong, F. Huang, H. Deng, C. Schaffrath, J.B. Spencer, D. O'Hagan and H.J. Naismith, “Crystal structure and mechanism of a bacterial fluorinating enzyme”, *Nature*, **427**, 561–565 (2004).
15. D. O'Hagan, C. Schaffrath, S.L. Cobb, J.T.G. Hamilton and C.D. Murphy, “Biochemistry: Biosynthesis of an organofluorine molecule”, *Nature*, **416**, 279–28, (2002).
16. H. Vilter, “Peroxidases from phaeophyceae: A vanadium(V)-dependent peroxidase from *Ascophyllum nodosum*”, *Phytochem.*, **23**, 1387–1390 (1984).
17. V. Vreeland, J.H. Waite and L. Epstein, “Polyphenols and oxidases in substratum adhesion by marine algae and mussels”, *J. Phycol.*, **34**, 1–8 (1998).
18. U Kusthardt, B. Hedman, K.O. Hodgson, R Hahn and H. Vilter, “High-resolution XANES studies on vanadium-containing haloperoxidase: pH-dependence and substrate binding”, *Federation of Eur. Biochem. Soc.*, **329**, 5–8 (1993).
19. A. Messerschmidt and R. Wever, “X-ray structure of a vanadium-containing enzyme: Chloroperoxidase from the fungus *Curvularia inaequalis*”, *Proc. Natl. Acad. Sci. U.S.A.*, **93**, 392–396 (1996).
20. A. Messerschmidt, L. Prade and R. Wever, “Implications for the catalytic mechanism of the vanadium-containing enzyme chloroperoxidase from the fungus *Curvularia inaequalis* by X-ray structures of the native and peroxide form”, *Biol. Chem.*, **378**, 309–315 (1997).
21. B.H. Simons, P. Barnett, E.G.M. Vollenbroek, H.L. Dekker, A.O. Muijsers, A. Messerschmidt, and R. Wever, “Primary structure and characterization of

the vanadium chloroperoxidase from the fungus *Curvularia inaequalis*", *Eur. J. Biochem.*, **229**, 566–574 (1995).

22. M.I. Isupov, A.R. Dalby, A. Brindley, Y. Izumi, T. Tanabe, G.N. Murshudov and J.A. Littlechild, "Crystal structure of vanadium dependent bromoperoxidase from *Corallina officinalis*", *J. Mol. Biol.*, **299**, 1035–1049 (2000).
23. P. Barnett, W. Hermrika, H.L. Dekker; A.O. Muijsers and R. Renirie, "Isolation, characterization, and primary structure of the vanadium chloroperoxidase from the fungus *Embellisia didymospora*", *J. Biol. Chem.*, **273**, 23381–23387 (1998).
24. M.P.J. van Deurzen, I.J. Remkes, F. van Rantwijk and R.A. Sheldon, "Chloroperoxidase catalyzed oxidations in *t*-butyl alcohol/water mixtures", *J. Mol. Catal. A: Chem.*, **117**, 329–337 (1997).
25. M.P.J. van Deurzen, F. van Rantwijk and R.A. Sheldon, "Selective oxidations catalyzed by peroxidases", *Tetrahedron*, **53**, 13183–13220 (1997).
26. W. Hemrika, R. Renirie, H L. Dekker, P. Barnett and R. Wever, "From phosphatases to vanadium peroxidases: A similar architecture of the active site", *Proc. Natl. Acad. Sci. U.S.A.*, **94**, 2145–2149 (1997).
27. A.F. Neuwald, "An unexpected structural relationship between integral membrane phosphatases and soluble haloperoxidases", *Protein Sci.*, **6**, 1764–1767 (1997).
28. H.B. ten Brink, H.E. Schoemaker and R. Wever, "Sulfoxidation mechanism of vanadium bromoperoxidase from *Ascophyllum nodosum*: Evidence for direct oxygen transfer catalysis", *Eur. J. Biochem.*, **268**, 132–138 (2001).
29. N. Jayme, Carter-Franklin, and A. Butler, "Vanadium bromoperoxidase-catalyzed biosynthesis of halogenated marine natural products", *J. Am. Chem. Soc.*, **126**, 15060–15066 (2004).
30. R.L. Robson, R.E. Eady, T.H. Richardson, R.W. Miller, M. Hawkins and J.R. Postgate, "The alternative nitrogenase of *Azotobacter chroococcum* is a vanadium enzyme", *Nature*, **322**, 388–390 (1986).

31. B.J. Hales, E.E. Case, J.E. Morningstar, M.F. Dzeda and L.A. Mauterer, "Isolation of a new vanadium-containing nitrogenase from *Azotobacter vinelandii*", *Biochem.*, **25**, 7251–7255 (1986).
32. B.J. Hales, D.J. Langosch and E.E. Case, "Isolation and characterization of a second nitrogenase Fe-protein from *Azotobacter vinelandii*", *J. Biol. Chem.*, **261**, 15301–15306 (1986).
33. J. Chen, J. Christiansen, R.C. Tittsworth, B.J. Hales, S.J. George, D. Coucouvanis and S.P. Cramer, "Iron EXAFS of *Azotobacter vinelandii* nitrogenase molybdenum-iron and vanadium-iron proteins", *J. Am. Chem. Soc.*, **115**, 5509–5515 (1993).
34. R.N. Pau, *Biology and Biochemistry of Nitrogen Fixation*, M.J. Dilworth and A.R. Glenn, (Eds.), Elsevier, Amsterdam, Ch. 3 (1991).
35. H.K. Chan, J. Kim and D.C. Res, The nitrogenase Fe Mo-cofactor and P-cluster pair: 2.2 Å resolution structures, *Science*, **260**, 792–794 (1993).
36. B.E. Smith, R.R. Eady, D.J. Lowe and C. Gormal, "The vanadium-iron protein of vanadium nitrogenase from *Azotobacter Chroococcum* contains an iron-vanadium cofactor", *Biochem.*, **250**, 299–302 (1988).
37. R. Wever and W. Hemrika, "*Vanadium in the Environment, Part One: Chemistry and Biochemistry*", J.O. Nriagu (Ed.), John Wiley & Sons, New York, Chapter 12 (1998).
38. R.H. Holm, P. Kennepohl and E.I. Solomon, "Structural and functional aspects of metal sites in biology", *Chem. Rev.*, **96**, 2239–2314 (1996).
39. A. Butler and C.J. Carrano, "Coordination chemistry of vanadium in biological systems", *Coord. Chem. Rev.*, **109**, 61–105 (1991).
40. M.R. Maurya, "Development of the coordination chemistry of vanadium through bis(acetylacetonato)oxovanadium(IV): Synthesis, reactivity and structural aspects", *Coord. Chem. Rev.*, **237**, 163–181 (2003).
41. C. R. Cornman, J. Kampf, M. S. Lah and V. L Pecoraro, "Modeling vanadium bromoperoxidase: Synthesis, structure, and spectral properties of vanadium(IV) complexes with coordinated imidazole", *Inorg. Chem.*, **31**, 2035–2043 (1992).

42. C. R. Cornman, G. J. Colpas, J. D. Hoeschele, J. Kampf and V. L. Pecoraro, "Implications for the spectroscopic assignment of vanadium biomolecules: Structural and spectroscopic characterization of monooxovanadium(V) complexes containing catecholate and hydroximate based noninnocent ligands", *J. Am. Chem. Soc.*, **114**, 9925–9933 (1992).
43. C. R. Cornman, J. Kampf and V. L. Pecoraro, "Structural and spectroscopic characterization of Vanadium(V)–oxoimidazole complexes", *Inorg. Chem.*, **31**, 1981–1983 (1992).
44. K. Fukui, H. Ohya–Nishiguchi and H. Kamada, "Electron spin–echo envelope modulation study of imidazole–coordinated oxovanadium(IV) complexes relevant to the active site structure of reduced vanadium haloperoxidase", *Inorg. Chem.*, **37**, 2326–2327 (1998).
45. M.R. Maurya, A. Arya, A. Kumar and J. Costa Pessoa, "Polystyrene bound oxidovanadium(IV) and dioxidovanadium(V) complexes of histamine derived ligand for the oxidation of methyl phenyl sulfide, diphenyl sulfide and benzoin", *Dalton Trans.*, 2185–2195 (2009).
46. M.R. Maurya, A. Arya, U. Kumar, A. Kumar, F. Avecilla and J. C. Pessoa, "Polymer-bound oxidovanadium(IV) and dioxidovanadium(V) complexes: synthesis, characterization and catalytic application for the hydroamination of styrene and vinyl pyridine", *Dalton Trans.*, 9555–9566 (2009).
47. V. Vergopoulos, W. Pribsch, M. Fritzsche and D. Rehder, "Binding of L–histidine to vanadium. Structure of $\text{exo-[VO}_2\{\text{N-(2-oxidonaphthal)-His}\}]$ ", *Inorg. Chem.*, **32**, 1844–1849 (1993).
48. D. C. Crans, A. D. Keramidas, S. S. Amin, O. P. Anderson and S. M. Miller, "Six–coordinated vanadium–(IV) and –(V) complexes of benzimidazole and pyridyl containing ligands", *J. Chem. Soc., Dalton Tans.*, 2799–2812 (1997).
49. L. J. Calviou, J. M. Arber, D. Collison, C. D. Garner and W. Clegg, "A structural model for vanadyl–histidine interactions: Structure determination of $[\text{VO(1-vinylimidazole)}_4\text{Cl}]\text{Cl}$ by a combination of X–ray crystallography and X–ray absorption spectroscopy", *J. Chem. Soc., Chem. Commun.*, 654–656 (1992).
50. A. D. Keramidas, S. M. Miller, O. P. Anderson and D. C. Crans, "Vanadium(V) hydroxylamido complexes: Solid state and solution properties", *J. Am. Chem. Soc.*, **119**, 8901–8915 (1997).

51. D. C. Crans, A. D. Keramidas, H. Hoover-Litty, O. P. Anderson, M. M. Miller, L. M. Lemoine, S. Pleasic-Williams, M. Vandenberg, A. J. Rossomando and L. J. Sweet, "Synthesis, structure, and biological activity of a new insulinomimetic peroxovanadium compound: Bisperoxovanadium imidazole monoanion", *J. Am. Chem. Soc.*, **119**, 5447–5448 (1997).
52. D. C. Crans, S. M. Schelble and L. A. Theisen, "Substituent effects in organic vanadate esters in imidazole-buffered aqueous solutions", *J. Org. Chem.*, **56**, 1266–1274 (1991).
53. S. K. Dutta, S. B. Kumar, S. Bhattacharyya, E. R. T. Tiekink and M. Chaudhury, "Intramolecular electron transfer in (BzImH)[(LOV)₂O] (H₂L = S-methyl 3-((2-hydroxyphenyl)methyl)dithiocarbazate): A novel μ -oxo dinuclear oxovanadium(IV/V) compound with a trapped-valence (V₂O₃)³⁺ core", *Inorg. Chem.*, **36**, 4954–4960 (1997).
54. S. K. Dutta, S. Samanta, S. B. Kumar, O. H. Han, P. Burckel, A. A. Pinkerton and M. Chaudhury, "Mixed-oxidation divanadium(IV,V) compound with ligand asymmetry: Electronic and molecular structure in solution and in the solid state", *Inorg. Chem.*, **38**, 1982–1988 (1999).
55. S. K. Dutta, S. Samanta, S. Mukhopadhyay, P. Burckel, A. A. Pinkerton and M. Chaudhury, "Spontaneous assembly of a polymeric helicate of sodium with LVO₂ units forming the strand: Photoinduced transformation into a mixed-valence product", *Inorg. Chem.*, **41**, 2946–2952 (2002).
56. S. Samanta, D. Ghosh, S. Mukhopadhyay, A. Endo, T. J. R. Weakley and M. Chaudhury, "Oxovanadium(IV) and (V) complexes of dithiocarbazate-based tridentate Schiff base ligands: Syntheses, structure, and photochemical reactivity of compounds involving imidazole derivatives as coligands", *Inorg. Chem.*, **42**, 1508–1517 (2003).
57. M.R. Maurya, A. Kumar, M. Ebel and D. Rehder, "Synthesis, characterization, reactivity and catalytic potential of model vanadium (IV & V) complexes with benzimidazole derived ONN donor ligands", *Inorg. Chem.*, **45**, 5924–5937 (2006).
58. M.R. Maurya, S. Khurana, C. Schulzke and D. Rehder, "Dioxo and oxovanadium(V) complexes of biomimetic hydrazone ONO donor ligands Synthesis, characterisation and reactivity", *Eur. J. Inorg. Chem.*, 779–788 (2001).

59. M. R. Maurya, S. Agarwal, C. Bader, M. Ebel and D. Rehder, "Synthesis, characterisation and catalytic potential of hydrazonato-vanadium(V) model complexes with $[\text{VO}]^{3+}$ and $[\text{VO}_2]^+$ cores", *Dalton Trans.*, 537–544 (2005).
60. T. Ghosh, "Dioxovanadium(V) complexes incorporating tridentate ONO donor hydrazone ligands derived from acetylhydrazide and 2-hydroxybenzaldehyde/2-hydroxyacetophenone. Synthesis, characterization and reactivity", *Transition Met. Chem.*, **31**, 560–565 (2006).
61. T. Ghosh, B. Mondal, T. Ghosh, M. Sutradhar, G. Mukherjee and M.G.B. Drew, "Synthesis, structure, solution chemistry and the electronic effect of *para* substituents on the vanadium center in a family of mixed-ligand $[\text{V}^{\text{VO}}(\text{ONO})(\text{ON})]$ complexes", *Inorg. Chim. Acta*, **360**, 1753–1761 (2007).
62. B. Mondal, M.G.B. Drew, R. Banerjee and T. Ghosh, "Chemistry of mixed-ligand methoxy bonded oxidovanadium(V) complexes with a family of hydrazone ligands containing VO_3^+ core and their substituent controlled methoxy-bridged dimeric forms", *Polyhedron*, **27**, 3197–3206 (2008).
63. B. Mondal, M.G.B. Drew and T. Ghosh, "Synthesis, structure and solution chemistry of quaternary oxovanadium(V) complexes incorporating hydrazone ligands", *Inorg. Chim. Acta*, **362**, 3303–3308 (2009).
64. S. Nica, M. Rudolph, H. Görls and W. Plass, "Structural characterization and electrochemical behavior of oxovanadium(V) complexes with N-salicylidene hydrazides", *Inorg. Chim. Acta*, **360**, 1743–1752 (2007).
65. M. R. Maurya, S. Agarwal, C. Bader and D. Rehder, "Dioxovanadium(V) complexes of ONO donor ligands derived from pyridoxal and hydrazides: Models of vanadate-dependent haloperoxidases", *Eur. J. Inorg. Chem.*, 147–157 (2005).
66. N. Vuletic and C. Djordjevic, "Oxodiperoxovanate(V) complexes with bidentate ligands", *J. Chem. Soc., Dalton Trans.*, 1137–1141 (1973).
67. C. Djordjevic, "Heteroligand peroxo transition metal complexes", *Chem. Br.*, **18**, 554–557 (1982).
68. C. Djordjevic, S. A. Craig and E. Sinn, "A polymeric peroxo heteroligand vanadate(V). Synthesis, spectra and structure of $\text{M(1)[VO}(\text{O}_2)(\text{C}_4\text{H}_5\text{O}_4\text{N})]$ ", *Inorg. Chem.*, **24**, 1281–1283 (1985).

69. C. Djordjevic, B. C. Puryear, N. Vuletic, C. J. Abelt and S. J. Sheffield, "Preparation, spectroscopic properties and characterization of novel peroxo complexes of vanadium(V) and molybdenum(VI) with nicotinic acid and nicotinic acid N-oxide", *Inorg. Chem.*, **27**, 2926–2932 (1988).
70. C. Djordjevic, M. Lee and E. Sinn, "Oxoperoxo(citrato) and dioxo(citrato)vanadates(V): Synthesis, spectra and structure of hydroxyl oxygen bridged dimer, $K_2[VO(O_2)(C_6H_6O_7)_2]_2 \cdot 2H_2O$ ", *Inorg. Chem.*, **28**, 719–723 (1989).
71. C. Djordjevic, P. L. Wilkins, E. Sinn and R. J. Butcher, "Peroxo aminopolycarboxylatovanadate(V) of an unusually low toxicity: Synthesis and structure of very stable $K_2[VO(O_2)(C_6H_6NO_6)] \cdot 2H_2O$ ", *Inorg. Chim. Acta*, **230**, 241–244 (1995).
72. C. Djordjevic, M. Lee–Renslo and E. Sinn, "Peroxo malato vanadates(V): Synthesis, spectra, and structure of the $(NH_4)_2[VO(O_2)(C_4H_4O_5)]_2 \cdot 2H_2O$ dimer with a rhomboidal V_2O_2 (hydroxyl) bridging core", *Inorg. Chim. Acta*, **233**, 97–102 (1995).
73. C. Djordjevic, N. Vuletic, M. Lee–Renslo, B. C. Puryear and R. Alimard, "Peroxo heteroligand vanadates(V): Synthesis, spectra–structure relationships, and stability toward decomposition", *Mol. Cellu. Biochem.*, **153**, 25–29 (1995).
74. M. Bhattacharjee, M. K. Chaudhuri, N. S. Islam and P. C. Paul, "Synthesis, characterization and physicochemical properties of peroxo–vanadium(V) complexes with glycine as the hetero ligand", *Inorg. Chim. Acta*, **169**, 97–100 (1990).
75. M. Sivák, D. Joniaková and P. Schwendt, "Nitrilotriacetato–monoperoxo complexes of vanadium(V): Formation in aqueous solution, synthesis and structure", *Trans. Met. Chem.*, **18**, 304–308 (1993).
76. L. Kuchta, M. Sivak and F. Pavelcik, "Synthesis, characterization and crystal structure of barium(nitrilotriacetato)oxoperoxovanadate(V) trihydrate", *J. Chem. Res. (S)*, 393 (1993).
77. F. W. B. Einstein, R. J. Batchelor, S. J. Angus–Dunne and A. S. Tracey, "A product formed from glycylglycine in the presence of vanadate and hydrogen peroxide: The (glycylde–N–hydroglycinato– $\kappa^3 N^2, N^N, O^1$)oxoperoxovanadate(V) Anion", *Inorg. Chem.*, **35**, 1680–1684 (1996).

78. M. Cásny, M. Sivák and D. Rehder, "Monoperoxo–vanadium(V) complexes of R,S–N–(carboxymethyl)aspartate", *Inorg. Chim. Acta*, **355**, 223–228 (2003).
79. V. Conte, O. Bortolini, M. Carraro and S. Moro, "Models for the active site of vanadium–dependent haloperoxidases: Insight into the solution structure of peroxo vanadium compounds", *J. Inorg. Biochem.*, **80**, 41–49 (2000).
80. B. J. Hamstra, G. J. Colpas and V. L. Pecoraro, "Reactivity of dioxovanadium(V) complexes with hydrogen peroxide: Implications for vanadium haloperoxidase", *Inorg. Chem.*, **37**, 949–955 (1998).
81. C. Kimblin, X. Bu and A. Butler, "Modeling the catalytic site of vanadium bromoperoxidase: Synthesis and structural characterization of intramolecularly H–bonded vanadium(V) oxoperoxo complexes, $[\text{VO}(\text{O}_2)(\text{NH}_2\text{pyg}_2)]\text{K}$ and $[\text{VO}(\text{O}_2)(\text{BrNH}_2\text{pyg}_2)]\text{K}$ ", *Inorg. Chem.*, **41**, 161–163 (2002).
82. H. Schmidt, I. Andersson, D. Rehder and L. Pattersson, "A potentiometric and ^{51}V NMR study of the aqueous $\text{H}^+/\text{H}_2\text{VO}_4^-/\text{H}_2\text{O}_2$ / L– α –alanyl–L–histidine", *Chem. Eur. J.*, **7**, 251–257 (2001).
83. J. A. Guevara–Garcia, N. Barba–Behrens, R. Contraras and Mendoza–Diaz, "Bis–peroxo–oxovanadium(V) complexes of histidine containing peptides as models for vanadium haloperoxidases, in Vanadium compounds: Biochemistry, chemistry and therapeutic applications", A. S. Tracy and D. C. Crans (Eds.), p.126 (1998).
84. W. Tsagkalidis, D. Rodewald and D. Rehder, "Coordination and oxidation of vanadium(II) by 1,2-bis(2-sulfidophenylsulfanyl)ethane(2-) (S_4): The structures of $[\text{V}(\text{S}_4)\text{tmeda}]$, the first example of vanadium(II)-sulfide coordination, and of $[\text{V}_3(\mu\text{-O})_2(\text{S}_2)_4(\text{tmeda})_2]$ [S_2 = 1,2-benzenedithiolate(2-)]", *J. Chem. Soc., Chem. Commun.*, 165–166 (1995).
85. A.J. Tasiopoulos, A.T. Vlahos, A.D. Keramidas, T.A. Kabanos, Y.G. Deligiannakis, C.P. Raptopoulou and A. Terzis, "Models of oxovanadium(IV) protein interactions: The first oxovanadium(IV) complexes with dipeptides", *Angew. Chem. Intl. Ed. Engl.*, **35**, 2531–2533 (1996).
86. M. Farahbakhsh, H. Nekola, H. Schmidt and D. Rehder, "Thio-ligation to vanadium: The NSSN and S'N'O donor sets (N equals pyridine, N' equals

- enamine; S equals thioether, S' equals thiolate)", *Chem. Ber. Recueil*, **130**, 1129–1133 (1997).
87. C.R. Cornman, T.C. Stauffer and P.D. Boyle, "Oxidation of a vanadium(V)-dithiolate complex to a vanadium(V)- $\eta^{(2)}$, $\eta^{(2)}$ -disulfenate complex", *J. Am. Chem. Soc.*, **119**, 5986–5987 (1997).
 88. W. Tsagkalidis and D. Rehder, "Characterization of bio-related vanadium and zinc complexes containing tetradentate dithiolate -disulphide, -diamine and -amine-amide ligands", *J. Biol. Inorg. Chem.*, **1**, 507–514 (1996).
 89. M. Milanesio, D. Viterbo, R. P. Hernandez, J. D. Rodriguez, J. Ramirez-Ortiz and J. Valdes-Martinez, "Synthesis, characterization and novel crystal structure of (salicylal-4-phenylthiosemicarbazidato) ammonium dioxovanadate(V) with a V–S bond", *Inorg. Chim. Acta*, **306**, 125–129 (2000).
 90. A. Sarkar and S. Pal, "Complexes of oxomethoxovanadium(V) with tridentate thiobenzhydrazide based Schiff bases", *Inorg. Chim. Acta*, **361**, 2296–2304 (2008).
 91. S.K.S. Hazari, J. Kopf, D. Palit, S. Rakshit and D. Rehder, "Oxidovanadium(IV) complexes containing ligands derived from dithiocarbazates—Models for the interaction of VO^{2+} with thiofunctional ligands", *Inorg. Chim. Acta*, **362**, 1343–1347 (2009).
 92. K. J. Ooms, S.E. Bolte, B. Baruah, M.A. Choudhary, D.C. Crans and T. Polenova, " ^{51}V solid-state NMR and density functional theory studies of eight-coordinate non-oxo vanadium complexes: oxidized amavadin", *Dalton Trans.*, 3262–3269 (2009).
 93. M. Sutradhar, G. Mukherjee, M.G.B. Drew and S. Ghosh, "Simple general method of generating non-oxo, non-amavadin model octacoordinated vanadium(IV) complexes of some tetradentate ONNO chelating ligands from various oxovanadium(IV/V) compounds and structural characterization of one of them", *Inorg. Chem.*, **46**, 5069–5075 (2007).
 94. H.H. Sky-Peck, "Trace metals and neoplasia", *Clin. Physiol. Biochem.*, **4**, 99–111 (1986).
 95. N.D. Chasteen, "The biochemistry of vanadium", *Struc. Bonding*, **53**, 105–138 (1983).

96. L.C. Cantley, L. Josephson, R. Warner, M. Yanaisawa, C. Lechene and G. Guidotti, "Vanadate is a potent (Na, K)-ATPase inhibitor found in ATP derived from muscle", *J. Biol. Chem.*, **252**, 7421–7423 (1977).
97. L. Josephson and L.C. Cantley, "Isolation of a potent (Na⁺-K⁺) stimulated ATPase inhibitor from striated muscle", *Biochem.*, **16**, 4572–4578 (1977).
98. L.C. Cantley and P. Aisen, "The fate of cytoplasmic vanadium. Implications on (Na,K)-ATPase inhibition", *J. Biol. Chem.*, **254**, 1781–1784 (1979).
99. B.R. Nechay, L.B. Nanninga and P.S.E. Nechay, "Vanadyl(IV) and vanadate(V) binding to selected endogenous phosphate, carboxyl, and amino ligands; calculations of cellular vanadium species distribution", *Arch. Biochem. Biophys.*, **251**, 128–138 (1986).
100. R.P. Sharma, S.G. Oberg and R.D. Parker, "Vanadium retention in rat tissues following acute exposures to different dose levels", *J. Toxicol. Environ. Health*, **6**, 45–54 (1980).
101. E. Sabbioni and E. Marafante, "Metabolic patterns of vanadium in the rat", *Bioinorg. Chem.*, **9**, 389–407 (1978).
102. R.A. Peckauskas, J.D. Termine and I. Pullman, "ESR investigation of the binding of acidic biopolymers to synthetic apatite", *Biopoly.*, **15**, 569–581 (1976).
103. R.A. Peckauskas, I. Pullman and J.D. Termine, "ESR investigation of the binding of some neutral polyamino acids to synthetic apatite", *Biopoly.*, **16**, 199–206 (1977).
104. M. Biagioli, L. Strinna-Erre, G. Micera, A. Panzanelli and M. Zema, "Molecular structure, characterization and reactivity of dioxo complexes formed by vanadium(V) with α -hydroxycarboxylate ligands", *Inorg. Chim. Acta*, **310**, 1–9 (2000).
105. D. Sanna, G. Micera, P. Buglyo and T. Kiss, "Oxovanadium(IV) complexes of ligands containing phosphonic acid moieties", *J. Chem. Soc., Dalton Trans.*, 87–92 (1996).
106. N. D. Chasteen, J. K. Grady and C. E. Holloway, "Characterization of the binding, kinetics and redox stability of vanadium(IV) and vanadium(V) protein complexes in serum", *Inorg. Chem.*, **25**, 2754–2760 (1986).

107. E. J. Baran, "Oxovanadium(IV) and oxovanadium(V) complexes relevant to biological systems", *J. Inorg. Biochem.*, **80**, 1–8 (2001).
108. J. Costa Pessoa, I. Tomaz, T. Kiss and P. Buglyo, "The system VO^{2+} + oxidized glutathione: A potentiometric and spectroscopic study", *J. Inorg. Biochem.*, **84**, 259–270 (2001).
109. T. Kiss, T. Jakusch, M. Kilyen, E. Kiss and A. Lakatos, "Solution speciation of bioactive Al(III) and VO(IV) complexes", *Polyhedron*, **19**, 2389–2401 (2000).
110. E. Kiss, E. Garribba, G. Micera, T. Kiss and H. Sakurai, "Ternary complex formation between VO(IV)–picolinic acid or VO(IV)–6–methylpicolinic acid and small blood serum bioligands", *J. Inorg. Biochem.*, **78**, 97–108 (2000).
111. T. Kiss, E. Kiss, E. Garribba and H. Sakurai, "Speciation of insulin–mimetic VO(IV)–containing drugs in blood serum", *J. Inorg. Biochem.*, **80**, 65–73 (2000).
112. E. L. Tolman, E. Barris, M. Burns, A. Pansini and R. Partridge, "Effects of vanadium on glucose metabolism *in vitro*", *Life Sci.*, **25**, 1159–1164 (1979).
113. G. R. Dubyak and A. Kleinzeller, "The insulin–mimetic effects of vanadate in isolated rat adipocytes. Dissociation from effects of vanadate as a (Na^+ – K^+) ATPase inhibitor", *J. Biol. Chem.*, **255**, 5306–5312 (1980).
114. Y. Shechter and S. J. Karlsh, "Insulin–like stimulation of glucose oxidation in rat adipocytes by vanadyl(IV) ions", *Nature (London)*, **284**, 556–558 (1980).
115. H. Sakurai, Y. Kojima, Y. Yoshikawa, K. Kawabe and H. Yasui, "Antidiabetic vanadium(IV) and zinc(II) complexes", *Coord. Chem. Rev.*, **226**, 187–198 (2002).
116. Y. Shechter, I. Goldwaser, M. Mironchik, M. Fridkin and D. Gefel, "Historic perspective and recent developments on the insulin–like actions of vanadium; toward developing vanadium based–drugs for diabetes", *Coord. Chem. Rev.*, **237**, 3–11 (2003).
117. K. H. Thompson, J. H. McNeill and C. Orvig, "Vanadium compound as insulin mimics", *Chem. Rev.*, **99**, 2561–2571 (1999).

118. O. Blondel, J. Simon, B. Chevalier and B. Portha, "Impaired insulin action but normal insulin receptor activity in diabetic rat liver: Effect of vanadate", *Am. J. Physiol.*, **258**, E459–E467 (1990).
119. C. E. Heyliger, A. G. Tahiliani and J. H. McNeill, "Effect of vanadate on elevated blood glucose and depressed cardiac performance of diabetic rats", *Science*, **227**, 1474–1477 (1985).
120. J. Meyerovitch, Z. Farfel, J. Sack and Y. Shechter, "Oral administration of vanadate normalizes blood glucose levels in streptozotocin-treated rats. Characterization and mode of action", *J. Biol. Chem.*, **262**, 6658–6662 (1987).
121. H. Sakurai, K. Tsuchiya, M. Nukatsuka, M. Sofue and J. Kawada, "Insulin-like effect of vanadyl ion on streptozotocin-induced diabetic rats", *J. Endocrinol.*, **126**, 451–459 (1990).
122. M. Halberstam, N. Cohen, P. Shlimovich, L. Rossetti and H. Shamoon, "Oral vanadyl sulfate improves insulin sensitivity in NIDDM but not in obese nondiabetic subjects", *Diabetes*, **45**, 659–666 (1996).
123. K. Cusi, S. Cukier, R. A. DeFronzo, M. Torres, F. M. Puchulu and J. C. P. Redondo, "Vanadyl sulfate improves hepatic and muscle insulin sensitivity in type 2 diabetes", *J. Clin. Endocrinol. Metab.*, **86**, 1410–1417 (2001).
124. K. Hamrin and J. Henriksson, "Local effect of vanadate on interstitial glucose and lactate concentrations in human skeletal muscle", *Life Sciences*, **76**, 2329–2338 (2005).
125. V. G. Yuen, C. Orvig and J. H. McNeill, "Glucose-lowering effects of a new organic vanadium complex, bis(maltolato)oxovanadium(IV)", *Can. J. Physiol. Pharmacol.*, **71**, 263–269 (1993).
126. J. H. McNeill, V. G. Yuen, H. R. Hoveyda, and C. Orvig, "Bis(maltolato)oxovanadium(IV) is a potent insulin mimic", *J. Med. Chem.*, **35**, 1489–1491 (1992).
127. C. Orvig, P. Caravan, L. Gelmini, N. Glover, F. G. Herring, H. Li, J. H. McNeill, S. J. Rettig, I. A. Setyawati, E. Shuter, Y. Sun, A. S. Tracey and V. G. Yuen, "Reaction chemistry of BMOV, bis(maltolato)oxovanadium(IV)—a potent insulin mimetic agent", *J. Am. Chem. Soc.*, **117**, 12759–12770 (1995).

128. Y. Sun, B. R. James, S. J. Rettig, and C. Orvig, "Oxidation kinetics of the potent insulin mimetic agent bis(maltolato)oxovanadium(IV) (BMOV) in water and in methanol", *Inorg. Chem.*, **35**, 1667–1673 (1996).
129. J. H. McNeill, V. G. Yuen, S. Dai and C. Orvig, "Increased potency of vanadium using organic ligands", *Mol. Cell. Biochem.*, **153**, 175–180 (1995).
130. B. D. Liboiron, K. H. Thompson, G. R. Hanson, E. lam, N. Aebischer and C. Orvig, "New insights into the interactions of serum proteins with bis(maltolato)oxovanadium(IV): Transport and biotransformation of insulin-enhancing vanadium pharmaceuticals", *J. Am. Chem. Soc.*, **127**, 5104–5115 (2005).
131. K. G. Peters, M. G. Davis, B. W. Howard, M. Pokross, V. Rastogi, C. Diven, K. D. Greis, E. Eby–Wilkens, M. Maier, A. Evdokimov, S. Soper and F. Genbauffe, "Mechanism of insulin sensitization by BMOV bis(maltolato)oxovanadium; unliganded vanadium(VO₄) as the active component", *J. Inorg. Biochem.*, **96**, 321–330 (2003).
132. K. H. Thompson, B. D. Liboiron, Y. Sun, K. D. D. Bellman, I. A. Setyawati, B. O. Patrick, V. Karunaratne, G. Rawji, J. Wheelar, K. Sutton, S. Bhanot, C. Cassidy, J. H. McNeill, V. G. Yuen and C. Orvig, "Preparation and characterization of vanadyl complexes with bidentate maltol-type ligands; *in vivo* comparisons of anti-diabetic therapeutic potential", *J. Biol. Inorg. Chem.*, **8**, 66–74 (2003).
133. K. H. Thompson and C. Orvig, "Metal complexes in medicinal chemistry: New vistas and challenges in drug design", *Dalton Trans.*, **761**–764 (2006).
134. Reapeat ref. H. Sakurai, Y. Kojima, Y. Yoshikawa, K. Kawabe and H. Yasui, "Antidiabetic vanadium(IV) and zinc(II) complexes", *Coord. Chem. Rev.*, **226**, 187 (2002).
135. Y. Adachi and H. Sakurai, "Insulin-mimetic vanadyl(IV) complexes as evaluated by both glucose-uptake and inhibition of free fatty acids (FFA)-release in isolated rat adipocytes", *Chem. Pharm. Bull.*, **52**, 428–433 (2004).
136. D. C. Crans, "Chemistry and insulin-like properties of vanadium(IV) and vanadium(V) compounds", *J. Inorg. Biochem.*, **80**, 123–131 (2000).
137. L. H. Gao, W. P. Liu, B. L. Wang, L. Li, M. J. Xie, Y. R. Li, Z. H. Chen and X. Z. Chen, "Effects of bis(α -furancarboxylato)oxovanadium(IV) on

non-diabetic and streptozotocin-diabetic rats”, *Clin. Chim. Acta*, **368**, 173–178 (2006).

138. M. Yamaguchi, K. Wakasugi, R. Saito, Y. Adachi, Y. Yoshikawa, H. Sakurai and A. Katoh, “Syntheses of vanadyl and zinc(II) complexes of 1-hydroxy-4,5,6-substituted 2(1H)-pyrimidinones and their insulin-mimetic activities”, *J. Inorg. Biochem.*, **100**, 260–269 (2006).
139. D. Rehder, J. Costa Pessoa, C. F. G. C. Geraldes, M. M. C. A. Castro, T. Kabanos, T. Kiss, B. Meier, G. Micera, L. Pettersson, M. Rangel, A. Salifoglou, I. Turel and D. Wang, “*In vitro* study of the insulin-mimetic behaviour of vanadium(IV, V) coordination compounds”, *J. Biol. Inorg. Chem.*, **7**, 384–396 (2002).
140. T. Takino, H. Yasui, A. Yoshitake, Y. Hamajima, R. Matsushita, J. Takada and H. Sakurai, “A new halogenated antidiabetic vanadyl complex, bis(5-iodopicolinate)oxovanadium(IV): in vitro and in vivo insulinomimetic evaluations and metalokinetic analysis”, *J. Biol. Inorg. Chem.*, **6**, 133–142 (2001).
141. J. J. Smee, J. A. Epps, K. Ooms, S. E. Bolte, T. Polenova, B. Baruah, L. Yang, W. Ding, M. Li, G. R. Willsky, A. la Cour, O. P. Anderson and D. C. Crans, “Chloro-substituted dipicolinate vanadium complexes: Synthesis, solution, solid-state, and insulin-enhancing properties”, *J. Inorg. Biochem.*, **103**, 575–584 (2009).
142. A. Shaver, D. A. Hall, J. Ng, A. M. Lehuis, R. C. Hynes and B. I. Posner, “Bisperoxovanadium compounds: Synthesis and reactivity of some insulin mimetic complexes”, *Inorg. Chim. Acta*, **229**, 253–260 (1995).
143. I. G. Fantus, S. Kadota, G. Deragon, B. Foster and B. I. Posner, “Pervanadate (peroxide(s) of vanadate) mimics insulin action in rat adipocytes via activation of the insulin receptor tyrosine kinase”, *Biochemistry*, **28**, 8864–8871 (1989).
144. S. Kadota, I. G. Fantus, G. Deragon, H. J. Guyda and B. I. Posner, “Stimulation of insulin-like growth factor II receptor binding and insulin receptor kinase activity in rat adipocytes. Effects of vanadate and H₂O₂”, *J. Biol. Chem.*, **262**, 8252–8256 (1987).
145. A. R. Sarkar and S. Mandal, “Insulin mimetic peroxo complexes of vanadium containing uracil and cytosine as ligand”, *Metal-based drugs*, **7**, 157–164 (2000).

146. C. C. McLauchlan, J.D. Hooker, M.A. Jones, Z. Dymon, E.A. Backhus, B.A. Greiner, N.A. Dorner, M.A. Youkhana and L.M. Manus, "Inhibition of acid, alkaline, and tyrosine (PTP1B) phosphatases by novel vanadium complexes", *J. Inorg. Biochem.*, **104**, 274–281 (2010).
147. C. Djordjevic and G. L. Wampler, "Antitumor activity and toxicity of peroxo heteroligand vanadates(V) in relation to biochemistry of vanadium", *J. Inorg. Biochem.*, **25**, 51–55 (1985).
148. P. Noblíia, M. Vieites, B. S. Parajón–Costa, E. J. Baran, H. Cerecetto, P. Draper, M. González, O. E. Piro, E. E. Castellano and A. Azqueta, "Vanadium(V) complexes with salicylaldehyde semicarbazone derivatives bearing in vitro anti-tumor activity toward kidney tumor cells (TK-10): crystal structure of $[V^VO_2(5\text{-bromosalicylaldehyde semicarbazone})]$ ", *J. Inorg. Biochem.*, **99**, 443–451 (2005).
149. P.I.D.S. Maia, F.R. Pavan, C.Q.F. Leite, S.S. Lemos, G.F. de Sousa, A.A. Batista, O.R. Nascimento, J. Ellena, E. E. Castellano, E. Niquet and V.M. Deflon, "Vanadium complexes with thiosemicarbazones: Synthesis, characterization, crystal structures and anti-Myco**ba**cterium tuberculosis activity", *Polyhedron*, **28**, 398–406 (2009).
150. D.I. Edwards, "Nitroimidazole drugs–action and resistance mechanisms. I. Mechanisms of action", *J. Antibiot. Chemother.*, 1993, **31**, 9–20.
151. K.B. Caylor and M.K. Cassimatis, "Metronidazole neurotoxicosis in two cats", *J. Am. Anim. Hosp. Assoc.*, **37**, 258–262 (2001).
152. M.R. Maurya, S. Khurana, Shailendra, A. Azam, W. Zhang and D. Rehder, "Synthesis, characterisation and antiamoebic studies of dioxovanadium(V) complexes containing ONS donor ligands derived from S–benzylidithiocarbazate", *Eur. J. Inorg. Chem.*, 1966–1973 (2003).
153. M.R. Maurya, A. Kumar, A.R. Bhat, A. Azam, C. Bader, and D. Rehder, "Dioxo– and oxovanadium(V) complexes of thiohydrazone ONS donor ligands: Synthesis, characterization, reactivity, and antiamoebic activity", *Inorg. Chem.*, **45**, 1260–1269 (2006).
154. M.R. Maurya, A. Kumar, M. Abid and A. Azam, "Dioxovanadium(V) and l–oxo bis[oxovanadium(V)] complexes containing thiosemicarbazone based ONS donor set and their antiamoebic activity", *Inorg. Chim. Acta*, **359**, 2439–2447 (2006).

155. A Butler, "Mechanistic considerations of the vanadium haloperoxidases", *Coord. Chem. Rev.*, **187**, 17–35 (1999).
156. A. Butler in J. Reedijk and E. Bouwman (Eds.), "Bioinorganic Catalysis", Marcel Dekker, New York, 2nd ed., Chapter 5 (1999).
157. C. Slebodnick, B.J. Hamstra and V.L. Pecoraro, "Modeling the biological chemistry of vanadium: Structural and reactivity studies elucidating biological function", *Struct. Bonding (Berlin)*, **89**, 51–108 (1997).
158. A.G.J. Ligtenbarg, R. Hage and B.L. Feringa, "Catalytic oxidations by vanadium complexes", *Coord. Chem. Rev.*, **237**, 89–101 (2003).
159. M.R. Maurya, A. Kumar, P. Manikandan and S. Chand, "Synthesis, characterisation and catalytic potential of oxovanadium(IV) based coordination polymers having a bridging methylene group", *Appl. Catal. A: Gen.*, **277**, 45–53 (2004).
160. M.R. Maurya and A. Kumar, "Oxovanadium (IV) based coordination polymers and their catalytic potentials for the oxidation of styrene, cyclohexene and *trans*-stilbene", *J. Mol. Catal. A: Chem.*, **250**, 190–198 (2006).
161. S. Rayati, M. Koliaei, F. Ashouri, S. Mohebbi, A. Wojtczak and A. Kozakiewicz, "Oxovanadium(IV) Schiff base complexes derived from 2,2'-dimethylpropandiamine: A homogeneous catalyst for cyclooctene and styrene oxidation", *Appl. Catal. A: Gen.*, **346**, 65–71 (2008).
162. P. Adão, J. Costa Pessoa, R.T. Henriques, M.L. Kuznetsov, F. Avecilla, M.R. Maurya, U. Kumar and I. Correia, "Synthesis, characterization and application of vanadium-salan complexes in oxygen transfer reactions", *Inorg. Chem.*, **48**, 3542–3561 (2009).
163. M.P. Weberski Jr., C.P. McLauchlan and C.G. Hamaker, "Synthesis and X-ray structural characterization of M(3,5-tBu₂-salophen) (M = Cu, VO)", *Polyhedron*, **25**, 119–123 (2006).
164. E. Kwiatkowski, G. Romanowski, W. Nowicki, M. Kwiatkowski and K. Suwińska, "Dioxovanadium(V) Schiff base complexes of N-methyl-1,2-diaminoethane and 2-methyl-1,2-diaminopropane with aromatic o-hydroxyaldehydes and o-hydroxyketones: Synthesis, characterisation, catalytic properties and structure", *Polyhedron*, **22**, 1009–1018 (2003).

165. G. Romanowski, E. Kwiatkowski, W. Nowicki, M. Kwiatkowski and T. Lis, "Chiral dioxovanadium(V) Schiff base complexes of 1,2-diphenyl-1,2-diaminoethane and aromatic o-hydroxyaldehydes: Synthesis, characterization, catalytic properties and structure", *Polyhedron*, **27**, 1601–1609 (2008).
166. P. Plitt, H. Pritzkow and R. Kraemer, "Biphenyl derived Schiff–base vanadium(V) complexes with pendant OH–groups–structure, characterization and hydrogen peroxide mediated sulfide oxygenation", *Dalton Trans.*, 2314–2320 (2004).
167. I. Lippold, K. Vlay, H. Görls and W. Plass, "Cyclodextrin inclusion compounds of vanadium complexes: Structural characterization and catalytic sulfoxidation", *J. Inorg. Biochem.*, **103**, 480–486 (2009).
168. G. Santoni, G. Licini and D. Rehder, "Catalysis of oxo transfer to prochiral sulfides by oxovanadium(V) compounds that model the active center of haloperoxidases", *Chem. Eur. J.*, **9**, 4700–4708 (2003).
169. D. Rehder, G. Santoni, G.M. Licini, C. Schulzke and B. Meier, "The medicinal and catalytic potential of model complexes of vanadate–dependent haloperoxidases", *Coord. Chem. Rev.*, **237**, 53–63 (2003).
170. V. Conte, F. Di Furia and G. Licini, "Liquid phase oxidation reactions by peroxides in the presence of vanadium complexes", *Appl. Catal. A: Gen.*, **157**, 335–361 (1997).
171. V. Conte and B. Floris, "Vanadium catalyzed oxidation with hydrogen peroxide", *Inorg. Chim. Acta*, **363**, 1935–1946 (2010).
172. F. Marchettia, C. Pettinari, C.D. Nicolaa, R. Pettinari, A. Crispini, M. Crucianelli and A.D. Giuseppe, "Synthesis and characterization of novel oxovanadium(IV) complexes with 4-acyl-5-pyrazolone donor ligands: Evaluation of their catalytic activity for the oxidation of styrene derivatives", *Appl. Catal. A: Gen.*, **378**, 211–220 (2010).
173. T.L. Fernández, E.T. Souza, L.C. Visentin, J.V. Santos, A.S. Mangrich, R.B. Faria, O.A.C. Antunes and M. Scarpellini, "A new oxo-vanadium complex employing an imidazole-rich tripodal ligand: A bioinspired bromide and hydrocarbon oxidation catalyst", *J. Inorg. Biochem.*, **103**, 474–479 (2009).

174. S. Groysman, I. Goldberg, Z. Goldschmidt and M. Kol, "Vanadium(III) and vanadium(V) amine tris(phenolate) complexes", *Inorg. Chem.*, **44**, 5073–5080 (2005).
175. R. Ando, H. Ono, T. Yagyu and M. Maeda, "Spectroscopic characterization of mononuclear, binuclear, and insoluble polynuclear oxovanadium(IV)–Schiff base complexes and their oxidation catalysis", *Inorg. Chim. Acta*, **357**, 817–823 (2004).
176. R. Ando, H. Inden, M. Sugino, H. Ono, D. Sakaeda, T. Yagyu and M. Maeda, "Spectroscopic characterization of amino acid and amino acid ester–Schiff–base complexes of oxovanadium and their catalysis in sulfide oxidation", *Inorg. Chim. Acta*, **357**, 1337–1344 (2004).
177. S.-H. Hsieh, Y.-P. Kuo and H.-M. Gau, "Synthesis, characterization, and structures of oxovanadium(V) complexes of Schiff bases of β -amino alcohols as tunable catalysts for the asymmetric oxidation of organic sulfides and asymmetric alkynylation of aldehydes", *Dalton Trans.*, 97–106 (2007).
178. S.K. Hanson, R.T. Baker, J.C. Gordon, B.L. Scott, A.D. Sutton, and D.L. Thorn, "Aerobic oxidation of pinacol by vanadium(V) dipicolinate complexes: Evidence for reduction to vanadium(III)", *J. Am. Chem. Soc.*, **131**, 428–429 (2009).
179. S.R. Reddy, S. Das and T. Punniyamurthy, "Polyaniline supported vanadium catalyzed aerobic oxidation of alcohols to aldehydes and ketones", *Tetrahedron Lett.*, **45**, 3561–3564 (2004).
180. M.R. Maurya, S. Sikarwar, T. Joseph, P. Manikandan and S. B. Halligudi, "Synthesis, characterisation and catalytic potentials of polymer anchored copper(II), oxovanadium(IV) and dioxomolybdenum(VI) complexes 2-(α -hydroxymethyl)benzimidazole", *React. Funct. Polymer*, **63**, 71–83 (2005).
181. Z.R. Tshentu, C. Togo and R.S. Walmsley, "Polymer-anchored oxovanadium(IV) complex for the oxidation of thioanisole, styrene and ethylbenzene", *J. Mol. Catal. A: Chem.*, **318**, 30–35 (2010).
182. R. Ando, T. Yagyu and M. Maeda, "Characterization of oxovanadium(IV)–Schiff–base complexes and those bound on resin, and their use in sulfide oxidation", *Inorg. Chim. Acta*, **357**, 2237–2244 (2004).

183. R. Ando, S. Mori, M. Hayashi, T. Yagyu and M. Maeda, "Structural characterization of pentadentate salen-type Schiff-base complexes of oxovanadium(IV) and their use in sulfide oxidation", *Inorg. Chim. Acta*, **357**, 1177–1184 (2004).
184. M.R. Maurya, U. Kumar and P. Manikandan, "Synthesis and Characterisation of polymer-anchored oxidovanadium(IV) complexes and their use for the oxidation of styrene and cumene", *Eur. J. Inorg. Chem.*, 2303–2314 (2007).
185. M.R. Maurya and S. Sikarwar, "Oxidation of phenol and hydroquinone catalysed by copper(II) and oxovanadium(IV) complexes of *N,N'*-bis(salicylaldene)diethylenetriamine ($H_2saldien$) covalently bonded to chloromethylated polystyrene", *J. Mol. Catal. A: Chem.*, **263**, 175–185 (2007).
186. M.R. Maurya, H. Saklani and S. Agarwal, "Oxidative bromination of salicylaldehyde by potassium bromide / H_2O_2 catalysed by dioxovanadium(V) complexes encapsulated in zeolite-Y: A functional model of haloperoxidases", *Catal. Commun.*, **5**, 563–568 (2004).
187. M.R. Maurya, H. Saklani, A. Kumar and S. Chand, "Dioxovanadium(V) complexes of dibasic tridentate ligands encapsulated in zeolite-Y for the liquid phase hydroxylation of phenol using H_2O_2 as oxidant", *Catal. Lett.*, **93**, 121–127 (2004).
188. M.R. Maurya, A.K. Chandrakar and S. Chand, "Zeolite-Y encapsulated metal complexes of oxovanadium(VI), copper(II) and nickel(II) as catalyst for the oxidation of styrene, cyclohexane and methyl phenyl sulfide", *J. Mol. Catal. A: Chem.*, **274**, 192–201 (2007).
189. A. Kozlov, K. Asakura and Y. Iwasawa, "Vanadium(IV) complexes with picolinic acids in NaY zeolite cages Synthesis, characterization and catalytic behavior", *J. Chem. Soc., Faraday Trans.*, **94**, 809–816 (1998).
190. A. Kozlov, A. Kozlova, K. Asakura and Y. Iwasawa, "Zeolite encapsulated vanadium picolinate peroxo complexes active for catalytic hydrocarbon oxidations", *J. Mol. Catal. A: Chem.*, **137**, 223–237 (1999).
191. K.J. Balkus Jr., A.K. Khanamedova, K.M. Dixon and F. Bedioui, "Oxidations catalyzed by zeolite ship-in-a-bottle complexes", *Appl. Catal. A: Gen.*, **143**, 159–173 (1996).

192. M.R. Maurya, M. Kumar, S.J.J. Titinchi and S. Chand, "Oxovanadium(IV) Schiff base complexes encapsulated in Zeolite-Y as catalysts for the liquid-phase hydroxylation of phenol", *Catal Lett.*, **86**, 97–105 (2003).
193. S. Raugei and P. Carloni, "Structure and Function of Vanadium Haloperoxidases", *J. Phys. Chem., B*, **110**, 3747–3758 (2006).
194. G. Santoni, G. Licini and D. Rehder, "Catalysis of oxo transfer to prochiral sulfides by oxovanadium(V) compounds that model the active center of haloperoxidases", *Chem. Eur. J.*, **9**, 4700–4708 (2003).
195. V.M. Dembitsky, "Oxidation, epoxidation and sulfoxidation reactions catalysed by haloperoxidases", *Tetrahedron*, **59**, 4701–4720 (2003).
196. G. Zampella, P. Fantucci, V.L. Pecoraro and L. De Gioia, "Reactivity of Peroxo Forms of the Vanadium Haloperoxidase Cofactor. A DFT Investigation", *J. Am. Chem. Soc.*, **127**, 953–960 (2005).
197. D.G. Fujimori and C.T. Walsh, "What's new in enzymatic halogenations", *Current Opinion Chemical Biology*, **11**, 553–560 (2007).
198. C. Drago, L. Caggiano and R.F.W. Jackson, "Vanadium-catalyzed sulfur oxidation/kinetic resolution in the synthesis of enantiomerically pure alkyl aryl sulfoxides", *Angew. Chem. Int. Ed.*, **44**, 7221–7223 (2005).
199. M.E. Cucciolito, R. Del Litto, G. Roviello and F. Ruffo, "O,N,O'-tridentate ligands derived from carbohydrates in the V(IV)-promoted asymmetric oxidation of thioanisole", *J. Mol. Catal. A: Chem.*, **236**, 176–181 (2005).
200. A.L. Maciucă, C.E. Ciocan, E. Dumitriu, F. Fajula and V. Hulea, "V-, Mo- and W-containing layered double hydroxides as effective catalysts for mild oxidation of thioethers and thiophenes with H₂O₂", *Catal. Today*, **138**, 33–37 (2008).
201. I. Lippold, J. Becher, D. Klemmb and W. Plass, "Chiral oxovanadium(V) complexes with a 6-amino-6-deoxyglucopyranoside-based Schiff-base ligand: Catalytic asymmetric sulfoxidation and structural characterization", *J. Mol. Catal. A: Chem.*, **299**, 12–17 (2009).
202. C. Wikete, P. Wu, G. Zampella, L. De Gioia, G. Licini and D. Rehder, "Glycine- and Sarcosine-Based Models of Vanadate-Dependent Haloperoxidases in Sulfoxxygenation Reactions", *Inorg. Chem.*, **46**, 196–207 (2007).

203. K.H. Thompson and C. Orvig, "Vanadium in diabetes: 100 years from Phase 0 to Phase I", *J. Inorg. Biochem.*, **100**, 1925–1935 (2006).
204. K.H. Thompson, J. Lichter, C. LeBel, M.C. Scaife, J.H. McNeill and C. Orvig, "Vanadium treatment of type 2 diabetes: A view to the future", *J. Inorg. Biochem.*, **103**, 554–558 (2009).
205. M. Tanyuksel and W.A. Petri Jr., "Laboratory diagnosis of amebiasis", *Clin. Microbiol. Rev.*, **16**, 713–729 (2003).
206. S.L. Stanley Jr., "Amoebiasis", *Lancet*, **361**, 1025–1034 (2003).
207. D.W. Kim, J.M. Park, B.W. Yoon, M.J. Baek, J.E. Kim and S. Kim, "Metronidazole-induced encephalopathy", *J. Neurol. Sci.*, **224**, 107–111 (2004).
208. A.F. el-Nahas and I.M. el-Ashmawy, "Reproductive and cytogenetic toxicity of metronidazole in male mice", *Basic Clin. Pharmacol. Toxicol.*, **94**, 226–31 (2004).
209. V. Purohit and A.K. Basu, "Mutagenicity of Nitroaromatic Compounds", *Chem. Res. Toxicol.*, **13**, 673–692 (2000).
210. P. Abboud, V. Lemee, G. Gargala, P. Brasseur, J.J. Ballet, F. Borsa-Lebas, F. Caron and L. Favennec, "Successful treatment of metronidazole- and albendazole-resistant giardiasis with nitazoxanide in a patient with acquired immunodeficiency syndrome", *Clin. Infectious Diseases*, **32**, 1792–1794 (2001).
211. W. Petri, "Therapy of intestinal protozoa", *Trends Parasitology*, **19**, 523–526 (2003).
212. Shailendra, N. Bharti, M.T. Gonzalez Garza, D.E. Cruz-Vega, J.C. Garza, K. Saleem, F. Naqvi and A. Azam, "Synthesis, characterization and antiamoebic activity of new thiophene-2-carboxaldehyde thiosemicarbazone derivatives and their cyclooctadiene Ru(II) complexes", *Bioorg. Med. Chem. Lett.*, **11**, 2675–2678 (2001).
213. Y.Q. Zuo, W.P. Liu, Y.F. Niu, C.F. Tian, M.J. Xie, X.Z. Chen and L. Li, "Bis(α -furancarboxylato)oxovanadium(IV) prevents and improves dexamethasone-induced insulin resistance in 3T3-L1 adipocytes", *J. Pharm. Pharmacol.*, **60**, 1335–1340 (2008).

4. D.A. Roess, S.M. Smith, P. Winter, J. Zhou, P. Dou, B. Baruah, A.M. Trujillo, N.E. Levinger, X. Yang, B.G. Barisas and D.C. Crans, "Effects of vanadium-containing compounds on membrane lipids and on microdomains used in receptor-mediated signaling", *Chem. Biodiver.*, **5**, 1558–1570 (2008).
5. A. Anwar-Mohamed and A.O. El-Kadi, "Down-regulation of the carcinogen-metabolizing enzyme cytochrome P450 1a1 by vanadium", *Drug Metab. Dispos.*, **36**, 1819–1827 (2008).
6. A.M. Evangelou, "Vanadium in cancer treatment", *Crit. Rev. Oncol. Hematol.*, **42**, 249–265 (2002).
7. R.L. Dutta and A. Syamal, "*Elements of Magnetochemistry*", Affiliated East-West Press, New Delhi, 2nd ed., p. 8 (1993).
8. A. Rockenbauer and L. Korecz, "Automatic computer simulations of ESR spectra", *Appl. Magn. Reson.*, **10**, 29–43 (1996).
9. (a) R.A. Rowe and M.M. Jones, "Vanadium(IV)oxy(acetylacetonate)", *Inorg. Synth.*, **5**, 113–116 (1957); (b) C.S. Maevell and N. Tarkoy, "Heat-stability studies on chelates from Schiff bases of salicylaldehyde derivatives", *J. Am. Chem. Soc.*, **79**, 6000–6003 (1957).
20. M.R. Maurya, D.C. Antony, S. Gopinathan and C. Gopinathan, "Synthesis, spectral and electrochemical studies of dioxotungsten(VI) complexes of binucleating Schiff bases derived from methylene- or dithio-bis(salicylaldehyde) and various hydrazides", *Indian J. Chem.*, **34A**, 967–970 (1995).
21. C.W. Wright, M.J.O' Neill, J.D. Phillipson and D.C. Warhurst, "Use of microdilution to assess in vitro antiamoebic activities of *Brucea javanica* fruits, *Simarouba amara* stem, and a number of quassinoids", *Antimicrob. Agents Chemother.*, **32**, 1725–1729 (1988).
22. L.S. Diamond, D.R. Harlow and C.C. Cunnick, "A new medium for the axenic cultivation of *Entamoeba histolytica* and other *Entamoeba*", *Trans. R. Soc. Trop. Med. Hyg.*, **72**, 431–432 (1978).
23. F.D. Gillin, D.S. Reiner and M. Suffnes, "Bruceantin, a potent amebicide from a plant, *Brucea antidysenterica*", *Antimicrob. Agents Chemother.*, **22**, 342–345 (1982).

224. A.T. Keen, A. Harris, J.D. Phillipson and D.C. Warhurst, "In vitro amoebicidal testing of natural products; part I. Methodolog", *Planta. Med.*, 278–284 (1986).
225. T. Mosmann, "Rapid colorimetric assay for cellular growth and survival: application to proliferation and cytotoxicity assays", *J. Immunol. Methods*, **65**, 55–63 (1983).
226. S.P. Perlepes, D. Nicholls and M.R. Harison, „Coordination compounds of benzildihydrazone", *Inorg. Chim. Acta*, **102**, 137–143 (1985).
227. O. Bortolini, M. Carraro, V. Conte and S. Moro, "Histidine-containing bisperoxovanadium(V) compounds. Insight into the solution structure by an ESI-MS and ^{51}V -NMR comparative study", *Eur. J. Inorg. Chem.*, 1489–1495 (1999).
228. O. Bortolini, V. Conte, F. Di Furia and S. Moro, "Direct evidence of solvent-peroxovanadium clusters by electrospray ionization mass spectrometry", *Eur. J. Inorg. Chem.*, **8**, 1193–1197 (1998).
229. C. Slebodnick and V.L. Pecoraro, "Solvent effects on ^{51}V NMR chemical shifts: characterization of vanadate and peroxovanadate complexes in mixed water/acetonitrile solvent", *Inorg. Chim. Acta*, **283**, 37–43 (1998).
230. P. Schwendt and K. Liscak, "Spectral investigation of stability of the peroxo complexes $\text{M}_2[\text{V}_2\text{O}_2(\text{O}_2)4\text{H}_2\text{O}]\cdot\text{aq}$ ($\text{M} = \text{N}(\text{CH}_3)_4$, $\text{N}(\text{C}_4\text{H}_9)_4$) in solutions", *Collect. Czech. Chem. Chem. Commun.*, **61**, 868–876 (1996).
231. M.J. Clague, N.L. Keder and A. Butler, "Biomimics of vanadium bromoperoxidase: Vanadium(V)-Schiff base catalyzed oxidation of bromide by hydrogen peroxide", *Inorg. Chem.*, **32**, 4754–4761 (1993).
232. M.R. Maurya, A. Arya, A. Kumar and J. Costa Pessoa, "Polystyrene bound oxidovanadium(IV) and dioxidovanadium(V) complexes of histamine derived ligand for the oxidation of methyl phenyl sulfide, diphenyl sulfide and benzoin", *Dalton Trans.*, 2185–2195 (2009).
233. M. Casný and D. Rehder, "Molecular and supramolecular features of oxo-peroxovanadium complexes containing O_3N , O_2N_2 and ON_3 donor sets", *Dalton Trans.*, 839–846 (2004).

234. J.S. Jaswal and A.S. Tracey, "Formation and decomposition of peroxovanadium(V) complexes in aqueous solution", *Inorg. Chem.*, **30**, 3718–3722 (1991).
235. Q. Zeng, H. Wang, T. Wang, Y. Cai, W. Weng and Y. Zhao, "Vanadium-catalyzed enantioselective sulfoxidation and concomitant, highly efficient kinetic resolution provide high enantioselectivity and acceptable yields of sulfoxides", *Adv. Synth. Catal.*, **347**, 1933–1936 (2005).
236. J.A. Bonadies, W.M. Butler, V.L. Pecoraro and C.J. Carrano, "Novel reactivity patterns of (N,N'-ethylenebis(salicylideneaminato))oxovanadium(IV) in strongly acidic media", *Inorg. Chem.*, **26**, 1218–1222 (1987).
237. A. Bonadies and C.J. Carrano, "Vanadium phenolates as models for vanadium in biological systems. 1. Synthesis, spectroscopy, and electrochemistry of vanadium complexes of ethylenebis[(o-hydroxyphenyl)glycine] and its derivatives", *J. Am. Chem. Soc.*, **108**, 4088–4095 (1986).
238. W. Plass, A. Pohlmann and H.-P. Yozgatli, "N-salicylidenehydrazides as versatile tridentate ligands for dioxovanadium(V) complexes", *J. Inorg. Biochem.*, **80**, 181–183 (2000).
239. K. Fukui, H. Ohya-Nishiguchi and H. Kamada, "Electron Spin-Echo Envelope Modulation Study of Imidazole-Coordinated Oxovanadium(IV) Complexes Relevant to the Active Site Structure of Reduced Vanadium Haloperoxidases", *Inorg. Chem.*, **37**, 2326–2327 (1998).
240. K. Wurthrich, "E.S.R. (electron spin resonance) investigation of VO₂⁺ complex compounds in aqueous solution. II", *Helv. Chim. Acta*, **48**, 1012–1017 (1965).
241. N.D. Chasteen in "*Biological Magnetic Resonance*", (Ed.: J. Reuben), Plenum, New York, p. 53 (1981).
242. D. Rehder, "*Bioinorganic Vanadium Chemistry*", John Wiley & Sons, New York, 2008.
243. I. Correia, J. Costa Pessoa, M.T. Duarte, R.T. Henriques, M.F.M. Piedade, L.F. Veiros, T. Jackush, A. Dornyei, T. Kiss, M.M.C.A. Castro, C.F.G.C. Geraldes and F. Avecilla, "N,N'-ethylenebis(pyridoxylideneiminato) and N,N'-ethylenebis(pyridoxylaminato): Synthesis, characterization,

- potentiometric, spectroscopic, and DFT studies of their vanadium(IV) and vanadium(V) complexes”, *Chem. Eur. J.*, **10**, 2301–2317 (2004).
244. A.G.J. Ligtenbarg, R. Hage and B.L. Feringa, “Catalytic oxidations by vanadium complexes”, *Coord. Chem. Rev.*, **237**, 89–101 (2003).
 245. B.J. Hamstra, G.J. Colpas and V.L. Pecoraro, “Reactivity of dioxovanadium(V) complexes with hydrogen peroxide: Implications for vanadium haloperoxidase”, *Inorg. Chem.*, **37**, 949–955 (1998).
 246. A. Giacomelli, C. Floriani, A.O.S. Duarte, A. Chiesi-Villa and C. Guastini, “Chemistry and structure of an inorganic analog of a carboxylic acid: hydroxobis(8-quinolinato)oxovanadium(V)”, *Inorg. Chem.*, **21**, 3310–3316 (1982).
 247. M.A. Anderson, A. Willets and S. Allenmark, “Asymmetric Sulfoxidation Catalyzed by a Vanadium-Containing Bromoperoxidase”, *J. Org. Chem.*, **62**, 8455–8458 (1997).
 248. H.B. ten Brink, H.E. Schoemaker and R. Wever, “Sulfoxidation mechanism of vanadium bromoperoxidase from *Ascophyllum nodosum*: evidence for direct oxygen transfer catalysis”, *Eur. J. Biochem.*, **268**, 132–138 (2001).
 249. G.J. Colpas, B.J. Hamstra, J.W. Kampf and V.L. Pecoraro, “Functional models for vanadium haloperoxidase: Reactivity and mechanism of halide oxidation”, *J. Am. Chem. Soc.*, **118**, 3469–3478 (1996).
 250. A. Butler, M.J. Clague and G.E. Meister, “Vanadium Peroxide Complexes”, *Chem. Rev.*, **94**, 625–638 (1994).
 251. C.J. Schneider, J.E. Penner-Hahn and V.L. Pecoraro, “Elucidating the Protonation Site of Vanadium Peroxide Complexes and the Implications for Biomimetic Catalysis”, *J. Am. Chem. Soc.*, **130**, 2712–2713 (2008).
 252. A.M. Ramadan, “Structural and biological aspects of copper (II) complexes with 2-methyl-3-amino-(3 H)-quinazolin-4-one”, *J. Inorg. Biochem.*, **65**, 183–189 (1997).
 253. B.J. Winer, “*Statistical Principals in Experimental Design*, vol. 22”, McGraw-Hill Book Company, 2nd ed., p. 45 (1971).

254. R.E. Berry, E.M. Armstrong, R.L. Beddoes, D. Collison, S.N. Ertok, M. Helliwell and C.D. Garner, "The structural characterization of amavadin", *Angew. Chem. Int. Ed.*, **38**, 795–797 (1999).
255. D.L. Parry, S.G. Brand and K. Kustin, "Distribution of Tunichrome in the Ascidiacea", *Bull. Marine Sci.*, **50**, 302–306 (1992).
256. T. Ishii, I. Nakai, C. Numako, K. Okoshi and T. Otake, "Discovery of a new vanadium accumulator, the fan worm *Pseudopotamilla ocellata*", *Naturwissenschaften*, **80**, 268–270 (1993).
257. M. Weyand, H.J. Hecht, M. Kiess, M.F. Liaud, H. Vilter and D. Schomburg, "X-ray Structure Determination of a Vanadium-dependent Haloperoxidase from *Ascophyllum nodosum* at 2.0 Å Resolution", *J. Mol. Biol.*, **293**, 595–611 (1999).
258. "Vanadium compounds: Chemistry, biochemistry and therapeutic applications", ed. V.L. Pecoraro, C. Sleboznick, B. Hamstra, D.C. Crans and A.S. Tracy, ACS Symposium Series, Ch. 12 (1998).
259. S.S. Amin, K. Cryer, B. Zhang, S.K. Dutta, S.S. Eaton, O.P. Anderson, S.M. Miller, B.A. Reul, S.M. Brichard and D.C. Crans, "Chemistry and insulin-mimetic properties of bis(acetylacetonate)oxovanadium(IV) and derivatives", *Inorg. Chem.*, **39**, 406–416 (2000).
260. D. Rehder, "Biological and medicinal aspects of vanadium", *Inorg. Chem. Commun.*, **6**, 604–617 (2003).
261. M. Xie, L. Gao, L. Li, W. Liu and S. Yan, "A new orally active antidiabetic vanadyl complex - bis(α -furancarboxylato)oxovanadium(IV)", *J. Inorg. Biochem.*, **99**, 546–551 (2005).
262. M.J. Gresser and A.S. Tracey, in: ed N.D. Chasteen, "*Vanadium in Biological Systems*", Kluwer Acad. Publ., Dordrecht, Ch. IV (1990).
263. M.R. Maurya, S. Sikarwar and P Manikandan, "Oxovanadium(IV) complex of 2-(α -hydroxyethyl)benzimidazole covalently bonded to chloromethylated polystyrene for oxidation of benzoin", *Appl. Catal. A: Gen.*, **315**, 74–82 (2006).
264. M.R. Maurya, A.K. Chandrakar and S. Chand, "Oxidation of phenol, styrene and methyl phenyl sulfide with H_2O_2 catalyzed by dioxovanadium(V) and copper(II) complexes of 2-

- aminomethylbenzimidazole-based ligand encapsulated in zeolite-Y", *J. Mol. Catal. A: Chem.*, **263**, 227–237 (2007).
265. M.R. Maurya and S. Sikarwar, "Oxovanadium(IV) complex of β -alanine derived ligand immobilised on polystyrene for the oxidation of various organic substrates", *Catal. Commun.*, **8**, 2017–2024 (2007).
 266. M.R. Maurya, U. Kumar, I. Correia, P. Adão and J. Costa Pessoa, "A polymer-bound oxidovanadium(IV) complex prepared from an L-cysteine-derived ligand for the oxidative amination of styrene", *Eur. J. Inorg. Chem.*, 577–587 (2008).
 267. M.R. Maurya, M. Kumar, A. Kumar and J. Costa Pessoa, "Oxidation of p-chlorotoluene and cyclohexene catalysed by polymer-anchored oxovanadium(IV) and copper(II) complexes of amino acid derived tridentate ligands", *Dalton Trans.*, 4220–4232 (2008).
 268. W. Plass, "Supramolecular interactions of vanadate species: vanadium(V) complexes with N-salicylidenehydrazides as versatile models", *Coord. Chem. Rev.*, **237**, 205–212 (2003).
 269. D. Rehder, "The coordination chemistry of vanadium as related to its biological functions", *Coord. Chem. Rev.*, **182**, 297–322 (1999).
 270. M.R. Maurya, "Development of the coordination chemistry of vanadium through bis(acetylacetonato)oxovanadium(IV): synthesis, reactivity and structural aspects", *Coord. Chem. Rev.*, **237**, 163–181 (2003).
 271. M.J. Clague and A. Butler, "On the mechanism of cis-dioxovanadium(v)-catalyzed oxidation of bromide by hydrogen peroxide: Evidence for a reactive, binuclear vanadium(V) peroxo complex", *J. Am. Chem. Soc.*, **117**, 3475–3484 (1995).
 272. A. Butler, H. Eckert and M.J. Danzitz, "Vanadium-51 NMR as a probe of metal-ion binding in metalloproteins", *J. Am. Chem. Soc.*, **109**, 1864–1865 (1987).
 273. D.I. Edwards, "Nitroimidazole drugs - action and resistance mechanisms. II. Mechanisms of resistance", *J. Antimicrob. Chemother.*, **31**, 201–210 (1993).
 274. M.M.L. Nigro, A.B. Gadano and M.A. Carballo, "Evaluation of genetic damage induced by a nitroimidazole derivative in human lymphocytes: Tinidazole (TNZ)", *Toxicol.*, **15**, 209–213 (2001).

275. S.N.J. Moreno and R. Docampo, "Mechanism of toxicity of nitro compounds used in the chemotherapy of trichomoniasis", *Environ. Health Perspect.*, **64**, 199–208 (1985).
276. Y. Akgun, I.H. Tacyldz and Y. Celik, "Amebic liver abscess: changing trends over 20 years", *World J. Surg.*, **23**, 102–106 (1999).
277. T.H. Conner, M. Stoeckel, J. Evrard, and M.S. Legator, "The contribution of metronidazole and two metabolites to the mutagenic activity detected in urine of treated humans and mice", *Cancer Res.*, **37**, 629–633 (1977).
278. K. Kapoor, M. Chandra, D. Nag, J.K. Paliwal, R.C. Gupta and R.C. Saxena, "Evaluation of metronidazole toxicity: a prospective study", *Int. J. Clin. Pharmacol. Res.*, **19**, 83–88 (1999).
279. H.S. Rosenkranz and W.T. Speck, "Mutagenicity of metronidazole. Activation by mammalian liver microsomes", *Biochem. Biophys. Res. Commun.*, **66**, 520–525 (1975).
280. D.A. Rowley, R.C. Knight, I.M. Skolimowski, and D.I. Edwards, "The relationship between misonidazole cytotoxicity and base composition of DNA", *Biochem. Pharmacol.*, **29**, 2095–2098 (1980).
281. N. Bharati, Shailendra, M.T.G. Garza, D.E. Cruz-Vega, J. Castro-Garza, K. Saleem, F. Naqvi, M.R. Maurya and A. Azam, "Synthesis, Characterization and Antiamoebic Activity of Benzimidazole Derivatives and Their Vanadium and Molybdenum Complexes", *Bioorg. Med. Chem. Lett.*, **12**, 869–871 (2002).
282. D.A. Dougherty, "Cation π -interactions in: *Encyclopedia of Supramolecular Chemistry*"; ed. J.L. Atwood and J.W. Steed, Marcel Dekker, Inc., New York; Vol. 1, 214–218 (2004).
283. M. Cametti, M. Nissinen, A. Dalla Cort, L. Mandonilini and K. Rissanen, "Recognition of Alkali Metal Halide Contact Ion Pairs by Uranyl-Salophen Receptors Bearing Aromatic Sidearms. The Role of Cation- π Interactions", *J. Am. Chem. Soc.*, **127**, 3831–3837 (2005).
284. M. Cametti, M. Nissinen, A. Dalla Cort, K. Rissanen and L. Mandolini., "Crystal Structure of a CsF-Uranyl-Salen Complex. An Unusual Cesium-Chlorine Coordination", *Inorg. Chem.*, **45**, 6099–6101 (2006).

285. T.A. Hanna, L. Liu, A.M. Angeles-Boza, X. Kou, C.D. Gutsche, K. Ejsmont, W.H. Watson, L.N. Zakharov, C.D. Incarvito and A.L. Rheingold, Synthesis, "Structures, and Conformational Characteristics of Calixarene Monoanions and Dianions", *J. Am. Chem. Soc.*, **125**, 6228–6238 (2003).
286. P. Thuéry, Z. Asfari, J. Vicens, V. Lamare and J.-F. Dozol, "Synthesis and crystal structure of sodium and caesium ion complexes of unsubstituted calix[4]arene. New polymeric chain arrangements", *Polyhedron*, **21**, 2497–2503 (2002).
287. K. Izod, W. Clegg and S.T. Liddle, "The First Structurally Authenticated Rb-PR₃ and Cs-PR₃ Contacts. Synthesis and Crystal Structures of [Rb{(Me₃Si)₂CP(C₆H₄-2-CH₂NMe₂)₂}]_n and [Cs{(Me₃Si)₂CP(C₆H₄-2-CH₂NMe₂)₂}(toluene)]_n", *Organometallics*, **20**, 367–369 (2001).
288. I. Lippold, H. Görls and W. Plass, "New aspects for modeling supramolecular interactions in vanadium haloperoxidases: β-cyclodextrin inclusion compounds of cis-dioxovanadium(V) complexes", *Eur. J. Inorg. Chem.*, 1487–1491 (2007).
289. D. Hoffmann, W. Bauer, P. von Ragué Schleyer, U. Pieper and D. Stalke, "Cation-induced structural alterations in the organo alkali metal derivatives of triphenylmethane: a combined x-ray and NMR study of the potassium-cesium salts", *Organometallics*, **12**, 1193–1200 (1993).
290. G.M. Sheldrick, "*SHELXL-97: An Integrated System for Solving and Refining Crystal Structures from Diffraction Data (Revision 4.1)*"; University of Göttingen, Germany, (1997).
291. G. Bernardinelli and H.D. Flack, "Least-squares absolute-structure refinement. Practical experience and ancillary calculations", *Acta Cryst., Sect. A: Crystallogr.*, **A41**, 500–511 (1985).
292. J.-W. Liu and S. Weng, "Diaquabis(3-hydroxybenzoato-κO)bis(1,10-phenanthroline-κ2N,N')barium(II)", *Acta Cryst. Section E*, **E63**, m808–m809 (2007).
293. A. Pohlman, S. Nica, T. Kim, K. Luong and W. Plass, "Dioxovanadium(V) complexes with side chain substituted N-salicylidenehydrazides modelling supramolecular interactions in vanadium haloperoxidases", *Inorg. Chem. Commun.*, **8**, 289–292 (2005).

294. C. Schade and P. von R. Schleyer, "Sodium, potassium, rubidium, and cesium: x-ray structural analysis of their organic compounds", *Adv. Organomet. Chem.*, **27**, 169–278 (1987).
295. J.D. Smith, "Organometallic compounds of the heavier alkali metals", *Adv. Organomet. Chem.*, **43**, 267–348 (1998).
296. C. Eaborn, P.B. Hitchcock, K. Izod and J.D. Smith, "The synthesis and crystal structures of $\text{RbC}(\text{SiMe}_3)_3$ and $\text{CsC}(\text{SiMe}_3)_3 \cdot 3.5\text{C}_6\text{H}_6$: a one-dimensional ionic solid and an ionic solid with a molecular structure", *Angew. Chem. Int. Ed. Engl.*, **34**, 687–688 (1995).
297. K. Izod, C. Wills, W. Clegg and R.W. Harrington, "Heavier Alkali Metal Complexes of a Silicon- and Phosphine-Borane-Stabilized Carbanion", *Organometallics*, **25**, 5326–5332 (2006).
298. A. Kojima, K. Okazaki, S. Ooi and K. Saito, "Crystal structures of vanadium(IV), vanadium(V), and vanadium(IV)vanadium(V) complexes of the (S)-[[1-(2-pyridyl)ethyl]imino]diacetate ion. Comparison of the molecular structure of the binuclear mixed-valence vanadium(IV)vanadium(V) complex with those of constituent vanadium(IV) and vanadium(V) complexes", *Inorg. Chem.*, **22**, 1168–1174 (1983).
299. X.-M. Zhang and X.-Zeng You, "Synthesis, characterization and crystal structure of a binuclear cis-dioxovanadium(V) Schiff base complex", *Polyhedron*, **15**, 1793–1796 (1996).
300. L. Pettersson, I. Andersson and A. Gorz s, "Speciation in peroxovanadate systems", *Coord. Chem. Rev.*, **237**, 77–87 (2003).
301. X. Li, M.S. Lah and V.L. Pecoraro, "Vanadium complexes of the tridentate Schiff base ligand N-salicylidene-N'-(2-hydroxyethyl)ethylenediamine: acid-base and redox conversion between vanadium(IV) and vanadium(V) imino phenolates", *Inorg. Chem.*, **27**, 4657–4664 (1988).
302. Z. Otwinowski and W. Minor in: "*Processing of X-ray Diffraction Data Collected in Oscillation Mode. Methods in Enzymology*", Ed. C.W. Carter and R.M. Sweet, Vol. 276, Macromolecular Crystallography; Academic Press: London; Part A, p 307 (1997).
303. M.A. Ali, and M.T.H. Tarafder, "Metal complexes of sulfur and nitrogen-containing ligands: complexes of S-benzylidithiocarbamate and a Schiff base

- formed by its condensation with pyridine-2-carboxaldehyde”, *J. Inorg. Nucl. Chem.*, **39**, 1785–1791 (1977).
304. M. Das and S.E. Livingstone, “Metal chelates of dithiocarbazic acid and its derivatives. IX. Metal chelates of ten new Schiff bases derived from S-methyldithiocarbazate”, *Inorg. Chim. Acta*, **19**, 5–10 (1976).
305. M.R. Maurya, D.C. Antony, S. Gopinathan and C. Gopinathan, Dioxomolybdenum(VI) complexes of flexibly-bridged hexadentate tetraanionic Schiff bases derived from methylene- or dithiobis(salicylaldehyde) and S-methyldithiocarbazate or S-benzoyldithiocarbazate, *Bull. Chem. Soc. Japan*, **68**, 554–565 (1995).
306. D. Rehder, “Transition metal nuclear magnetic resonance”, Ed., P.S. Pregosin, Elsevier, New York, pp 1–58 (1991).
307. D. Rehder, C. Weidemann, A. Duch, W. Pribsch; *Inorg. Chem.*, **27**, 584–587 (1988).

*Summary
&
Conclusion*

SUMMARY AND CONCLUSION

The active center of vanadate-dependent haloperoxidases (VHPO) is constituted by vanadate(V) covalently linked to the imidazole moiety of a histidine side-chain of the protein. Vanadium is in a trigonal-bipyramidal environment, with the imidazole-N and an HO^- in the axial positions. Several model complexes have been reported in the literature. We have used binucleating hydrazones, $\{\text{CH}_2(\text{H}_2\text{sal-nah})_2, \text{CH}_2(\text{H}_2\text{sal-inh})_2, \text{CH}_2(\text{H}_2\text{sal-bhz})_2 \text{ and } \text{CH}_2(\text{H}_2\text{sal-fah})_2\}$ and thiohydrazones $\{\text{CH}_2(\text{H}_2\text{sal-sbdt})_2 \text{ and } \text{CH}_2(\text{H}_2\text{sal-smdt})_2\}$ derived from 5,5'-methylenebis (salicylaldehyde) $\{\text{CH}_2(\text{Hsal})_2\}$ and hydrazide {nicotinoylhydrazide (nah), isonicotinoylhydrazide (inh), benzoylhydrazide (bhz) and 2-furoylhydrazide (fah)} or thiohydrazide {S-benzylthiocarbamate (sbdt) and S-methylthiocarbamate (smdt)} to design oxidovanadium(IV) and dioxovanadium(V) complexes. Thus, $\text{V}^{\text{IV}}\text{O}-$ and $\text{V}^{\text{V}}\text{O}_2$ -complexes have been synthesized and characterized. For one of the $\text{V}^{\text{V}}\text{O}_2$ -complexes, $\text{Cs}_2[\text{CH}_2\{\text{V}^{\text{V}}\text{O}_2(\text{sal-bhz})\}_2]\cdot 2\text{H}_2\text{O}$ the crystal and molecular structure was determined. Each $\text{Cs}_2[\text{CH}_2\{\text{V}^{\text{V}}\text{O}_2(\text{sal-bhz})\}_2]\cdot 2\text{H}_2\text{O}$ moiety contains two cis-dioxovanadium(V) units, forming a dinuclear compound with no relevant interactions between the V^{V} -centres.

Dioxidovanadium(V) complexes have been shown to be functional models of vanadium dependent haloperoxidases, satisfactorily catalyzing the oxidative bromination of salicylaldehyde to give 5-bromosalicylaldehyde, 3,5-dibromosalicylaldehyde and 2,4,6-tribromophenol using $\text{H}_2\text{O}_2/\text{KBr}$ in the presence of HClO_4 in aqueous solution at room temperature. Complexes $\text{Cs}_2[\text{CH}_2\{\text{V}^{\text{V}}\text{O}_2(\text{sal-sbdt})\}_2]\cdot 2\text{H}_2\text{O}$ and $\text{Cs}_2[\text{CH}_2\{\text{V}^{\text{V}}\text{O}_2(\text{sal-smdt})\}_2]\cdot 2\text{H}_2\text{O}$ also catalyze oxidative bromination of styrene to give 1,2-dibromo-1-phenylethane, 2-bromo-1-phenylethane-1-ol and 1-(4-bromophenyl)ethane-1,2-diol. Oxidovanadium(IV) complexes have also been shown to be catalyst precursors for

the catalytic oxidation, by peroxide, of methyl phenyl sulfide and diphenyl sulfide, yielding the corresponding sulfoxide and sulfone at room temperature.

The reactivity in methanol and DMSO of the $V^{IV}O$ - and V^VO_2 -complexes was studied by UV-Vis, EPR and ^{51}V NMR spectroscopy, by either adding H_2O_2 or acid (HCl or $HClO_4$) or both, the formation of several species being established, some of them probably being intermediates in the catalytic processes studied, namely $[CH_2\{V^VO(O_2)(L)\}_2]^{2-}$ and $[CH_2\{V^VO(OH)(L)\}_2]$.

Medicinal aspects of vanadium compounds were increased with the discovery of insulin-mimetic property of vanadium ions in 1979. Vanadium(IV) and vanadium(V) salts have been extensively tested both in vivo and in vitro in a considerable variety of experimental models of diabetes. Several types of neutral and low molecular weight vanadium(IV) complexes with organic ligands have been designed and investigated in animal model systems for the treatment of diabetes. We have tested isolated vanadium complexes for their antiamoebic activity. Amoebiasis is caused by *Entamoeba histolytica*, the second leading cause of death among parasite diseases. For the treatment of amoebiasis metronidazole has been till now the drug of choice. The vanadium(IV) and vanadium(V) were screened against HM1:IMSS strains of *Entamoeba histolytica*, the results and determined IC_{50} values showing that they are significantly more active than metronidazole, suggesting that these vanadium compounds may be promising drugs for the treatment of this disease. Moreover, toxicity tests carried out with the HeLa cell line showed that some of the complexes offer remarkable viability (>90%), further supporting that these vanadium compounds may be promising drugs for the treatment of Amoebiasis.